THE ROLE OF DOXAZOSIN IN PROSTATE AND BLADDER CANCERS

Mr Nevil Mallet Pavithran MBBS, MS (Gen Surgery), MRCS (Edin)

Division of Surgical & Interventional Sciences
University College London

Submitted for award of PhD.

Principal Supervisor: Prof Faiz Mumtaz

Second Supervisor: Dr Cecil Thompson

Declaration

I, Nevil Mallet Pavithran, confirm that the work presented in my thesis is my own. Where information has been derived from other sources, I confirm that this has been indicated in the thesis.

Nevil Pavithran

15 March 2023

Abstract

Introduction: Doxazosin, an alpha-1 adrenergic receptor antagonist, is used to treat hypertension and benign prostatic enlargement. Additionally, it has shown antineoplastic effects on various cancers, including prostate and bladder cancer. These anticancer effects are unrelated to its alpha-adrenergic activity and are instead linked to its quinazoline-based chemical structure. The specific mechanisms and receptors involved in doxazosin's antineoplastic activity remain unclear. This study aimed to elucidate the cellular mechanisms by which doxazosin induces cell death in prostate and bladder cancer cells.

Methods: Using UniProtKB/PSI-Search 2, we identified that 5- hydroxy tryptamine receptors have structural similarity to alpha-1 adrenergic receptors. Subsequently, we investigated if the antineoplastic actions of doxazosin were mediated via 5-hydroxy tryptamine due to its structural similarity to alpha-1 adrenergic receptors. In parallel, we also attempted to develop doxazosin-resistant cell lines with a view to investigate the up regulation and/or down regulation of such receptors. As both the above did not yield any results, we subsequently investigated non-receptor mediated pathways (such as endocytosis and pinocytosis).

During our experiments to develop doxazosin-resistant cells, we had incidentally observed that granulations appeared within cells when exposed to doxazosin. We explored this further using SEM, TEM, and immunostaining techniques. Subsequently, we investigated the changes in gene expression following exposure to doxazosin. Finally, we conducted *In Vivo* experiments to

ascertain if the experiments findings translated to similar actions in nude athymic mice.

Results: We were able to demonstrate that dynamin-mediated and clathrin-dependent endocytic trafficking of doxazosin resulted in widespread autophagy (mitophagy) in prostate, bladder and fibroblast cells undergoing cell death following exposure to doxazosin. Furthermore, doxazosin increased the gene expression of several gene families related to autophagy, apoptosis, anoikis, and lipid metabolism. Doxazosin also inhibited the growth of HT1376 bladder cancer cell implants *In Vivo* in nude athymic mice.

Conclusion: Our results raise the possibility that doxazosin could be useful in the management of advanced urological malignancy.

Impact Statement

This study titled 'The Role of Doxazosin in Prostate and Bladder Cancers,' was the first to demonstrate that the dynamin-mediated endocytic trafficking of doxazosin resulted in widespread autophagy (mitophagy) in prostate, bladder and fibroblast cells undergoing cell death following exposure to doxazosin.

This study was also the first to demonstrate that doxazosin increased the gene expression of several gene families related to autophagy, apoptosis, anoikis, and lipid metabolism in PC-3 cell line. Using next generation transcriptome sequencing we have also identified a gene LOC100271832 that remains uncharacterized to date. This gene was incidentally to have the second- highest fold change when cells were exposed to doxazosin. This opens to a promising subject for future research.

We were also able to demonstrate that the *In Vitro* actions of doxazosin translate to *In Vivo* by demonstrating that it inhibited the growth of HT1376 bladder cancer cell implants *In Vivo* in nude athymic mice.

Collectively, these findings suggest that doxazosin (or development of alternate molecules based on a similar quinazoline structure) could be potential candidates for development of anticancer agents that may have novel mechanisms of action. These may complement existing chemotherapeutic options, especially in the management of androgen-resistant metastatic prostate cancers. It may also have a role in local treatment of bladder cancers along with existing agents.

UCL Research Paper Declaration Form

referencing the doctoral candidate's own published work(s)

Please use this form to declare if parts of your thesis are already available in another format, e.g. if data, text, or figures:

- have been uploaded to a preprint server.
- are in submission to a peer-reviewed publication.
- have been published in a peer-reviewed publication, e.g. journal, textbook.

This form should be completed as many times as necessary. For instance, if you have seven thesis chapters, two of which containing material that has already been published, you will complete this form twice.

- 1. For a research manuscript that has already been published (if not yet published, please skip to section 2)
 - a) What is the title of the manuscript?
 - DOXAZOSIN-INDUCED CELL DEATH OF HT1376 BLADDER CANCER CELLS IS MEDIATED BY AUTOPHAGY BOTH IN VITRO AND IN VIVO Authors: Nevil Pavithran, Majed Shabbir, Soha El Shiekh, Faiz Mumtaz, JM Cooper, Rajai Al Jehani, Cecil Thompson Poster AND Abstract BAUS Oncology 2016. (Pavithran, Shabbir et al. 2017) https://doi.org/10.1177/2051415816682423
 - 2. DOXAZOSIN CAUSES CELL DEATH BY AUTOPHAGY (MITOPHAGY) IN HORMONE RESISTANT PROSTATE CANCER CELLS.

Authors: Nevil Pavithran, Cecil Thompson.

Poster, Physiology 2012. Proc Physiol Soc 27 (2012), PC309.

(Pavithran and Thompson 2012)

doi: not available

- b) Please include a link to or doi for the work
 - <u>1. https://doi.org/10.1177/2051415816682423</u>
 - 2. Doi: not available (not indexed to doi)
- c) Where was the work published?
- 1. Journal of Clinical Urology 2017. Volume 10, Issue 4.
- 2. Proc Physiol Soc 2012. PC309.
- d) Who published the work? (e.g. OUP)
- 1. Physiological Society
- 2. Sage Publications.
- e) When was the work published?
- 1. 2012
- 2. 2017.

| f) | List the manuscript's authors in the order they appear on the publication. |
|-----|--|
| 1. | Nevil Pavithran, Majed Shabbir, Soha El Shiekh, Faiz Mumtaz, JM Cooper, Rajai Al Jehani, Cecil Thompson |
| 2. | Nevil Pavithran, Cecil Thompson. |
| g) | Was the work peer reviewed? |
| Yes | 3. |
| h) | Have you retained the copyright? |
| Yes | S. |
| i) | Was an earlier form of the manuscript uploaded to a preprint server? (e.g. medRxiv). If 'Yes', please give a link or doi) |
| No. | <u>.</u> |
| | No', please seek permission from the relevant publisher and check the box next to the below tement: |
| | |
| | cknowledge permission of the publisher named under 1d to include in this thesis portions of the blication named as included in 1c . |
| Fo | r a research manuscript prepared for publication but that has not yet been |

2. published (if already published, please skip to section 3)

Not applicable.

3. For multi-authored work, please give a statement of contribution covering all authors (if single author, please skip to section 4)

DOXAZOSIN-INDUCED CELL DEATH OF HT1376 BLADDER CANCER CELLS IS MEDIATED BY AUTOPHAGY BOTH IN VITRO AND IN VIVO Authors: Nevil Pavithran (hypothesis, study planning, conducted cell culture experiments and wrote first draft and subsequent updates),

Majed Shabbir (conducted In vivo experiments),

Soha El Shiekh (enabled immunostaining experiments),

Faiz Mumtaz (study planning and review of drafts),

JM Cooper (study planning and review of drafts),

Rajai Al Jehani (enabled next generation transcriptome sequencing),

Cecil Thompson (study planning and review of drafts)

4. In which chapter(s) of your thesis can this material be found?

Chapters 3,5,6,7 and 8.

| 5. | e-Signatures confirming that the information above is accurate (this form should be co-signed by the supervisor/ senior author unless this is not appropriate, e.g. if the paper was a single-author work) |
|----|---|
| | Candidate |
| | Nevil Mallet Pavithran |
| | Date: |
| | 23/03/2023 |
| | Supervisor/ Senior Author (where appropriate) |
| | Prof Faiz Mumtaz and Dr Cecil Thompson |
| | Date |
| | 24/03/2023 |
| | |
| | |

Acknowledgements

I am very grateful and highly indebted to my supervisors Dr Cecil Thompson and Prof Faiz Mumtaz; the research and submission of this thesis would not have been possible without their constant encouragement and help at every stage of the research and write up.

I am very grateful to Prof Marilena Loizidou, Prof Vivek Mudra and Prof Umber Cheema for their encouragement and allowing me to submit the thesis.

I am very thankful to Dr Jehani Al Rajai for her help and guidance with the Next Generation Sequencing – this would not have been possible without her encouragement and generous use of research space and equipment. I am very grateful for Dr Mark Cooper for allowing me to use his lab to conduct research and for his guidance.

I am very grateful to Dr Anita Jagroop for her encouragement and support especially at times when things were not going well in the lab. I am very grateful to Dr Korsa Khan for the help and guidance in use of lab space for conducting fluorescent microscopy experiments. I am very grateful to Dr Soha El-Sheikh for her help and guidance with immunostaining experiments. I am very grateful to Mr Majed Shabir for the experiments involving *In Vivo* studies. I am very grateful to the team at the Electron Microscope lab at Royal Free Hospital for their support and guidance in this work. I am very grateful to Dr Dimitri Mikhailidis for the financial support.

I am very grateful to Dr Simon Bignall, Dr Emer O'Connor, Dr RS Prasad (Ricky) and Mr Sritharan Kadirkamanathan for the advice and moral support they had provided.

I am also grateful to Professor RB Singh who introduced me to academic writing and for supporting me over the last 2 decades. I will also be forever indebted to Mr Mario Caruana, Mr Peter Laws, Mr Ilangovan and Mrs Corona.

I am very grateful to Dr Rajesh MP (Yempee) who supported me morally and financially to come to the UK and to Mr Vikas VK with whom I set up a home lab at age 14 and continue to collaborate on projects, for several decades and even to date.

Lastly but not the least, I am most highly indebted to my parents and my sister who have always been a pillar of support. This would not have been possible without their commitment, moral support the sacrifices they had made.

Table of contents

| <u>Contents</u> | | <u>Page</u> |
|------------------|--|-------------|
| Title page | | 1 |
| Declaration | | 2 |
| Abstract | | 3-4 |
| Impact stat | ement | 5 |
| Research p | paper declaration | 6-8 |
| Acknowledgements | | 9-10 |
| Table of co | ntents | 11-12 |
| Abbreviatio | ns | 13-14 |
| Chapters | | |
| Chapter 1 | Introduction | 15-59 |
| Chapter 2 | Materials and methods | 60-79 |
| Chapter 3 | In Vitro evaluation of receptors that may mediate doxazosin-induced cell death in prostate and | |
| | bladder cancer cells | 80-107 |

| Cnapter 4 | lines | 108-134 |
|------------|---|---------|
| Chapter 5 | Investigating the role of endocytosis and pinocytosis in doxazosin-induced cell death of prostate and bladder cancer cell lines | 135-177 |
| Chapter 6 | Investigating the role of autophagy in doxazosin-induced cell death of prostate and bladder cancer cell lines | 178-207 |
| Chapter 7 | Investigating changes in gene expression in PC-3 cells following exposure to doxazosin | 208-260 |
| Chapter 8 | Investigating the effect of doxazosin on growth of high grade bladder cancer In Vivo | 261-272 |
| Chapter 9 | Discussion | 273-300 |
| Chapter 10 | Suggestions for future work | 301-303 |
| Chapter 11 | Summary | 304-307 |
| References | | 308-334 |

Abbreviations

2DG 2-deoxyglucose 3-MA 3-methyl adenine

5-HT 5-hydroxy tryptamine or serotonin ADI-PEG20 Pegylated arginine deaminase

Akt AK-Strain transforming

AMPK AMP- activated protein kinase

ANOVA Analysis of variance AP-1 Activator protein 1 AR Androgen receptor **ATG** Autophagy-related gene ATP Adenosine triphosphate BC Background control BCa Bladder cancer Bcl-2 B-cell lymphoma 2

BL Blank

BLAST Basic local alignment search tool

BLEND Study Bladder cancer and nutritional determinants study

BPE Benign prostate enlargement
CBCV Assay Cell-Titer Blue® cell viability assay

CoA Coenzyme A
CPZ Chlorpromazine

DAPI 4,6-diamidino-2-phenylindole
DAPS Diastase periodic acid Schiff

DMEM Dulbecco's minimum essential media

DMSO Dimethyl sulfoxide
DNA Deoxyribonucleic acid

EDTA Ethyl diamine tetra acetic acid EGF Epidermal growth factor

EGFR Endothelial growth factor receptor

ER Endoplasmic reticulum

FADD Fas associated protein with death domain

FGF Fibroblast growth factor
GPCR G-protein coupled receptor
GSK Glycogen synthase kinase
GTPase Guanosine-5-triphosphatase

HARE Hyaluronan receptors for endocytosis

HDAC Histone deactylase

HEGR Ligand Human early growth response ligand

HIF Hypoxia inducible factor

HIFU High intensity focused ultrasound
HRPC Hormone refractory prostate cancer

IUPAC International union of pure and applied chemistry

JNK Jun-N-terminal kinase LDH Lactate dehydrogenase

LDL Low-density lipoprotein

LHRH Luteinizing hormone releasing hormone

LPDS Lipoprotein deficient serum

MBCD Methyl beta cyclodextrin

MEM Minimum essential medium

MEME Minimum essential medium Eagle

MG 132 Carbo-benzoxy-L-leucyl-L-leucyl-leucinal

MMP Mitochondrial membrane potential

MOPS 3-N(morpholino) propane sulfonic acid

MT Microtiter

mRNA Messenger ribonucleic acid

mROS Mitochondrial reactive oxygen species mTOR Mammalian target of rapamycin

MTS [3-(4,5-dimethylthiazol-2-yl)-5-(3-carboxythoxyphenyl)- 2-4

-sulfophenyl-2H-tetrazolium

OD Optical density

PBS Phosphate buffer solution

PCa Prostate cancer

PEITC Phenylethyl isothiocyanate
PI3K Phosphatidylinositol 3-kinase
PIN Prostatic intraepithelial neoplasia

PKB Protein kinase B

Prec Prostate epithelial cell line
PSA Prostate specific antigen

RAB Retigeric acid B

REDUCE Trial Reduction by dutasteride of prostate cancer events trial

RNA Ribonucleic acid

ROS Reactive oxygen species

SCID Severe combined immunodeficiency

s.e.m Standard error of the mean
SEM Scanning electron microscopy
SIP Sphingosine-1-phosphate
siRNA Small interfering RNA

TEM Transmission electron microscopy

TGF Tumour growth factor
TNF Tumour necrosis factor

TRAMP Transgenic adenocarcinoma of the mouse prostate

VEGF Vascular endothelial growth factor

VEGFR Vascular endothelial growth factor receptor

Chapter 1

General Introduction

1.1 Prostate Cancer

Prostate cancer (PCa) is the most common to be diagnosed in men living in developed nations; worldwide, it is the second most common (Bray, Ren et al. 2013, Torre, Bray et al. 2015, Shah, loffe et al. 2022, Siegel, Miller et al. 2023). More than one million cases are diagnosed worldwide annually, and accounts for over 300,000 deaths annually (Cooperberg and Chan 2017). Among men currently alive today, it has been estimated that 1 in 7 will develop PCa which will also account for 1 in 38 deaths (Wein, Kavoussi et al. 2016).

1.1.1 Prevalence of PCa:

There is a wide variation in the worldwide prevalence of PCa - two thirds of all PCa occur among 17% of the world's male population within developed countries (Torre, Bray et al. 2015). Compared to Asian nations (where the incidence is low), the incidence of PCa is 25-fold more in North and West Europe, North America, Caribbean nations, and Australia-New Zealand (Torre, Bray et al. 2015). PCa has recently surpassed oesophageal cancer in terms of mortality burden and is currently the fifth leading cause of cancer death worldwide, with highest mortality in Caribbean and Southern and Middle African nations (Torre, Bray et al. 2015, Cooperberg and Chan 2017, Hinata and Fujisawa 2022, Vickers, Elfiky et al. 2022).

A large factor in the variation in the prevalence has been attributed to the availability of serum prostate specific antigen (PSA) screening (Hird, Dvorani et al. 2022). This is a blood test that measures the elevated antigen that rises proportionately as the disease progresses. Nonetheless, the prevalence of PCa is high in Caucasian and African American men. This is confirmed in a recent study that involved the autopsy of 6024 men aged 70 to 79 years, which found a 36% and 51% incidence of PCa in

Caucasian and African American men, respectively (Jahn, Giovannucci et al. 2015, Vickers, Elfiky et al. 2022). The combination of this high prevalence of PCa and the high sensitivity of PSA screening has led to a marked increase in apparent incidence of the disease in countries where there is routine PSA screening (Jahn, Giovannucci et al. 2015, Hird, Dvorani et al. 2022).

PSA screening has a long lead time of approximately 3 to 12 years, and so other factors such as age, life expectancy, Gleason Score and stage of the disease are important consideration in the management (Draisma, Etzioni et al. 2009). A large percentage of these elderly men with PCa will die of other causes unrelated to the PCa (Lee, Mallin et al. 2017). Therefore, the focus has recently been on identifying high-risk PCa that carries a significantly higher mortality (Daniyal, Siddiqui et al. 2014). Recent studies have shown that death from PCa with a primary or secondary Gleason pattern of 5 histology without definitive treatment is high. The cancer specific survival in this group was 86.6% and 57.4% for those receiving and not receiving definitive local treatment, respectively when followed up for 4.3 years (Frandsen, Orton et al. 2017).

1.1.2 Risk factors:

Risk factors for PCa are multifactorial and include both genetic and environmental factors. Family history of PCa in a first –or –second degree relative increases the relative risk of an individual developing PCa (Zeegers, Jellema et al. 2003). Factors that promote inflammation in the prostate have also been implicated in the aetiology of PCa. A history of sexually transmitted infection and prostatitis were found to be associated with a significantly higher incidence of PCa, although the mechanisms

remain unclear and no specific infectious agent has been implicated (Dennis and Dawson 2002).

The role of hormones such as androgens, oestrogens, and insulin-like growth factors, leptin and vitamin-D have been investigated. Androgens play a key role in the carcinogenesis and maintenance of PCa, but the precise molecular mechanisms remain to be fully elucidated. The REDUCE trial [Reduction by Dutasteride of Prostate cancer Events] has shown that the incidence of PCa is reduced by 25% to 30% in patients on 5-alpha reductase inhibitors for benign prostate enlargement (BPE) (Andriole, Bostwick et al. 2010). However, androgen levels did not correlate with the risk of developing the disease. Besides the role of androgens, there is also increasing evidence that oestrogens act as pro-carcinogens in the prostate. Estrogen receptor alpha expression is supressed in the early stages of PCa and subsequently re-emerges in hormone-resistant prostate cancer (HRPC) (Prins and Korach 2008). In the aetiology of PCa, the roles of insulin-like growth factors, leptin and vitamin-D have not revealed a definitive link as causative factors.

1.1.3 Treatment options:

PCa localized to the organ are amenable to surgical treatment or by radiotherapy whilst androgen ablation therapy is the mainstay of treatment strategy once the disease is locally advanced or has metastasized.

In elderly men with short life expectancy, 'watchful waiting' is an option when there is low volume, moderately differentiated cancer, and other significant comorbidities.

Less than 0.5% of elderly men with small PCa would die of the disease, and 99.5% will die from other unrelated causes (Ross, Jennings et al. 2003). Hence, deferred treatment has been reserved for men with a life expectancy of less than 10 years,

and low grade PCa (Gleason score 2 to 6) (Wein, Kavoussi et al. 2016). However, this is not the case for younger men or where life expectancy is over 10 years, or those with more advanced or aggressive disease. All PCa patients are at risk of disease progression and approximately 25% to 50% of patients, depending on their individual risk factors, will demonstrate objective evidence of tumour progression within 5 years of active surveillance (Neulander, Duncan et al. 2000, Warlick, Allaf et al. 2006, Duffield, Lee et al. 2009). In a study of 407 men (median age 65.7 years) with T1c PCa, 59% remained on active surveillance, 25% underwent treatment, 16% withdrew from the study, were lost to follow up, or died of other causes (Carter, Kettermann et al. 2007).

Radical prostatectomy was the first treatment used for PCa and has been performed for nearly 150 years (Wein, Kavoussi et al. 2016). To date, no treatment has supplanted radical prostatectomy and it remains as the gold standard for curative treatment of PCa. The surgical approach to radical prostatectomy can be by perineal or retropubic approach and can be done as robot-assisted or laparoscopically. Besides surgery and radiotherapy, newer modalities of treatment such as cryoablation and (high intensity focussed ultrasound) have been described more recently, but long term data on the success of these procedures are lacking (Wein, Kavoussi et al. 2016). Hormonal therapy and chemotherapy are never curative, and radiotherapy and other physical forms of energy have not been shown to eradicate all cancer cells consistently (Wein, Kavoussi et al. 2016). More recently, Lutetium-177 PSMA (prostate-specific membrane antigen) radioligand therapy has emerged as one of the options for treatment of metastatic PCa (Fanti, Briganti et al. 2022). In tumours that are not localized to the prostate, androgen ablation therapy aimed at decreasing the level of circulating testosterone is the mainstay of treatment. This can

be achieved surgically by bilateral orchiectomy, or pharmacologically by prescribing anti-androgens (cyproterone acetate, flutamide, bicalutamide, nilutamide and enzalutamide), LHRH inhibitors (diethylstilbesterol, leuprolide, goserelin, triptorelin, histrelin, cetrorelix, abarelix and degarelix) or androgen synthesis inhibitors (aminoglutethimide, ketoconazole and abiraterone). However, regardless of the methods employed to reduce circulating androgen, the response to androgen ablation therapy is always short lived; eventually, all patients relapse into HRPC. Furthermore, HRPC also develops resistance to a wide variety of cytotoxic agents.

Approximately 20% to 30% of men with localized tumour present with high-risk characteristics and a large percentage of men (approximately 1 in 5) have advanced or disseminated disease at initial diagnosis (Cooperberg, Cowan et al. 2008). Life expectancy from disseminated HRPC has not significantly improved by current treatment modalities and resistance to chemotherapy is common.

The focus of this research, therefore, was to evaluate the role of adrenergic receptor antagonists in PCa that would be of value in the management of advanced and disseminated HRPC. Additionally, we also investigated the role of adrenergic receptor antagonists in high grade cancer of the bladder.

1.2 Bladder Cancer

Bladder cancer (BCa) is the ninth most common cancer worldwide and accounted for 430,000 cases in 2012 (Malats and Real 2015, Halaseh, Halaseh et al. 2022, Lobo, Afferi et al. 2022). In the same year in Europe, 118,000 new cases of BCa were reported, which accounted for 52,000 deaths (Wong, Fung et al. 2018). Sixty three percent of BCa occurred in developed countries with 55% of these case came from

North America and Europe (Wein, Kavoussi et al. 2016). BCa is 3 to 4 times more prevalent in men than women and are rare before the age of 40 years (Pelucchi, Bosetti et al. 2006, Halaseh, Halaseh et al. 2022). Over 90% of cases are diagnosed in individuals over 55 years (Cheluvappa, Smith et al. 2014) and the incidence peaks in the seventh and eighth decades of life (Malats and Real 2015).

1.2.1 Histological types:

The predominant histological type of BCa is urothelial (transitional cell) carcinoma in Western Europe and United States and accounts for 95% of all cases in white populations and 85% in black American populations (Pelucchi, Bosetti et al. 2006, Malats and Real 2015). In Africa, 60% to 90% are urothelial and 10 to 40% are squamous cell BCa, the latter being more prevalent and secondary to schistosomiasis (*Schistosoma haematobium*) infection (Mostafa, Sheweita et al. 1999, El-Sebaie, Zaghloul et al. 2005, Parkin 2008).

1.2.2 Risk factors:

BCa is caused by a genetic predisposition as well as external risk factors (Brownson, Chang et al. 1987, Vineis, Martone et al. 1995, Chu, Wang et al. 2013). First degree relatives of patients with BCa have a two-fold increased risk of developing urothelial cancers (Wu, Ros et al. 2008). Genetic polymorphisms that increase susceptibility to environmental toxins can also lead to development of BCa. N-acetyl transferase detoxifies nitrosamines, which are known bladder carcinogens; slow acetylation polymorphism of N-acetyl transferase 2 is associated with BCa and an odds ratio of 1.4 when compared to the fast polymorphism genotype (Lower, Nilsson et al. 2007). Likewise, glutathione S-transferase conjugates arylamines and nitrosamines; null

glutathione S-transferase 1 polymorphisms are associated with BCa with a relative risk of 1.5 (Lower, Nilsson et al. 2007).

Among the various environmental carcinogens implicated in BCa, tobacco, especially cigarette smoking, is the leading cause and accounts for 60% and 30% of all urothelial cancers in males and females, respectively (Brownson, Chang et al. 1987, Vineis 1992, Burger, Catto et al. 2013, Scherr 2014). The relationship between diet and BCa is less consistent. Nutrients and their metabolites are excreted in urine which lead to prolonged contact with the bladder urothelium and can modulate the risk of developing the disease. The 'Bladder Cancer and Nutritional Determinants' (BLEND) study was setup in 2016 to collect data from 11,261 BCa and 675,532 non-BCa cases from 18 case control and 6 cohort studies worldwide to investigate the association between individual food items, nutrients and dietary patterns and the risk of developing BCa (Goossens, Isa et al. 2016).

Patients chronically infected with *Schistosoma haematobium* are at risk of squamous cell carcinoma of the bladder. Human papilloma virus infection is associated with a 2.3 fold higher relative risk of developing BCa (Akhtar, Al-Shammari et al. 2018). A recent meta-analysis of 18 case control and 3 cohort studies found that chronic urinary tract infection is associated with a significant and independent higher risk of developing BCa (Akhtar, Al-Shammari et al. 2018). The chemotherapeutic agent cyclophosphamide, besides causing chronic interstitial cystitis, also lead to development of BCa (Murta-Nascimento, Schmitz-Drager et al. 2007).

1.2.3 Treatment options:

The most common presentation of BCa is painless gross haematuria which occurs in 85% of cases whilst microscopic haematuria occurs in almost all cases (Wein,

Kavoussi et al. 2016). Evaluation is based on urine cytology, urinary tract imaging and cystoscopy. Several urinary markers are being evaluated for diagnosis, evaluation of grade of tumours as well as for surveillance (van Rhijn, van der Poel et al. 2005, Zwarthoff 2008, de Bekker-Grob, van der Aa et al. 2009). Pathological staging of urothelial cancer is based on the TNM grading system and the presence or absence of detrusor muscle invasion is an important factor in treatment planning. Radical cystectomy with bilateral pelvic node dissection is the gold standard treatment for patients with muscle invasive disease at diagnosis and within the clinical staging T2-T4a, N0, M0 (Wein, Kavoussi et al. 2016). Neoadjuvant cisplatin-based chemotherapy is advocated as 50% of muscle-invasive BCa treated with cystectomy alone will progress to metastatic disease (Ghoneim and Abol-Enein 2008). In patients with metastatic disease, cisplatin-based combination chemotherapy is the standard of care though prognosis remains poor with median survival of 14 months and overall 5-year survival rates of 5% to 20% (Wein, Kavoussi et al. 2016).

1.3 Adrenergic Receptors

Adrenergic receptors are among the best characterized G-protein coupled receptor (GPCR) superfamily. GPCRs, also known as hepta-helical receptors, 7-transmembrane receptors or serpentine receptors, are a class of receptors that signal through the $G_{q/11}$ signalling pathway (Chen and Minneman 2005). GPCRs are known to have 4 distinct signalling roles: (a) direct ligand-GPCR signalling, (b) signal regulation by receptor trafficking, (3) altering receptor pharmacology and function by associating with GPCR proteins, and (4) acting as a scaffold to physically link with other receptors and in turn modulate the functions via the latter (Hall and Lefkowitz 2002).

1.3.1 Adrenergic receptor subtypes:

There are 9 subtypes of adrenergic receptors: alpha-1A, alpha-1B, alpha-1D, alpha-2A, alpha-2B, alpha-2C, beta-1, beta-2, and beta-3 (Docherty 1998). This classification is based on the use of recent molecular biological techniques and takes into account the receptor structure, pharmacology, and second messengers involved in signalling pathways (Schwinn and Roehrborn 2008). A distinct phenotype of the alpha-1A receptors was described as alpha-1AL due to their low affinity for prazosin; however, these are no longer classed as a distinct subtype and are classified under the alpha-1A subtype (Hennenberg, Stief et al. 2014). Similarly, alpha-1C were initially considered to be a distinct subtype (Tseng-Crank, Kost et al. 1995) but were later found to be identical to the alpha-1A receptor (Perez, Piascik et al. 1994).

1.3.2 Anatomical distribution of adrenergic receptors:

It has been shown that there is wide variability in the differences in expression of the adrenergic receptors between individual species as well the type of tissue. Human liver expresses the highest levels of alpha-1A subtype, whilst the alpha-1B subtype is most expressed in spleen and kidney, and the alpha-1D subtype is most expressed in the cerebral cortex and aorta (Schwinn and Roehrborn 2008).

In the prostate, alpha-1A receptors are the predominant subtype in prostatic stromal tissue (Nishimune, Yoshiki et al. 2012). The ratios between the three subtypes are altered in hyperplastic and non-hyperplastic prostatic tissue. The alpha-1A: alpha-1B: alpha-1D ratio is 63:6:31 in non-hyperplastic prostate tissue and 85:1:14 in hyperplastic prostates. This variation is thought to be due to an upregulation of the alpha-1A subtype (Hennenberg, Stief et al. 2014). Furthermore, the location and the relative ratios of receptor subtypes are also altered in PCa where there is higher

expression of alpha-1A subtypes within the epithelium as well as an increase in the mRNA (messenger RNA) levels of alpha-1B and alpha-1D subtypes (Tseng-Crank, Kost et al. 1995). It is currently unknown if these alterations in expression and localization of alpha-adrenergic receptors contribute to the development or progression of PCa.

In the bladder detrusor, the predominant subtype of adrenergic receptors in the order of abundance are beta > alpha 2 > alpha 1 (Goepel, Wittmann et al. 1997).

1.3.3 Cellular distribution of adrenergic receptors:

At the cellular level, adrenergic receptors have been traditionally classically described as cell membrane receptors. However, all the alpha receptor subtypes have been shown to take up antagonist ligand into intracellular compartments by endocytosis (McGrath 2015). Single cell confocal microscopy studies using BIODIPY-FL prazosin in live, single, human vascular smooth muscle cells have shown that 40% of binding sites for the alpha-1 receptors were located intracellularly (Mackenzie, Daly et al. 2000). Similarly, in prostatic smooth muscle cells 40% of specific binding sites for alpha-1 adrenergic receptors were also located intracellularly and particularly around the nucleus and around the Golgi apparatus (McGrath, Mackenzie et al. 1999, Mackenzie, Daly et al. 2000). Moreover, it has been shown that agonists or antagonists can enter the cells by diffusion or by their lipophilicity and can bind to these intracellular receptors to transduce downstream signalling (Mackenzie, Daly et al. 2000). Additionally, the intracellular alpha-1 adrenergic receptors have been shown to interact with a variety of intracellular proteins and can also act as a scaffold, physically linking the receptor to other effectors and modulate the functions of the latter (Hall and Lefkowitz 2002).

In Vitro and animal studies have shown that chronic alpha-1 adrenergic receptor stimulation secondary to increased catecholamine levels leads to increased prostatic growth (McVary, Razzaq et al. 1994). Chronic activation of alpha-1A receptors modulated calcium influx via diacylglycerol calcium permeable gating channels and promoted proliferation of LNCaP cells (Thebault, Roudbaraki et al. 2003). Daily subcutaneous administration of phenylephrine induced prostatic hyperplasia in adult male C57/BL6 mice (Marinese, Patel et al. 2003) and Wistar mice (Golomb, Kruglikova et al. 1998).

1.3.4 Adrenergic receptor signalling and cancer:

In humans such direct evidence between higher catecholamine levels leading to chronic alpha-1A receptor stimulation and prostatic hyperplasia is lacking.

Nonetheless, epidemiological studies have pointed to a correlation between incidence of BPE and hypertension leading to the increased annual rate of growth of established BPE (Hammarsten and Hogstedt 1999). Furthermore, in patients with spinal cord injuries with severe paralysis, it has been observed that the prostate glands are relatively smaller (Frisbie, Kumar et al. 2006). Also the incidence of PCa is lower in patients with spinal cord injury above the level of T10 vertebrae compared to those with lesions below T10 (Vaidyanathan, Soni et al. 2009).

Beta adrenergic signalling is thought to be protective against human PCa by inhibiting apoptosis in PCa cells (Sastry, Karpova et al. 2007, Sun, Bao et al. 2013), which has been found to play a key role in the aetiology of several cancers (Cole and Sood 2012, Tang, Li et al. 2013, Wang, Li et al. 2015). However, a similar role of alpha-adrenergic receptor signalling in the pathogenesis of cancer in humans is lacking and the available data is limited to a few *In Vivo* studies (Poulet, Berardi et al.

2004, Bruner, Novilla et al. 2009). Alpha adrenergic signalling has been implicated in the development of benign and malignant hibernomas in Sprague-Dawley rats (Bruner, Novilla et al. 2009). Also, long-term oral administration of phentolamine (alpha adrenergic agonist) resulted in development of hibernomas in a dosedependent fashion in approximately 5% of male Sprague-Dawley rats while the incidence was less than 0.5% in females (Poulet, Berardi et al. 2004). The role of alpha adrenergic receptor antagonist in the inhibition of cell growth was reported in 1994 (Patane 2015).

Currently, there is an increasing body of evidence that alpha-1A adrenergic receptor antagonists inhibit the growth of several types of cancer, including PCa and BCa. Conversely, these actions are independent of their ability to bind with the alpha-1A receptors and dependent on the quinazoline-based structure of the antagonists.

1.3.5 Alpha-1A adrenergic receptor antagonists:

Alpha-1 adrenergic receptors antagonists or alpha-1 blockers are compounds that possess a high affinity to bind to the alpha-1 receptors and block the downstream signal pathway. This binding can be selective to alpha-1A, 1B or 1D receptor or non-selective. The earlier developed alpha-1antagonists were non-selective and were derived from a quinazoline-based structure while the more recent selective alpha-1A antagonists are compounds with a sulphonamide-based structure. The quinazoline-based adrenoceptor antagonists, namely doxazosin, prazosin and terazosin exhibit antineoplastic activity; in contrast, none of the sulphonamide-based antagonist drugs exhibit such cytotoxic effects.

The early concepts for the management of BPE were derived from endocrine treatments using drugs such as finasteride that acted on the static component of

BPE through a reduction in volume, whilst the alpha-1 antagonists exerted its effect on the dynamic component of BPE by inducing a relaxation of smooth muscle cells. However, this concept was soon challenged and it was suggested that alpha-1 antagonists additionally affect the natural history of BPE progression through its ability to induce apoptosis of prostatic tissue, (Kyprianou, Litvak et al. 1998, Chon, Borkowski et al. 1999, Michel, Schafers et al. 2000). Kyprianou et al, biopsied the prostates of 22 men with BPE before treatment with doxazosin and after 3 months treatment, and found that the mean apoptotic indices were significantly increased after 3 months of post-treatment with evidence of smooth muscle cell apoptosis, prostatic stromal degeneration, and decreased alpha-smooth muscle actin expression (Kyprianou, Litvak et al. 1998).

Keledjian et al, compared the histology from prostate glands from 34 men treated with terazosin for BPE undergoing surgery for concomitant PCa with that of 25 untreated patients with PCa. The results clearly showed that there was significant induction of apoptosis in cancerous prostatic glands in the terazosin treated group as compared to the untreated group, together with a significant reduction in the microvessel density in the terazosin treated group (Keledjian, Borkowski et al. 2001). In a retrospective epidemiological analysis of medical records of 27,138 males, it was found that the cumulative incidence of developing BCa in those who were prescribed alpha-1 antagonists (doxazosin or terazosin) for either BPE or hypertension was 0.24% as compared to 0.42% in the untreated group (Martin, Harris et al. 2008). This data indicated that there were 1.8 few cases of BCa per 1000 men treated with alpha-1 antagonists. The study concluded that men treated with alpha adrenoceptor antagonists have a 43% lower attributable relative risk of developing than untreated men (p=0.083) (Martin, Harris et al. 2008). In a similar

study by the same research group using the same cohort of patients in relation to the development of PCa, it was found that the cumulative incidence of developing the disease was less in those who were prescribed alpha-1 antagonists (doxazosin or terazosin) for BPE or hypertension. In the treated group this was 1.65% as compared to 2.41% in the untreated group (Harris, Warner et al. 2007). There were 7.6 fewer cases of PCa per 1000 men treated with alpha-1 antagonists and they had a 31.7% lower attributable relative risk of developing the disease than untreated men (Harris, Warner et al. 2007).

More recently, the incidence of PCa in patients treated with the quinazoline-based alpha-1 antagonist, naftopidil was compared to those treated with tamsulosin. It was found that naftopidil preferentially induced apoptosis of PCa cells as compared to non-cancerous cells whilst tamsulosin showed no effect on either cell type (Yamada, Nishimatsu et al. 2013). These retrospective data suggests that quinazoline-based alpha-1 receptor antagonists may play an important role in preventing the development of PCa and BCa; moreover, they may preferentially induce apoptosis of cancerous cells in patients with established PCa.

1.3.5.1 Doxazosin:

Doxazosin is a small water-soluble molecule (Molecular Weight, 451.483 g/M) belonging to the class of organic compounds known as n-aryl piperazines and it contains a piperazine ring where the nitrogen ring atom carries an aryl group. Its designated IUPAC (International Union of Pure and Applied Chemistry) name is [4-(4-amino-6,7-dimethoxyquinazolin-2-yl) piperazin-1-yl] -(2,3-dihydro-1,4-benzodioxin-3-yl) methanone.

Following the oral administration of doxazosin, about 60% is absorbed in the gut and in the circulatory system and is 98% protein bound, with a half-life of 18.6 to 20.5 hours (Kaye, Cussans et al. 1986). It is primarily metabolized in the liver and this is mainly by o-methylation and hydroxylation (Fulton, Wagstaff et al. 1995). About 5% of the drug is excreted unchanged in faeces and 9% of the radioactive dose can be recovered from urine (Kaye, Cussans et al. 1986, Fulton, Wagstaff et al. 1995).

The most common clinical indications for doxazosin were for the treatment of hypertension and BPE; however, it is no longer used as the first line management of either clinical condition in the UK. Other uncommon indications for which doxazosin have been tested in clinical trials include management of: pheochromocytoma (van der Zee and de Boer 2014), stress-induced smoking (Verplaetse, Weinberger et al. 2017), post-traumatic stress disorder (Rodgman, Verrico et al. 2016), cocaine abuse and dependence (Newton, De La Garza et al. 2012), alcoholism (Leggio and Kenna 2013), methamphetamine dependence (Munzar and Goldberg 1999), ureteric stones and symptomatic relief of lower urinary tract symptoms (Belayneh and Korownyk 2016).

More recently, doxazosin has been found to have antineoplastic activity against several types of cancers both *In Vitro* and *In Vivo* (Batty, Pugh et al. 2016). Its antineoplastic actions are dependent on its quinazoline structure but independent of its activity on the alpha receptor and several mechanisms have been proposed to account for this action. Moreover, normal human prostate epithelial cells exhibited very low sensitivity to its antineoplastic actions of doxazosin (Benning and Kyprianou 2002). These factors have made it an attractive candidate for the treatment of PCa and other cancers (Tahmatzopoulos, Rowland et al. 2004).

Despite extensive investigations, the exact molecular and cell signalling mechanisms of doxazosin (and other piperazinyl quinazoline alpha receptors antagonists) remains elusive. This has, in part, been compounded by the findings that in addition to its alpha-1 antagonist activity, doxazosin can act as a human early growth response (HEGR) ligand, (Bilbro, Mart et al. 2013) epidermal growth factor (EGF) receptor inhibitor (Hui, Fernando et al. 2008), vascular endothelial growth factor (VEGF) mediated angiogenic antagonist (Park, Kim et al. 2014), fibroblast growth factor (FGF) receptor-2 antagonist (Ballou, Cross et al. 2000), and tyrosine kinase receptor agonist (Keledjian, Garrison et al. 2005, Petty, Myshkin et al. 2012). Not surprisingly, doxazosin modulates several signalling pathways (Walden, Globina et al. 2004, Garrison and Kyprianou 2006, Park, Kim et al. 2014, Batty, Pugh et al. 2016). Doxazosin acts on the extrinsic apoptotic pathway via the death receptor and induces tumour growth factor receptor (TGF) beta 1 and tumour necrosis factor (TNF) alpha leading to adaptor protein complex formation, caspase-3 and caspase-8 activation, which in turn led to Fas associated protein with death domain (FADD) dependent apoptosis in the PCa cell lines PC-3 and BPH-1(Garrison and Kyprianou 2006). On the other hand, doxazosin has been shown to mediate apoptosis through the intrinsic pathway by release of calcium from endoplasmic reticulum (ER) leading to mitochondrial release of cytochrome-c and caspase-9 activation (Batty, Pugh et al. 2016). Additionally, it can directly exert its action on DNA (deoxyribonucleic acid) either by DNA fragmentation or by inhibiting topoisomerase 1 leading to DNA damage, intercalation of DNA and cell death (Batty, Pugh et al. 2016). In addition to these actions, doxazosin modulates phosphatidyl inositol 3-kinase/AK strain transforming (PI3K/Akt) signalling pathways by inhibiting downstream VEGFR-2 (vascular endothelial growth factor-2), Akt, mTOR (mammalian target of rapamycin)

signalling as well as reducing hypoxia inducible factor 1a (HIF) expression and VEGF expression, and these have been postulated to explain its ability to inhibit angiogenesis (Park, Kim et al. 2014). We were the first to report extensive autophagy in PCa and BCa cell lines as well as in fibroblasts following exposure to doxazosin (Pavithran and Thompson 2012, Pavithran, Shabbir et al. 2017).

1.3.5.2 Prazosin:

Prazosin is a synthetic piperazine derivative with a quinazoline based structure and used in the management of hypertension and BPE. Its IUPAC name is [4-(4-amino-6,7-dimethoxyquinazolin-2-yl) piperazine-1-yl] -(furan-2-yl) methanone. It has a shorter half-life than doxazosin and primarily metabolized in the liver with 6-10% of the oral dose excreted via urine.

Prazosin has been shown to induce cell death of PCa and BCa cells. Prazosin inhibits endothelial growth factor receptor (EGFR) (Han, Bowen et al. 2008), acts as an HEGR ligand (Alberti 2007), (Bilbro, Mart et al. 2013) and induces Cd1k inactivation and G2 check point arrest (Patane 2015). Prazosin has been shown to induce mitochondria mediated apoptosis via a p53 dependent mechanism (Kyprianou and Jacobs 2000) and also have been shown to induce autophagy (Pavithran and Thompson 2012, Forbes, Anoopkumar-Dukie et al. 2016, Pavithran, Shabbir et al. 2017). Nonetheless, the exact mechanisms that mediate prazosin induced cell death of PCa and BCa cells remains unclear.

1.3.5.3 Terazosin:

Terazosin is an alpha adrenoceptor antagonist with a quinazoline-based structure like that of doxazosin and prazosin. Its IUPAC name is [4-(4-amino-6,7-dimethoxyquinazolin-2-yl) piperazin-1-yl] -(oxolan-2-yl) methanone and used as an

antihypertensive and in the management of BPE. It is well absorbed in the gut with 90% bioavailability, metabolized primarily in the liver, and approximately 20% is excreted in faeces and 10% in urine.

Terazosin can act as an HEGR ligand but unlike doxazosin and prazosin it has not been shown to have an inhibitor action on EGFR (Patane 2015). Terazosin induces caspase-3-meidated apoptosis, causes cell cycle arrest in G1 phase in PCa and BCa cells (Keledjian, Borkowski et al. 2001, Papadopoulos, Vlachodimitropoulos et al. 2013). Additionally, terazosin has been shown to downregulate proteasomes leading to accumulation of ubiquitinated proteins in PC-3 cells (Patane 2015). Nonetheless, as with other quinazoline based adrenoceptor antagonists, the underlying mechanism of terazosin induced cell death remains uncertain.

1.3.5.4 Naftopidil:

Naftopidil is an alpha-1 antagonist with a quinazoline based structure (Kanda, Ishii et al. 2008). It has been shown to inhibit PCa growth by inducing G1 phase cell cycle arrest in PC3 and LNCaP cell lines (Kanda, Ishii et al. 2008). More recently, HUHS1015, an analogue of naftopidil has been shown to have antineoplastic action against several human cancer cell lines (Nishizaki, Kanno et al. 2014). The exact mechanisms have not fully been elucidated. Moreover, the cytotoxic actions of naftopidil, terazosin, alfuzosin have been the least studied when compared to other alpha receptor antagonists such as doxazosin and prazosin.

1.3.6 Sulphonamide-based adrenoceptor antagonists:

These include the selective alpha-1A antagonist tamsulosin and silodosin and have a sulphonamide-based structure. Neither tamsulosin nor silodosin have been shown

to induce cell death of PCa or BCa cells suggesting that the quinazoline-based structure (and not the adrenergic activity) plays a key role in this activity.

Besides quinazoline structure based adrenergic receptor antagonists, several other small molecules have been shown to induce apoptosis of PCa cells via a variety of cellular signalling pathways. Below is a list of compounds that have been shown to have an antiproliferative action on PCa and/or BCa cells (Table 1). A brief summary of the mechanism of the action is also included in this table.

Table 1: List of compounds shown to have antiproliferative effect in PCa and BCa along with a brief description of the mechanism of action.

| Drug | Mechanism of action on PCa and/or BCa. | Reference |
|--|--|--|
| Acacetin (flavonoid compound) | G ₁ /G _{2M} cell cycle arrest associated with decrease cyclin B1, significant apoptosis induction, and dose-dependent inhibition of DU145 and LNCaP cells. | (Singh, Agrawal et al. 2005) |
| Adenovirus p21 and p53 (Ad5CMV-vector-p21 – and –p53) | Growth suppression of 148-1PA cells by cyclin dependent kinase inhibition. It also reduced tumour volumes and improved survival in mice. | (Eastham, Hall et al. 1995) |
| Anandamide (endogenous lipid and cannabinoid receptor ligand) | Reduced EGFR levels in LNCaP, DU145 and PC3 cells by acting through cannabinoid CB ₁ receptor subtype thereby reducing EGFR stimulated growth, resulting in apoptosis and cytotoxic effects. | (Mimeault, Pommery et al. 2003) |
| Arsenic trioxide | Growth inhibition and apoptosis of BIU-87 BCa cells and apoptosis by downregulating expression of bcl-2 gene and DNA synthesis. | (Tong, Zeng et al. 2001) |
| Berberine (naturally occurring isoquinoline alkaloid) | G₁ phase arrest and caspase-3-dependent apoptosis of LNCaP, DU145 and PC3 cells. | (Mantena, Sharma et al. 2006) |
| 12-methyltetradecanoic acid (branched chain fatty acid from sea cucumber) | Inhibited cell proliferation and caspase dependent apoptosis by impairing eicosanoid metabolism through selective inhibition of 5-lipoxygenase in PC3 cell line. | (Yang, Collin et al. 2003) |
| Carboxy amido-triazole (transmembrane ca ²⁺ influx inhibitor) | Reduced cell viability and apoptosis by reduced bcl-2 protein expression in transitional cell carcinoma (TCC) BCa cell lines, namely, RT1, RT112, T24 and SUP. | (Perabo, Wirger et al. 2004) |
| Cefazolin (cephalosporin antibiotic) | Dose-dependent cytotoxic action of BCa cells (HTB9, T24 and TccSuP lines <i>In Vitro</i>). | (Kamat and Lamm 2004) |
| Ciprofloxacin (fluoroquinolone antibiotic) | S/G _{2M} cell cycle arrest, downregulation of cyclin B, cyclin E and cdk2 and apoptosis of bladder TCC cell line HTB9. | (Aranha, Wood et al. 2000, Kamat and Lamm 2004) |
| Curcumin (polyphenol compound in turmeric) | Decreased growth of T24 and 5637 BCa cells and promoted apoptosis by suppression of matrix metalloproteinase pathways. | (Shi, Zhang et al. 2017) |
| Celecoxib and piroxicam (Cyclooxygenase: Cox-1 and cox-2 inhibitors) | Induced apoptosis in HT1376 and RT4 cell lines. Also delayed progression of xenografts in athymic mice. | (Pruthi, Derksen et al. 2003, Mohammed, Dhawan et al. 2006) |
| Decursin (coumarin compound in Korean angelica roots) | G ₁ cell cycle arrest, cdk inhibition and apoptosis through caspase- dependent and independent pathways in LNCaP and DU145 cells. | (Yim, Singh et al. 2005) |
| Endothelin receptor antagonist (zibotentan and atrasentan) | Acts through multiple pathways with efficacy demonstrated <i>In Vitro</i> and <i>In Vivo</i> and tested clinically in humans. However, meta-analysis of 8 RCTs (6065 patients) have shown no proven benefit of combining either drug (with docetaxel) in improving survival rates or progression-free survival over that of docetaxel alone. | (Qi, Chen et al. 2015) |
| Equiguard (dietary supplement from 9 Chinese herbs) | Disrupting cell cycle control by downregulating retinoblastoma protein Rb and cytochrome-c release to induce apoptosis in LNCaP cells. | (Lu, Hsieh et al. 2004) |
| Epigallocatechin gallate catechin compound in green tea) | Reduced growth of PC-3 via MEK dependent ERK-1/2 activation in PC3 cells. Alters genes involved in transcription, RNA processing, protein folding, phosphorylation, protein degradation and ion transport in DU145. | (Kobalka, Keck et al. 2015) |

| Drug | Mechanism of action on PCa and/or BCa. | Reference |
|---|--|---|
| Essiac® (extract made from 4 herbs) | Decreased proliferation of LNCaP and CHO cells and immunogenic response to antigenic stimulation in spleen cells isolated from mice. | (Ottenweller, Putt et al. 2004) |
| Flavopiridol (G2/M cell cycle inhibitor) | Growth inhibition and apoptosis byG2/M cell cycle arrest in RT4, UMUC-3 and 5637 bladder cell lines, and HUC-E6, HUC-E7 human urothelial cell lines as well as synergistic effect in doxorubicin resistant cell lines from RT4 and 5637. | (Chien, Astumian et al. 1999) |
| Genistein (isoflavone present in soy products) | G ₁ cell cycle arrest and reduced proliferation in lower doses, and apoptosis in higher doses in LNCaP cells. | (Shen, Klein et al. 2000) |
| Bee honey | Inhibited proliferation by reduction in S-phase of cell cycle and apoptosis of T24, RT4, 253J and MBT-2 BCa cell lines. <i>In Vitro</i> , it inhibited growth of subcutaneously implanted BCa in mice. | (Swellam, Miyanaga et al. 2003) |
| Hypericum perforatum (methanolic plant extract) | Anti-proliferative action by serotonin (5HT) uptake inhibition <i>In Vitro</i> and in mice models. | (Martarelli, Martarelli et al. 2004) |
| HUHS1015 (naftopidil analogue) | Growth inhibition, caspase-dependent apoptosis, and necrosis of PCa cell lines (DU145, LNCaP and PC3) and BCa cell lines (MKN-28 and MKN-45). | (Nishizaki, Kanno et al. 2014, Zhan, Zhang et al. 2022) |
| Imatinib (tyrosine kinase inhibitor) | Antiproliferative to PC-3, DU145 and LNCaP cell lines by inhibiting PDGF-r and interrupting PDGF signalling pathway; additive effects with estramustine phosphate or 4-hydroxyperoxy-cyclophosphamide. However, clinical Phase II trials combining imatinib with docetaxel for head and neck squamous cell cancers closed due to lack of efficacy and potential antagonistic effect. | (Kubler, van Randenborgh et al. 2005, Tsao, Liu et al. 2011) |
| Indole-3-carbinol | G1 phase cell cycle arrest, <i>Bcl</i> -2 downregulation, and apoptosis in PC3 cell lines. | (Chinni, Li et al. 2001) |
| Inositol hexaphosphatase | G1 phase cell cycle arrest, <i>Bcl-2</i> downregulation, inhibition of Akt phosphorylation and apoptosis in LNCaP cells. | (Agarwal, Dhanalakshmi et al. 2004) |
| Levamisole | Biological response modulator. Inhibits growth of MBT-2 cells but was not superior to BCG in efficacy. Prevented recurrence in 4 out of 10 patients with recurrent superficial BCa. | (Morales and Pang 1986, Zlotta and Schulman 2000) |
| Liver x receptor agonist- T0901317 (transcriptional regulator for lipid homeostasis) | Growth inhibition by shortened S-phase of cell cycle associated with an increase in cdk inhibitors. Inhibited growth of LNCaP xenografts in athymic nude mice. | (Fukuchi, Kokontis et al. 2004, Chuu, Hiipakka et al. 2006) |
| Lipoxygenase (Lox) inhibitors – NDGA, AA861, baicalein | Baicalein (12-Lox inhibitor) induced apoptosis of MBT-2 cells in dose dependent manner, and to a lesser extent by AA81 (5-Lox inhibitor). Also, AA861 inhibits growth of 5-Lox expressing bladder cell lines (BOY, T24, HT1376 and ScaBeR). | (Ikemoto, Sugimura et al. 2004, Hayashi, Nishiyama et al. 2006) |
| Nitrofurantoin | Shown to have a dose-dependent cytotoxic action of BCa cells. Contrarily, other reports based on carcinogenesis studies in rats have suggested it as a potential carcinogen in BCa. | (Bulbul, Chin et al. 1985, Hasegawa, Murasaki et al. 1990, Kamat and Lamm 2004) |

| Drug | Mechanism of action on PCa and/or BCa. | Reference |
|---|---|--|
| Nitroxide tempo (nitroxide-based free radical) | Inhibition of cell growth, G2/M cell cycle arrest, decreased S-phase, and caspase mediated apoptosis in LNCaP, PC3 and DU145 cells and reduced growth in LNCaP tumour bearing mice. Additive effects with doxorubicin and mitoxantrone. | (Suy, Mitchell et al. 2005) |
| NSAID (Ibuprofen and R-flurbiprofen) | Inhibited survival of T24 BCa cells by induced expression of p75NTR tumour suppressor protein. | (Khwaja, Allen et al. 2004) |
| OK-432 (streptococcal preparation) Oleic acid | Inhibited growth of T24 and KK-47 cell lines and potent inducer of IL-2 in <i>In Vitro</i> models, therefore, acting as an immune modulating agent. Inhibits DNA synthesis and induced apoptosis in TSU-Pr1 human | (Zlotta and Schulman 2000) (Oh, Lee et al. |
| | BCa cell lines. | 2003) |
| PC-SPES (small molecule) | Inhibited growth of DU145, LNCaP and PC3 cell lines with G2/M cell cycle arrest and reduced S-phase, downregulation of <i>Bcl-2</i> and apoptosis. | (Kubota, Hisatake et al. 2000) |
| Resveratrol (polyphenolic compound in grapes) | Dose dependent inhibition of DU145 cells and caspase-dependent apoptotic cell death associated with Cdk inhibition and upregulation of Bax proteins. | (Kim, Rhee et al. 2003) |
| Retinoic acid receptor antagonist (AGN194310) | Inhibited growth of DU145, LNCaP and PC3 cell lines and was associated with G1 cell cycle arrest, mitochondrial depolarization, caspase dependent apoptosis. | (Keedwell, Zhao et al. 2004) |
| 5HT receptor antagonists | 5HT1A and 5HT1B receptor antagonists induced cell cycle arrest and apoptosis in PC3 and HT1376 cells <i>In Vitro</i> . | (Siddiqui, Shabbir et al. 2005, Siddiqui, Shabbir et al. 2006) |
| Silibinin and Silymarin (polyphenolic flavonoids in milk thistle) | Inhibited growth, induced G1 and G2-M cell cycle arrest and cell death by apoptosis in PC3 cells. | (Deep, Singh et al. 2006) |
| Trimethoprim- sulfamethoxazole (sulphonamide antibiotic) | Dose-dependent cytotoxic action on BCa cells (HTB9, T24 and TccSuP lines <i>In Vitro</i>). | (Kamat and Lamm 2004) |
| Vitamin D (calcitriol) | Antiproliferative action of BCa cell lines 253J and T24 and cell death by apoptosis. In N-methyl nitrosourea induced BCa models of mice, they resulted in fewer tumours of lower grade and invasiveness. | (Konety, Lavelle et al. 2001) |

1.4 Autophagy and Cancer

Dysregulated autophagy is emerging as a hallmark of malignancy (Leone and Amaravadi 2013). Autophagy is an evolutionarily conserved process of degradation of cytoplasm and organelles in the lysosomes for amino acid recycling and energy

(Klionsky, Abeliovich et al. 2008). Autophagy serves as a survival strategy during starvation and plays a pivotal role in energy homeostasis. It is also a critical component of the cellular recycling mechanism and quality control of macromolecules and intracellular organelles, with an important role in maintaining cellular fitness both in healthy and stressful conditions. Interestingly, it has both pro- and anti-tumorigenic roles and can crosstalk with apoptosis, and has a role in senescence; however, autophagy can lead to cell death if the process is uncontrolled. Autophagy thus plays a dual role in both cell survival and cell death (Klionsky, Abeliovich et al. 2008, Klionsky, Abdalla et al. 2012, Zhang 2015).

One of the strategies that cancer cells utilize to 'survive chemotherapy' is to upregulate autophagy as a cytoprotective response. Recent clinical trials in PCa are exploring, by inhibiting autophagy, the strategy of preventing a 'survival response' in cancer cells following chemotherapy (Farrow, Yang et al. 2014) and is currently under investigation by several groups (Ashrafizadeh, Paskeh et al. 2022). Furthermore, there are several compounds with the potential to modulate autophagy in PCa (Loizzo, Pandolfo et al. 2022). Over 60 compounds that have been associated with PCa cell death and autophagy are listed below (Table 2).

Table 2: List of compounds that can modulate autophagy in PCa, the mechanism of action and their effect on survival.

| Drug/ experimental condition | Reference | Actions | Effect on survival | Mechanism | Cell Line |
|--|--|-----------------------------------|-------------------------------|--|---------------------------|
| Neuregulin | (Tal-Or, Di-Segni et al. 2003, Schmukler, Shai et al. 2012) | Induce incomplete autophagy | Cell death | ErbB-2/ErbB-3, JNK (Jun-N- terminal kinase) and Beclin 1 activation Independent of mTOR | LNCaP |
| MG132 | (Yang, Monroe et al. 2006) | Autophagy, Apoptosis | Cell death | Proteasome Inhibitor | PC-3 |
| PDT | (Xue, Chiu et al. 2007) | Autophagy | Cell death | Possible (reactive oxygen species) ROS generation | DU145 |
| CRAds | (Ito, Aoki et al. 2006) | Autophagy | Cell death | Unknown | PC-3 |
| Sulforaphane | (Herman- Antosiewicz, Johnson et al. 2006, Xiao, Powolny et al. 2009) | Autophagy | Cell death | ROS generation | PC-3, LNCaP |
| Everolimus + radiation | (Tai, Sun et al. 2012) | Autophagy | Cell death | Increased radiosensitivity | PC-3, DU145 |
| Everolimus + propachlor (synergy) | (Tai, Sun et al. 2012) | Autophagy and apoptosis | Cell death | Increased beclin-1, LC-3, autophagy-related gene (ATG) ATG5 and ATG12 expression | |
| A23187, Tunicamycin, thapsigargin and brefeldin-A | (Ding, Ni et al. 2007) | Autophagy | Cell death | Endoplasmic reticulum (ER) stress | DU145 |
| Lysophosphatidic acid | (Chang, Liao et al. 2007) | Inhibits Autophagy | Survival in serum deprivation | Inhibit formation of autophagosomes | PC-3 |
| 4 IBP | (Megalizzi, Mathieu et al. 2007) | Autophagy and apoptosis | Cell death | Sigma 1 receptor antagonist | PC-3 |
| Prenylflavonoids | (Delmulle, Vanden Berghe et al. 2008) | Autophagy | Cell death | Not specified | PC-3, DU145 |
| Soraphen A | (Beckers, Organe et al. 2007) | Autophagy | Cell death | Blocks fatty acid synthesis | PC-3M |
| Androgen deprivation | (Li, Jiang et al. 2008) | Autophagy | Survival | Several pathways (see below under section 1.4.2) | LNCaP |
| PDT + photosensitiser Pc4 | (Xue, Chiu et al. 2008) | Autophagy | Cell death | ER stress, non-specified | DU145 |
| Cysmethynil | (Wang, Tan et al. 2008) | Autophagy | Cell death | Decreased mTOR signalling | PC-3 |
| CCL2 | (Roca, Varsos et al. 2008) | Inhibits autophagy | Survival | PI3K/Akt/Survivin pathway involved | PC-3, DU145, C4- 2B |
| 2-deoxy-D- glucose | (DiPaola, Dvorzhinski et al. 2008) | Autophagy | Cell death | cdk4, cdk6 involved | PC-3, LNCaP |

| Drug/ experimental condition | Reference | Actions | Effect on survival | Mechanism | Cell Line |
|---|--|-------------------------|--------------------|---|--|
| 2-deoxyglucose | (Stein, Lin et al. 2010) | Autophagy | Cell Death | Increased p62 (autophagic resistance marker). | Phase III trials |
| H40 | (Long, Zhao et al. 2009) | Autophagy | Cell death | Histone deacetylase inhibition. | PC-3M |
| Arginine deiminase (ADI- PEG20) | (Kim, Yang et al. 2009) | Autophagy | Survival | Arginine deprivation. | CWR22Rv1 PC-3, LNCaP |
| Trptorelix-1 | (Kim, Bold et al. 2009) | Autophagy | Growth inhibition | GnRH-II antagonist; mitochondrial dysfunction and ROS release. | PC-3 |
| Phenethyl isothiocyanate | (Bommareddy, Hahm et al. 2009) | Autophagy, Apoptosis | Cell death | ATG5 dependent process; inhibition of oxidative phosphorylation and adenosine triphosphate (ATP) depletion leading to ROS production; over expression of E cadherin in TRAMP mouse model. | PC-3, LNCaP |
| Dimethyl oxalyl glycine | (Farrall and Whitelaw 2009) | Autophagy | Survival | Hypoxia mimetic; SIM2 mediated repression of BNIP3 gene expression by crosstalk with HIF1-alpha. | PC-3AR+ cells |
| 2,2'-dipyridyl (DP) | (Farrall and Whitelaw 2009) | Autophagy | Survival | Same as for dimethyl oxalyl glycine. | PC-3 AR+ |
| Sphingosine 1- phosphate (SIP) | (Chang, Ho et al. 2009) | Autophagy | Cell death | Inhibition of mTOR; SIP (5) activation. | PC-3 |
| Radiation followed by oncolytic adenovirus | (Rajecki, af Hallstrom et al. 2009) | Autophagy | Cell death | Mre11 inhibition. | |
| Liquorice & licochalone-A | (Yo, Shieh et al. 2009) | Autophagy | Cell death | Suppression of <i>Bcl-2</i> expression, inhibition of mTOR. | LNCaP |
| MYC expression | (Balakumaran, Porrello et al. 2009, Balakumaran, Herbert et al. 2010) | Inhibit Autophagy | Survival | Inhibit mTOR through over expression of 4EBP1 gene. | PrEC |
| Penta galloyl glucose | (Hu, Chai et al. 2009) | Autophagy | Cell death | Inhibition of downstream targets of mTOR (S6K and 4EBP1); increased Akt phosphorylation. | PC-3, TRAMP-C2 |
| PPAR gamma knock out | (Jiang, Fernandez et al. 2010, Jiang, Jerome et al. 2010) | Autophagy | Cell Death | Dysregulation of cell cycle, and metabolic signalling networks linked to peroxisomal and lysosomal maturation, lipid oxidation and degradation. | Prostatic epithelium of PPAR gamma knock out mice |

| Drug/ experimental condition | Reference | Actions | Effect on survival | Mechanism | Cell Line |
|--|---|-------------------------------|---|---|--------------------------|
| Proteasome inhibitors | (Zhu, Dunner et al. 2010) | Autophagy | Cell death | Upregulation of ATG5 and ATG7 genes; activates autophagy through a phospho-eIF2alphadependent mechanism to eliminate protein aggregates and alleviate proteotoxic stress. | PCa |
| Atorvastatin | (Parikh, Childress et al. 2010) | Autophagy in PC-3 cells | Cell death in PC3 | Inhibition of geranylgeranyl biosynthesis; mediated by Erk and JNK pathways. | PC-3, RWPE1, LNCaP |
| Atorvastatin + radiation synergy | (He, Mangala et al. 2012) | Autophagy | Cell death | Mediated through <i>ATG7</i> and/or <i>ATG12</i> . | PC-3 |
| Glycogen synthase kinase-3 beta (GSK-3- beta) inhibition | (Yang, Takahashi et al. 2010) | Autophagy/ necrosis | Cell death | GSK-3-beta inhibition; increased Bif-dependent autophagy. | PCa |
| ABC294640 | (Beljanski, Knaak et al. 2010) | Autophagy | Cell death | Sphingosine kinase 2 inhibitor. | PC-3 |
| Red-Br-nos | (Bhutia, Dash et al. 2010, Karna, Zughaier et al. 2010) | Autophagy | Cell death | ROS release. | PC-3 |
| MDA-7/IL-24 | (Bhutia, Das et al. 2011) | Autophagy/ Apoptosis | Survival | Interaction with Beclin-1, ATG 5, and hVps34. | |
| Sorafenib | (Ullen, Farnebo et al. 2010) | Autophagy/ Apoptosis | Not specified | Not specified. | PC-3, DU145, 22Rv1 |
| Fisetin | (Suh, Afaq et al. 2010) | Autophagy | Cell death | Supress mTOR signalling. | PC-3 |
| Metformin + 2deoxyglucose | (Ben Sahra, Laurent et al. 2010, Ben Sahra, Tanti et al. 2010) | Inhibits autophagy | Augments cell death by apoptosis | Switch from autophagy to p53 and AMPK dependent apoptosis. | |
| (-)-Gossypol | (Lian, Karnak et al. 2010, Lian, Wu et al. 2011) | Apoptosis/ Autophagy | Cell death | BH3 mimetic; inhibits <i>Bcl-2</i> ; modulates <i>ATG5</i> ; interrupts the interaction between beclin 1 and Bcl-2/Bcl-xL at ER. | PCa xenografts |
| (-)- Gossypol + Sorafenib (synergy) | (Lian, Ni et al. 2012) | Apoptosis/ Autophagy | Cell death | Mcl-1 inhibition and Bak activation. | DU-145; PC-3 |
| Apogossypolone | (Zhang, Huang et al. 2010) | Autophagy | Cell death | Not specified. | PC-3, LNCaP |
| BI-9C1 (sabutoclax) | (Dash, Azab et al. 2011) | Autophagy | Cell death | Targets Mcl-1; mda-7/IL-24- mediated toxicity. | PCa xenografts |
| Src family of tyrosine kinase inhibitors, e.g.: saracatinib | (Wu, Chang et al. 2010, Kung 2011) | Autophagy | Protects from apoptosis when given alone. Increased cell death in combination with autophagy inhibitors | Inhibit PI3K1/Akt/mTOR signalling pathway. | PC-3 |

| Drug/ experimental condition | Reference | Actions | Effect on survival | Mechanism | Cell Line |
|--|--|--|---|--|---------------------------------------|
| Irinotecan +/- cisplatin | (Tung, Wang et al. 2011) | Apoptosis/ Autophagy | Not specified | Topoisomerase 1 inhibitor in small cell carcinoma of prostate xenograft in NOD-SCID mice. | xenograft |
| Sirt1 gene homozygous deletion | (Powell, Casimiro et al. 2011) | Decreased Autophagy | Survival and development of prostatic intraepithelial neoplasia | Sirt1 repress androgen- responsive gene expression and induce autophagy. | Sirt1 (-/-) mice |
| Oridonin | (Ye, Li et al. 2012) | Autophagy | Cell death | Not specified. | PC-3 cells |
| YM155 | (Wang, Chen et al. 2011) | Autophagy & Apoptosis | Not known | Survivin suppressant. | PC3 |
| Redox-active polymer capsules for small interfering RNA (siRNA) delivery | (Becker, Orlotti et al. 2011) | Autophagy | Not known | Not known. | PC-3 |
| Curcumin | (Teiten, Gaascht et al. 2011) | Autophagy an AD PCa but not in Al cells | Decreased proliferation | Activation of the Wnt/beta- catenin pathway. | PCa |
| Zoledronic Acid | (Lin, Lin et al. 2011) | Autophagy | Cell death | Not known. | PC-3, DU145, LNCaP, CRW22Rv1 |
| Di geranyl bisphosphonate | (Wasko, Dudakovic et al. 2011) | Autophagy | | Depletion of geranylgeranyl diphosphate. | PC-3 |
| Androgen receptor (AR) | (Bennett, Fleming et al. 2010, Bennett, Stockley et al. 2013) | Inhibit serum deprivation autophagy | Survival | Promote ER stability by upregulation of GrP78/BiP. | LNCaP |
| Gamma- tocotrienol | (Jiang, Rao et al. 2012) | Apoptosis, necrosis & Autophagy | Cell death | Accumulation of sphingolipids. | Xenografts in mice |
| Pancratistatin | (Griffin, McNulty et al. 2011) | Apoptosis & Autophagy | Cell death by apoptosis | Accumulation of ROS species. | DU145, LNCaP, Xenografts |
| Compound 22 | (Lee, Hsu et al. 2011) | Autophagy and apoptosis | Cell death | Integrin-linked kinase inhibitor; dephosphorylation of Akt; suppressed expression of YB-1 and its targets HER2 and EGFR. | PC-3; PC-3 xenografts |
| Celastrol | (Wang, Feng et al. 2012) | Paraptosis; Autophagy; Apoptosis | Cell death | Influence on proteasome, mitogen activated protein kinase and p38; ER stress, and Hsp90. | PC-3 |

| Drug/experiment al condition. | Reference | Effect | Effect on survival | Mechanism | Cell Line |
|-------------------------------|--|-------------------------------|-------------------------|---|---------------------------|
| Ursolic acid | (Shin, Kim et al. 2012) | Autophagy | Cell death | Not specified. | PCa |
| Geraniol | (Kim, Park et al. 2012) | Apoptosis and autophagy | Cell death | Inhibited Akt, activated AMP- activated protein kinase (AMPK); mTOR inhibition. | PC-3 |
| Ascorbate | (Chen, Yu et al. 2012) | Autophagy | Cell death | H2O2 production; ATP depletion. | PCa |
| Arsenic trioxide + radiation | (Chiu, Chen et al. 2012) | Autophagy/ Apoptosis | Cell death | ROS production; inhibition of Akt/mTOR pathways. | PC-3, LNCaP |
| Chloroquine | (Farrow, Yang et al. 2014, Xu, Yang et al. 2022) | Autophagy | Not Specified | Increased autophagic flux. | PC-3 |
| E1201 | (Ibanez, Agliano et al. 2012) | Autophagy | Cell death | inhibits the PI3K/Akt/mTOR pathway. | PC-3 |
| TDFP3 | (Ren, Ma et al. 2012) | Autophagy and apoptosis | Not known | Not known. | LNCaP |
| PI3K inhibitor + PDT | (Fateye, Li et al. 2012) | Autophagy | Cell death | ROS generation. | PCa |
| Nelfinavir | (Guan, Fousek et al. 2012) | Autophagy Apoptosis | Survival from apoptosis | SREBP-1 translocation to nucleus, ATF6-EGFP fusion. | PC-3 |
| Recombinant human arginase | (Hsueh, Knebel et al. 2012) | Autophagy | Cell death | Decreased phosphorylation of 4E-BPI; arginosuccinate synthase deficiency. | LNCaP; DU-145; PC-3 |

1.4.1 Autophagic flux:

Autophagy is a dynamic process whereby double membraned vesicles (autophagosome) sequester cargo (cytoplasm and organelles) for delivery to the vacuole/lysosome for degradation and recycling (Klionsky, Abdalla et al. 2012, Parzych and Klionsky 2014). The sequestration process begins within double membrane structures called phagophores (in macro autophagy) - henceforth referred to as autophagy (Klionsky, Abdalla et al. 2012, Parzych and Klionsky 2014). The entire process of autophagy commencing from the delivery of cargo to lysosomes (by fusion of latter with autophagosomes) and its subsequent breakdown leading to the release

of macromolecules back into cytosol is referred to as autophagic flux (Klionsky, Abdalla et al. 2012).

At least 30 autophagy related genes have been identified in yeast; in mammalian cells, the complete molecular mechanisms for autophagy induction remains to be fully understood (Chen, Liu et al. 2014).

1.4.2. Autophagy and cancer:

There is a clear link between autophagy and cancer (Mathew, Karantza-Wadsworth et al. 2007, Li, Han et al. 2011, Das, Shravage et al. 2012, Wu, Coffelt et al. 2012); however, the intricate mechanism of how autophagy prevents or causes cancer remains unclear (Reyjal, Cormier et al. 2014). Several alterations in autophagy process have been observed in PCa, which is similar in many other cancers, however, their implications to the disease development and progression remains to be fully addressed (Wu, Coffelt et al. 2012). It has been suggested that the autophagic response may be a survival strategy in conditions of androgen deprivation in PCa (Bennett, Fleming et al. 2010, Bennett, Stockley et al. 2013, Boutin, Tajeddine et al. 2013). It is conceivable that, autophagy may be impaired in PCa due to either activation of the PI3K/Akt/mTOR pathway or by allelic loss of *Beclin 1*, an essential autophagy gene (DiPaola-11). In prostate, breast, ovarian and lung cancers, loss of *Beclin 1* or inhibition of *Beclin 1* by the BCL-2 family of protein has been shown to cause a defective autophagy process, increased DNA damage, metabolic stress and genomic instability (Powell, Casimiro et al. 2011).

1.4.3 Androgens and autophagy:

The relationship between androgens and autophagy has been demonstrated at various stages in the progression of PCa, from prostatic intraepithelial neoplasia (PIN) to established cancer (Kim, Song et al. 2011, Powell, Casimiro et al. 2011). Genetic

studies have revealed an association between the development of PIN and autophagy. Homozygous deletion of *Sirt1* (*Sirt1*-/-) in mice results in PIN and reduced autophagy (Powell, Casimiro et al. 2011). *Sirt1*, belongs to the family of NAD+-dependent histone deacetylase (HDAC) and is the ortholog of *Sirt2* gene, an important regulator cell growth and aging. *Sirt1* inhibits androgen receptor (AR) signalling and apoptosis, while promoting autophagy in mice prostate. The AR co-localizes with *Sirt1* in the nuclear compartment, where *Sirt1* inhibits AR activity by binding to, and deacetylating the AR (Powell, Casimiro et al. 2011).

AR expression and activity are crucial determinants of PCa onset and progression (Powell, Casimiro et al. 2011). In early androgen-sensitive PCa, AR-mediated prosurvival signalling plays a key role in prostate carcinogenesis enabling the cell to survive in tumour microenvironments that are nutrient-poor, hypoxic, or acidified. AR signalling prevents an autophagic response in such environments where cellular stress and androgen deprivation leads to activation of autophagy. Following castration, the epithelial cells of rat prostate gland exhibit increased autophagosomes (Nikoletopoulou, Markaki et al. 2013, Feng, He et al. 2014, Parzych and Klionsky 2014). A combination of androgen deprivation and hypoxia resulted in autophagy via AMP-activated protein kinase (AMPK) activation whereas neither condition alone was sufficient to activate AMPK. Such activation of AMPK in conditions of combined hypoxia and androgen deprivation was mediated by Beclin-1 (Powell, Casimiro et al. 2011).

LNCaP cells subjected to AR activation by mibolerone temporarily abrogated the autophagic response to serum starvation. This attenuation of autophagic response to starvation was not mediated by mTOR, and therefore the abrogation of autophagy by AR signalling is not initiated by nutrient sensing. On the other hand, inhibition of pro-

survival AR signalling (by androgen deprivation) leads to activation of autophagy as a survival response. Androgen removal resulted in inhibition of mTOR, leading to autophagy and growth arrest of LNCaP cells (Li, Jiang et al. 2008). Conversely, androgen administration to LNCaP cells stimulated mTOR activity, and augmented the expression of genes that were related to the transport of glucose and amino acids (Li, Jiang et al. 2008). Suppression of autophagy by pharmacological inhibitors and Beclin-1 siRNA in LNCaP cells resulted in an increased apoptosis of LNCaP cells to both androgen deprivation and serum deprivation suggesting that autophagy served as protective or survival mechanism in response to androgen deprivation.

In summary, the molecular pathways that mediate the relationship between androgen and autophagy remain interdependent on several signalling networks and the precise mechanisms are largely unknown. Current evidence suggests that androgens mediate autophagy by pathways dependent on mTOR, and its downstream effector p70S6K as well as through alternate pathways (independent of mTOR) such as ER signalling (Li, Jiang et al. 2008, Powell, Casimiro et al. 2011). An example of the latter is the AR activation by mibolerone that was independent of mTOR and instead modulated by ER stress response pathways. Nonetheless, early androgen-dependent PCa exploits the autophagic pathways to antagonize apoptosis during androgen ablation therapy, at least temporarily. Such survival involves a myriad of networks of signalling events, some of which may be influential in contributing to the development of HRPC itself.

1.4.4 PI3K/Akt/mTOR survival pathway:

Growth factor mediated activation of the PI3K-Akt-mTORC1 pathway suppresses autophagy in healthy cells in nutrient replete conditions (Klionsky, Abdalla et al. 2012, Feng, He et al. 2014, Parzych and Klionsky 2014). The PI3K-protein kinase B

(PKB)/Akt pathway plays a pivotal role in promoting normal cell growth and proliferation. Constitutive activation of PI3K-PKB/Akt is implicated in several cancers including prostate. Akt plays an important role in the progression of early PCa to HRPC. Inhibition of Akt impairs the AR mediated pro-survival signalling, and the progression to HRPC required an intact upstream PI3K signalling pathway. Phosphatase and tensin homolog heterozygous mice (+/-) develop PIN with nearly 100% frequency, (Cao, Subhawong et al. 2006) and its inactivation has also been found in a significant proportion of PCa (Klionsky, Abdalla et al. 2012). Conversely, inactivation of this pathway downstream using mTORC1 using Rad001, a potent and specific inhibitor of mTORC1, had been unsuccessful in a clinical setting against HRPC due to activation of compensatory signalling pathways that countered mTORC1 inhibition (Cao, Subhawong et al. 2006, Tai, Sun et al. 2012). Agents known to have synergistic action with everolimus (Rad001) have therefore been investigated (Tai, Sun et al. 2012). The mTOR inhibitor everolimus sensitized PC-3 cells to radiation, and there was further sensitization using Z-VAD and Bax/BakSiRNA, which blocked caspase-dependent apoptosis. The herbicide, propachlor (Lee, Hsu et al. 2011) was also found to be synergistic with everolimus in PC-3 and C4-2 cells by inducing autophagy and apoptosis - ATG5, ATG12 and Beclin 1 were induced by this combination (Tai, Sun et al. 2012).

1.4.5 Phenethyl isothiocyanate (PEITC):

PEITC is a naturally occurring isothiocyanate with known anticancer properties, while having no cytotoxic action on the normal human prostate epithelial cell lines (PrEC). In contrast, it induced predominantly autophagic cell death in PC-3 and LNCaP cells by suppressing of Akt/ mTOR, which and this was regulated by ATG 5 protein (Xiao, Powolny et al. 2010). Knockout of *ATG5* abrogated the cytotoxic actions of PEITC, but

the molecular mechanism connecting *ATG5* and PEITC remains unclear (Bommareddy, Hahm et al. 2009). In a separate study, PEITC was found to induce autophagy and apoptosis in LNCaP and PC-3 cells (but not in PrEC) by ROS production, suppression of complex III (mitochondrial site of ROS production), inhibition of oxidative phosphorylation, and ATP depletion. Whilst apoptosis was found to be mediated by Bax activation leading to cytochrome-*c* release and caspase activation, the mechanisms by which ROS regulated autophagy was independent of catalase degradation remains unclear, at least in part (Xiao, Powolny et al. 2009).

1.4.6 ROS:

A number of structurally diverse substances like sulforaphane, (Herman-Antosiewicz, Johnson et al. 2006) Red-Br-nos, (Karna, Zughaier et al. 2010, Pannu, Rida et al. 2012) trptorelix-1, (Kim, Yang et al. 2009) pancratistatin, (Griffin, McNulty et al. 2011) and arsenic trioxide (Chiu, Chen et al. 2012) have been shown to modulate autophagy in PCa via ROS production. The primary sources for mitochondrial ROS (mROS) production are the mitochondrial respiratory chain complexes I and III. The released mROS induce cellular stress and modulate cell signalling (Chen and Karantza-Wadsworth 2009, Karna, Zughaier et al. 2010, Chhipa, Wu et al. 2011, Chae, Caino et al. 2012, Farrow, Yang et al. 2014). Briefly, ROS production leads to a decrease in mitochondrial membrane potential (MMP) and the release of cytochrome-c release into the cytosol, which in turn activates caspase mediated apoptosis (Karna, Zughaier et al. 2010). On the other hand, autophagosomes may sequester the mitochondria that has been damaged by ROS and inhibit apoptosis by preventing the release of cytochrome-c into the cytosol. Alternatively, cleavage of beclin-1 by activated caspase can also promote autophagy. The molecular pathways that determine the pathway to undergo apoptosis or autophagy, in response to ROS mediated signalling remains

needs further clarity (Karna, Zughaier et al. 2010). Nevertheless, ROS is capable of modulating autophagic and apoptotic pathways and can thus determine the fate of the cell in response to chemotherapeutic agents (Janssen, Horn et al. 2009).

Retigeric acid B (RAB) is a naturally pentacyclic triterpenic acid isolated from the fungus *Lobaria retigera* (*Liu*, *Ji et al. 2013*). In PC-3 and LNCaP cells, RAB induced ROS production, was mitochondriotoxic as demonstrated by mitochondrial membrane depolarization and the stimulation of mitophagy. RAB also inhibited the PI3K/Akt/mTOR pathway, which can also predispose to autophagy. However, inhibition of autophagy by pre-treatment with 3-methyl adenine (3-MA) or chloroquine potentiated RAB-induced cell death via apoptosis (Wang, Feng et al. 2012, Liu, Ji et al. 2013).

Pancratistatin, a plant alkaloid can lead to an increased mROS production with resultant loss of MMP selectively in PCa cell lines (DU-145 and LNCaP) but not in normal human fibroblast cells. In LNCaP cells, the mode of cell death was primarily apoptotic. In DU-145 cells both autophagic and apoptotic responses were observed suggesting that ROS mediated autophagy by pancratistatin in DU-145 cells were modulated through p-53 dependent pathways (Griffin, McNulty et al. 2011).

Red-Br-nos can also cause an increase in ROS generation, and mitochondrial membrane disruption, inducing autophagy and caspase-dependent apoptosis in PC-3 cells (Karna, Zughaier et al. 2010). Autophagy is an early and cytoprotective event following ROS-mediated mitochondrial damage, and cells eventually undergo apoptosis (Karna, Zughaier et al. 2010).

Trptorelix-1, a GHRH-II antagonist, increases mROS, decreased MMP and induced autophagy *In Vivo* and *In Vitro*. These effects of trptorelix-1 were partially prevented

by the antioxidant N-acetyl cysteine. Thus, trptorelix-1 directly induces mitochondrial dysfunction and increased ROS production, leading to autophagy of PCa cells (Kim, Yang et al. 2009).

Sulforaphane belongs to the isothiocyanate class of dietary chemopreventive agents that are present in several edible cruciferous vegetables, which have been shown to have a protective role in several cancers including PCa (Herman-Antosiewicz, Johnson et al. 2006). Sulforaphane induce apoptosis in PC-3 cells by initiating mitochondrial-mediated and non-mitochondrial mediated generation of ROS leading to disruption of MMP and cytochrome-*c* release from mitochondria into the cytosol. Sulforaphane also induces autophagy which serves as a survival response to inhibit apoptosis induced cell death in PC-3 and LNCaP cells, by preventing sulforaphane-induced cytosolic release of cytochrome-*c* due to sequestration of mitochondria in autophagosomes (Herman-Antosiewicz, Johnson et al. 2006, Xiao, Powolny et al. 2009, Wiczk, Hofman et al. 2012, Vyas, Hahm et al. 2013).

1.4.7 Modulation of ER stability:

Accumulation of unfolded or misfolded proteins leads to ER stress, which in turn induces autophagy to sequestrate and clear the misfolded proteins. ER stress signalling results in the unfolded protein response, whose key regulator is glucose-regulated protein 78/BiP (Grp78/BiP). This results in a global halt in translation and reduction in the ER protein overload. AR activation of LNCaP cells by mibolerone in serum starved conditions upregulated Grp78/BiP, independently of mTOR, to temporarily abolish the autophagic response to serum starvation. Interestingly, compounds that cause the accumulation of misfolded or unfolded proteins within ER (tunicamycin - inhibits glycosylation; brefeldin A - inhibits transportation to Golgi

complex; A23187 and thapsigargin disturbs the calcium homeostasis) improved survival of androgen-independent DU-145 cells but not in non-transformed cell lines (Ding, Ni et al. 2007). The molecular mechanisms that regulate autophagy in relation to the level of ER stress remains to be fully understood. Transcription upregulation of *ATG* such as *ATG12* and *ATG8* have been associated with ER stress (Ding, Ni et al. 2007, Janssen, Horn et al. 2009). Such upregulation of autophagy may be to mitigate the ER stress to clear the ubiquitinated and unfolded proteins. In support of this, deletion of *ATG5* or *ATG7* in mice, has led to accumulation of polyubiquitinated proteins (Ding, Ni et al. 2007, Janssen, Horn et al. 2009).

1.4.8 Modulation of nutrient metabolism:

Autophagy is a survival response that allows the cells to degrade cytoplasmic contents, which are recycled and used to generate energy during starvation. The cancer cell metabolism differs from that of a normal cell, and this difference has been exploited to selectively target cancer cells (Altman and Rathmell 2012). Several metabolic manipulations have been used to induce or inhibit autophagy in PCa (Ben Sahra, Laurent et al. 2010). These include: (a) inhibition of glycolysis (b) arginine deprivation (c) inhibition of geranylgeranyl synthesis (d) inhibition of fatty acid synthesis (Ben Sahra, Laurent et al. 2010, Altman and Rathmell 2012, Beauchamp and Platanias 2013, Boya, Reggiori et al. 2013).

(a) Inhibition of glycolysis:

2-deoxyglucose (2DG) (Beljanski, Knaak et al. 2010), a prototypic glycolysis inhibitor, caused dose-dependent death of the cells by modulation of check point proteins cdk4 and cdk6. This autophagic response was also mediated by Beclin 1 (Ben Sahra, Laurent et al. 2010, Ben Sahra, Tanti et al. 2010). Quantification of Beclin 1 in PCa

served as a predictive marker for the autophagic response to therapeutic starvation with 2DG (DiPaola, Dvorzhinski et al. 2008). On the other hand, increased p62 levels served as a marker for resistance to autophagy (Stein, Lin et al. 2010). Combining metformin with 2DG was more cytotoxic than either drug alone, and metformin inhibited 2DG-induced autophagy, decreased *beclin 1* expression, and triggered a switch from autophagy-mediated survival to apoptotic cell death. Thus, 2DG is capable of inducing cell death directly by initiating uncontrolled autophagy, and also by inhibiting survival-mediated autophagy when combined with other potent apoptosis-inducing agents to enhance the cytotoxic potential of the latter (DiPaola, Dvorzhinski et al. 2008).

(b) Arginine deprivation:

Pegylated arginine deaminase (ADI-PEG20) induces depletion of arginine and its efficacy can be correlated to resultant deficiency of argininosuccinate synthetase (Kim, Bold et al. 2009, Kim, Coates et al. 2009, Hsueh, Knebel et al. 2012, Changou, Chen et al. 2014). This rate limiting enzyme for arginine synthesis has been found to be lacking in human PCa tissues. PCa cell lines such as CWR22Rv1 lack the enzyme, while PC-3 has reduced levels and LNCaP cells highly express the enzyme (Kim, Bold et al. 2009). ADI-PEG20 treatment of CWR22Rv1 cells led to the early induction of autophagy (1-4 h post treatment). Inhibition of autophagy by chloroquine or beclin 1 siRNA led to accelerated cell death by non-canonical, caspase-independent apoptosis, whereas LNCaP cells were resistant to both ADI-PEG20 and autophagic inhibition (Kim, Bold et al. 2009, Kim, Coates et al. 2009). Decreased phosphorylation of 4E-BP1, which is the downstream effector of mTOR, was observed in DU-145 and PC-3 following treatment of DU-145, PC-3, and LNCaP cells to recombinant human arginine (Balakumaran, Porrello et al. 2009, Hsueh, Knebel et al. 2012). Moreover,

combining arginine deaminase with docetaxel, a caspase-dependent chemotherapeutic agent, was shown to decrease tumour growth *In Vivo* (Kim, Coates et al. 2009). This shows that arginine deprivation can modulate autophagy and cause caspase-independent cell death. This effect of arginine deprivation is executed via multiple cell death pathways when combined with traditional caspase-dependent chemotherapeutic agents (Kim, Bold et al. 2009, Kim, Coates et al. 2009, Hsueh, Knebel et al. 2012, Changou, Chen et al. 2014).

(c) Inhibition of geranylgeranyl biosynthesis:

Epidemiological studies have shown that statins (cholesterol lowering drugs) decrease the incidence of advanced PCa thereby protecting against tumour progression (Parikh, Childress et al. 2010, Toepfer, Childress et al. 2011, He, Mangala et al. 2012, Peng, Li et al. 2013, Zhang, Yang et al. 2013, Babcook, Sramkoski et al. 2014). A high fat diet, which elicits the opposite clinical effect of statin treatment, correlates with a higher incidence of PCa (Parikh, Childress et al. 2010, Zhang, Yang et al. 2013). *In Vitro* studies have shown that statins caused autophagic cell death by inhibiting geranylgeranyl biosynthesis in HRPC cell lines (PC-3), but this was less pronounced in androgen-sensitive (LNCaP) cells and absent in the normal prostate cell line (RWPE1) (Toepfer, Childress et al. 2011, Wasko, Dudakovic et al. 2011). The combination of statins with radiation, resulted in a synergistic cytotoxic effect (He, Mangala et al. 2012).

Malonyl coenzyme A (Co-A), an intermediate metabolite of fatty acid synthesis and negative regulator of fatty acid oxidation, is formed by carboxylation of acetyl Co-A by the enzyme acetyl Co-A carboxylase (Beckers, Organe et al. 2007). Inhibition of acetyl Co-A carboxylase using soraphen A, had no cytotoxic effects on pre-malignant BPH-

1 cells (Beckers, Organe et al. 2007). However, soraphen A, at nano molar concentrations, inhibited cancer cell proliferation and resulted in cellular death of LNCaP and PC-3M-luc-C6 cells by blocking lipogenesis and enhancing fatty acid oxidation (Beckers, Organe et al. 2007). Increased lipogenesis is a feature of PCa cells, and these data suggest that such an acceleration of lipogenesis is dependent on acetyl Co-A carboxylase activity in PCa (Kaini, Sillerud et al. 2012, Knaevelsrud and Simonsen 2012). Soraphen A induced inhibition of acetyl Co-A carboxylase resulted in cell death by apoptosis in LNCaP cells whereas the PC-3M-luc-C6 underwent autophagic cell death. The difference in the mode of cell death in response to inhibition of lipogenesis between these two cell lines is intriguing and remains unclear (Wu, Coffelt et al. 2012).

1.4.9 Genetic manipulation:

HDAC inhibitors: HDAC inhibitors are target anticancer agents that have shown promising results (Long, Zhao et al. 2009). They induce histone H3 hyperacetylation, which correlates with their ability to inhibit cancer cell proliferation, induce cell differentiation and cell cycle blockade (Shubassi, Robert et al. 2012). Three structurally unrelated HDAC inhibitors (trichostatin A, FR901228, and sodium butyrate) induced apoptotic cell death in LNCaP and DU-145 cells but PC-3 cells were largely resistant to all the 3 inhibitors (Long, Zhao et al. 2009). In a separate study that used two other HDAC inhibitors H40 and SAHA on several cancer cell lines, cytotoxicity in the PCa cell line (PC-3M) and promyelocytic leukaemia cell line (HL-60) was found to be mediated by autophagy instead of apoptosis; the molecular mechanisms underlying the switch towards autophagic cell death in selective cell lines remains poorly understood (Powell, Casimiro et al. 2011, Klionsky, Abdalla et al. 2012).

1.4.10 Modulation by external radiation:

Radiotherapy has an important role in the treatment of early and inoperable locally advanced PCa (Gillmore, Laurence et al. 2010). Induction of autophagy by mTOR inhibition increased the susceptibility of PCa to irradiation (Hsueh, Knebel et al. 2012). In a separate study, the mTOR inhibitor everolimus sensitized PC-3 cells to radiation, with further sensitization by the addition of blocking caspase-dependent apoptosis using Z-VAD and Bax/BakSiRNA. Moreover, Z-VAD, independently induced radio sensitization through promotion of autophagy (Cao, Subhawong et al. 2006). As mentioned previously, statins when combined with radiation produced a synergistic response (He, Mangala et al. 2012). These findings suggest that radiotherapy induces the cell death by both autophagy and apoptosis in PCa cells when combined with other agents and the mode of cell death is dependent on the agent in context.

1.4.11 Proteasome inhibitors:

MG 132: MG 132 (carbo-benzoxy-L-leucyl-L-leucyl-L-leucinal) is a potent proteasome inhibitor (Yang, Monroe et al. 2006). Gene profile expression of MG 132- treated PC-3 cells activated multiple signalling pathways notably heat shock proteins and ubiquitination proteins. Additionally, there was increased expression of *ATG12*, *ATG7* and *ATG5* as well as pro-apoptotic genes. Conceivably, cells treated with MG132 demonstrated both apoptosis and autophagy, and it remains inconclusive if cell death was 'induced by autophagy' or 'associated with autophagy' (Yang, Monroe et al. 2006).

1.4.12 Modulation of growth factor signalling:

Neuregulin: Neuregulins are polypeptide growth factors from the EGF family (Montero, Rodriguez-Barrueco et al. 2008). Potential mechanisms of actions by neuregulin involves modulation of the JNK mediated signalling by increased JNK phosphorylation, and also the inhibition of interactions between beclin-1and Bcl-2, ROS, and Pl3K pathways (Tal-Or, Di-Segni et al. 2003, Soler, Mancini et al. 2009, Schmukler, Shai et al. 2012). Cell death associated with neuregulin induced autophagy was inhibited by SP600125 (JNK inhibitor), Bcl-2 over-expression, *Beclin-1* silencing, 3-MA, and N-acetyl cysteine (Schmukler, Shai et al. 2012). The broadspectrum caspase inhibitor [Z-VAD-FMK] did not inhibit neuregulin-associated cell death (Tal-Or, Di-Segni et al. 2003).

It is abundantly clear that several mechanisms are involved in inducing autophagy in PCa. However, the potential outcome of the autophagy process may vary depending on the specific conditions under which the process is activated, even when using the same drug but under a different experimental condition. The aim of the current study is aimed to identify the mechanism(s) through which alpha adrenergic receptor antagonists with quinazoline structure-based compounds induce cell death with a predominantly autophagic picture using well established commercial cell lines of PCa and BCa. Doxazosin is used as the primary prototype drug for these experiments and is also supplemented using prazosin.

1.5 Endocytosis and PCa

Endocytosis was first discovered by Ilya Metchnikoff in the late 19th century (Schmid, Sorkin et al. 2014). It is the process by which plasma membrane vesicles move

inwardly from the cell surface into the interior of the cell; the opposite process is termed exocytosis.

The three main pathways of endocytosis are clathrin-dependent endocytosis and clathrin-independent endocytosis and dynamin-dependent endocytosis (Ivanov 2008). The former is characterized by the formation of clathrin coated vesicles on the cytoplasmic side of cell membrane, whilst in the latter, dynamin acts as a critical regulator of vesicle separation. In general, clathrin dependent pathways of internalization mediates recycling whilst clathrin independent pathways mediate degradation of receptors (Le Roy and Wrana 2005).

Clathrin independent pathways involve several internalization pathways amongst which the most important is the lipid raft or caveolae mediated pathway. This is where caveolin containing invaginations called caveosomes effect transport inwardly. Caveolae are regions in the plasma membrane that have a high content of cholesterol and sphingolipids content (Nabi and Le 2003).

Dynamin is a GTPase (guanosine-5-triphosphatase) molecule that is an adaptor protein capable of self-assembly and oligomerization around plasma membrane vesicles and regulates the fission of the vesicles, thus regulating the final step in vesicle formation (Hinshaw 2000). Hence dynamin is also a critical regulator of both clathrin-dependent and clathrin-independent endocytosis.

Receptor mediated endocytosis is the process by which membrane localized receptors are internalized – this can be either constitutive or ligand-induced. In constitutive endocytosis, membrane receptors are spontaneously internalized into cytoplasm and then recycled back to cell membrane, after sorting in the endosomal compartments (Schmid 1997, Di Fiore 2009). In ligand-induced endocytosis, the internalization is

triggered upon binding to a ligand to remove active, signalling receptors from cell membrane and transport them to lysosomal compartments for degradation. Thus, ligand-mediated endocytosis serves to extinguish receptor signalling and is the major mechanism of long-term attenuation of signalling receptors (Di Fiore 2009). Endocytosis of receptors and their ligands can therefore modulate signalling at the cell surface, and endocytosis can itself be considered as a signalling pathway initiated by activation of surface receptors that lead to their internalization and degradation (Polo, Pece et al. 2004). The internalization of the receptor controls the duration, intensity and specificity of signalling (Sorkin 2001).

Endocytic trafficking of receptors are important processes in the pathogenesis of cancer and disturbances in receptor trafficking have been shown to modulate the clinical behaviour of PCa (Polo, Pece et al. 2004). In PC-3M PCa cells, nanoparticles composed of titanium dioxide conjugated with Alizarin Red S has been shown to undergo temperature, time, and concentration dependent intracellular transport mediated by clathrin pits, caveolae and micropinocytosis (Thurn, Arora et al. 2011). Inhibition of hyaluronan receptors for endocytosis (HARE) using monoclonal antibodies blocked the formation of lymph node metastasis in orthotopic mice models (Simpson, Weigel et al. 2012). Furthermore, the specific blockade of HARE did not have any effect on the primary tumour growth or on other tissues, suggesting that endocytic processes could promote tissue-specific dissemination of PCa (Simpson, Weigel et al. 2012). Another similar example is the clathrin-mediated internalization of the cell adhesion molecule cadherin-11, which regulates the migratory function in PCa cells (Satcher, Pan et al. 2015).

Androgen independent growth of advanced PCa is dependent on growth factors such as EGFR. Endocytosis of growth factor receptors, one of the mechanisms that

facilitate growth factor signalling, have been found to be markedly different in metastatic PCa (Oosterhoff, Kuhne et al. 2005, Xie, Zuhair et al. 2023). AR affects clathrin-mediated endocytic pathways of EGFR, which plays a key role in the pathogenesis of several tumours including PCa (Aguilar and Wendland 2005). Moreover, increased re-expression of AR by endocytic trafficking is in itself a determinant of less aggressive phenotypes of PCa (Bonaccorsi, Nosi et al. 2007).

More recently, endocytosis have been exploited to develop novel mechanisms of drug delivery using nanoparticles (Chen, Li et al. 2017) and PEGylated agents have been used to enhance cancer imaging (Chuang, Wang et al. 2010). The endocytic process of the glycoprotein molecule transferrin, which functions primarily as an iron chelator, have been exploited as an useful target for cancer therapy (Tortorella and Karagiannis 2014). Transferrin is upregulated in several metastatic and drug-resistant cancers including PCa and BCa (Zhou, Zhao et al. 2018). Transferrin based targeting using nanoparticle delivery systems have shown to result in 70% growth inhibition of PC3 cells *In Vitro* with paclitaxel as compared to 35% with free paclitaxel; *In Vivo*, the former was able to cause complete tumour regression and improved survival in mice (Sahoo, Ma et al. 2004).

In summary, endocytosis has immense ramifications in receptor trafficking and cell signalling, and many of these have been intrinsically linked to cancer growth modulation, cell division, autophagy, and apoptosis. In chapter 5, we investigated the role of endocytosis in doxazosin-induced cell death of PCa and BCa cell lines.

Chapter 2

Materials and Methods

2.1 Cell Culture

2.1.1 In Vitro monolayer culture of PCa cell lines:

Three PCa cell lines (PC-3, DU145 and LNCaP) were used for *In Vitro* experiments. The PC-3 and DU-145 cell lines were obtained from ATCC (American Type Culture Collection). LNCaP cells were kindly provided by Prof. J Masters from University College of London, London.

PC-3 cells are HRPC cells established from the bone metastasis in a 62-year-old male Caucasian with high-grade prostatic adenocarcinoma. PC-3 cells were grown in Ham's F12K medium with 2 mM L-glutamine supplemented with 7.5% foetal calf serum and 1% antibiotic solution containing penicillin, streptomycin, and amphotericin B.

DU145 cells are also HRPC cells derived from a brain metastasis in a 69-year-old Caucasian male reported to be grade II adenocarcinoma by ATCC, which corresponds to Gleason score 8 (Gordetsky and Epstein 2016). DU145 cells were grown in minimum essential medium (MEM) containing 2 mM L-glutamine supplemented with 10% foetal calf serum, and 1% antibiotic solution containing penicillin, streptomycin, and amphotericin B.

The LNCaP cell line is derived from a human prostate adenocarcinoma cell from a 50-year-old Caucasian male in 1977, taken from a needle aspiration biopsy from a metastatic lesion in the left supraclavicular lymph node (Kyprianou N, 2005). LNCaP cells were maintained in DMEM (Dulbecco's minimum essential media) supplemented with 10% foetal bovine serum containing 2 mM L-glutamine

supplemented with 10% foetal calf serum, and 1% antibiotic solution containing penicillin, streptomycin, and amphotericin B.

2.1.2 In Vitro monolayer culture of BCa cell lines:

HT 1376 cell lines was obtained from the European Collection of Cell Cultures (Salisbury, Wiltshire, UK). These cells were derived from a 58-year-old woman with high grade (G3) transitional cell carcinoma of the bladder who was not originally treated with chemotherapy or radiotherapy. The cells were maintained in MEME (minimum essential media Eagle) supplemented with 10% foetal calf serum and 1% antibiotic solution containing penicillin, streptomycin, and amphotericin B, 1% non-essential amino acids and 2 mM L-Glutamine. The cells were maintained in a humidified atmosphere at 37 C containing 5% CO2 in a sterile environment.

2.1.3 In Vitro monolayer culture of non-cancerous cell lines:

2.1.3.1 Fibroblast cell lines:

The fibroblast cell lines were derived from human skin fibroblasts. The cells were grown in MEME supplemented with 10% foetal calf serum and 1% antibiotic solution containing penicillin, streptomycin, and amphotericin B.

2.1.3.2 Lipid receptor-deficient cells:

This cell line was developed from a patient with homozygous familial hypercholesterolemia with Pro664Leu mutation in the low-density lipoprotein (LDL) receptor gene (Bourbon, Fowler et al. 1999) and was kindly provided by Prof A Soutar from the Medical Research Council Laboratory, Hammersmith Hospital, London, United Kingdom. The cells were grown in MEME supplemented with 10% foetal calf

serum and 1% antibiotic solution containing penicillin, streptomycin, and amphotericin B.

2.1.4 Establishment of doxazosin-resistant cell lines *In Vitro*:

We attempted to develop doxazosin-resistant cell lines in this study. The methodology adopted are detailed in chapter 4.

2.2 Cell Culture Methods and Protocols

Cells were handled in a class II microbiological safety cabinet hood in accordance with local and manufacturer's safety guidelines. All cells were maintained in the incubator in a humidified atmosphere containing 5% CO₂ at 37 C. The cells were used for experiments (after they had undergone a minimum of 2 passages from thawing) and used for a maximum of 10 to 12 passages. Low passage cells were stored by following the standard protocol for that cell line and placed in liquid nitrogen flasks for future experimental use as stock. Incubators were subjected to autoclave cleaning every 3 to 4 months.

Typically, cells were grown in 75 cm² flasks, seeded at 20% to 25% confluence and allowed to grow to 60% to 70% confluence after which they were detached using 3 to 5 ml trypsin-EDTA (ethyl diamine tetra acetic acid) solution for 2 to 6 minutes at 37 C. Fresh serum containing media was added to inactivate the trypsin, cells pelleted by centrifugation, and re-suspended. Cell counts were performed on the pellet suspension prior to use for subsequent passages or for experiments.

2.2.1 Cell counting:

The re-suspended cells were placed in 10 ml of media and were mixed thoroughly using a mixer. 40 μL of the sample was pipetted out and transferred to an

Eppendorf tube. Subsequently, 40 μ L of trypan blue solution was also added to the Eppendorf tube and mixed thoroughly using a vortex mixer. This was loaded (20 μ L) onto the chambers of a Neubauer's haemocytometer covered with a cover slip. The live cells appear colourless and refractile while dead cells take up the trypan blue dye and are stained blue.

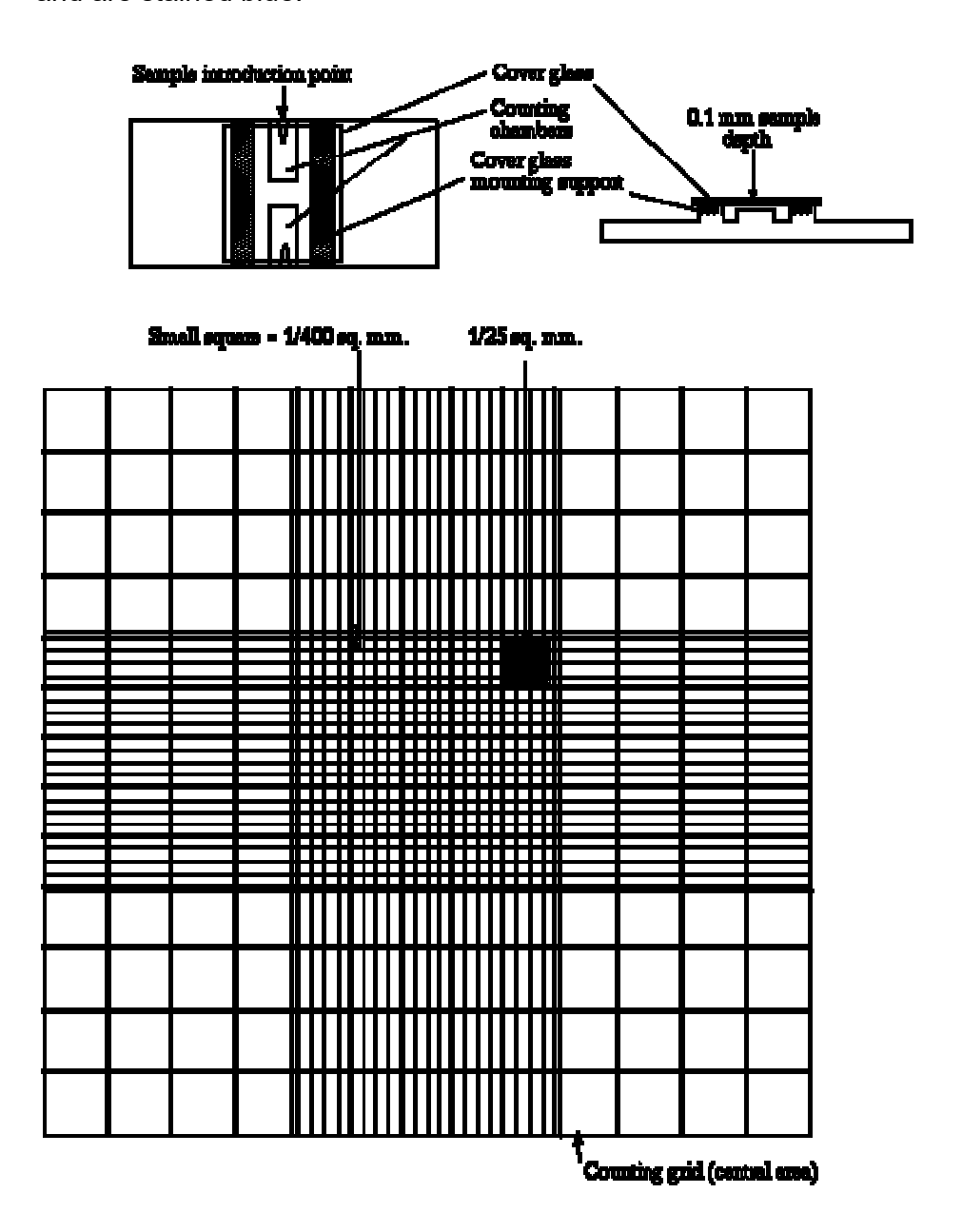


Figure 1: Neubauer's haemocytometer (top left). Method of applying cover slip (top right). Grids within each chamber of the haemocytometer (bottom).

The number of cells in the outer 4 grids (16 squares with thick lines only) and the central grid (one with the thick as well as transverse and vertical thin lines) was counted in each chamber under the low power objective of a light microscope.

For example, to obtain 5000 cells/well for experiments the calculation used was as follows:

[(Live cells in chamber 1 + Live cells in chamber 2) x 2 x 1000] / 50,000

2.3 In Vitro Proliferation Studies

We tested 4 different assays for *In Vitro* proliferation studies, namely:

- (a) Crystal violet dye elution assay
- (b) Cell-Titer 96® aqueous one solution cell proliferation MTS assay [see note below]
- (c) Cell-Titer Blue® cell viability (CBCV) assay
- (d) Cell proliferation BrdU colorimetric ELISA (BrdU ELISA) assay

[Note: MTS contains tetrazolium compound [3-(4,5-dimethylthiazol-2-yl)-5-(3-carboxymethoxyphenyl)-2-(4-sulfophenyl)-2H-tetrazolium, inner salt; abbreviated henceforth as MTS]

After extensive testing, we opted to not use crystal violet dye elution assays in any of the experimental protocols given the lack of reproducibility due to several artefactual errors from this assay. In brief, the assay involved the addition of 100 µL of absolute ethanol which was particularly difficult to pipette accurately as the volatility of the ethanol solution resulted in artefactual errors due to evaporation and pipetting errors due to its very low viscosity. Moreover, crystal violet assays require 3 cycles of

washing. Treatment with doxazosin induces anoikis and cells become less adherent - the washing process was found to remove the less adherent cells. Hence an assay that does not involve a wash step was considered more reliable. For most experiments the Cell-Titer 96® aqueous one cell proliferation MTS assay (henceforth referred to as Cell-Titer 96® aqueous MTS assay) was used as the results were reproducible, did not involve wash steps, and the methodology was relatively simple to perform on a routine basis.

2.3.1 Cell-Titer 96[®] aqueous MTS assay:

Cells were seeded in a 96-well microtiter (MT) plate at densities of 2500 to 5000 cells in 100 µL (per well) of serum containing medium and incubated at 37 C. After 24 h of incubation, 10 µL of the serum containing medium were removed and replaced with 10 µL solutions of the test compound at varying final concentrations. In control wells, an equal volume (10 µL) of solvent was used in the preparation of the solution. This served as a vehicle control, alongside a no-cell blank control (BL) and background controls (BC). Following the incubation period, cell viability was assessed using Cell-Titer 96® aqueous solution and an electron coupling reagent phenazine ethosulphate as per the manufacturer's (Promega®) instructions. In brief, 20 µL of the above reagent was added to each well and incubated at 37 C for 4 h. The MT plates were read on a spectrophotometric plate reader (Sunrise, Tecan, UK) using the appropriate reading and reference wavelength. Using data reduction software (Tecan, UK) the optical densities (OD) were calculated as follows:

$$OD = OD_{xxx} - OD_{yyy} - [OD_{BC} + OD_{BL}]$$

Proliferation studies were carried out after 24, 48 or 72 h of incubation with the drug or control solutions. Each experiment was carried out in triplicate and repeated three

times (n=9). Using the GraphPad Prism 6[®] software dose response curves were generated and IC₅₀ were calculated where applicable.

2.3.2 Cell proliferation BrdU ELISA assay:

Cells were seeded in a 96-well MP at densities of 2500 to 5000 cells in 100 µL (per well) serum containing medium and incubated at 37 C. After 24 h of incubation, the medium was replaced with 100 µL serum free medium containing 1% antibiotic solution containing penicillin, streptomycin, and amphotericin B. After a further 24 h of incubation, 10 µL of the serum containing medium was removed and replaced with 10 µL solutions of the test compound at varying final concentrations. In control wells, an equal volume (10 µL) of solvent used in the preparation of the solution was added this served as a standard or vehicle control. Also, BL and BC were used as per manufacturer's instructions. Following the incubation period, cell proliferation assays were performed as per the instruction manual provided in the BrdU ELISA assay kit (Roche, UK).

The MP were read on a spectrophotometric plate reader (Sunrise, Tecan, UK) using the appropriate wavelength. Using Magellan® data reduction software (Tecan, UK) the OD was calculated as follows:

$$OD = OD_{xxx} - OD_{yyy} - [OD_{BC} + OD_{BL}]$$

Proliferation studies were carried out after 24, 48 or 72 h of incubation with the drug or control. Each experiment was carried out in triplicate and repeated three times (n=9). Using the GraphPad Prism 6[®] software dose response curves were generated and IC₅₀ were calculated where applicable.

2.3.3 CBCV assay:

Cells were seeded in 96-well MT plates at densities of 2500 to 5000 cells in 100 μL (per well) serum containing medium and incubated at 37 C. After a 24 h interval, 10 μL of the serum containing medium were removed using a multichannel pipette and replaced with 10 μL solutions of test compound at varying final concentrations. In control wells, an equal volume (10 μL) of solvent used in the preparation of the solution served as a vehicle control, alongside no-cell BL control and BC wells. Following the incubation period, cell viability was assessed using Cell-Titer Blue® cell viability reagent (highly purified resazurin) as per manufacturer's instruction (Promega, UK). Briefly, 20μl of the Cell-Titer Blue® reagent is added to the cells. Incubation is maintained for a period of 1 to 4 h. Finally, fluorescence was recorded at 560_{Ex}/590_{Em} using Fluoroskan Ascent® plate reader.

Proliferation studies were carried out after 24, 48 or 72 h of incubation with the drug or control. Each experiment was carried in triplicate and repeated three times (n=9).

2.3.4 Cytotoxicity detection kit for lactate dehydrogenase (LDH):

LDH, a cytoplasmic enzyme, from damaged cells leaks out into to the culture supernatant, and the amount of enzymatic activity corresponds to the proportion of lysed cells. The assay is based on the cleavage of a tetrazolium salt when LDH is present in the culture supernatant.

Batch cultures of cells grown in 4 well plates were incubated with the drug or the vehicle control. At the end of the incubation period, the cells were harvested in trypsin-EDTA, centrifuged at 500 rpm for 5 min. The supernatant was removed and transferred to a 96-well MP. The substrate mixture (100 μ L/well) were added to the supernatant and incubated for 30 min.

The MP was measured on a spectrophotometric plate reader (Sunrise, Tecan, UK) at 500 nm. Using the existing Magellan® data reduction software (Tecan, UK) the OD was calculated as described in the proliferation assays.

Cytotoxicity studies were carried out following 24, 48 or 72 h of incubation with the drug or control. Each experiment was carried out in triplicate and measurements repeated three times (n=9). Using the GraphPad Prism 6[®] software dose response curves were generated and IC₅₀ were calculated where applicable.

2.4 Statistical Analysis

Data was expressed in as standard error of mean (s.e.m). Cumulative response curves were plotted and compared using 2-way analysis of variance (ANOVA). The significance of the results obtained were assessed using Student's 2-tail *t* test. Results were considered significant if p < 0.05. Statistical software Prism V4.0® or V6.0® (GraphPad Software Inc.) was used for statistical calculations and to obtain graphical representations of the experimental data.

<u>2.5 Transmission Electron Microscopy (TEM) and Scanning Electron Microscopy (SEM)</u>

Low passage PC-3 cells were thawed from -80C, subjected to 2 passages at sub-confluence, harvested (using EDTA-trypsin), seeded in 25 cm² pre-labelled flasks and incubated for 24 h. The flasks were divided into test group (exposed to 37.5 μM doxazosin) and control group exposed to solvent (sterile water) and incubated for the requisite period, after which the cells were washed 3 times with phosphate buffer

solution (PBS), fixed (using 2% glutaraldehyde) and stored at 4C. TEM and SEM of glutaraldehyde-fixed cell samples were carried out in collaboration with the Dept. of Electron Microscopy Unit, Royal Free Hospital. Initially samples and their matched controls at 24, 48 and 72 h were examined.

2.6 Identification of Lipofuscin Granules

Low passage PC-3, DU-145 and LNCaP cells were thawed from -80C, subjected to 2 passages at sub-confluence, harvested (EDTA-trypsin), seeded in 25 cm² pre-labelled flasks and incubated for 24 h. The flasks were divided into test group (exposed to 37.5 µM doxazosin) and control group exposed to solvent (sterile water) and incubated for the requisite period, after which the cells were detached using trypsin-EDTA, pelleted and washed.

The cell pellets were processed into paraffin blocks and stained for lipofuscin using the DAPS (diastase periodic acid Schiff) which stains lipofuscin that appear as a magenta colour, and with aldehyde fuchsin which demonstrates lipofuscin in deep purple.

2.7 Fluorescent Microscopy

Cells were grown on cover slips at a density of 5000 cells/well. Cells were allowed to attach for 24 h and then treated with doxazosin 37 μ M whilst controls were exposed to solvent (H₂O) for 48 h. Both groups were then exposed to dansylcadaverine (100 μ M) and stained using 4,6-diamidino-2-phenylindole (DAPI) blue-fluorescent stained nucleus (DNA). Dansylcadaverine is an inhibitor of

autophagy; it also has auto fluorescent properties and concentrates within the autophagosomes of cells undergoing autophagy.

2.8 Immunohistochemistry

These studies were used to identify the presence of LC-3 as a marker of autophagy in PCa cell lines. Established LC-3 positive breast cancer cell lines that were known to demonstrate autophagy were used as positive controls for the study.

Low passage cells were thawed from -80C, subjected to 2 passages at subconfluence, harvested (using EDTA-trypsin), seeded in 25 cm² pre-labelled flasks and incubated for 24 h. The flasks were divided into test group (exposed to 37.5 μM doxazosin) and control group exposed to solvent (sterile water) and incubated for 48 h, after which the cells were detached using trypsin-EDTA, and pelleted. The freshly pelleted cells were treated to anti-LC3 antibody (Catalogue No: ab51520, Abcam Plc, UK) in 1/2000 dilution, fixed and mounted on slides.

2.9 In Vitro Synergism Studies

Low passage cells were seeded in in 96-well MP at densities of 2500 to 5000 cells in 100L (per well) serum containing medium and incubated at 37 C. After a 24 h interval, 10-20 μ L of the serum containing medium were removed from each well using a multichannel pipette and replaced with: (i) 5 – 10 μ L each of two or more test compounds at individual IC50 concentrations to make a final volume of 100 μ L (ii) 10 - 20 μ L of the serum containing medium of the individual test compounds at the IC50 concentration. (iii) an equal volume of solvent (sterile water) served as the vehicle control, alongside BL and BC wells. Following the incubation period, cell viability or

cell proliferation were assessed using CBCV or MTS assay, respectively. BrdU ELISA assays were used when experimental conditions require a serum free incubation period prior to the addition of test compounds, (to reset the cells in G₀ phase). The MT plates were read in accordance with the assay protocols (as described earlier) using the appropriate equipment and wavelength.

Proliferation studies were carried out after 24, 48 or 72 h of incubation with the drug or control. Each experiment was carried out in triplicate and repeated three times (n=9). Statistical analyses were carried out as previously mentioned in section 2.4.

2.10 In Vitro Competitive Agonism and Antagonism Studies

Low passage cells were seeded in a 96-well MP at densities of 2500 to 5000 cells in 100 μ L (per well) serum containing medium and incubated at 37 C. After a 24 h interval, 10 -20 μ L of the serum containing medium was removed and replaced with 5 – 10 μ L of drug solution containing the first test compound at a chosen concentration to make a final volume of 100 μ L. The plates were returned to the incubator for 30 min to 4 h. At the end of this period all the media in the wells were discarded by aspiration and replaced with 100 μ L of media containing the second test compound at a chosen concentration. In some wells, the 100 μ L were made up with the media and an equivalent volume (10 - 20 μ L) of solvent used in the preparation of the solution which served as the vehicle control, alongside BL and BC wells. Following the incubation period, cell viability or cell proliferation were assessed using CBCV or MTS assay, respectively. The MT plates were read in accordance with the assay protocols using a spectrophotometer at the appropriate wavelength. Proliferation studies were carried out after 24, 48 and 72 h of incubation with the drug or control. Each experiment

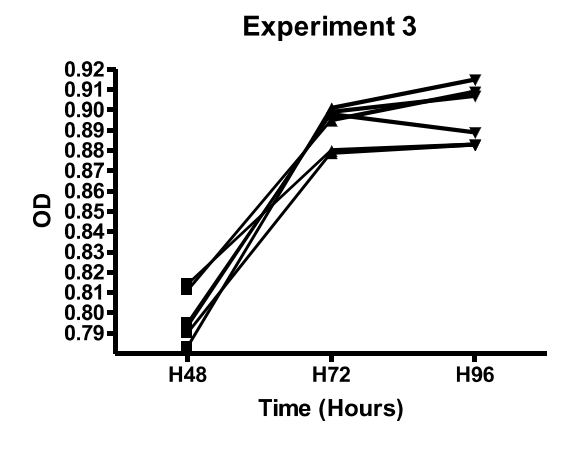
was carried out in triplicate and repeated 3 times (n=9). Statistical analysis was carried out as previously mentioned in section 2.4.

2.11 Methodology - Experiments and Results

2.11.1 Measuring the sensitivity of Cell-Titer 96® aqueous MTS assay to evaluate the growth of PC-3, DU-145, LNCaP, HT-1376 and fibroblast cells in 96 well plates:

Cells were plated at densities of 2500 cells/well or 5000 cells/well in 96-well plates and assays were performed at 24 h intervals for a period of 168 h, to assess the growth curve of the cells. It was observed that the growth of cells was maximal between 48 and 72 h, after which the growth plateaued. A representative graph for the curves obtained for fibroblasts is shown below.

Figure 2: Representative graphs for growth of fibroblast cells seeded at 5000 cells/well and assessed after 48 h, 72 h and 96 h. OD = optical density (in Y-axis) measured by Cell-Titer 96® aqueous MTS Assay.



There is a steep growth curve of fibroblasts between 48 and 72 h, after which the growth plateaus during the further period of incubation. This could be due to either

the cell reaching full confluence or diminishing availability of nutrient or both. The experiments were repeated for all individual PCa and BCa cells lines used in this study, and a similar representative curve profile was obtained in each case.

2.11.2 Evaluating the sensitivities CBCV and Cell-Titer 96® aqueous MTS assays on different cell densities:

Subsequently, cells were plated at varying densities from 1000 cells per well to 20,000 cells per well and assessed with Cell-Titer 96® aqueous MTS assay and with CBCV assay to determine if the OD corresponded to the cell densities.

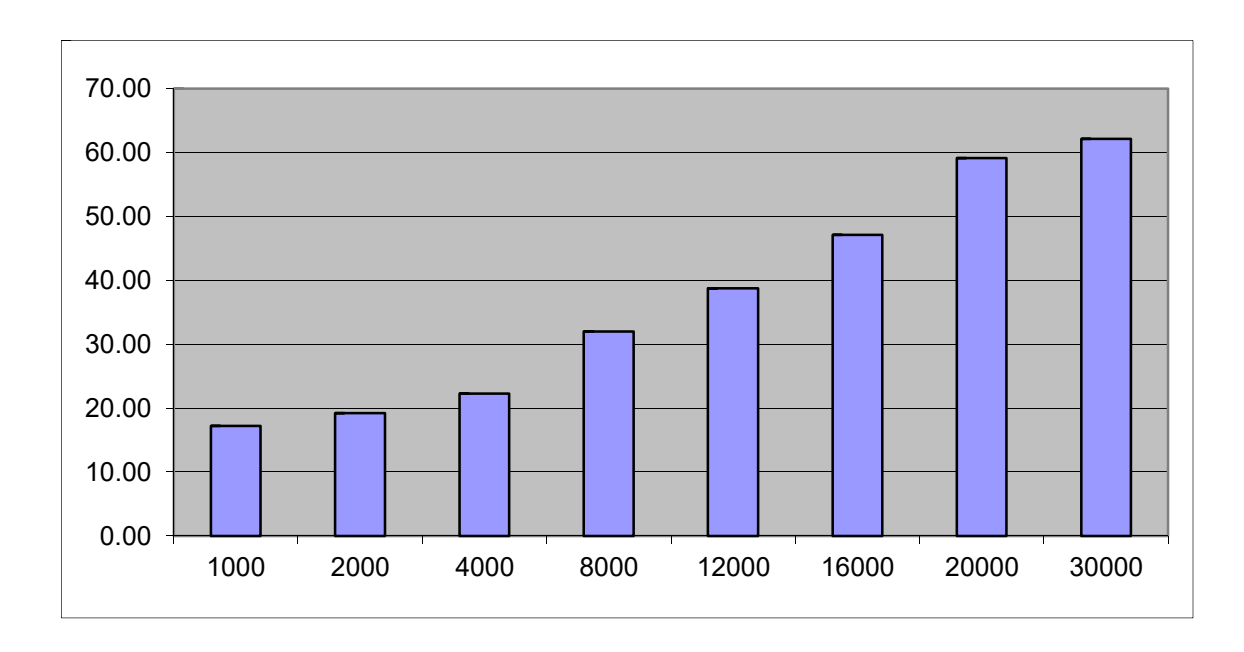


Figure 3: Graph showing increasing densities (X-axis) of PC-3 cells plated in 96 well MT plates and assessed for cell viability using CBCV assay at 72 h; Y-axis represents the optical density (OD).

Similarly, the sensitivity of Cell-Titer 96® aqueous MTS assay was assessed from 625 cells/well to 40,000 cells per 100 per well. The assay was found to be sensitive and provide consistent readings between cell counts of 1250 cells per well to 20,000 cells/well.

2.11.3 Measuring the effect of alpha-adrenergic receptor antagonists on cell viability:

PC-3, DU145, LNCaP, HT-1376 and human skin fibroblast cells were seeded in 96-well MP at densities of 2500 and 5000 cells in (100 μL per well) in serum containing medium and incubated overnight at 37 C. The cells were treated with doxazosin [10⁻¹⁰ to 10⁻⁴], prazosin [10⁻¹⁰ to 10⁻⁴], terazosin [10⁻¹⁰ to 10⁻⁴], or tamsulosin [10⁻¹⁰ to 10⁻⁴] and control wells treated with solvent (sterile water). Cell-Titer 96[®] aqueous MTS assay was performed as described in section 2.3.1 after incubating with the drug or control for 24h, 48h or 72h. Each experiment was carried out in triplicate and measurements repeated 3 times (n=9). Statistical analysis was performed as previously described in section 2.4. Dose response curves were generated and IC₅₀ were calculated where applicable.

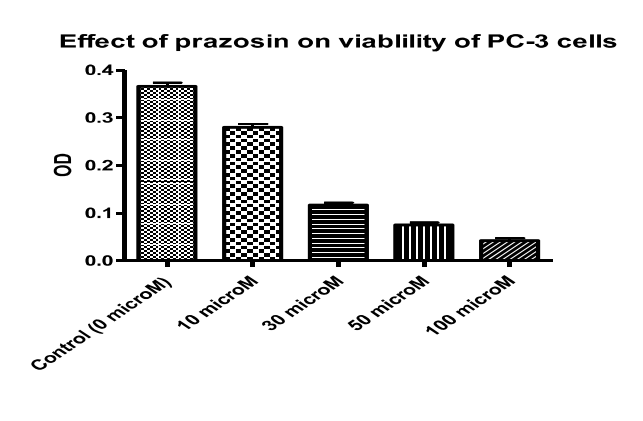
The above experiments were repeated using serum free media. This involved seeding PC-3, DU145, LNCaP, HT-1376 and human skin fibroblast cells in 96-well MP at densities of 2500 and 5000 cells (100 μL per well) in serum containing medium and incubated overnight at 37 C. The media in the wells were aspirated and the cells washed thrice with PBS and then 90 μL (per well) of serum free medium was added. Subsequently, 10 μL (per well) of the respective drug was added to achieve the final concentration ranges of doxazosin [10⁻¹⁰ to 10⁻⁴], prazosin [10⁻¹⁰ to 10⁻⁴], terazosin [10⁻¹⁰ to 10⁻⁴], or tamsulosin [10⁻¹⁰ to 10⁻⁴] whilst control wells treated with 10 μL water/well. These were then incubated for a further 24h, 48h or 72h. Cell-Titer 96® aqueous MTS assay was performed as described earlier [Section 2.3.1] after incubating with the drug or control for 24h, 48h or 72h. Each experiment was carried out in triplicate and measurements repeated three times (n=9). Statistical

analysis was performed as described in section 2.4. Dose response curves were generated and IC₅₀ were calculated where applicable.

2.11.4 *In Vitro* evaluation of the effects of quinazoline-based alpha adrenergic receptor antagonists on PCa and BCa cell lines:

To evaluate the effects of prazosin on the cell viability, cells were seeded at 5000 cells/well/100 μ L in serum containing media in 96 well MP and incubated at 37 C for 24 h. During this period the cells attached to the base of the MP wells and also resumes normal growth. At the end of this 24 h period, prazosin (10, 30, 50 and 100 μ M) or vehicle control were added and incubated for a further 72 h. Cell-Titer 96® aqueous MTS assay was used to determine cell viability to obtain a dose-dependent curve for PC-3 cells. As seen below (Figure 4) at all concentrations (10-100 μ M) that were used in this experiment, prazosin caused death of PC-3 cells as compared to untreated control.

Figure 4: Graph showing prazosin-induced dose-dependent cell death of PC-3 cells; Y-axis represents the OD (optical density).



Prazosin

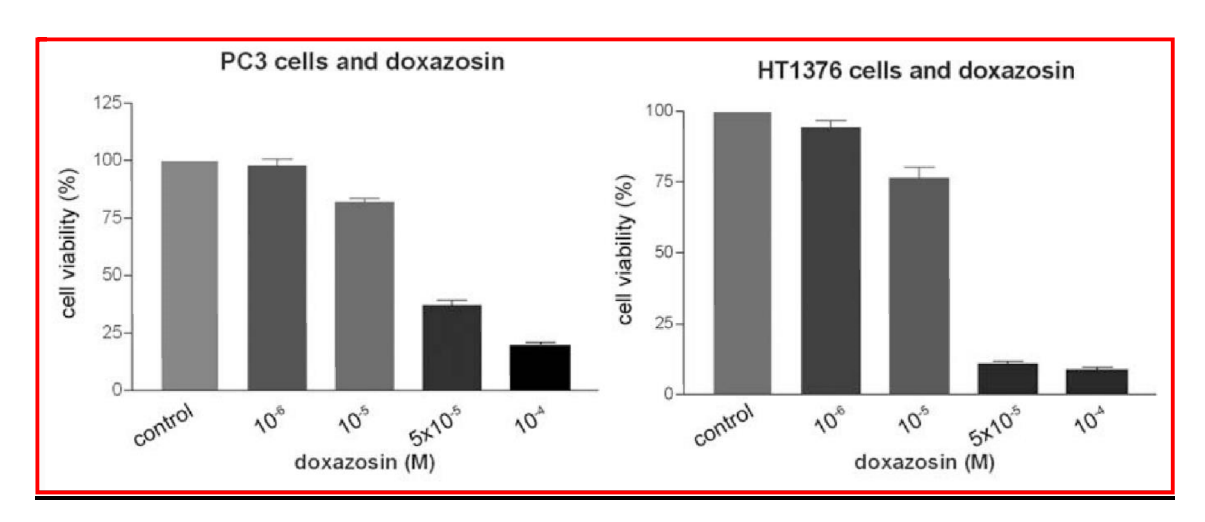


Figure 5: Dose-dependent inhibition of PC3 cell growth by doxazosin with a maximum effect seen at a concentration of 10⁻⁴ M after 72 h. The bars represent the standard error of the mean (left), and right: Dose-dependent inhibition of HT1376 cell growth by doxazosin with a maximum effect seen at a concentration of 10⁻⁴ M after 72 h. The bars represent the standard error of the mean.

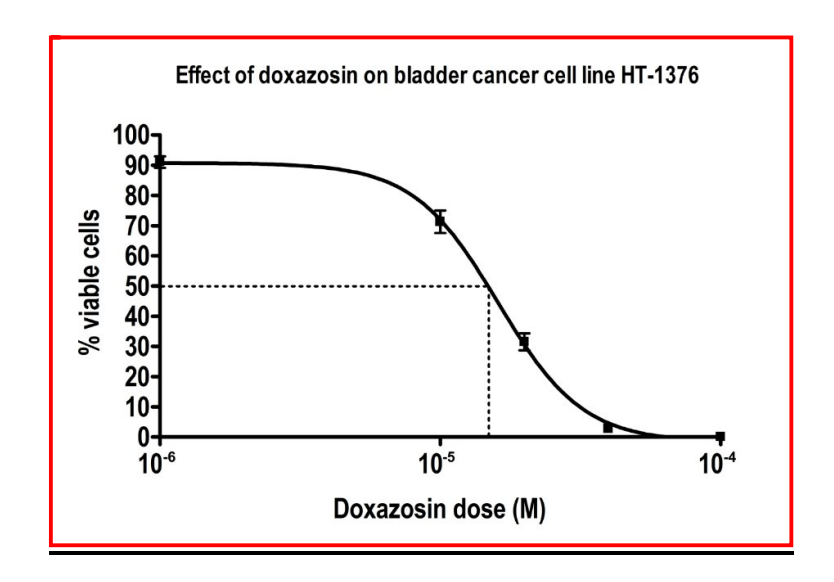


Figure 6: Dose-response curve for HT1376 after exposure to doxazosin for 72 h.

2.11.5 *In Vitro* evaluation of the effects of quinazoline-based alpha adrenergic receptor antagonists on PCa and BCa cell lines treated with tamsulosin:

To evaluate the effects of tamsulosin on PCa and BCa cell viability, cells were seeded at 2500 cells/well/100 μ L of serum supplemented F-12 HAM media in 96 well MP and incubated at 37 C for 24 h. During this period the cells attached to the base of the MP wells, and also resume their normal growth. At the end of this 24 h period, tamsulosin (10, 30, 50 and 100 μ M) or vehicle control were added and incubated for a further 72 h after which MTS assay were performed. At all concentrations (10 to 100 μ M) that were used in this experiment, tamsulosin had no effect on cell viability when compared to the untreated control.

2.11.6 Evaluation of the effects of doxazosin on viability of cells pre-treated with phenoxybenzamine:

To evaluate whether pre-treatment with phenoxybenzamine (an alpha agonist) would prevent cell death induced by doxazosin the following experiments were conducted. Cells were seeded in a 96-well MP at densities of 2500 cells in 100 μL (per well) serum containing medium and incubated at 37 C. After a 24 h interval, 10 μL of the serum containing medium was removed and replaced with 10 μL each of solutions of phenoxybenzamine (10⁻⁵ M) in a volume of 100 μL. The plates were returned to the incubator for 30 min. Subsequently, 10 μL was aspirated and replaced with doxazosin or control solutions. Cell-Titer 96® aqueous MTS assay was used to determine cell viability after 72 h of incubation. All concentrations of doxazosin used caused death of PC-3 cells as compared to untreated control. Hence, the cell death induced by doxazosin (an alpha antagonist) was not prevented

by pre-treatment with phenoxybenzamine (alpha agonist). Doxazosin-induced cell death was therefore independent of its action on alpha receptors.

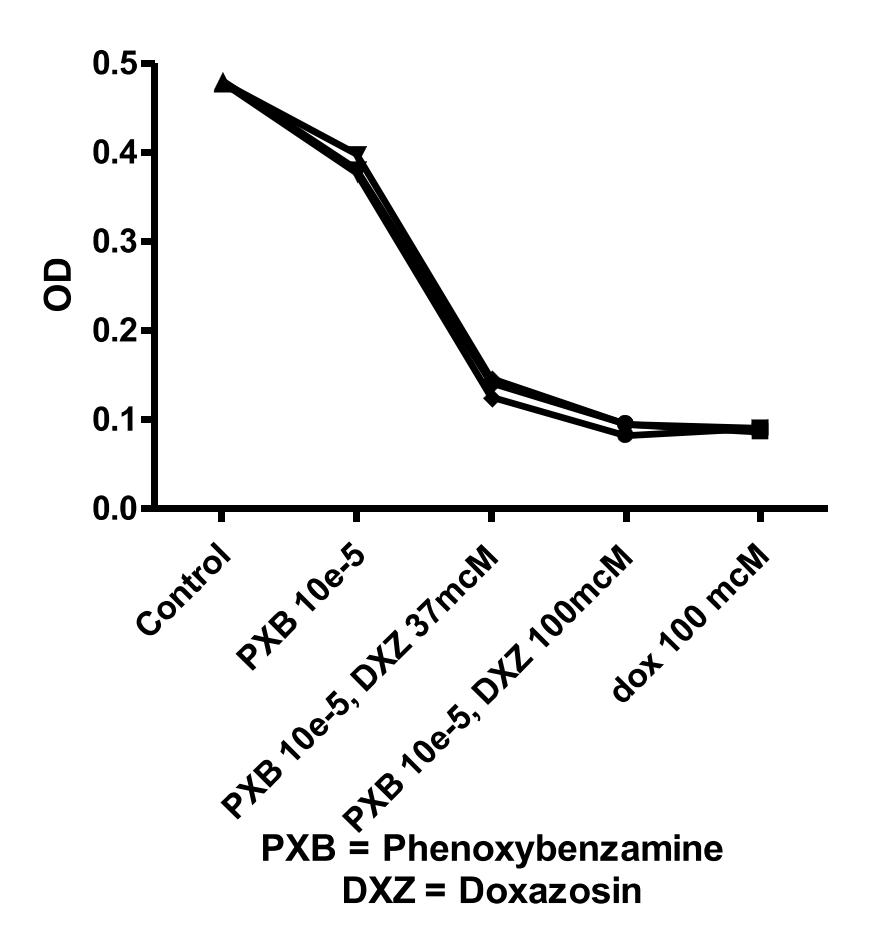


Figure 7: Graph showing doxazosin-induced dose-dependent cell death of PC-3 cells, and pre-exposure to phenoxybenzamine (PXB) had no effect on doxazosin-induced cell death of PC-3 cells; DXZ = Doxazosin; Y-axis represents the optical density (OD).

The above experiment was repeated for other cell lines, and they yielded similar findings to those obtained with PC-3 cells, confirming that doxazosin-induced cell death was independent of the alpha receptor in PCa and BCa cell lines. This finding is in agreement with the findings of others who have also used prostate as well as other cancer cell lines (Gotoh, Nagaya et al. 2012).

Chapter 3

Evaluation of receptors that may mediate doxazosin-induced cell death in prostate and bladder cancers *In Vitro*.

3.1 Introduction

Doxazosin and its related quinazoline-based compounds have receptor affinities to several structurally similar receptor domains. Those receptors that are likely to have affinity to doxazosin were identified through PubMed search, and via the UniProtKB/PSI-Search 2 using P35348, which corresponds to the *ADRA1A* gene encoding for the alpha-1 adrenergic receptor. Furthermore, BLAST (Basic Local Alignment Search Tool) searches were conducted to identify those receptors that have a structural similarity to the alpha-1 adrenergic receptor (Lussi, Magrane et al. 2023). From these searches, it was evident that several members of the adrenergic receptor family and the serotonin receptors had overlapping morphology [Figure 8].

It was therefore hypothesised that at higher concentrations, doxazosin could be exerting its cytotoxic action through an alternate, structurally similar receptor such as the 5HT receptor to which it has an affinity even at nanomolar concentration although this affinity was weak.

Doxazosin has been shown to interact with serotonin receptors. It has been demonstrated that pre-treatment with doxazosin inhibits the shape change of platelets – an early step in platelet activation (Jagroop and Mikhailidis 2001). Furthermore, doxazosin attenuated 5HT-mediated contractility of cavernous smooth muscles (Lau, Thompson et al. 2006). Taken together these findings suggested that doxazosin can mediate the action of the 5HT receptors.

We therefore investigated the role of 5HT receptors on doxazosin-induced cell death in PC3, DU145, LNCaP and HT1376 cell lines.

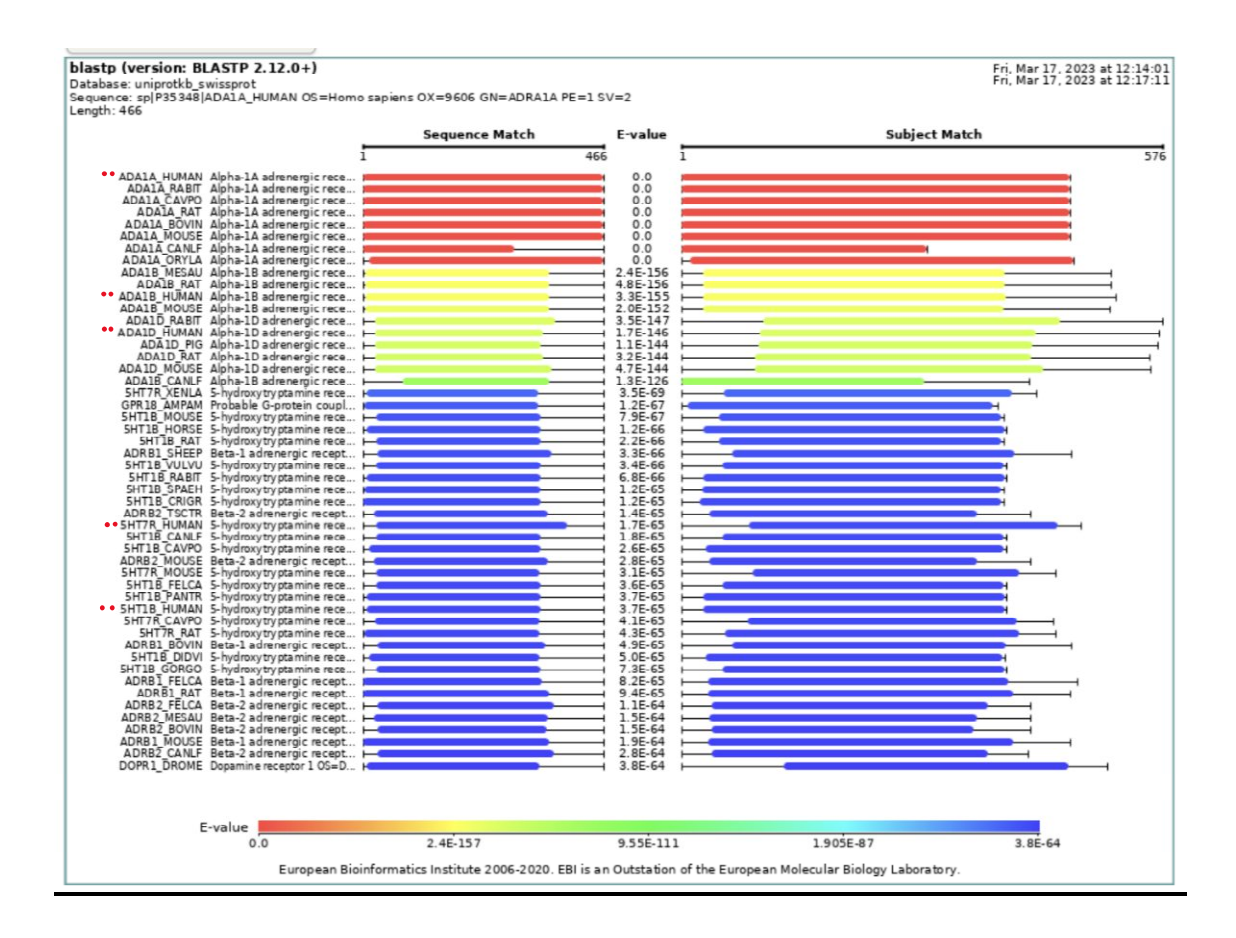


Figure 8: UniProtKB/EMBL and PSI-Search 2 (combined) database search results for showing structural similarity of human alpha-1 adrenergic receptor to that of other human adrenergic receptors and human 5HT receptors. The two red dots on the left point to data specifically pertaining to humans (Homo sapiens).

3.2 Experiments

3.2.1 Evaluation of the effects of doxazosin on PC-3, DU145, LNCaP and HT1376 cells pre-incubated with serotonin hydrochloride:

PC-3, DU145, LNCaP or HT1376 cells were seeded in a 96-well MP at densities of 5000 cells in 100 μ L (per well) in serum containing medium and incubated at 37 C. After a 24 h interval, 10 μ L of the serum containing medium was removed and replaced with 10 μ L each of solutions of serotonin hydrochloride [to final concentration of 1 x 10⁻¹² to 1 x10⁻⁶ M/L] (Sigma-Aldrich, catalogue number – H9523) to make a final

volume of 100 μ L. The plates were returned to the incubator for 4 h. At the end of this period, in test wells, 10 μ L of the medium was removed and replaced with 10 μ L of doxazosin to make a final concentration of 37 μ M of doxazosin in 100 μ L of media. In control wells, the 100 μ L were made up with the media and 10 μ L of solvent (sterile water with addition of hydrochloric acid) used in the preparation of the serotonin hydrochloride solution to serve as the vehicle control. Also, cell free BL and BC were used for quality control. Following an incubation period of 72 h, cell viability was assessed using Cell-Titer 96® aqueous MTS assay. Each experiment was carried out in triplicate and repeated three times (n=9). Statistical analyses were carried out as mentioned earlier in section 2.4.

3.2.2 Evaluation of the effects of doxazosin on PC-3, DU145, LNCaP and HT1376 cells pre-incubated with serotonin creatinine sulphate:

The experiment was repeated using serotonin creatinine sulphate complex as serotonin hydrochloride was soluble only with addition of hydrochloric acid that may influence several metabolic processes within the cell. Also, serotonin is light sensitive and likely to degrade during preparation and pipetting into MP. Serotonin creatinine sulphate complex on the other hand is water soluble, more stable, and not prone to degradation by light.

PC-3, DU145, LNCaP or HT1376 cells were seeded in a 96-well MP at densities of 5000 cells in 100 μ L (per well) in serum containing medium and incubated overnight at 37 C. The media was replaced with serum free media (100 μ L) and incubated for a further 24h. Subsequently, by 10 μ L each was pipetted out and replaced with solutions of serotonin creatinine sulphate [1 x10⁻⁷ to 1 x 10⁻⁹M/L] (Sigma-Aldrich, catalogue number – H7752) to make a final volume of 100 μ L. The plates were returned to the incubator for 4 h. At the end of this period, in test wells, 10 μ L of

the medium was removed and replaced with 10 μ L of doxazosin to make a final concentration of 37 μ M of doxazosin in 100 μ L of media. In control wells, the 100 μ L were made up with the serum free media and 10 μ L of solvent (sterile water) used in the preparation of the serotonin creatinine sulphate solution to serve as the vehicle control. Also, cell free BL and BC were used for quality control. Following an incubation period of 48 h to 72 h, cell viability was assessed using BrdU ELISA assay as described earlier in section 2.2.2. Each experiment was carried out in triplicate and repeated 3 times (n=9). Statistical analyses were carried out as mentioned in section 2.4 in the previous chapter.

3.2.3 Evaluation of the effects of doxazosin on PC-3, DU145, LNCaP and HT1376 cells pre-incubated with clonidine:

PC-3, DU145, LNCaP or HT1376 cells were seeded in a 96-well MP at densities of 5000 cells in 100 μ L (per well) in serum containing medium and incubated at 37 C. After a 24 h interval, 10 μ L of the serum containing medium was removed and replaced with 10 μ L each of solutions of clonidine hydrochloride [final concentration of 100 μ M] (Catalogue Number C7897, Sigma Aldrich, Amersham, UK), to make a final volume of 100 μ L. The plates were returned to the incubator for 4 h. At the end of this period, in test wells, 10 μ L of the medium was removed and replaced with 10 μ L of doxazosin to make a final concentration of 37 μ M of doxazosin in 100 μ L of media. In control wells, the 100 μ L were made up with the media and 10 μ L of solvent (sterile water) used in the preparation of the clonidine to serve as the vehicle control. Also, cell free BL and BC were used for quality control. Following an incubation period of 72 h, cell viability was assessed using Cell-Titer 96® aqueous MTS assay. Each experiment was carried out in triplicate and repeated three times (n=9). Statistical analysis was carried out as mentioned earlier.

3.2.4 Evaluation of the effects of doxazosin on PC-3, DU145, LNCaP and HT1376 cells pre-incubated with yohimbine:

PC-3, DU145, LNCaP or HT1376 cells were seeded in a 96-well MP at densities of 5000 cells in 100 μ L (per well) in serum containing medium and incubated at 37 C. After a 24 h interval, 10 μ L of the serum containing medium was removed and replaced with 10 μ L each of solutions of yohimbine hydrochloride [final concentration of 1 to 4mM] (Sigma Aldrich- catalogue number – Y3125) to make a final volume of 100 μ L. The plates were returned to the incubator for 4 h. At the end of this period, in test wells, 10 μ L of the medium was removed and replaced with 10 μ L of doxazosin to make a final concentration of 37 μ M of doxazosin in 100 μ L of media. In control wells, the 100 μ L were made up with the media and 10 μ L of solvent (sterile water) used in the preparation of the yohimbine to serve as the vehicle control. Also, cell free BL and BC were used for quality control. Following an incubation period of 72 h, cell viability was assessed using Cell-Titer 96® aqueous MTS assay. Each experiment was carried out in triplicate and repeated three times (n=9). Statistical analyses were carried out as mentioned earlier.

3.2.5 Evaluation of the effects of doxazosin on PC-3, DU145, LNCaP and HT1376 cells pre-incubated with propranolol:

PC-3, DU145, LNCaP or HT1376 cells were seeded in a 96-well MP at densities of 5000 cells in 100 μ L (per well) in serum containing medium and incubated at 37 C. After a 24 h interval, 10 μ L of the serum containing medium was removed and replaced with 10 μ L each of solutions of propranolol [final concentration of 10 to 25 μ M] (Sigma Aldrich, catalogue number – P0884) to make a final volume of 100 μ L. The plates were returned to the incubator for 4 h. At the end of this period, in test wells, 10 μ L of

the medium was removed and replaced with 10 μ L of doxazosin to make a final concentration of 37 μ M of doxazosin in 100 μ L of media. In control wells, the 100 μ L were made up with the media and 10 μ L of solvent (sterile water) used in the preparation of the propranolol to serve as the vehicle control. Also, cell free BL and BC were used for quality control. Following an incubation period of 72 h, cell viability was assessed using Cell-Titer 96® aqueous MTS assay. Each experiment was carried out in triplicate and repeated 3 times (n=9). Statistical analyses were carried out as mentioned earlier under section 2.4.

3.2.6 Evaluation of the effects of doxazosin on PC-3, DU145, LNCaP and HT1376 cells pre-incubated with imiloxan:

PC-3, DU145, LNCaP or HT1376 cells were seeded in a 96-well MP at densities of 5000 cells in 100 μ L (per well) in serum containing medium and incubated at 37 C. After a 24 h interval, 10 μ L of the serum containing medium was removed and replaced with 10 μ L each of solutions of imiloxan hydrochloride [final concentration of 0.5 μ M to 1 μ M] (Sigma Aldrich, catalogue number – 19531) to make a final volume of 100 μ L. The plates were returned to the incubator for 4 h. At the end of this period, in test wells, 10 μ L of the medium was removed and replaced with 10 μ L of doxazosin to make a final concentration of 37 μ M of doxazosin in 100 μ L of media. In control wells, the 100 μ L were made up with the media and 10 μ L of solvent (sterile water) used in the preparation of the imiloxan to serve as the vehicle control. Also, cell free BL and BC were used for quality control. Following an incubation period of 72 h, cell viability was assessed using Cell-Titer 96® aqueous MTS assay. Each experiment was carried out in triplicate and repeated three times (n=9). Statistical analyses were carried out as mentioned earlier.

3.2.7 Evaluation of the effects of doxazosin on PC-3, DU145, LNCaP and HT1376 cells pre-incubated with guanabenz:

PC-3, DU145, LNCaP or HT1376 cells were seeded in a 96-well MP at densities of 5000 cells in 100 μ L (per well) in serum containing medium and incubated at 37 C. After a 24 h interval, 10 μ L of the serum containing medium was removed and replaced with 10 μ L each of solutions of guanabenz acetate salt [0.5 μ M to 10 μ M] (Sigma Aldrich, catalogue number – G110) to make a final volume of 100 μ L. The plates were returned to the incubator for 4 h. At the end of this period, in test wells, 10 μ L of the medium was removed and replaced with 10 μ L of doxazosin to make a final concentration of 37 μ M of doxazosin in 100 μ L of media. In control wells, the 100 μ L were made up with the media and 10 μ L of solvent solution [sterile water 7620 μ L + DMSO 1000 μ L + 1% acetic acid 200 μ L] used in the preparation of the guanabenz to serve as the vehicle control. Also, cell free BL and BC were used for quality control. Following an incubation period of 72 h, cell viability was assessed using Cell-Titer 96® aqueous MTS assay. Each experiment was carried out in triplicate and repeated three times (n=9). Statistical analyses were carried out as mentioned earlier in section 2.4.

3.2.8 Evaluation of the effects of doxazosin on PC-3, DU145, LNCaP and HT1376 cells pre-incubated with idazoxan:

PC-3, DU145, LNCaP or HT1376 cells were seeded in a 96-well MP at densities of 5000 cells in 100μ L (per well) in serum containing medium and incubated at 37 C. After a 24 h interval, $10~\mu$ L of the serum containing medium was removed and replaced with $10~\mu$ L each of solutions of idazoxan hydrochloride [1 to $10~\mu$ M] (Sigma Aldrich, catalogue number – 16138) to make a final volume of $100~\mu$ L. The plates were returned

to the incubator for 4 h. At the end of this period, in test wells, 10 μ L of the medium was removed and replaced with 10 μ L of doxazosin to make a final concentration of 37 μ M of doxazosin in 100 μ L of media. In control wells, the 100 μ L were made up with the media and 10 μ L of solvent (sterile water) used in the preparation of the idazoxan to serve as the vehicle control. Also, cell free BL and BC were used for quality control. Following an incubation period of 72 h, cell viability was assessed using Cell-Titer 96® aqueous MTS assay. Each experiment was carried out in triplicate and repeated three times (n=9). Statistical analyses were carried out as mentioned earlier (section 2.4).

3.3 RESULTS:

3.3.1 Effect of doxazosin on PC-3 cells pre-incubated with serotonin:

PC3 cells treated with serotonin had a proliferative effect when compared to solvent treated controls, and this was significant (p = 0.0052) for a serotonin concentration of 1 x 10^{-8} M/L. However, pre-incubation of serotonin did not attenuate the cytotoxic effect of doxazosin on PC3 cells when compared to doxazosin treated controls (p = 0.3240 at 10^{-8} M/L).

3.3.2 Effect of doxazosin on DU-145 cells pre-incubated with serotonin:

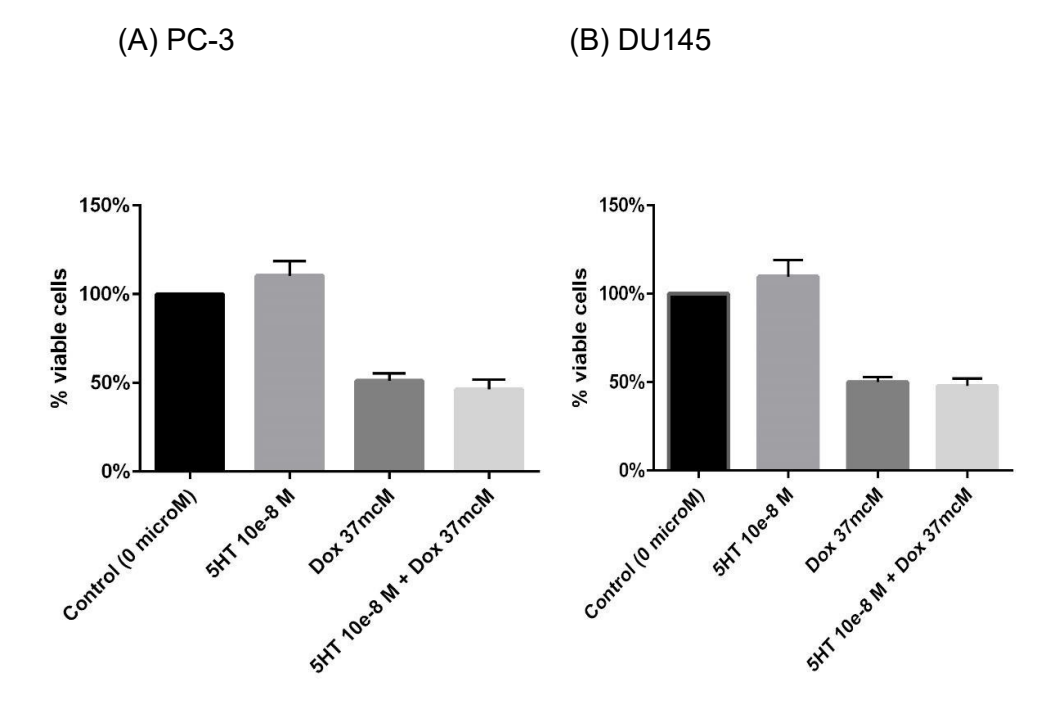
DU145 cells treated with serotonin had a proliferative effect when compared to solvent treated controls, and this was significant (p = 0.0071) for a serotonin concentration of 1 x 10^{-8} M/L. However, pre-incubation of serotonin did not attenuate the cytotoxic effect of doxazosin on DU145 cells when compared to doxazosin treated controls (p = 0.8396).

3.3.3 Effect of doxazosin on LNCaP cells pre-incubated with serotonin:

LNCaP cells treated with serotonin had a proliferative effect when compared to solvent treated controls, and this was significant (p < 0.001) for a serotonin concentration of 1 x 10^{-8} M/L. However, pre-incubation of serotonin did not attenuate the cytotoxic effect of doxazosin on LNCaP cells when compared to doxazosin treated controls (p = 0.5574).

3.3.4 Effect of doxazosin on HT1376 cells pre-incubated with serotonin:

HT1376 cells treated with serotonin has a proliferative effect when compared to solvent treated controls, and this was significant (p = 0.0080) for a serotonin concentration of 1 x 10^{-8} M/L. However, pre-incubation of serotonin did not attenuate the cytotoxic effect of doxazosin on HT1376 cells when compared to doxazosin treated controls (p = 0.8381).



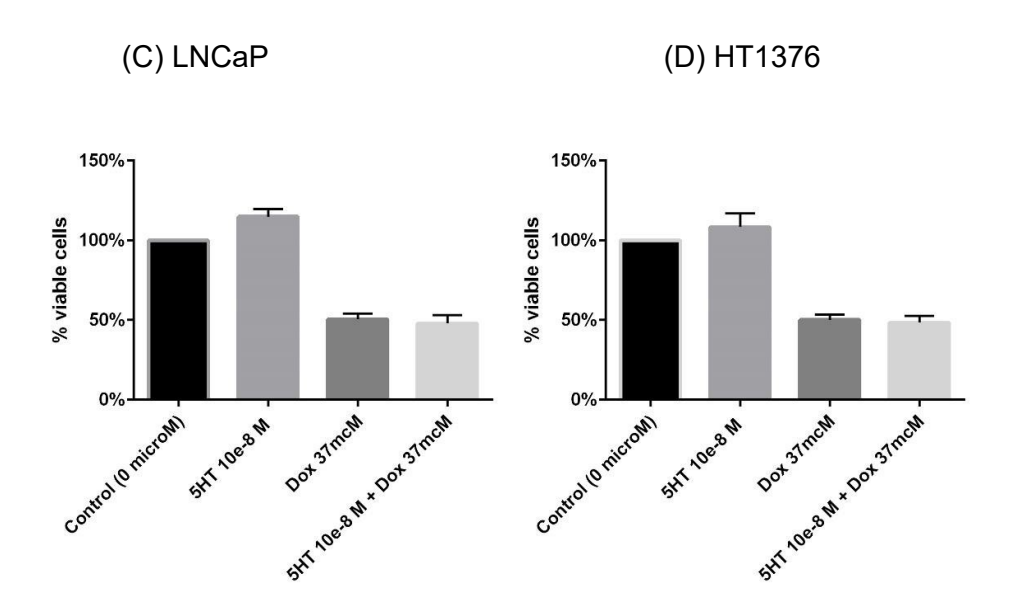


Figure 9: PC3 cells (a), DU145 cells (b), LNCaP cells (c) and HT1376 cells (d) preincubated with 10e-8 M/L 5HT for 4 h followed by doxazosin 37 μ M for 72 h.

3.3.5 Effect of doxazosin on PC-3 cells pre-incubated with serotonin creatinine sulphate:

PC3 cells treated with serotonin sulphate had a proliferative effect when compared to solvent treated controls, and this was significant (p <0.0001) for a serotonin creatinine sulphate concentration of 1 x 10^{-8} M/L. However, pre-incubation of serotonin creatinine sulphate did not attenuate the cytotoxic effect of doxazosin on PC3 cells when compared to doxazosin treated controls (p = 0.9763).

3.3.6 Effect of doxazosin on DU-145 cells pre-incubated with serotonin creatinine sulphate:

DU145 cells treated with serotonin creatinine sulphate had a proliferative effect when compared to solvent treated controls, and this was significant (p <0.0001) for a serotonin creatinine sulphate concentration of 1 x 10⁻⁸ M/L. However, pre-incubation of serotonin creatinine sulphate did not attenuate the cytotoxic effect of doxazosin on DU145 cells when compared to doxazosin treated controls (p = 0.7360).

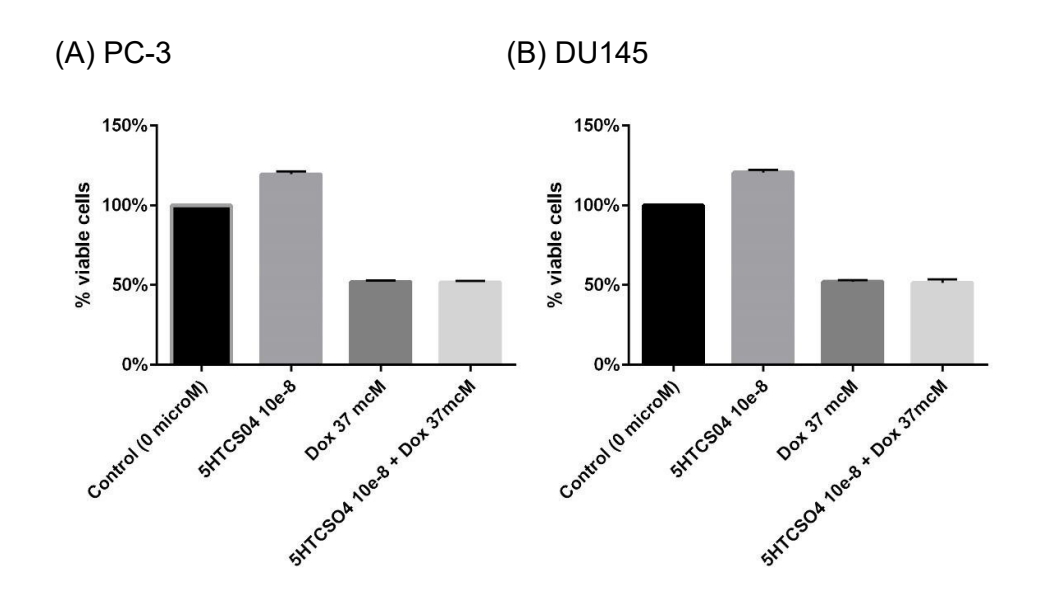
3.3.7 Effect of doxazosin on LNCaP cells pre-incubated with serotonin creatinine sulphate:

LNCaP cells treated with serotonin creatinine sulphate had a proliferative effect when compared to solvent treated controls, and this was significant (p <0.0001) for a serotonin creatinine sulphate concentration of 1 x 10^{-8} M/L. However, pre-incubation of serotonin creatinine sulphate did not attenuate the cytotoxic effect of doxazosin on LNCaP cells when compared to doxazosin treated controls (p = 0.9316).

3.3.8 Effect of doxazosin on HT1376 cells pre-incubated with serotonin creatinine sulphate:

HT1376 cells treated with serotonin creatinine sulphate had a proliferative effect when compared to solvent treated controls, and this was significant (p <0.0001) for a serotonin creatinine sulphate concentration of 1 x 10^{-8} M/L. However, pre-incubation

of serotonin creatinine sulphate did not attenuate the cytotoxic effect of doxazosin on HT1376 cells when compared to doxazosin treated controls (p = 0.9892).



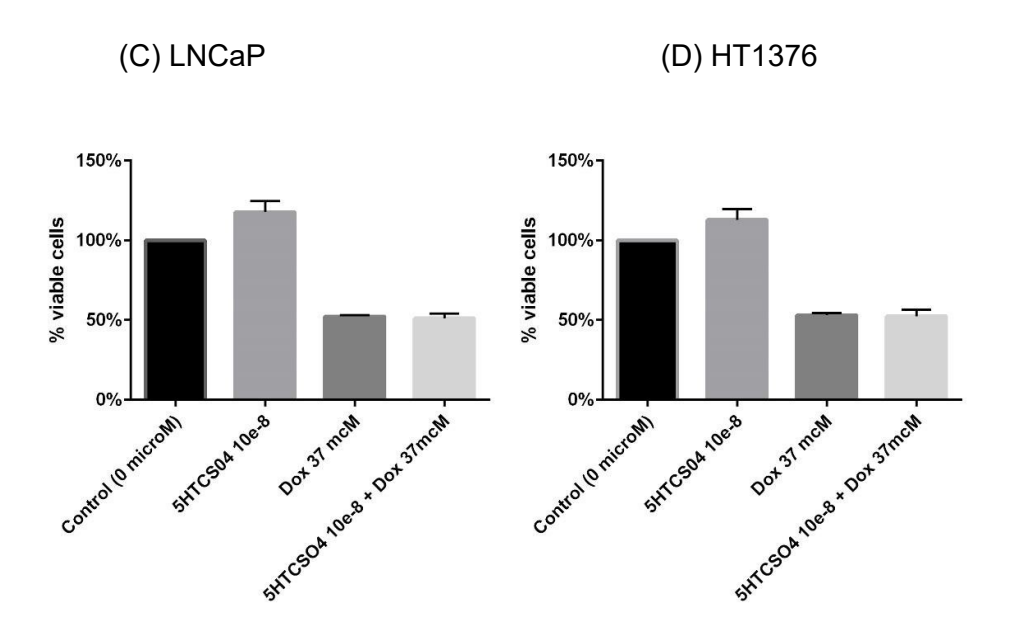


Figure 10: PC3 cells (a), DU145 cells (b), LNCaP cells (c) and HT1376 cells (d) preincubated with 10e-8 M/L serotonin creatine sulphate (5HTCSO4) for 4 h followed by doxazosin (Dox) 37 μ M for 72 h.

3.3.9 Effect of doxazosin on PC3 cells pre-incubated with clonidine:

PC3 cells treated with clonidine demonstrated no effect on growth when compared to solvent treated controls (p = 0.2387)). Moreover, pre-incubation of clonidine did not attenuate the cytotoxic effect of doxazosin on PC3 cells when compared to doxazosin treated controls (p = 0.9965).

3.3.10 Effect of doxazosin on DU145 cells pre-incubated with clonidine:

DU145 cells treated with clonidine demonstrated no effect on growth when compared to solvent treated controls (p = 0.8640). Moreover, pre-incubation of clonidine did not attenuate the cytotoxic effect of doxazosin on DU145 cells when compared to doxazosin treated controls (p = 0.9982).

3.3.11 Effect of doxazosin on LNCaP cells pre-incubated with clonidine:

LNCaP cells treated with clonidine demonstrated no effect on growth when compared to solvent treated controls (p = 0.8343). Moreover, pre-incubation of clonidine did not attenuate the cytotoxic effect of doxazosin on LNCaP cells when compared to doxazosin treated controls (p = 0.8327).

3.3.12 Effect of doxazosin on HT1376 cells pre-incubated with clonidine:

HT1376 cells treated with clonidine demonstrated no effect on growth when compared to solvent treated controls (p = 0.5762). Moreover, pre-incubation of clonidine did not attenuate the cytotoxic effect of doxazosin on HT1376 cells when compared to doxazosin treated controls (p = 0.4873).

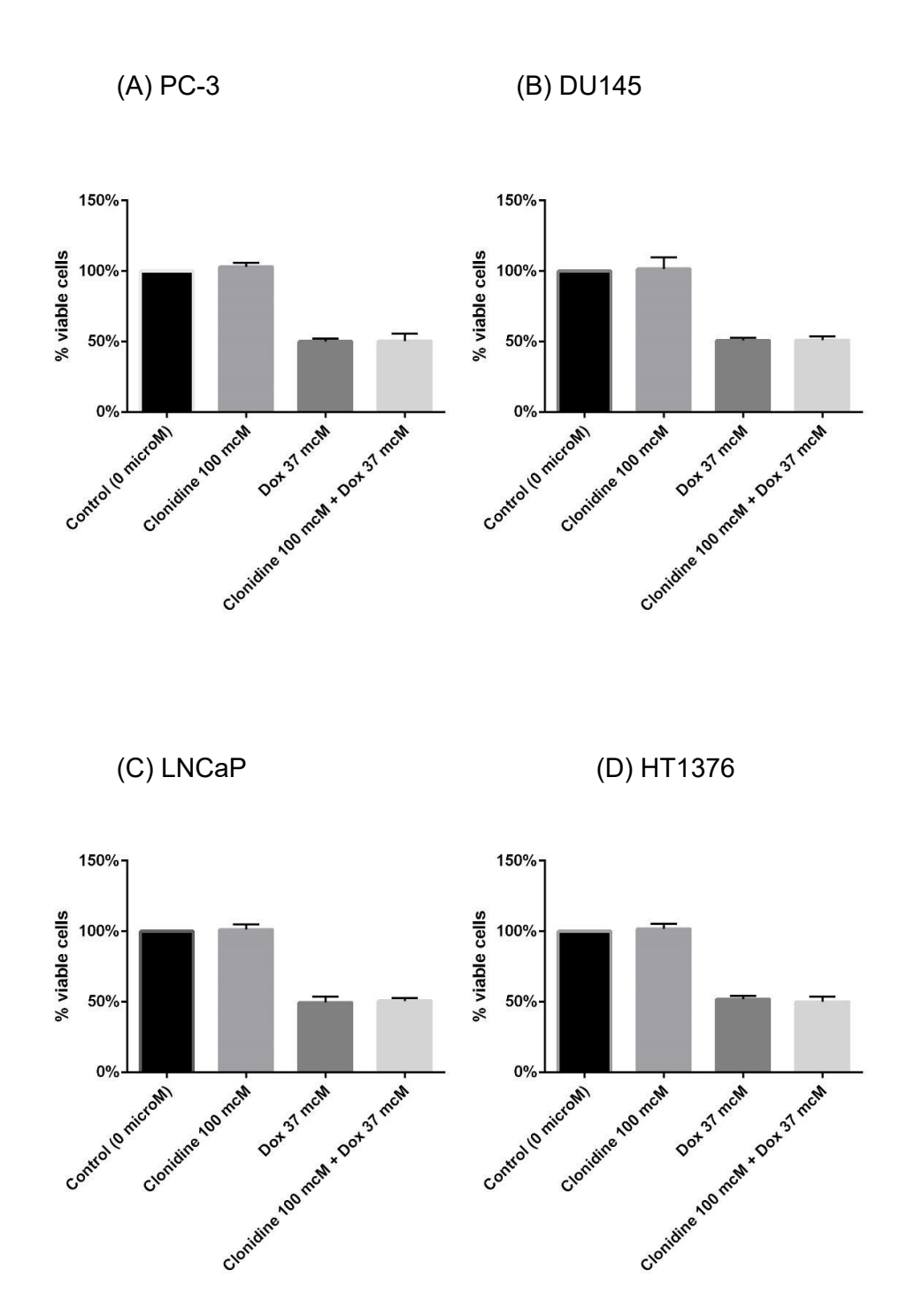


Figure 11: PC3 cells (a) DU145 cells (b) LNCaP cells (c) and HT1376 cells (d) preincubated with 100 μ M clonidine for 4 h followed by doxazosin (Dox) 37 μ M for 72 h.

3.3.13 Effect of doxazosin on PC3 cells pre-incubated with yohimbine:

PC3 cells treated with yohimbine demonstrated no effect on growth when compared to solvent treated controls (p = 0.9998). Moreover, pre-incubation of yohimbine did not attenuate the cytotoxic effect of doxazosin on PC3 cells when compared to doxazosin treated controls (p = 0.7283).

3.3.14 Effect of doxazosin on DU145 cells pre-incubated with yohimbine:

DU145 cells treated with yohimbine demonstrated no effect on growth when compared to solvent treated controls (p = 0.1139). Moreover, pre-incubation of yohimbine did not attenuate the cytotoxic effect of doxazosin on DU145 cells when compared to doxazosin treated controls (p = 0.9699).

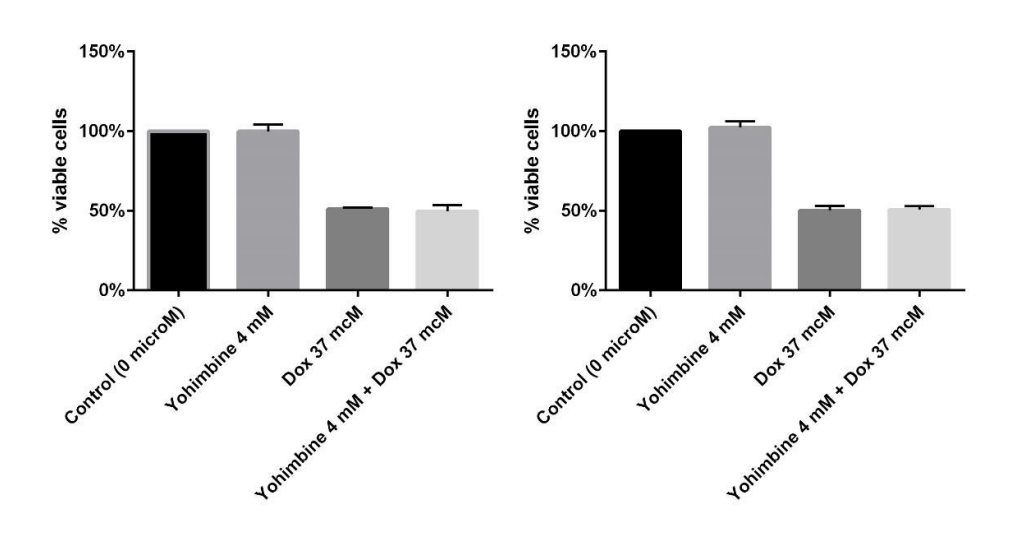
3.3.15 Effect of doxazosin on LNCaP cells pre-incubated with yohimbine:

LNCaP cells treated with yohimbine demonstrated no effect on growth when compared to solvent treated controls (p = 0.0866). Moreover, pre-incubation of yohimbine did not attenuate the cytotoxic effect of doxazosin on LNCaP cells when compared to doxazosin treated controls (p = 0.9324).

3.3.16 Effect of doxazosin on HT1376 cells pre-incubated with yohimbine:

HT1376 cells treated with yohimbine demonstrated no effect on growth when compared to solvent treated controls (p = 0.7426). Moreover, pre-incubation of yohimbine did not attenuate the cytotoxic effect of doxazosin on PC3 cells when compared to doxazosin treated controls (p = 0.8612).





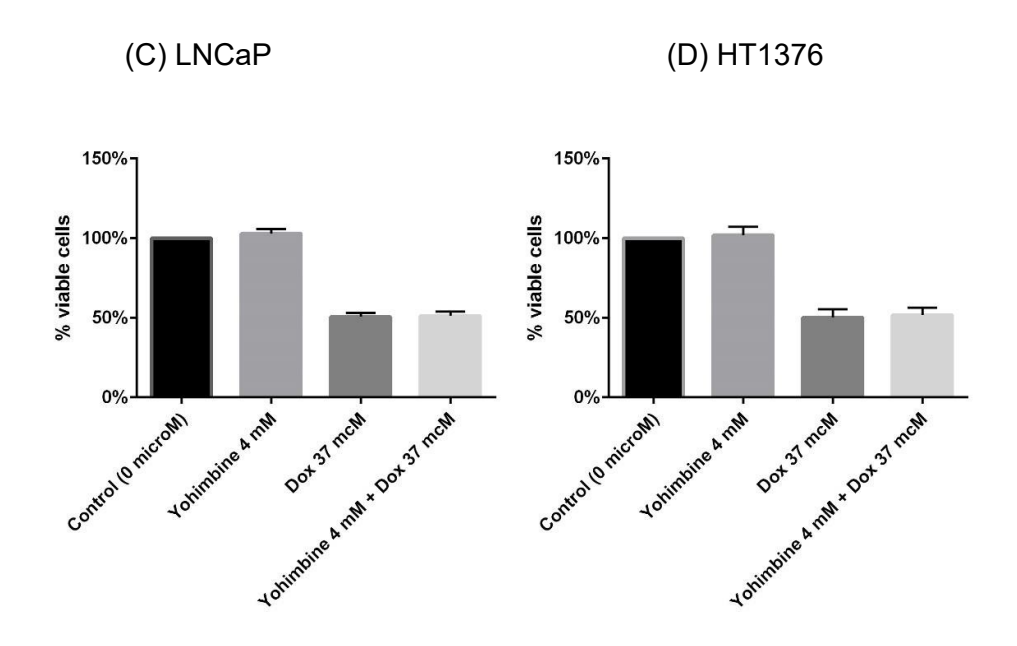


Figure 12: PC3 cells (a) DU145 cells (b) LNCaP cells (c) and HT1376 cells (d) preincubated with yohimbine (4 mM) for 4 h followed by doxazosin (Dox) 37 μ M for 72 h.

3.3.17 Effect of doxazosin on PC3 cells pre-incubated with propranolol:

PC3 cells treated with propranolol demonstrated no effect on growth when compared to solvent treated controls (p = 0.9816). Moreover, pre-incubation of propranolol did not attenuate the cytotoxic effect of doxazosin on PC3 cells when compared to doxazosin treated controls (p = 0.7939).

3.3.18 Effect of doxazosin on DU145 cells pre-incubated with propranolol:

DU145 cells treated with propranolol demonstrated no effect on growth when compared to solvent treated controls (p = 0.2519). Moreover, pre-incubation of propranolol did not attenuate the cytotoxic effect of doxazosin on DU145 cells when compared to doxazosin treated controls (p = 0.9986).

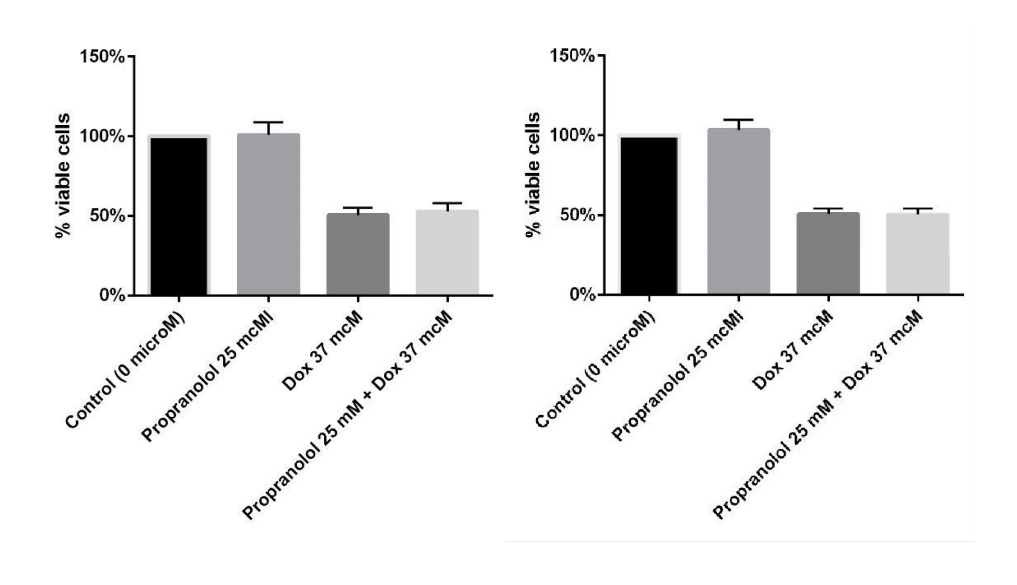
3.3.19 Effect of doxazosin on LNCaP cells pre-incubated with propranolol:

LNCaP cells treated with propranolol demonstrated no effect on growth when compared to solvent treated controls (p = 0.3708). Moreover, pre-incubation of propranolol did not attenuate the cytotoxic effect of doxazosin on LNCaP cells when compared to doxazosin treated controls (p = 0.3770).

3.3.20 Effect of doxazosin on HT1376 cells pre-incubated with propranolol:

HT1376 cells treated with propranolol demonstrated no effect on growth when compared to solvent treated controls (p = 0.2528). Moreover, pre-incubation of propranolol does not attenuate the cytotoxic effect of doxazosin on HT1376 cells when compared to doxazosin treated controls (p = 0.9522).





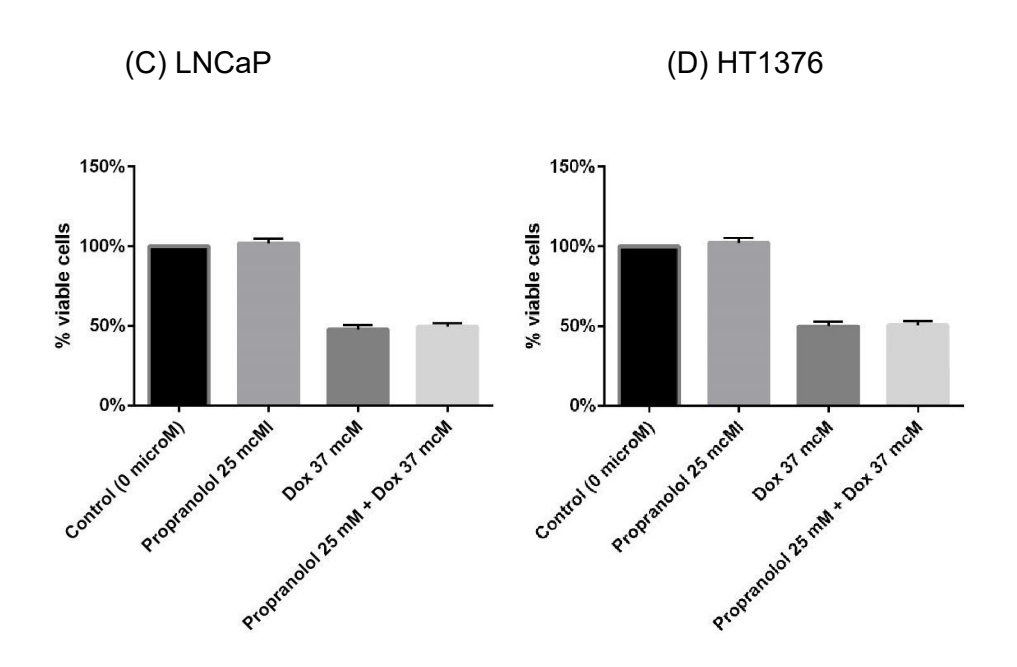


Figure 13: PC3 cells (a) DU145 cells (b) LNCaP cells (c) and HT1376 cells (d) preincubated with propranalol (25 μ M) for 4 h followed by doxazosin (Dox) 37 μ M for 72 h.

3.3.21 Effect of doxazosin on PC3 cells pre-incubated with imiloxan:

PC3 cells treated with imiloxan demonstrated no effect on growth when compared to solvent treated controls (p = 0.6579). Moreover, pre-incubation of imiloxan did not attenuate the cytotoxic effect of doxazosin on PC3 cells when compared to doxazosin treated controls (p = 0.9236).

3.3.22 Effect of doxazosin on DU145 cells pre-incubated with imiloxan:

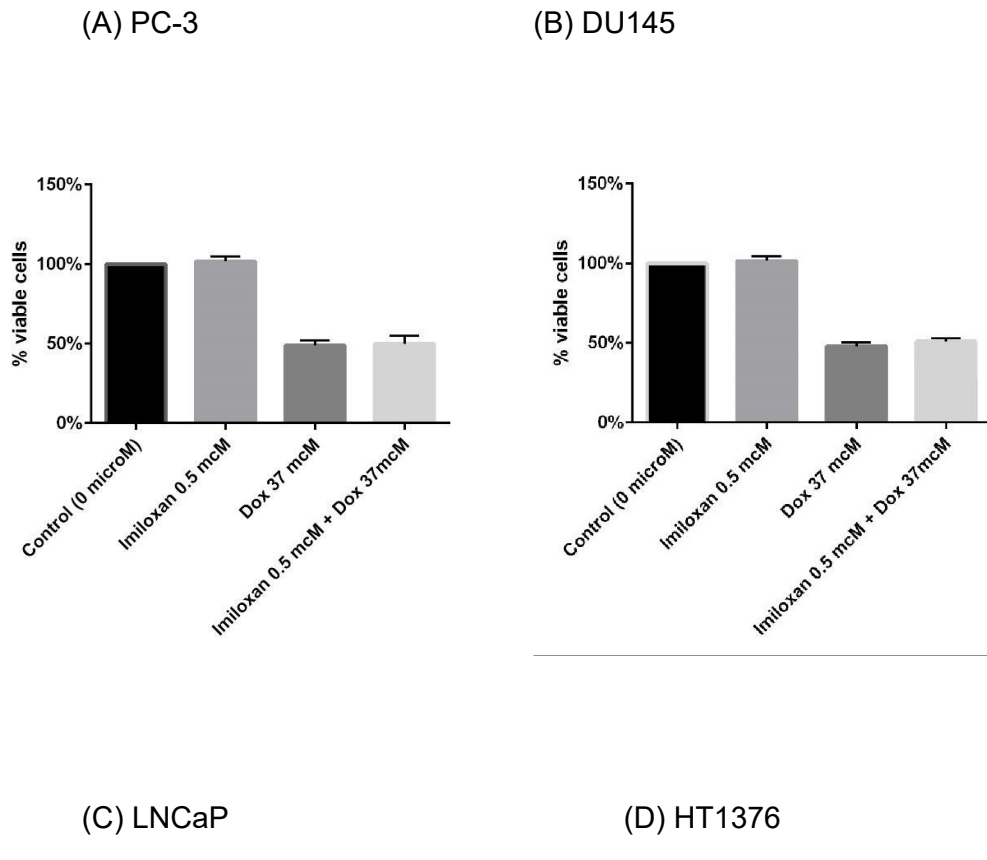
DU145 cells treated with imiloxan demonstrated no effect on growth when compared to solvent treated controls (p = 0.3565). Moreover, pre-incubation of imiloxan did not attenuate the cytotoxic effect of doxazosin on DU145 cells when compared to doxazosin treated controls (p = 0.238).

3.3.23 Effect of doxazosin on LNCaP cells pre-incubated with imiloxan:

LNCaP cells treated with imiloxan demonstrated no effect on growth when compared to solvent treated controls (p = 0.4733). Moreover, pre-incubation of imiloxan did not attenuate the cytotoxic effect of doxazosin on LNCaP cells when compared to doxazosin treated controls (p = 0.9023).

3.3.24 Effect of doxazosin on HT1376 cells pre-incubated with imiloxan:

HT1376 cells treated with imiloxan demonstrated no effect on growth when compared to solvent treated controls (p = 0.5662). Moreover, pre-incubation of imiloxan not attenuate the cytotoxic effect of doxazosin on HT1376 cells when compared to doxazosin treated controls (p = 0.8215).



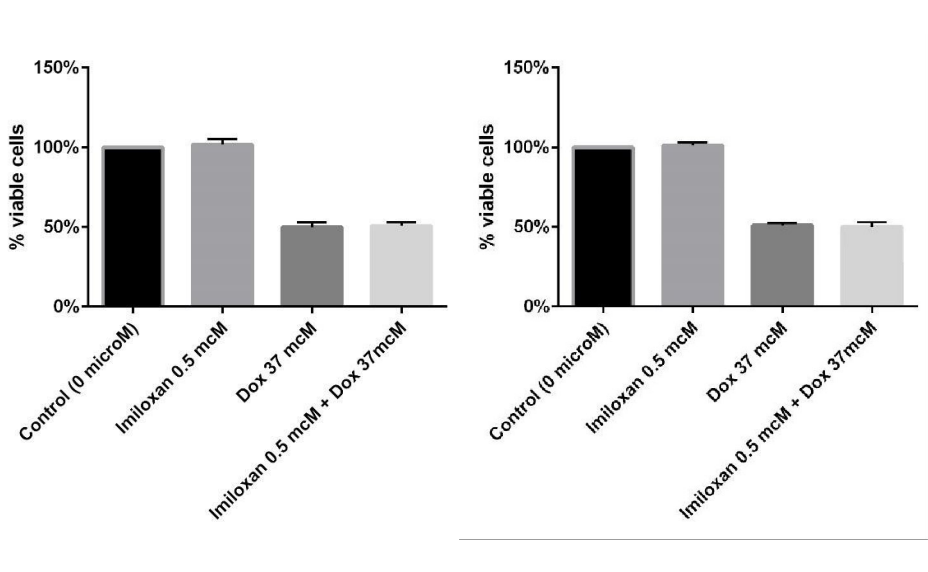


Figure 14: PC3 cells (a) DU145 cells (b) LNCaP cells (c) and HT1376 cells (d) preincubated with imiloxan (0.5 μ M) for 4 h followed by Doxazosin (Dox) 37 μ M for 72 h.

3.3.25 Effect of doxazosin on PC3 cells pre-incubated with guanabenz:

PC3 cells treated with guanabenz demonstrated no effect on growth when compared to solvent treated controls (p = 0.9412). Moreover, pre-incubation of guanabenz did not attenuate the cytotoxic effect of doxazosin on PC3 cells when compared to doxazosin treated controls (p = 0.6310).

3.3.26 Effect of doxazosin on DU145 cells pre-incubated with quanabenz:

DU145 cells treated with guanabenz demonstrated no effect on growth when compared to solvent treated controls (p = 0.4052). Moreover, pre-incubation of guanabenz did not attenuate the cytotoxic effect of doxazosin on DU145 cells when compared to doxazosin treated controls (p = 0.9862).

3.3.27 Effect of doxazosin on LNCaP cells pre-incubated with guanabenz:

LNCaP cells treated with guanabenz demonstrated no effect on growth when compared to solvent treated controls (p = 0.4561). Moreover, pre-incubation of guanabenz did not attenuate the cytotoxic effect of doxazosin on LNCaP cells when compared to doxazosin treated controls (p = 0.9136).

3.3.28 Effect of doxazosin on HT1376 cells pre-incubated with guanabenz:

HT1376 cells treated with guanabenz demonstrated no effect on growth when compared to solvent treated controls (p = 0.1723). Moreover, pre-incubation of guanabenz did not attenuate the cytotoxic effect of doxazosin on HT1376 cells when compared to doxazosin treated controls (p = 0.4290).

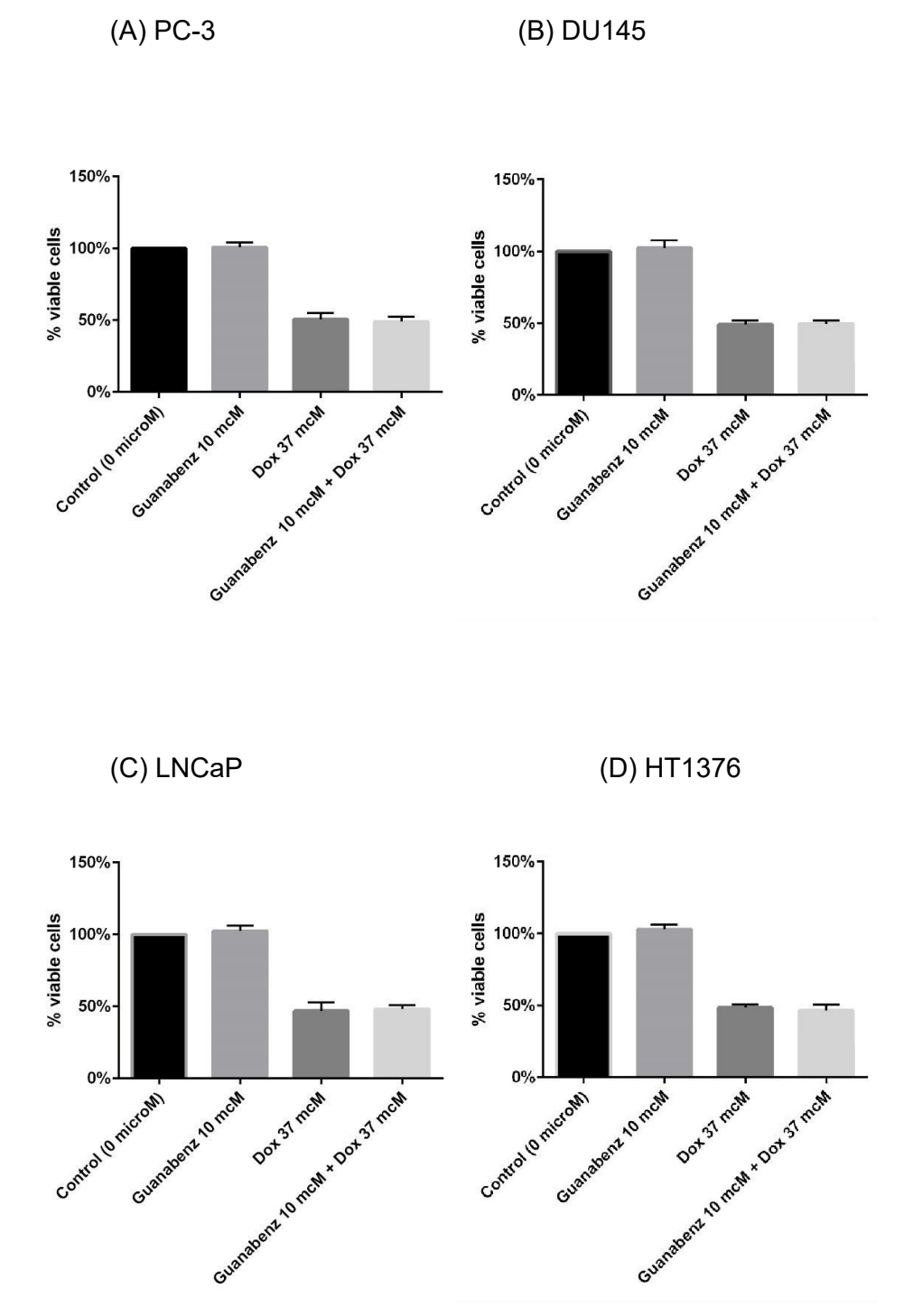


Figure 15: PC3 cells (a) DU145 cells (b) LNCaP cells (c) and HT1376 cells (d) preincubated with guanabenz (10 μ M) for 4 h followed by doxazosin (Dox) 37 μ M for 72 h.

3.3.29 Effect of doxazosin on PC3 cells pre-incubated with idazoxan:

PC3 cells treated with idazoxan demonstrated a significant reduction in growth when compared to solvent treated controls (p = 0.0027). However, pre-incubation of idazoxan did not attenuate the cytotoxic effect of doxazosin on PC3 cells when compared to doxazosin treated controls (p = 0.9700).

3.3.30 Effect of doxazosin on DU145 cells pre-incubated with idazoxan:

DU145 cells treated with idazoxan demonstrated a significant reduction in growth when compared to solvent treated controls (p = 0.0394). However, pre-incubation of idazoxan did not attenuate the cytotoxic effect of doxazosin on DU145 cells when compared to doxazosin treated controls (p = 0.9636).

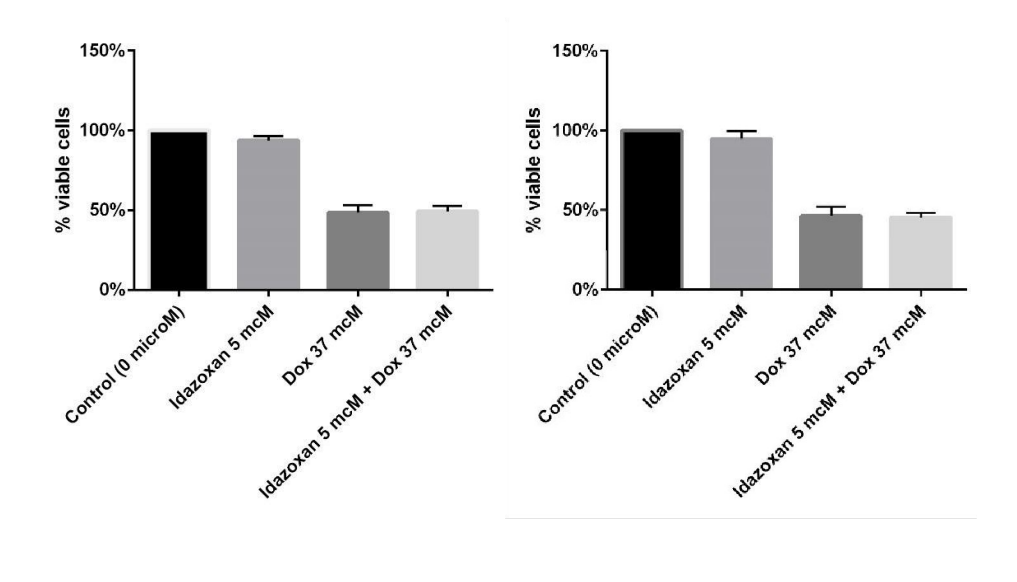
3.3.31 Effect of doxazosin on LNCaP cells pre-incubated with idazoxan:

LNCaP cells treated with idazoxan demonstrated no effect on growth when compared to solvent treated controls (p = 0.9332). Moreover, pre-incubation of idazoxan did not attenuate the cytotoxic effect of doxazosin on LNCaP cells when compared to doxazosin treated controls (p = 0.5466).

3.3.32 Effect of doxazosin on HT1376 cells pre-incubated with idazoxan:

HT1376 cells treated with idazoxan demonstrated no effect on growth when compared to solvent treated controls (p = 0.1117). Moreover, pre-incubation of idazoxan not attenuate the cytotoxic effect of doxazosin on HT1376 cells when compared to doxazosin treated controls (p = 0.9835).







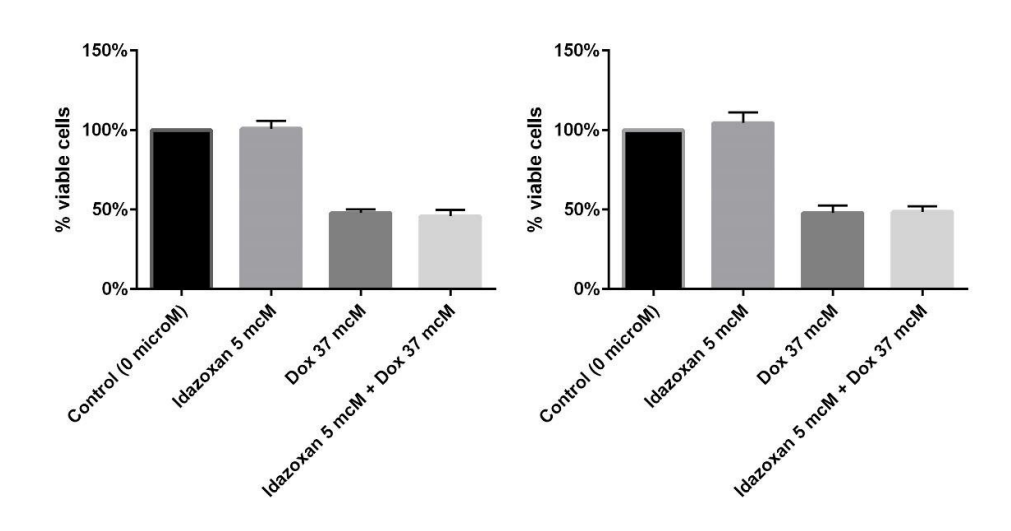


Figure 16: PC3 cells (a) DU145 cells (b) LNCaP cells (c) and HT1376 cells (d) preincubated with idazoxan (5 μ M) for 4 h followed by doxazosin (Dox) 37 μ M for 72 h. Idazoxan significantly inhibited growth of PC3 cells and DU145 cells but not in the LNCaP cells and HT1376 cell lines.

3.4 Discussion

The adrenergic compounds tested included several adrenergic agonists and antagonists namely clonidine, idazoxan and guanabenz (alpha-2 selective agonist), yohimbine (non-selective alpha antagonist), propranolol (non-selective beta antagonist) and imiloxan (alpha-2B antagonist).

We found 5HT induced proliferation of the cell lines we tested, however, pretreatment with 5HT did not attenuate cell death induced by doxazosin. These results were similar to previous studies that had shown that serotonin induces proliferation of PCa and BCa cells *In Vitro* (Siddiqui, Shabbir et al. 2005) and that their effects on proliferation is inhibited by 5HT antagonists (Abdul, Anezinis et al. 1994). The relationship between 5HT receptors and doxazosin has been reported in studies on platelet activation (Jagroop and Mikhailidis 2001) and in cavernous smooth muscle contraction (Lau, Thompson et al. 2006). Furthermore, it has been hypothesized that 5HT receptors could possibly mediate the growth inhibitory effects of doxazosin (Siddiqui, Shabbir et al. 2005).

Our experiments involving pre-treatment by serotonin hydrochloride [1 x 10⁻¹² to 1 x 10⁻⁶] for 4 h was unable to demonstrate that 5HT receptors mediated doxazosin induced growth inhibition using Cell-Titer 96[®] aqueous MTS assay. Subsequently, we repeated the experiments using serotonin creatinine sulphate [1 x 10⁻⁹ to 1 x 10⁻⁶], which had better solubility in water as well as being more stable and not photo degradable. In these experiments too, we were unable to demonstrate that doxazosin mediated growth was mediated by 5HT receptors. We also repeated the experiment using BrdU assay with serotonin creatinine sulphate [1 x 10⁻⁹ to 1 x 10⁻⁶], obtained similar results to that of Cell-Titer 96[®] aqueous MTS assay. Taken together,

we concluded that 5HT receptors did not mediate the cytotoxic effects of doxazosin in the PCa and BCa cell lines we tested.

Subsequently, we investigated the role of other adrenergic receptors that had a structural similarity to alpha-1 adrenergic receptors. Whilst we had already shown that pre-treatment with phenoxybenzamine did not attenuate the growth effects of doxazosin, we used another non-selective alpha antagonist, namely, yohimbine to confirm these results. Not surprisingly, yohimbine did not attenuate the growth inhibition by doxazosin.

Given the structural similarity of alpha-1 receptors to alpha-2 adrenergic receptors, we tested if clonidine, idazoxan and guanabenz (alpha-2 agonists), imiloxan (selective alpha-2B antagonist) and propranolol (non-selective beta antagonist) would have any effect on the growth inhibition by doxazosin. Idazoxan inhibited the growth of PC3 cells and DU145 cells but not of LNCaP and HT1376 cells. The growth inhibition of DU145 cells by idazoxan had already been reported previously though the mechanism of action remains to be fully elucidated (Eilon, Weisenthal et al. 2009). PC3 and DU145 cells are androgen resistant cell lines whilst LNCaP is androgen-dependent, and HT1376 is a cell line developed from high grade BCa with no relation to androgen. These findings suggest that growth inhibitory actions of idazoxan could be related to the androgen-resistant status of PC3 and DU145 cells. Nonetheless, idazoxan did not have any effect on growth inhibition by doxazosin in any of the cell lines we tested. Pre-treatment with clonidine, guanabenz, imiloxan, and propranolol compounds did not attenuate the cell death induced by doxazosin.

We concluded that doxazosin did not mediate its actions on cell viability via receptors that have structural similarity to alpha-1 adrenergic receptor. Nonetheless, at this stage of experiments the receptor that mediated the cytotoxic actions of doxazosin remained elusive. After these results we embarked on developing doxazosin-resistant cells as these cells could potentially lead to the up regulation or down regulation of the receptors that mediated the growth inhibiting actions of doxazosin and these are described in further detail in the next chapter.

Chapter 4

Development of doxazosin-resistant prostate cancer cells

4.1 Introduction

In PCa, not confined to the prostate gland, androgen ablation is the mainstay of treatment. However, this is not curative as eventually the cancer cells develop resistance to androgen ablation treatment (becomes androgen-independent) and to subsequent chemotherapeutic agents. Thus, progression of PCa during treatment can be seen as selective survival and proliferation of resistant cells. Understanding the differences in cells that survive chemotherapy would help to determine the adaptive mechanisms involved in development of resistance by cancer cells. As the mechanism of action of doxazosin was receptor-mediated, development of a cell line that is resistant to doxazosin could potentially be a useful substrate to investigate those receptors that will be upregulated or down regulated when rendered resistant to doxazosin. Also, doxazosin-resistant cancer cells had not been developed to date, and development of a resistant cell line would serve as a valuable tool for future studies.

We attempted to develop drug-resistant cancer cell lines of prostate (PC-3, DU-145 and LNCaP) using previously established experimental protocols (Chien, Astumian et al. 1999). In brief, logarithmically growing cells were exposed *In Vitro* to: (a) serially increasing concentrations of doxazosin to a maximum dose of 100 μ M, and (b) exposure of cells to a low dose doxazosin for longer periods.

However, the protocols were not specific for developing cells that can be rendered resistant to doxazosin as doxazosin-resistant cell lines had not been established previously. The first step in establishment of successful development of resistance was to compare the IC₅₀ with control cell populations.

4.2 Development of Cell Lines Resistant to Doxazosin

4.2.1 Treatment of PC-3, DU-145 and LNCaP cell lines to serially increasing concentrations of doxazosin:

Cell lines (PC-3, DU-145 and LNCaP) grown in serum containing media were exposed to serially increasing concentrations (12.5, 25, 37.5, 50, 75 and 100 µM doxazosin) in an attempt to develop doxazosin resistant cell lines.

The cells were grown in serum containing media in 75 cm² flasks (n=12) to nearly confluence (60-70%). The cells were washed twice with PBS and fresh serum containing media (18 ml) containing doxazosin (final doxazosin concentration of 12.5 µM) was added. The cells were observed under light microscope daily for progress in proliferation, excessive cell death and anoikis. The media (with addition of doxazosin) was changed every 48 h.

Following 7 to 14 days of treatment, the concentration of doxazosin was increased - in a serial stepwise manner every week – from initial first chosen concentrations of 12.5 μ M and 25 μ M, with a view to serially increase to 37.5,50, 75 and 100 μ M of doxazosin.

Controls (n=12) were maintained in separate flasks and treated in the same manner without the addition of doxazosin. Where full confluence necessitated splitting the growth over a larger surface area, trypsin-EDTA was used for detaching the cells. Once detached, the cells were pelleted by centrifugation at 500 rpm for 5 minutes. The cell pellet was re-suspended in 1ml of serum free media. Half of this volume was seeded into 75 cm² flasks and the newly seeded cells were allowed to attach overnight prior to adding appropriate concentration of doxazosin.

The doxazosin-treated cells and the controls were treated with 37.5 μ M doxazosin and the IC₅₀ compared every 7 days. The concentration was serially increased if there was a statistically significant reduction in doxazosin-induced cell death to 37.5 μ M in doxazosin pre-treated cells as compared to solvent pre-treated control cells.

4.2.2 Treatment of PC-3, DU-145 and LNCaP cell lines to prolonged, low-dose concentrations of doxazosin:

Cell lines (PC-3, DU-145 and LNCaP) grown in serum containing media were exposed to low dose concentrations (3.125, 6.25 µM doxazosin) for 3 weeks in an attempt to develop doxazosin-resistant cell lines.

DU-145, PC-3 or LNCaP cells grown in serum containing media 75 cm² were grown to near confluence (60-70%). The cells were washed twice with PBS and grown in serum containing media (18 ml) containing appropriate concentrations of doxazosin (to obtain final doxazosin concentrations of 3.125 μ M, 6.25 μ M were added (n=12 for each group). The cells were observed under light microscope every 48 to 72 h for progress in proliferation, excessive cell death and anoikis. The media (with doxazosin) was changed every 48 h.

Controls (n=12) were maintained in separate flasks and treated in the same manner with the addition of diluent (water) only. Where full confluence necessitated splitting the growth over a larger surface area, trypsin-EDTA was used for detaching the cells. Once detached, the cells were pelleted by centrifugation at 500 rpm for 5 minutes. The cell pellet was re-suspended in 1ml of serum free media. Half of this volume was seeded into 75 cm² flasks and the newly seeded cells were allowed to attach overnight prior to adding appropriate concentration of doxazosin or diluent.

The doxazosin-treated cells and the controls were treated with 37.5 μ M doxazosin and the IC₅₀ compared every 7 days. The concentration was serially increased if there was a statistically significant reduction in doxazosin-induced cell death to 37.5 μ M in doxazosin pre-treated cells as compared to solvent pre-treated control cells.

4.3 Investigation of Effects of Doxazosin in Serum Deprived Conditions on PC-3, DU-145 and LNCaP Cells

4.3.1 Evaluation of the effects of doxazosin on PC-3, DU-145 and LNCaP cell lines in serum free media:

DU-145, PC-3 or LNCaP cells were seeded in 96-well MT plates at 5000 cells per 100 μ L in appropriate serum containing media and 1% antibiotic solution. After overnight incubation at 37C, the media from the test wells were decanted, washed thrice with PBS, and replaced with serum free media (90 μ L) containing 1% antibiotic solution of grown in serum containing penicillin, streptomycin, and amphotericin B and doxazosin (12.5 μ M, 25 μ M, 37 μ M and 50 μ M or water).

In control wells, the media from the wells were decanted, washed thrice with PBS, and replaced with appropriate serum containing media and 1% antibiotic solution and doxazosin (12.5 μ M, 25 μ M, 37 μ M and 50 μ M or water). After 72 h of incubation, Cell-Titer 96® aqueous MTS assay was performed. The IC50 in serum free condition were calculated for the individual cell lines.

4.3.2 Evaluation of the effects of doxazosin on PC-3, DU-145 and LNCaP cell lines in serum free media supplemented with lipoprotein deficient serum (LPDS) and/or cholesterol:

DU-145, PC-3 or LNCaP cells were seeded in 96 well MT plates at 5000 cells per 100 µL in appropriate serum containing media and 1% antibiotic solution. After overnight

incubation at 37C, the media from the test wells were decanted, washed thrice with PBS, and replaced with one of the following: (a) serum free media (90 μ L), (b) serum added media (90 μ L), (c) serum free media (90 μ L) and 10% LPDS, (d) serum free media (90 μ L), and 10% LPDS and cholesterol (1:1000 solution)

Additionally, doxazosin 20 µM was added to test well whilst water was added to control wells. After 72 h of incubation, Cell-Titer 96® aqueous MTS assay was performed.

4.4 Evaluation of the effects of Doxazosin on Lipid Receptor-deficient Fibroblasts:

This cell line was developed from a patient with homozygous familial hypercholesterolemia with Pro664Leu mutation in the LDL receptor gene (Bourbon, Fowler et al. 1999). The cells were grown in MEME supplemented with 10% foetal calf serum and 1% antibiotic solution containing penicillin, streptomycin, and amphotericin B.

Low passage cells were grown to 40% confluence and detached by EDTA-trypsin and plated at a density of 2500 cells per well in 96 well MP for overnight incubation at 37 C. Subsequently 10 μ L of media was aspirated out and replaced with 10 μ L of doxazosin [12.5 μ M, 25 μ M, 37 μ M and 50 μ M, 75 μ M] and control wells received 10 μ L water (solvent). Dose-response curves at 48 h was performed using Cell-Titer 96® aqueous MTS assay and onset of any granulations were noted by inspection under light microscopy.

4.5 Results

4.5.1 Observations using light microscopy:

All cells treated with doxazosin developed a granular appearance of the cytoplasm on light microscopy. Control samples were devoid of the granular changes. When treated with doxazosin, amongst all the cell lines tested (PC3, DU145, LNCaP), PC-3 cells showed the most marked granular appearance whilst in HT-1376 cells these granulations were difficult to appreciate as these cells do not form a uniform monolayer and tend to grow into several layers.

The onset of granular appearance was directly proportional to the concentration of doxazosin - the higher the concentration of doxazosin the faster the granulation appeared with the cytoplasm. We, therefore, embarked on identifying and further characterizing the appearance of granulations that were observed on light microscopy.

4.5.1.1 Further experiments conducted in view of light microscopy findings:

First, we looked at the lowest concentration required for the appearance of granulations and the time taken for these to be observable by light microscopy. We treated the above cell lines (n=6 each) at 60% confluence with doxazosin 1, 2 and 5 µM/L or water (controls) until granulations became noticeable on light microscopy. The cells were observed under light microscope every 24 h for progress in proliferation, excessive cell death or anoikis. The media (with doxazosin or control) was changed every 48 to 72 h. Where full confluence necessitated splitting the growth over a larger surface area, trypsin-EDTA was used for detaching the cells. Once detached, the cells were pelleted by centrifugation at 500 rpm for 5 minutes.

The cell pellet was re-suspended in 1ml of serum free media. Half of this volume was seeded into 75 cm² flasks and the newly seeded cells were allowed to attach overnight prior to adding appropriate concentration of doxazosin or diluent.

We did not observe the appearance of granulations in the first 96 of exposure in any of the low-dose exposures. At 96 h, granulations were observed in the cells exposed to 5 μ M doxazosin; similarly, the granulations appeared at 144 and 168 h for 2 μ M and 1 μ M, respectively.

Next, we investigated if the granular appearance of cytoplasm could be reversed if exposure to doxazosin was terminated and cells were continued to grow in the absence of doxazosin. The above cell lines (n=6 each) were exposed to doxazosin (water for controls). Once granulations were observable the cells were incubated with doxazosin (or water) for a further 24 h. Subsequently, cells were washed with PBS twice and allowed to grow in their respective media (without doxazosin). The media (with doxazosin or control) was changed every 48 to 72 h. Where full confluence necessitated splitting the growth over a larger surface area, trypsin-EDTA was used for detaching the cells. Once detached, the cells were pelleted by centrifugation at 500 rpm for 5 minutes. The cell pellet was re-suspended in 1ml of serum free media. Half of this volume was seeded into 75 cm² flasks and the newly seeded cells were allowed to attach overnight prior to adding appropriate concentration of doxazosin or diluent. The granulations were found to gradually disappear when exposure to doxazosin was removed. The time taken for the disappearance of granular appearance was proportional to the concentration of doxazosin exposed - the lower the concentration of doxazosin the faster the granulations disappeared from the cytoplasm [Table 3].

Table 3. Data showing the various time points for the onset of granulation (middle column) following exposure of PC-3, DU-145 and LNCaP cells to various concentrations of and right column shows time taken to observe disappearance of granulations after the exposure had been terminated; ICD = irreversible cell death.

| Doxazosin concentration | Time taken for onset of granulation (Hours) | | | Time taken for disappearance of granulation (Hours) | | |
|-------------------------|---|-------|-------|---|-------|-------|
| | PC-3 | DU145 | LNCaP | PC-3 | DU145 | LNCaP |
| 1 μM/L | 168 | 168 | 168 | 24 | 24 | 24 |
| 2 μM/L | 144 | 144 | 144 | 24 | 24 | 24 |
| 5 μM/L | 96 | 96 | 96 | 48 | 24 | 24 |
| 6.25 μM/L | 72 | 96 | 72 | 48 | 48 | 48 |
| 12.5 μM/L | 48 | 72 | 72 | 48 | 48 | 48 |
| 25 μM/L | 36 | 48 | 48 | 72 | 48 | 72 |
| 37.5 μM/L | 24 | 36 | 24 | 72 | 72 | 96 |
| 50 μM/L | 18 | 18 | 18 | 96-144 | 96 | 144 |
| 75 μM/L | 4 | ICD* | ICD* | ICD* | ICD* | ICD* |
| 100 μM/L | 1 | ICD* | ICD* | ICD* | ICD* | ICD* |

4.5.1.2 Measurement of maximum tolerable dose of doxazosin:

The maximum dose that cells tolerated exposure for 24 h was 50 μ M/L. At 60 μ M/L and beyond, most cells underwent cell death or anoikis and were detached (floating) from the monoculture. It was also observed that those cells that remained attached were unable to re-attach following EDTA-trypsinization. If doxazosin exposure was terminated (without subjecting the cells to EDTA-trypsinization), the cells took more than 21 days to resume back to the same pace of growth (doubling time) as compared to matched controls.

4.5.2 Preparation of cells for identification of lipofuscin granules:

Low passage PC-3, DU-145 and LNCaP cells were thawed from -80C, subjected to 2 passages at sub-confluence, harvested (EDTA-trypsin), seeded in 25 cm² pre-labelled flasks and incubated for 24 h. The flasks were divided into test group (exposed to 37.5 µM doxazosin) and control group. Doxazosin was added to test flasks and water added to controls and incubated for the requisite period, after which the cells were detached using trypsin-EDTA, pelleted and washed.

The cell pellets were processed into paraffin blocks and stained for lipofuscin using the DAPS which stains lipofuscin in magenta colour, and with aldehyde fuchsin which demonstrates lipofuscin in deep purple.

All 3 cell lines tested were negative for lipofuscin as compared to controls, thus demonstrating the granules observed in TEM were not due to lipofuscin formation in doxazosin treated cells.

4.5.3 Evaluation of the effects of treatment of PC-3 cells to serially increasing concentrations of doxazosin:

There was no difference in the number of viable cells in the PC-3 control group versus the PC-3 DR group (p = 0.1737). Exposure of PC-3 cells to 12.5 μ M doxazosin for one week resulted in a significant (p = 0.0209) increase in cell death induced by doxazosin (37 μ M) in PC3-DR cells when compared to control PC-3 cells (Figure.17A).

We incubated the PC3-DR cells with the same concentration of doxazosin 12.5 μ M for another week and the experiment repeated after another 8 days of incubation (week 2). We observed that the number of viable cells in PC3-DR cells were significantly less (p = 0.0008) when compared to PC-3 control group. Also, there was a significant (p =

0.0003) increase in cell death induced by doxazosin (37 µM) in PC3-DR cells when compared to control PC-3 cells (Figure.17B).

These results suggested that treatment with 12.5 µM doxazosin for 1-2 weeks did not render the cells resistant to doxazosin. On the contrary, the doxazosin-treated cells underwent significantly more cell death as compared to solvent treated controls, suggesting that pre-exposure to doxazosin rendered the cells more susceptible to cell death and not vice versa.

4.5.4 Evaluation of the effects of treatment of DU-145 cells to serially increasing concentrations of doxazosin:

When the DU-145 control cells were compared to DU145-DR controls, there was a significant reduction in the in the number of viable cells in the DU145-DR (p = 0.0081), suggesting that growth DU-145 cells were impeded following exposure to DU-145 cells to 12.5 μ M doxazosin for one week. However, there was no significant difference (p = 0.3518) when these were incubated with 37 μ M doxazosin for a further 72 h (Figure.18A)

We then incubated the DU145-DR cells with the same concentration of doxazosin 12.5 μ M for another week and the experiment repeated after another 8 days of incubation (week 2). We observed that the number of viable cells in DU145-DR cells were again significantly less (p = 0.0027) when compared to DU-145 control group. Also, there was a significant (p = 0.0230) increase in cell death induced by doxazosin (37 μ M) in DU145-DR cells when compared to control DU-145 cells (Figure 18B).

These results suggested that treatment with 12.5 μ M doxazosin for 2 weeks did not render the DU-145 cells resistant to doxazosin. On the contrary, the doxazosin-treated cells underwent significantly more cell death as compared to solvent treated controls,

suggesting that pre-exposure to doxazosin rendered the cells more susceptible to cell death and not vice versa.

4.5.5 Evaluation of the effects of treatment of LNCaP cells to serially increasing concentrations of doxazosin:

When the LNCaP control cells were compared to LNCaP-DR controls, there was a significant reduction in the in the number of viable cells in the LNCaP-DR (p = 0.0020), suggesting that growth LNCaP cells were impeded following exposure to LNCaP cells to 12.5 μ M doxazosin for one week. However, there was no significant difference (p = 0.158) when these were incubated with 37 μ M doxazosin for a further 72 h (Figure.19A).

We then incubated the LNCaP-DR cells with the same concentration of doxazosin 12.5 μ M for another week and the experiment repeated after another 8 days of incubation (week 2). We observed that the number of viable cells in LNCaP-DR cells were again significantly less (p = 0.0001) when compared to LNCaP control group. Also, there was a significant (p = 0.0008) increase in cell death induced by doxazosin (37 μ M) in LNCaP-DR cells when compared to control LNCaP cells (Figure.19B).

These results suggested that treatment with 12.5 μ M doxazosin for 2 weeks did not render the LNCaP cells resistant to doxazosin. On the contrary, the doxazosin-treated cells underwent significantly more cell death as compared to solvent treated controls, suggesting that pre-exposure to doxazosin rendered the cells more susceptible to cell death and not vice versa.

Not surprisingly, when PC-3, DU-145 and LNCaP cells were treated with an initial concentration of 25 μ M of doxazosin for 1 week, all the doxazosin-treated cell lines

showed a significant reduction in cell numbers when compared to untreated controls (p = 0.0001). Also, there was a significant (p = 0.0008) increase in cell death induced by doxazosin (37 μ M) in doxazosin pre-treated cells when compared to controls. We did not proceed to the second week of incubation given the lack of results and the inability to produce doxazosin-resistant cells in any of the cell lines.

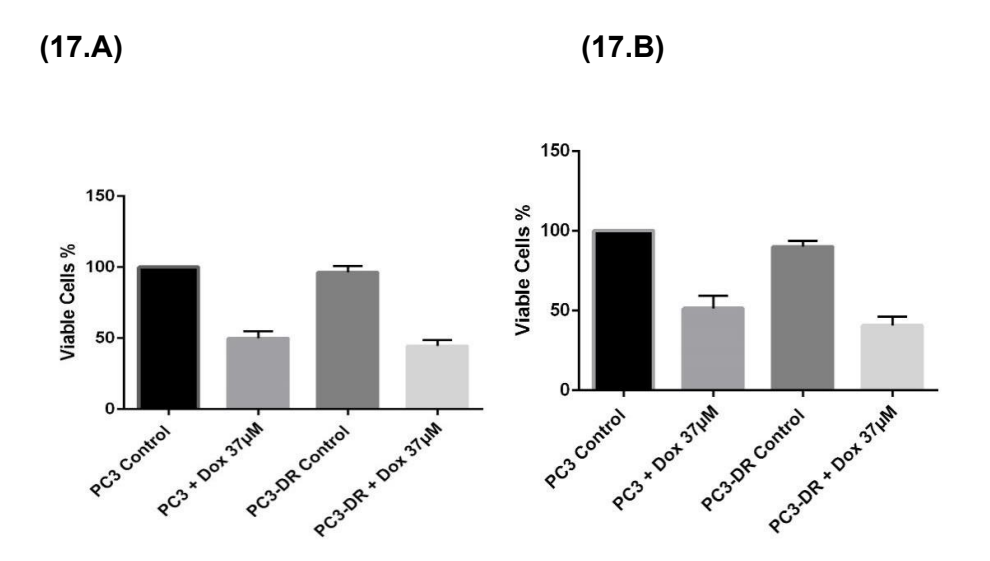


Figure 17: PC-3 cells incubated with doxazosin (Dox) 12.5 μ M for 1 week (A) and for 2 weeks (B) after which they were exposed to doxazosin 37 μ M for 72 h. PC3-DR = drug resistant PC3 cells

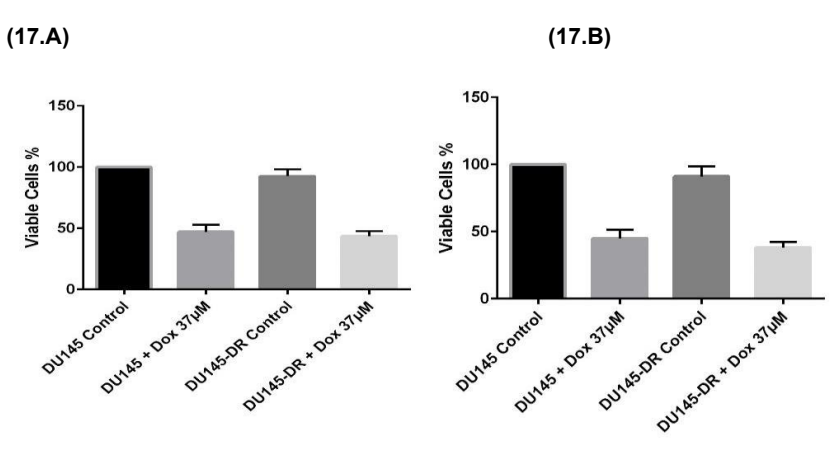


Figure 18: DU145 cells incubated with doxazosin (Dox) 12.5 μ M for 1 week (A) and for 2 weeks (B) after which they were exposed to doxazosin 37 μ M for 72 h. DU145-DR = drug resistant DU-145 cells.

(19.A) (19.B)

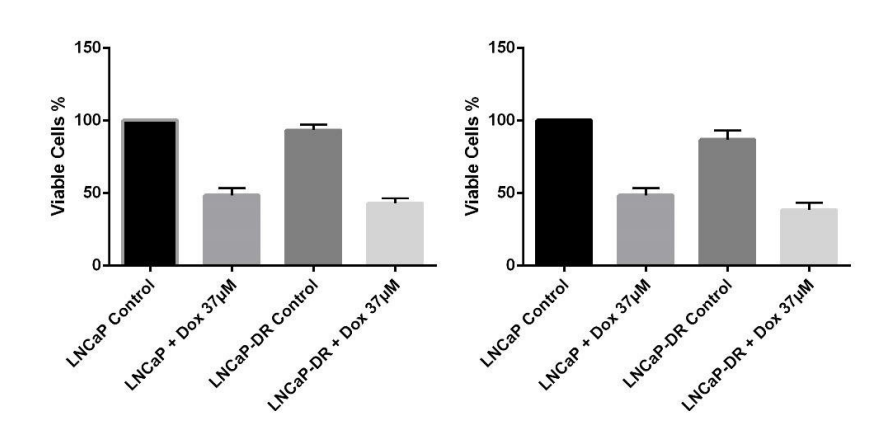


Figure 19: LNCaP cells incubated with doxazosin (Dox) 12.5 μ M for 1 week (A) and for 2 weeks (B) after which they were exposed to doxazosin 37 μ M for 72 h. LNCaP-DR = drug resistant LNCaP cells.

4.5.6 Evaluation of the effects of prolonged, low-dose concentrations of doxazosin on PC3 cells:

When the PC-3 control cells were compared to PC3-DR controls, there was no significant reduction in the in the number of viable cells in the PC3-DR (p = 0.9734), suggesting that growth LNCaP cells were impeded following exposure to LNCaP cells to 3.125 μ M doxazosin for 3 weeks. Also, there was no significant difference (p = 0.1958) when these were incubated with 37 μ M doxazosin for a further 72 h.

We then incubated the PC3-DR cells with the same concentration of doxazosin 3.125 μ M for another week and the experiment repeated after another 7 days of incubation (week 4). We observed that the number of viable cells in PC3-DR cells were again significantly less (p = 0.0002) when compared to PC3 control group. Also, there was a significant (p = 0.0008) increase in cell death induced by doxazosin (37 μ M) in PC3-DR cells when compared to control PC3 cells (Figure. 20 A, B).

These results suggested that treatment with 3.125 µM doxazosin for 4 weeks did not render the PC-3 cells resistant to doxazosin. On the contrary, the doxazosin-treated cells underwent significantly more cell death as compared to controls, suggesting that pre-exposure to doxazosin rendered the cells more susceptible to cell death and not vice versa. Therefore, we did not proceed to the next week of incubation given the lack of results and the inability to produce doxazosin-resistant cells in PC-3 cell lines by prolonged low dose exposure.

4.5.7 Evaluation of the effects of prolonged, low-dose concentrations of doxazosin on DU145 cells:

When the DU145 control cells were compared to DU145-DR controls, there was no significant reduction in the number of viable cells in the DU145-DR (p = 0.9734), suggesting that growth DU-145 cells were impeded following exposure to DU-145 cells to 3.125 μ M doxazosin for 3 weeks. Also, there was no significant difference (p = 0.1958) when these were incubated with 37 μ M doxazosin for a further 72 h (Figure.21).

We then incubated the DU145-DR cells with the same concentration of doxazosin 3.125 μ M for another week and the experiment repeated after another 7 days of incubation (week 4). We observed that the number of viable cells in DU145-DR cells were again significantly less (p = 0.0002) when compared to DU-145 control group. Also, there was a significant (p = 0.0008) increase in cell death induced by doxazosin (37 μ M) in DU145-DR cells when compared to control DU145 cells.

These results suggested that treatment with 3.125 µM doxazosin for 4 weeks did not render the DU-145 cells resistant to doxazosin. On the contrary, the doxazosin-treated cells underwent significantly more cell death as compared to controls, suggesting that

pre-exposure to doxazosin rendered the cells more susceptible to cell death and not vice versa. Therefore, we did not proceed to the next week of incubation given the lack of results and the inability to produce doxazosin-resistant cells in DU-145 cell lines by prolonged low dose exposure.

4.5.8 Evaluation of the effects of prolonged, low-dose concentrations of doxazosin on LNCaP cells:

When the LNCaP control cells were compared to LNCaP-DR controls, there was a significant reduction in the in the number of viable cells in the LNCaP-DR (p = 0.0001), suggesting that growth LNCaP cells were impeded following exposure to LNCaP cells to 3.125 μ M doxazosin for 3 weeks. Also, there was a significant difference (p = 0.0001) when these were incubated with 37 μ M doxazosin for a further 72 h (Figure.22).

We then incubated the LNCaP -DR cells with the same concentration of doxazosin 3.125 μ M for another week and the experiment repeated after another 7 days of incubation (week 4). We observed that the number of viable cells in LNCaP-DR cells were again significantly less (p = 0.0001) when compared to LNCaP control group. Also, there was a significant (p = 0.0001) increase in cell death induced by doxazosin (37 μ M) in LNCaP-DR cells when compared to control LNCaP cells.

These results suggested that treatment with 3.125 µM doxazosin for 4 weeks did not render the LNCaP cells resistant to doxazosin. On the contrary, the doxazosin-treated cells underwent significantly more cell death as compared to controls, suggesting that pre-exposure to doxazosin rendered the cells more susceptible to cell death and not vice versa. Therefore, we did not proceed to the next week of incubation given the lack

of results and the inability to produce doxazosin-resistant cells in LNCaP cell lines by prolonged low dose exposure.

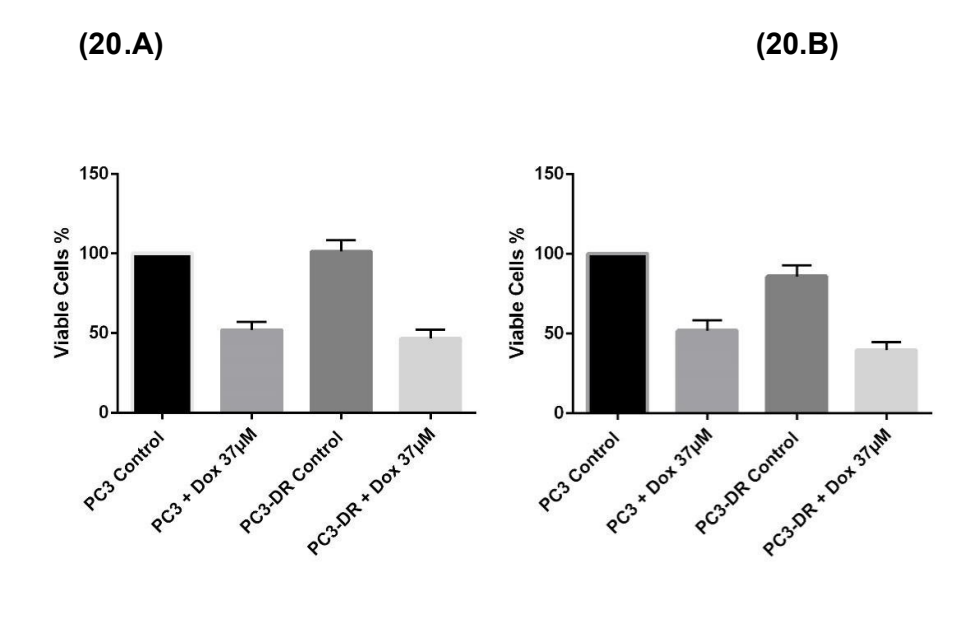


Figure 20: PC-3 incubated with doxazosin (Dox) 3.125 μ M for 3 weeks (A) and for 4 weeks (B) after which they were exposed to doxazosin 37 μ M for 72 h. PC3-DR = drug resistant PC3 cells.

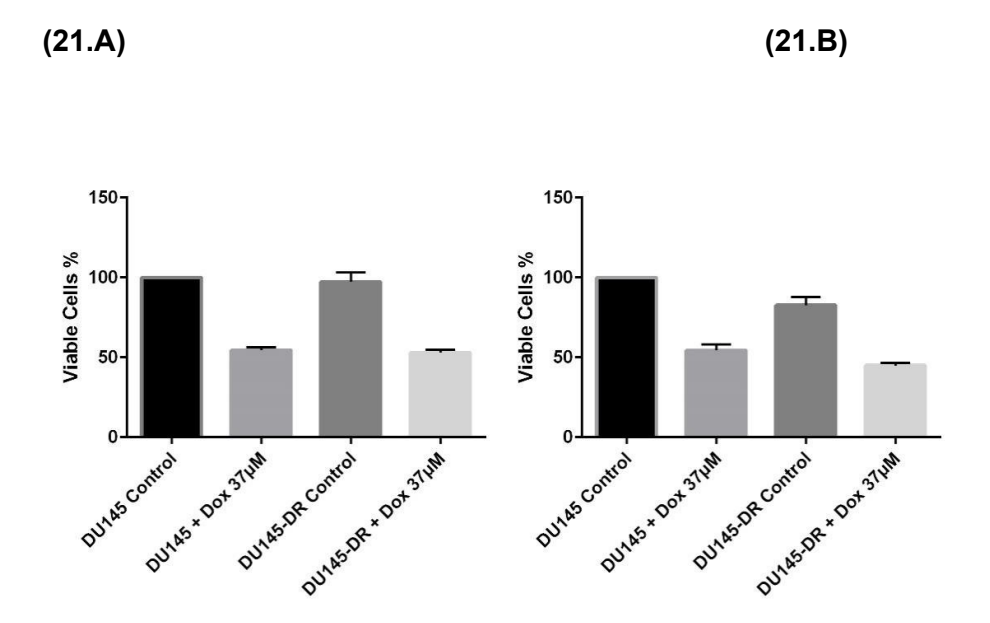


Figure 21: DU145 cells incubated with doxazosin (Dox) 3.125 μ M for 3 weeks (A) and for 4 weeks (B) after which they were exposed to doxazosin 37 μ M for 72 h. DU145-DR = drug resistant DU-145 cells.

(22.A) (22.B)

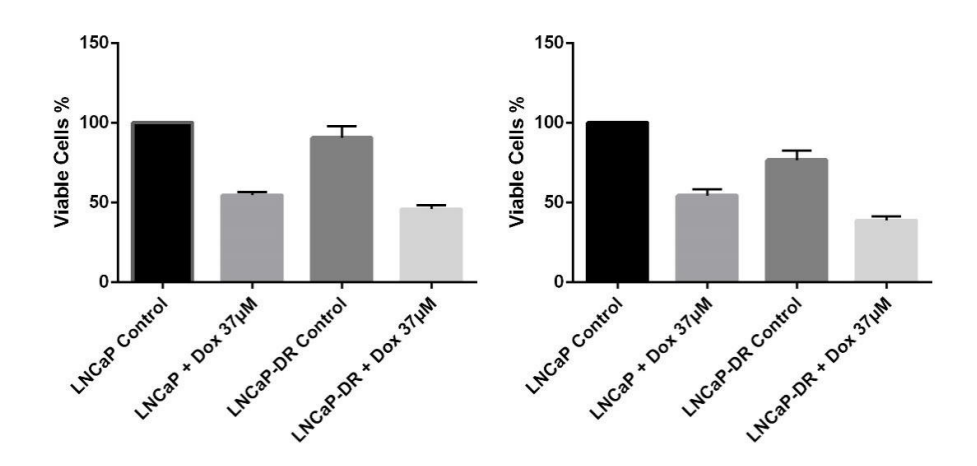


Figure 22: LNCaP cells incubated with (Dox) 3.125 μ M for 3weekS (A) and for 4 weeks (B) after which they were exposed to doxazosin 37 μ M for 72 h. LNCaP-DR = drug resistant LNCaP cells.

4.5.9 Evaluation of the effects of doxazosin on PC-3 cells in serum free media:

When the PC-3 serum free control cells were compared to PC-3 serum controls, there was a significant reduction in the in the number of viable cells in the former in the serum free wells (p = 0.0001), suggesting that growth PC3 cells were impeded following serum deprivation (Figure 23).

4.5.10 Effect of doxazosin on DU-145 cells in serum free media:

When the DU-145 serum free controls were compared to DU-145 serum controls, there was a significant reduction in the in the number of viable cells in the former (p = 0.0001), suggesting that growth DU-145 cells were impeded following serum deprivation (Figure 24).

4.5.11 Evaluation of the effects of doxazosin on LNCaP cells in serum free media:

When the LNCaP serum free controls were compared to LNCaP serum controls, there was a significant reduction in the in the number of viable cells in the former (p = 0.0001), suggesting that growth LNCaP cells were impeded following serum deprivation (Figure 25).

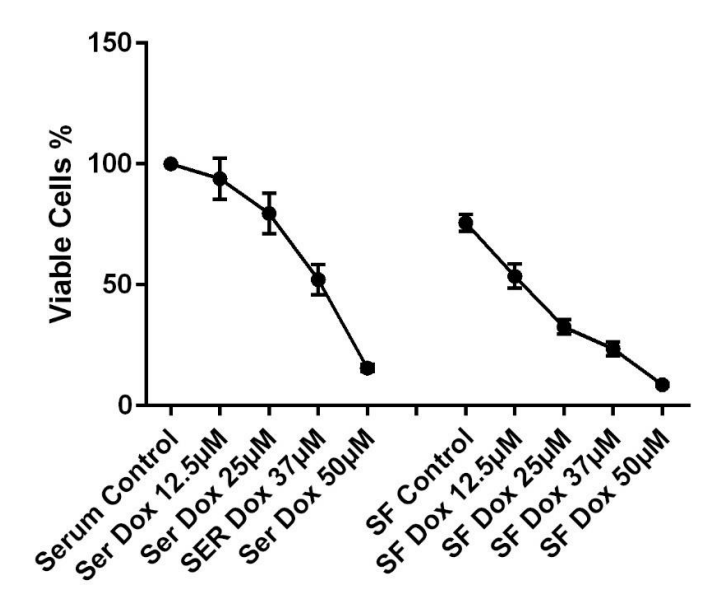


Figure 23: PC-3 cells treated with varying concentrations of doxazosin (Dox) for 72 h in serum containing media (left) and serum free (SF) media.

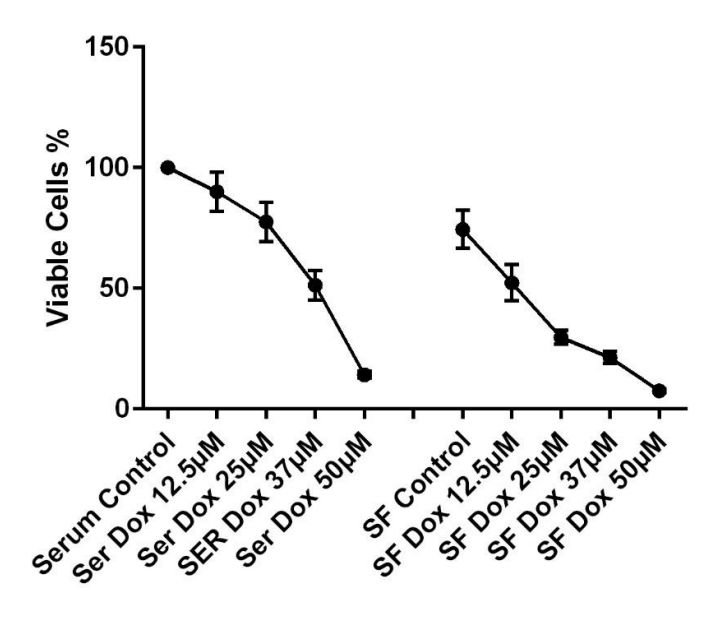


Figure 24: DU145 cells treated with varying concentrations of doxazosin (Dox) for 72 h in serum containing media (left) and serum free (SF) media.

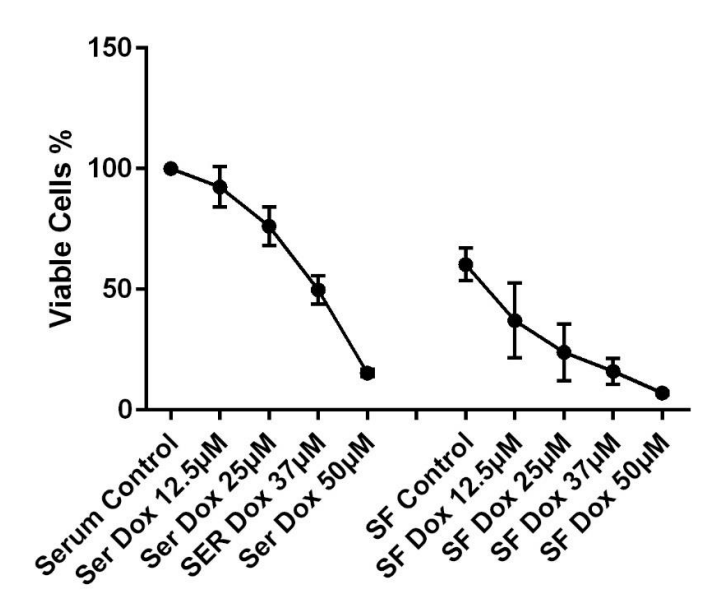


Figure 25: LNCaP cells treated with varying concentrations of doxazosin (Dox) for 72 h in serum containing media (left) and serum free (SF) media.

4.5.12 Effect of doxazosin on PC-3 cells in serum containing media, serum free media and LPDS and cholesterol supplemented medium:

When compared to PC-3 cells grown in serum containing media to that of serum free media, there was a significant reduction in growth in the latter (p = 0.0001). This reduction in growth due to serum deprivation was not abrogated by the addition of LPDS or a combination of LPDS and cholesterol solution (1:1000).

We then compared how the viability of PC-3 cells were affected by doxazosin in the different experimental conditions. The addition of LPDS to serum free media improved cell viability (p = 0.0001). However, when the viability of doxazosin-treated cells with addition of LPDS were compared to doxazosin-treated cells in complete serum, the former showed significantly less viable cells (p = 0.0001). When a combination of LPDS and cholesterol was added, it resulted in an even more significant abrogation of the cell death induced by doxazosin as compared to LPDS alone (Figure 26).

4.5.13 Effect of doxazosin on DU145 cells in serum containing media, serum free media and LPDS and cholesterol supplemented medium:

When compared to DU-145 cells grown in serum containing media to that of serum free media, there was a significant reduction in growth in the latter (p = 0.0001). This reduction in growth due to serum deprivation was not abrogated by the addition of LPDS or a combination of LPDS and cholesterol solution (1:1000).

We then compared how the viability of DU-145 cells were affected by doxazosin in the different experimental conditions. The addition of LPDS to serum free media improved cell viability (p = 0.0001). However, when the viability of doxazosin-treated cells (with addition of LPDS) were compared to doxazosin-treated cells in complete serum, the former showed significantly less viable cells (p = 0.0001). When a combination of

LPDS and cholesterol was added, it resulted in an even more significant abrogation of the cell death induced by doxazosin as compared to LPDS alone (Figure 27).

4.5.14 Effect of doxazosin on LNCaP cells in serum containing media, serum free media and LPDS and cholesterol supplemented medium:

When compared to LNCaP cells grown in serum containing media to that of serum free media, there was a significant reduction in growth in the latter (p = 0.0001). This reduction in growth due to serum deprivation was not abrogated by the addition of LPDS or a combination of LPDS and cholesterol solution (1:1000).

We then compared how the viability of LNCaP cells were affected by doxazosin in the different experimental conditions. The addition of LPDS to serum free media improved cell viability (p = 0.0001). However, when the viability of doxazosin-treated cells (with addition of LPDS) were compared to doxazosin-treated cells in complete serum, the former showed significantly less viable cells (p = 0.0001). When a combination of LPDS and cholesterol was added, it resulted in an even more significant abrogation of the cell death induced by doxazosin as compared to LPDS alone (Figure 28).

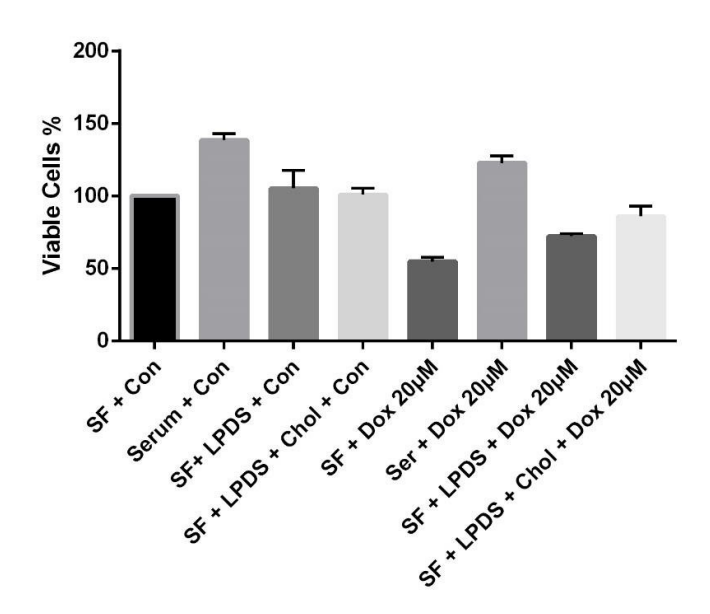


Figure 26: PC3 cells in serum free media control or serum control and LPDS or LPDS+ cholesterol controls treated compared to treatment with 20 μ M of doxazosin (Dox). LPDS = lipoprotein deficient serum.

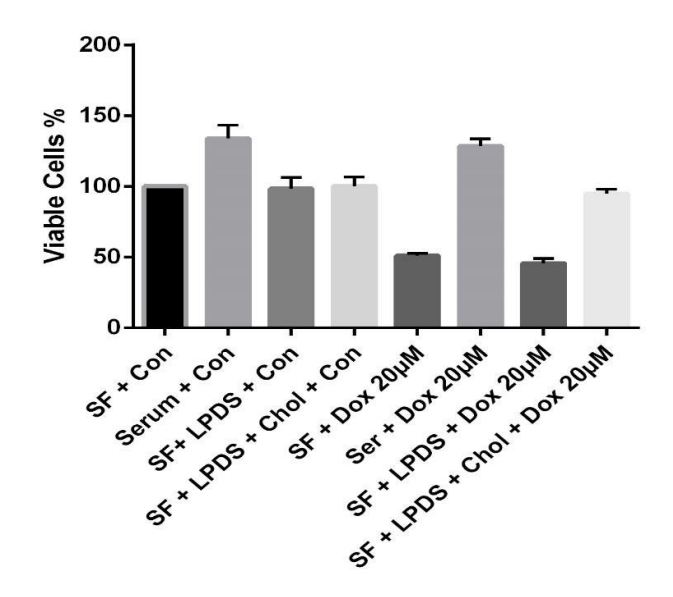


Figure 27: DU145 cells in serum free media control or serum control and LPDS or LPDS + cholesterol controls treated compared to treatment with 20 μ M of doxazosin (Dox). LPDS = lipoprotein deficient serum.

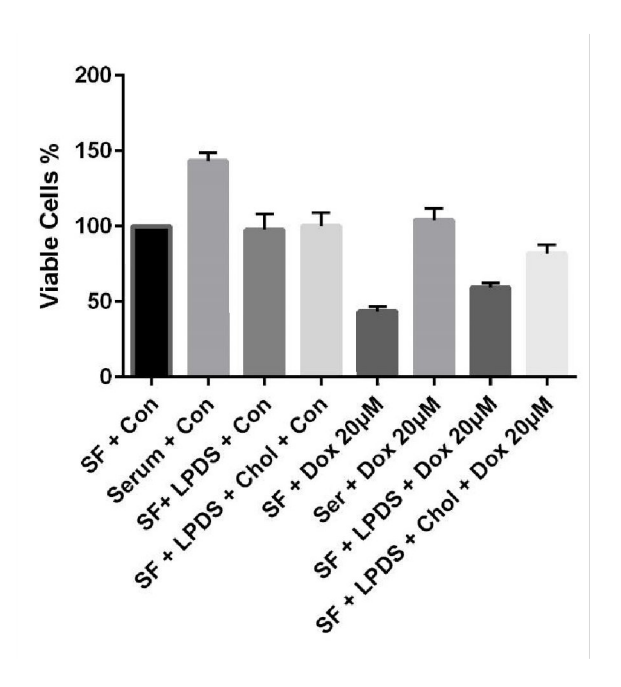


Figure 28: LNCaP cells in serum free media control or serum control and LPDS or LPDS + cholesterol control treated compared to treatment with 20 μ M of doxazosin (Dox).

4.3.15 Effect of doxazosin on lipid receptor-deficient fibroblast cell lines:

Doxazosin had no effect on cell viability at concentration of 12.5 μ M and 25 μ M. At concentrations of 37 μ M we observed that 84% of the cells were viable, and concentrations of 75 μ M, 57% of the cells were viable (Figure 29).

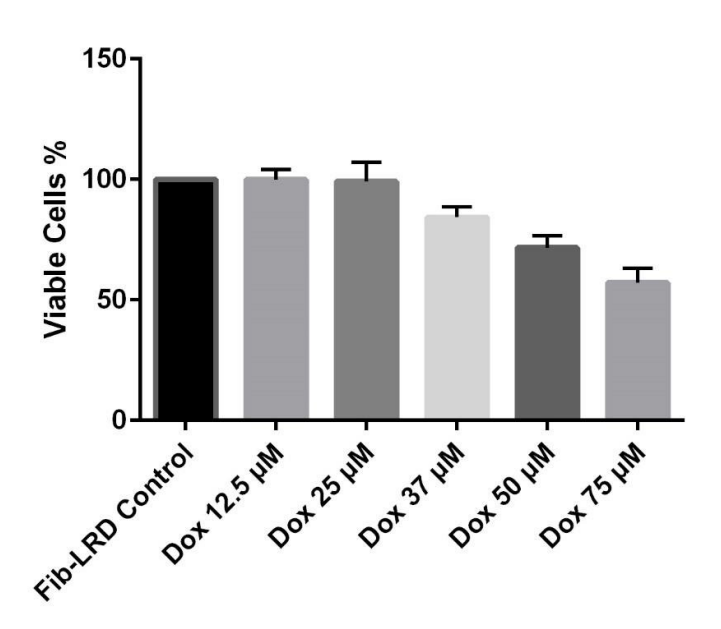


Figure 29: LDL receptor deficient fibroblasts (Fib-LRD) treated with different concentrations of doxazosin (Dox).

4.6 Discussion

Developing cancer cell lines that are resistant to a drug is an important strategy in the study of drug development. Our results suggest that our attempts to develop cell lines that are resistant to doxazosin were unsuccessful. However, morphological examination of the cell lines using light microscopy during these experiments suggested that:

- (a) the appearance of granular cytoplasm preceded cell death induced by doxazosin,
- (b) the effects on the cell even in low doses were cumulative over time,
- (c) the effects of doxazosin were reversible over time if the cells were not exposed to concentrations over $60~\mu\text{M}$
- (d) doxazosin-induced cell death was potentiated when the cells were in nutrient-depleted conditions (serum free media +/- EAA supplements), and this effect seen with nutrient depletion can be reversed by the addition of lipoproteins.
- (e) also, the addition of cholesterol solution (1:1000) further abrogated the cell death induced by doxazosin.

Given the cumulative effects of doxazosin and its reversibility, we concluded that the development of doxazosin-resistant cell lines using the above strategy would not be feasible; therefore, we did not extend our experiments into BCa cells. The results from our experiments with PCa cell lines led us to believe that doxazosin is probably transported into the cell whereby it induces it cytotoxic actions within the cell. This finding also led us to postulate that the effects of doxazosin could be mediated by a receptor that is endocytosed upon binding with doxazosin – possibly the lipid receptor, given the increased cell death in serum free conditions and the protective effect of lipoproteins in nutrient-depleted conditions. We therefore used LDL receptor mutant fibroblast cell lines to test this hypothesis. Interestingly, doxazosin had no effect on cell viability at lower concentrations (12.5μM and 25μM) on these cells and over 50% of the cells were viable at 75 μM of doxazosin.

LDL receptor mutant cell lines were difficult to grow in cell cultures and did not grow beyond 40% - 50% confluence. Despite our best efforts, establishing new batches of cells for experiments proved futile and therefore further experiments using this cell

line had to be terminated. Hence, it is difficult to conclude if LDL receptors can be implicated in doxazosin-mediated toxicity.

LDL receptors were the first receptors that were identified to be transported within the cell via endocytosis, which then led to its downstream functions intracellularly and eventually would be transported back to the cell surface. This led us to hypothesize that endocytic process could be involved in the transport of the receptor that mediated doxazosin induced cell death in PCa and BCa cells. In the next chapter we look at the various endocytic pathways that could mediate doxazosin induced cell death.

Chapter 5

Investigating the role of endocytosis and pinocytosis in doxazosin mediated cell death of prostate and bladder cancer cells

5.1 Introduction

Cells are capable of internalizing plasma membrane, surface receptors and their bound ligands, nutrients, bacterial toxins, immunoglobulins, viruses and various extracellular soluble molecules by endocytosis (Lanzetti and Di Fiore 2008). Endocytosis had been considered in the past to be an attenuator of cell signalling though recent evidence has shown that endocytic signalling persists throughout the signalling route giving rise to the concept of signalling endosomes (von Zastrow and Sorkin 2007, Lanzetti and Di Fiore 2008).

Our previous experiments had led us to hypothesize that doxazosin may mediate its actions intracellularly, following its entry into the cell by endocytic process.

Quinazoline molecules are small molecules and therefore can be trafficked into the cell directly by endocytosis. Alternatively, the molecule could bind to a receptor which then is trafficked intracellularly or could be trafficked directly in view of the lipophilic nature of the quinazoline molecules. It has been shown by single cell quantitative fluorescence imaging of BIODIPY-FL prazosin that 40% of adrenergic binding sites are located intracellularly (Mackenzie, Daly et al. 2000).

In this chapter we investigated the role of the common endocytic pathways as well as pinocytosis in doxazosin-induced cell death. We used chemical inhibitors of clathrin –and –caveolin mediated as well as inhibitors of pinocytosis to ascertain the effects of these inhibitors on doxazosin-induced cell death. Also, we used dynasore, an inhibitor of dynamin, which regulated dynamin-dependent endocytic processes. In brief, our results shows that inhibition of clathrin and dynamin-dependent endocytic process resulted in significant attenuation of doxazosin-induced cell death.

5.2 Experiments on *In Vitro* inhibition of clathrin-mediated endocytosis, caveolin-mediated endocytosis, and pinocytosis in PCa and BCa cell lines

5.2.1 Inhibition of endocytosis by cooling on ice:

5.2.1.1 Evaluation of the effects of doxazosin on PC-3, DU-145, LNCaP and HT1376 cells incubated on ice:

PC-3, DU145, LNCaP and HT1376 cells were seeded into 96-well MP at 5000 cells in 100 μ L/well and incubated at 37 C. After 24h, 10 μ L of media was removed from all plates, and the MP were paired into test and control plates. The subsequent steps for test and control plates are as follows.

Test plates: Test plates were incubated on ice for 30 minutes to ensure cooling prior to experiments. Then 10 μL of doxazosin (diluted in water at 4 C) at different concentrations (10⁻⁷, 10⁻⁶, 10⁻⁵, 10⁻⁴) were added to the wells whilst 10 μL was added to control wells. The plates were then incubated for a further 2 h on ice. After this, the media from all wells were decanted and fresh media (100 μL at 37 C) added to each well. The plates were incubated for 4 h at 37 C and cell viability was assessed using Cell-Titer 96[®] aqueous MTS assay.

Positive control plates: In contrast to test plates, the positive control plates were incubated at 37 C throughout, and all drug and media added were at 37C. These plates were incubated at 37 C for 30 minutes and 10 µL of doxazosin (diluted in water at 37 C) at different concentrations (10^{-7,} 10⁻⁶, 10⁻⁵, 10⁻⁴) were added to test wells and 10 µL was added to control wells. The plates were incubated for a further 2 h at 37 C. After this, the media from all wells were decanted and fresh media (100 µL at 37 C) added to each well. The plates were incubated for 4 h at 37 C and cell viability was assessed using Cell-Titer 96® aqueous MTS assay.

5.3 Experiments on Inhibition of endocytosis using chemical inhibitors of clathrin-mediated endocytic pathway:

5.3.1 Evaluation of the effects of doxazosin on PC-3, DU145, LNCaP and HT1376 cells pre-incubated with hypertonic sucrose solution:

PC-3, DU145, LNCaP and HT1376 cells were seeded into 96-well MP at 5000 cells in 100 μL/well and incubated at 37 C. After 24h, 20 μL was pipetted out from each well. Test and control wells were treated as follows:

Test wells: Test wells were incubated with 10 μ L sucrose (0.25 M and 0.4M, final concentration) for 30 minutes followed by doxazosin in 10 μ L (10⁻⁶, 10⁻⁵, 10⁻⁴). These were incubated for 6 h, and Cell-Titer 96[®] aqueous MTS assay performed.

Control wells: Control well were incubated with 10 µL water for 30 minutes followed by doxazosin in in 10 µL (final concentration of 10⁻⁶, 10⁻⁵, 10⁻⁴). These were incubated for 6 h, and Cell-Titer 96[®] aqueous MTS assay performed.

5.3.2 Evaluation of the effects of doxazosin on PC-3, DU145, LNCaP and HT1376 cells pre-incubated with chlorpromazine:

PC-3, DU145, LNCaP and HT1376 cells were seeded into 96-well MP at 5000 cells in 100 μL/well and incubated at 37 C in serum containing media. After 24h, serum contained media was replaced with 90 μL serum free medium and plates were incubated for 30 minutes at 37 C. Test and control wells were treated as follows:

Test wells: 10 μ L each of solutions of chlorpromazine hydrochloride 100 μ M (Sigma Aldrich, UK, Catalogue No: C8138) was added to make up a total volume of 100 μ L. The plates were returned to the incubator for 30 minutes. Subsequently, 10 μ L was

aspirated and replaced with doxazosin in 10 μL (final concentration 37 μM). These were incubated for 72 h, and Cell-Titer 96[®] aqueous MTS assay performed.

Control wells: 10 μ L each of solutions of diluent (water) was added to make up a total volume of 100 μ L. The plates were returned to the incubator for 30 minutes. Subsequently, 10 μ L was aspirated and replaced with doxazosin in 10 μ L (final concentration of 37 μ M). These were incubated for 72 h, and Cell-Titer 96® aqueous MTS assay performed.

5.3.3 Evaluation of the effects of doxazosin on PC-3, DU145, LNCaP and HT1376 cells pre-incubated with dansylcadaverine:

PC-3, DU145, LNCaP and HT1376 cells were seeded into 96-well MP at 5000 cells in 100 μ L/well and incubated at 37 C in serum containing media for 24h. After this, 10 μ L was pipetted out from each well and test and control wells were treated as follows:

Test wells: 10 μ L each of solutions of dansylcadaverine 75 μ M (Sigma Aldrich, Catalogue No: D4808) to make up a total volume of 100 μ L. The plates were returned to the incubator for 4 h. Subsequently, 10 μ L was aspirated and replaced with doxazosin in 10 μ L (37 μ M). These were incubated for 72 h, and Cell-Titer 96® aqueous MTS assay performed.

Control wells: 10 μ L each of solutions of the diluent used for preparing stock solutions of dansylcadaverine (160 μ L of 1% acetic acid and 6160 μ L of sterile water) was added to make up a total volume of 100 μ L. The plates were returned to the incubator for 4 h. Subsequently, 10 μ L was aspirated and replaced with doxazosin in 10 μ L (final concentration of 37 μ M). These were incubated for 72 h, and Cell-Titer 96® aqueous MTS performed.

<u>5.4 Experiments on Inhibition of endocytosis using chemical inhibitors of caveolae-mediated (lipid raft) endocytic pathway:</u>

<u>5.4.1 Evaluation of the effects of doxazosin on PC-3, DU145, LNCaP and</u> HT1376 cells pre-incubated with mevastatin:

PC-3, DU145, LNCaP and HT1376 cells were seeded into 96-well MP at 5000 cells in 100 μ L/well and incubated at 37 C in serum containing media. After 24h the media was decanted from all the wells and replaced with serum free media (100 μ L/well) and the plates transferred to incubator for 30 minutes. After this period, 10 μ L was pipetted out from all the wells and test and control wells were treated as follows:

Test wells: 10 μ L each of solutions of mevastatin 20 μ M (Sigma Aldrich, Catalogue No: M2537) to make up a total volume of 100 μ L. The plates were returned to the incubator for 4 h. Subsequently, 10 μ L was aspirated and replaced with doxazosin in 10 μ L (final concentration 37 μ M). These were incubated for 72 h, and Cell-Titer 96® aqueous MTS assay performed.

Control wells: 10 μ L each of solutions of diluent used for mevastatin preparing stock solutions of mevastatin (4502 μ L of DMSO and 1900 μ L of water) was added to make up a total volume of 100 μ L. The plates were returned to the incubator for 4 h. Subsequently, 10 μ L was aspirated and replaced with doxazosin in 10 μ L (final concentration of 37 μ M). These were incubated for 48 h, and Cell-Titer 96® aqueous MTS assay performed.

5.4.2 Evaluation of the effects of doxazosin on PC-3, DU145, LNCaP and HT1376 cells pre-incubated with methyl beta cyclodextrin (MBCD):

PC-3, DU145, LNCaP and HT1376 cells were seeded into 96-well MP at 5000 cells in 100 μ L/well and incubated at 37 C in serum containing media. After 24h the media was decanted from all the wells and replaced with serum free media (100 μ L/well) and the plates transferred to incubator for 30 minutes. After this period, 10 μ L was pipetted out from all the wells and test and control wells were treated as follows:

Test wells: 10 μL each of solutions of MBCD1mM (Sigma Aldrich, Catalogue No: C4555) to make up a total volume of 100 μL. The plates were returned to the incubator for 1 h. Subsequently, 10 μL was aspirated and replaced with doxazosin in 10 μL (final concentration 37 μM). These were then incubated for 72 h, and Cell-Titer 96® aqueous MTS assay performed.

Control wells: 10 μ L each of solutions of diluent (sterile water) used for MBCD was added to make up a total volume of 100 μ L. The plates were returned to the incubator for 60 minutes. Subsequently, 10 μ L was aspirated and replaced with doxazosin in 10 μ L (final concentration of 37 μ M). These were incubated for 72 h, and Cell-Titer 96® aqueous MTS assay performed.

<u>5.4.3 Evaluation of the effects of doxazosin on PC-3, DU145, LNCaP and</u> HT1376 cells pre-incubated with cholesterol oxidase:

PC-3, DU145, LNCaP and HT1376 cells were seeded into 96-well MP at 5000 cells in 100 μ L/well and incubated at 37 C in serum containing media. After 24h the media was decanted from all the wells and replaced with serum free media (100 μ L/well) and the plates transferred to incubator for 30 minutes. After this period, 10 μ L was pipetted out from all the wells and test and control wells were treated as follows:

Test wells: 10 μ L each of solutions of cholesterol oxidase 2 units/ml (Sigma Aldrich, Catalogue No: C48649) to make up a total volume of 100 μ L. The plates were returned to the incubator for 2 h. Subsequently, 10 μ L was aspirated and replaced with doxazosin in 10 μ L (final concentration 37 μ M). These were then incubated for 72 h, and Cell-Titer 96® aqueous MTS assay performed.

Control wells: 10 μ L each of solutions of diluent (potassium phosphate buffer adjusted to pH 7.0) used for cholesterol oxidase was added to make up a total volume of 100 μ L. The plates were returned to the incubator for 2 h. Subsequently, 10 μ L was aspirated and replaced with doxazosin in 10 μ L (final concentration of 37 μ M). These were incubated for 72 h, and Cell-Titer 96® aqueous MTS assay performed.

5.5 Experiments on Inhibition of endocytosis using chemical inhibitors of micropinocytosis:

5.5.1 Evaluation of the effects of doxazosin on PC-3, DU145, LNCaP and HT1376 cells pre-incubated with amiloride:

PC-3, DU145, LNCaP and HT1376 cells were seeded into 96-well MP at 5000 cells in 100 μ L/well and incubated at 37 C in serum containing media. After this period, 10 μ L was pipetted out from all the wells and test and control wells were treated as follows:

Test wells: 10 μ L each of solutions of amiloride 50 μ M (Sigma Aldrich, Catalogue No: A7410) to make up a total volume of 100 μ L. The plates were returned to the incubator for 4 h. Subsequently, 10 μ L was aspirated and replaced with doxazosin in 10 μ L (final concentration 37 μ M). These were then incubated for 72 h and Cell-Titer 96® aqueous MTS assay performed.

Control wells: 10 μ L each of solutions of diluent used for amiloride (sterile water) was added to make up a total volume of 100 μ L. The plates were returned to the incubator for 4 h. Subsequently, 10 μ L was aspirated and replaced with doxazosin in 10 μ L (final concentration of 37 μ M). These were incubated for 72 h, and Cell-Titer 96® aqueous MTS assay performed.

5.6 Experiments on Inhibition of endocytosis using chemical inhibitors of dynamin-mediated endocytic vesicle development:

5.6.1 Evaluation of the effects of doxazosin on PC-3, DU145, LNCaP and HT1376 cells pre-incubated with dynasore:

PC-3, DU145, LNCaP and HT1376 cells were seeded into 96-well MP at 5000 cells in 100 μ L/well and incubated at 37 C in serum containing media. After 24 h, serum contained media was replaced with 100 μ L serum free medium and plates were incubated for 30 minutes at 37 C. After this, 10 μ L was pipetted out from each well and test and control wells were treated as follows:

Test wells: 10 μ L each of solutions of dynasore 20 μ M (Sigma Aldrich, Catalogue No: D7693) to make up a total volume of 100 μ L. The plates were returned to the incubator for 60 minutes. Subsequently, 10 μ L was aspirated and replaced with doxazosin in 10 μ L (final concentration of 37 μ M or 100 μ M). These were incubated for 72 h and Cell-Titer 96® aqueous MTS assay performed.

Control wells: 10 μ L each of solutions of diluent used for dynasore (stock solutions prepared from 5 mg in 2898 μ L of DMSO and 8586 μ L of water) was added to make up a total volume of 100 μ L. The plates were returned to the incubator for 60

minutes. Subsequently, 10 μ L was aspirated and replaced with doxazosin in 10 μ L (final concentration of 37 μ M or100 μ M). These were incubated for 72 h and Cell-Titer 96® aqueous MTS assay performed.

5.6.2 Evaluation of the effects of doxazosin on PC-3, DU145, LNCaP and HT1376 cells pre-incubated with Mdivi-1:

PC-3, DU145, LNCaP and HT1376 cells were seeded into 96-well MP at 5000 cells in 100 μL/well and incubated at 37 C in serum containing media. After 24 h, serum contained media was replaced with 100 μL serum free medium and plates were incubated for 30 minutes at 37 C. After this, 10 μL was pipetted out from each well using a multichannel pipette. Test and control wells were treated as follows:

Test wells: 10 μ L each of solutions of Mdivi-1 50 μ M (Sigma Aldrich; Catalogue No: M0199) to make up a total volume of 100 μ L. The plates were returned to the incubator for 30 minutes. Subsequently, 10 μ L was aspirated and replaced with doxazosin in 10 μ L (final concentration of 37 μ M). These were incubated for 72 h and Cell-Titer 96® aqueous MTS assay performed.

Control wells: 10 μ L each of solutions of diluent used for Mdivi-1 (DMSO and sterile water) was added to make up a total volume of 100 μ L. The plates were returned to the incubator for 30 minutes. Subsequently, 10 μ L was aspirated and replaced with doxazosin in 10 μ L (final concentration of 37 μ M). These were incubated for 72 h and Cell-Titer 96® aqueous MTS assay performed.

5.7 RESULTS:

5.7.1 Inhibition of endocytosis by cooling on ice:

5.7.1.1 Effect of doxazosin on PC-3 cells incubated on ice:

Incubation on ice caused a significant inhibition of doxazosin-induced cell death of PC-3 cells particularly at higher concentrations of doxazosin, with a maximum inhibition at 10⁻⁴ of doxazosin. At 10⁻⁴ and 10⁻⁵ concentrations of doxazosin, the attenuation of doxazosin-induced cell death was 11.54 % and 6.9 % respectively, while at concentrations of 10⁻⁶ and 10⁻⁷, the difference was not significant.

5.7.1.2 Effect of doxazosin on DU-145 cells incubated on ice:

Incubation on ice caused a significant inhibition of doxazosin-induced cell death of D145 cells particularly at higher concentrations of doxazosin. At 10⁻⁴ and 10⁻⁵ concentrations of doxazosin, the attenuation of doxazosin-induced cell death was 12.3 % and 7.68 % respectively, while at concentrations of 10⁻⁶ and 10⁻⁷, the difference was not significant.

5.7.1.3 Effect of doxazosin on LNCaP cells incubated on ice:

Incubation on ice cause a significant inhibition of doxazosin-induced cell death of LNCaP cells particularly at higher concentrations of doxazosin. At 10⁻⁴ there was marked anoikis of doxazosin treated cells in the control group and following the decanting of the media, many cells were seen detached. At 10⁻⁴ and 10⁻⁵ concentrations of doxazosin, the attenuation of doxazosin-induced cell death was 4.43 % and 18.13 % respectively, while at concentrations of 10⁻⁶ and 10⁻⁷, the difference was not significant.

5.7.1.4. Effect of doxazosin on HT1376 cells incubated on ice:

Incubation on ice cause a significant inhibition of doxazosin-induced cell death of HT1376 cells at higher concentrations of doxazosin, with a maximum inhibition of 13.44 % at 10⁻⁴ of doxazosin. At 10⁻⁴ and 10⁻⁵ concentrations of doxazosin, the attenuation of doxazosin-induced cell death was 8.35 % and 13.44 % respectively, while at concentrations of 10⁻⁶ and 10⁻⁷, the difference was not significant.

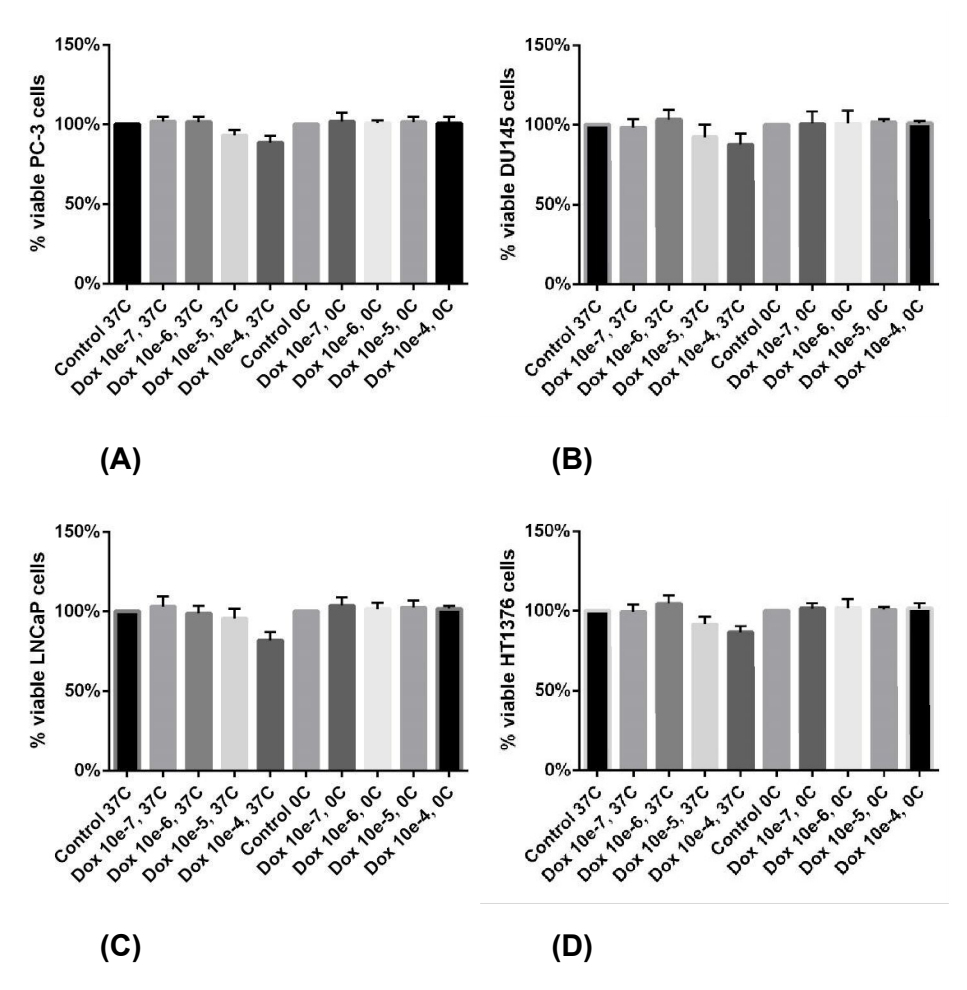


Figure 30: Effect of temperature on doxazosin-induced cell death in the cell lines PC-3 (A), DU145 (B), LNCaP (C), and HT1376 (D) showing significant (p>0.0001) attenuation of cell death at higher concentrations of doxazosin (10⁻⁴ and 10⁻⁵⁾ when cells are cooled 0 C to 4 C on ice. Dox = doxazosin.

5.7.2 Inhibition of endocytosis using chemical inhibitors of clathrin-mediated endocytic pathway:

<u>5.7.2 .1 Effect of doxazosin on PC-3 cells pre-incubated with hypertonic sucrose solution:</u>

We observed doxazosin-induced cell death in PC-3 was attenuated by pre-treatment with sucrose of 0.25 M and followed by exposure to doxazosin (10⁻⁵) significantly (p=0.0256). At a higher concentration of sucrose of 0.4 M, this effect was significant for two different concentrations of doxazosin (p=0.0122 for 10⁻⁵ and 0.0016 for 10⁻⁵ of doxazosin). The results are detailed in below (Figure 31 and Table 4).

5.7.2 .2 Effect of doxazosin on DU-145 cells pre-incubated with hypertonic sucrose solution:

Pre-treatment with sucrose 0.25 M and 0.4 M and followed by exposure to doxazosin (10⁻⁶) significantly (p=0.0147 and 0.0475, respectively) attenuated the cell death induced by doxazosin in DU145 cells. The results are detailed in below (Figure 32 and Table 5).

5.7.2 3 Effect of doxazosin on LNCaP cells pre-incubated with hypertonic sucrose solution:

Sucrose had no significant effect on viability of at all the concentrations tested. The results are detailed in below Figure 33 and Table 6).

5.7.2.4 Effect of doxazosin on HT1376 cells pre-incubated with hypertonic sucrose solution:

In HT1376 cells, the only significant (p=0.0004) attenuation of the doxazosin cytotoxicity was observed when pre-treatment with sucrose 0.25 M was followed by exposure to doxazosin (10⁻⁶). The results are detailed in below (Figure 34 and Table 7).

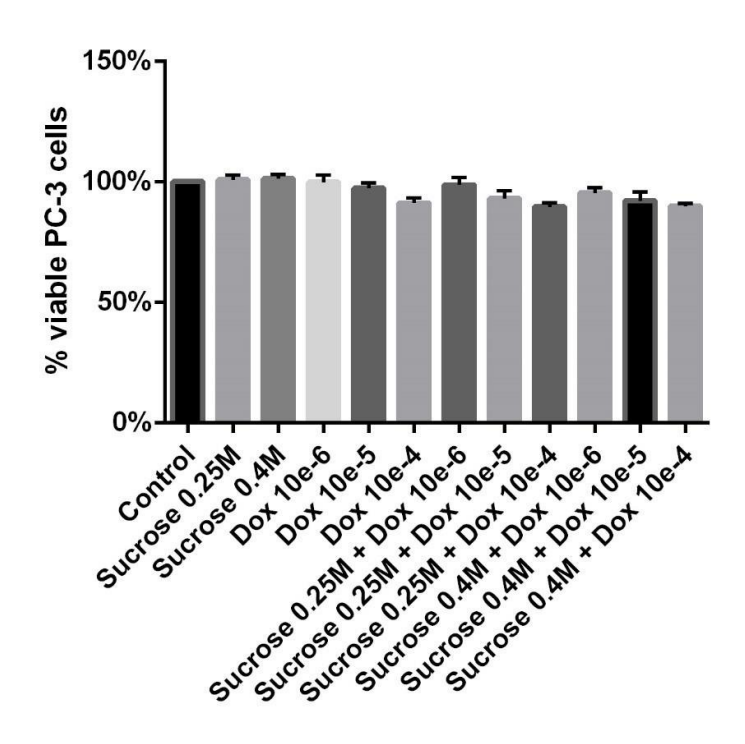


Figure 31: Effect of sucrose 0.25M and 0.4 M on doxazosin-induced cell death on PC-3 cells. Dox = doxazosin.

Table 4: Effect of sucrose 0.25M and 0.4M on PC3 cell line.

| Parameters Compared | Mean Difference | p value |
|---|--------------------|---------|
| Control vs Sucrose 0.25M | -0.7780 | >0.9999 |
| Control vs Sucrose 0.4M | -1.301 | 0.9934 |
| Dox 10 ⁻⁶ vs Sucrose 0.25M + Dox 10 ⁻⁶ | 1.084 | 0.9987 |
| Dox 10 ⁻⁵ vs Sucrose 0.25M + Dox 10 ⁻⁵ | 4.204 | 0.0256 |
| Dox 10 ⁻⁴ vs Sucrose 0.25M + Dox 10 ⁻⁴ | 1.602 | 0.9667 |
| Dox 10 ⁻⁶ vs Sucrose 0.4M + Dox 10 ⁻⁶ | 4.484 | 0.0122 |
| Dox 10 ⁻⁵ vs Sucrose 0.4M + Dox 10 ⁻⁵ | 5.172 | 0.0016 |
| Dox 10 ⁻⁴ vs Sucrose 0.4M + Dox 10 ⁻⁴ | 1.391 | 0.9887 |
| (Sucrose 0.25M + Dox 10 ⁻⁶) vs (Sucrose 0.4M + Dox 10 ⁻⁶) | 3.401 | 0.1581 |
| (Sucrose 0.25M + Dox 10 ⁻⁵) vs (Sucrose 0.4M + Dox 10 ⁻⁵) | 0.9681 | 0.9995 |
| (Sucrose 0.25M + Dox 10 ⁻⁴) vs (Sucrose 0.4M + Dox 10 ⁻⁴) | -0.2110 | >0.9999 |

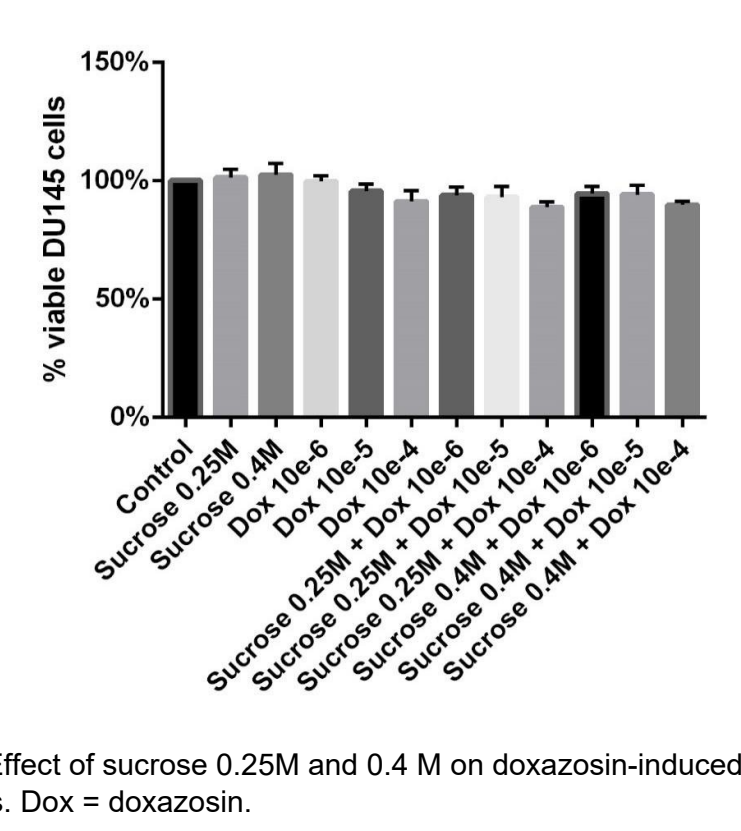


Figure 32: Effect of sucrose 0.25M and 0.4 M on doxazosin-induced cell death on DU-145 cells. Dox = doxazosin.

Table 5: Effect of sucrose 0.25M and 0.4M on DU145 cell line

| Parameters Compared | Mean Difference | p value |
|---|--------------------|---------|
| Control vs Sucrose 0.25M | -1.304 | 0.9996 |
| Control vs Sucrose 0.4M | -2.485 | 0.9161 |
| Dox 10 ⁻⁶ vs Sucrose 0.25M + Dox 10 ⁻⁶ | 5.976 | 0.0147 |
| Dox 10 ⁻⁵ vs Sucrose 0.25M + Dox 10 ⁻⁵ | 2.573 | 0.8961 |
| Dox 10 ⁻⁴ vs Sucrose 0.25M + Dox 10 ⁻⁴ | 2.505 | 0.9117 |
| Dox 10 ⁻⁶ vs Sucrose 0.4M + Dox 10 ⁻⁶ | 5.354 | 0.0475 |
| Dox 10 ⁻⁵ vs Sucrose 0.4M + Dox 10 ⁻⁵ | 1.532 | 0.9980 |
| Dox 10 ⁻⁴ vs Sucrose 0.4M + Dox 10 ⁻⁴ | 1.455 | 0.9988 |
| (Sucrose 0.25M + Dox 10 ⁻⁶) vs (Sucrose 0.4M + Dox 10 ⁻⁶) | -0.6225 | >0.9999 |
| (Sucrose 0.25M + Dox 10 ⁻⁵) vs (Sucrose 0.4M + Dox 10 ⁻⁵) | -1.040 | >0.9999 |
| (Sucrose 0.25M + Dox 10 ⁻⁴) vs (Sucrose 0.4M + Dox 10 ⁻⁴) | -1.050 | >0.9999 |

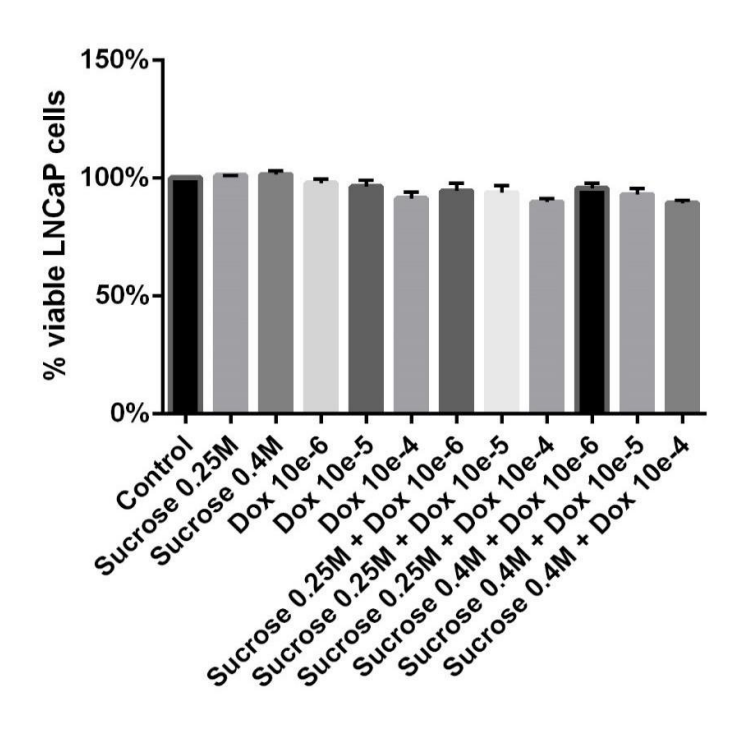


Figure 33: Effect of sucrose 0.25M and 0.4 M on doxazosin-induced cell death on LNCaP cells. Dox = doxazosin.

Table 6: Effect of sucrose 0.25M and 0.4M on LNCaP cell line

| Parameters Compared | Mean Difference | p value |
|---|--------------------|---------|
| Control vs Sucrose 0.25M | -1.024 | 0.9976 |
| Control vs Sucrose 0.4M | -1.430 | 0.9637 |
| Dox 10 ⁻⁶ vs Sucrose 0.25M + Dox 10 ⁻⁶ | 3.329 | 0.0722 |
| Dox 10 ⁻⁵ vs Sucrose 0.25M + Dox 10 ⁻⁵ | 2.678 | 0.3006 |
| Dox 10 ⁻⁴ vs Sucrose 0.25M + Dox 10 ⁻⁴ | 1.621 | 0.9154 |
| Dox 10 ⁻⁶ vs Sucrose 0.4M + Dox 10 ⁻⁶ | 2.227 | 0.5853 |
| Dox 10 ⁻⁵ vs Sucrose 0.4M + Dox 10 ⁻⁵ | 3.388 | 0.0620 |
| Dox 10 ⁻⁴ vs Sucrose 0.4M + Dox 10 ⁻⁴ | 1.938 | 0.7706 |
| (Sucrose 0.25M + Dox 10 ⁻⁶) vs (Sucrose 0.4M + Dox 10 ⁻⁶) | -1.102 | 0.9953 |
| (Sucrose 0.25M + Dox 10 ⁻⁵) vs (Sucrose 0.4M + Dox 10 ⁻⁵) | 0.71.6 | >0.9999 |
| (Sucrose 0.25M + Dox 10 ⁻⁴) vs (Sucrose 0.4M + Dox 10 ⁻⁴) | 0.3168 | >0.9999 |

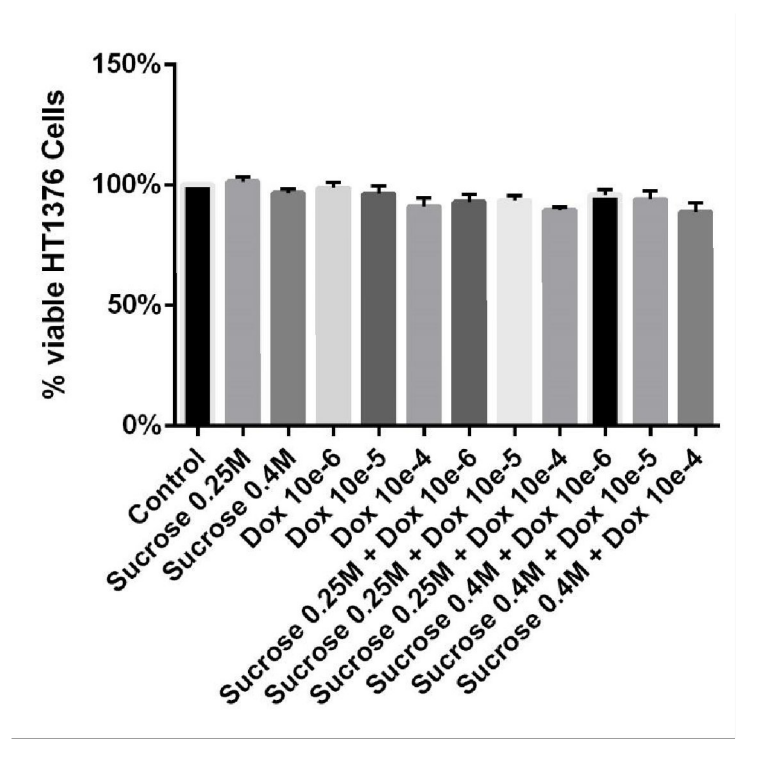


Figure 34: Effect of sucrose 0.25M and 0.4 M on doxazosin-induced cell death on HT1376 cells. Dox = doxazosin.

Table 7: Effect of sucrose 0.25M and 0.4M on HT1376 cell line

| Parameters Compared | Mean Difference | p value |
|---|--------------------|---------|
| Control vs Sucrose 0.25M | -1.350 | 0.9936 |
| Control vs Sucrose 0.4M | 3.454 | 0.1853 |
| Dox 10 ⁻⁶ vs Sucrose 0.25M + Dox 10 ⁻⁶ | 5.865 | 0.0004 |
| Dox 10 ⁻⁵ vs Sucrose 0.25M + Dox 10 ⁻⁵ | 2.697 | 0.5463 |
| Dox 10 ⁻⁴ vs Sucrose 0.25M + Dox 10 ⁻⁴ | 1.512 | 0.9840 |
| Dox 10 ⁻⁶ vs Sucrose 0.4M + Dox 10 ⁻⁶ | 2.905 | 0.4294 |
| Dox 10 ⁻⁵ vs Sucrose 0.4M + Dox 10 ⁻⁵ | 2.154 | 0.8314 |
| Dox 10 ⁻⁴ vs Sucrose 0.4M + Dox 10 ⁻⁴ | 2.258 | 0.7848 |
| (Sucrose 0.25M + Dox 10 ⁻⁶) vs (Sucrose 0.4M + Dox 10 ⁻⁶) | -2.961 | 0.3993 |
| (Sucrose 0.25M + Dox 10 ⁻⁵) vs (Sucrose 0.4M + Dox 10 ⁻⁵) | -0.5429 | >0.9999 |
| (Sucrose 0.25M + Dox 10 ⁻⁴) vs (Sucrose 0.4M + Dox 10 ⁻⁴) | 0.7459 | >0.9999 |

5.7.2.5 Effect of doxazosin on PC-3 cells pre-incubated with chlorpromazine:

When PC-3 cells were incubated with chlorpromazine 100 μ M there was a small reduction in viable cells when compared to controls, though this difference was not statistically significant (p = 0.55). Pre-incubation with chlorpromazine hydrochloride 100 μ M did not abrogate the cell death induced by 37 μ M of doxazosin, (p = 0.8738).

5.7.2.6 Effect of doxazosin on DU145 cells pre-incubated with chlorpromazine:

When DU-145 cells were incubated with chlorpromazine 100 μ M there was a small reduction in viable cells when compared to controls, though this difference was not statistically significant (p = 0.1605). Pre-incubation with chlorpromazine hydrochloride 100 μ M did not abrogate the cell death induced by 37 μ M of doxazosin, (p = 0.8544).

5.7.2.7 Effect of doxazosin on LNCaP cells pre-incubated with chlorpromazine:

When LNCaP cells were incubated with chlorpromazine 100 μ M there was a small reduction in viable cells when compared to controls, though this difference was not statistically significant (p = 0.4139). Pre-incubation with chlorpromazine hydrochloride 100 μ M did not abrogate the cell death induced by doxazosin (37 μ M), (p = 0.9973).

5.7.2.8 Effect of doxazosin on HT1376 cells pre-incubated with chlorpromazine:

When HT1376 cells were incubated with chlorpromazine 100 μ M there was a small reduction in viable cells when compared to controls, though this difference was not statistically significant (p = 0.2071). Pre-incubation with chlorpromazine hydrochloride 100 μ M did not abrogate the cell death induced by doxazosin (37 μ M), (p = >0.9999).

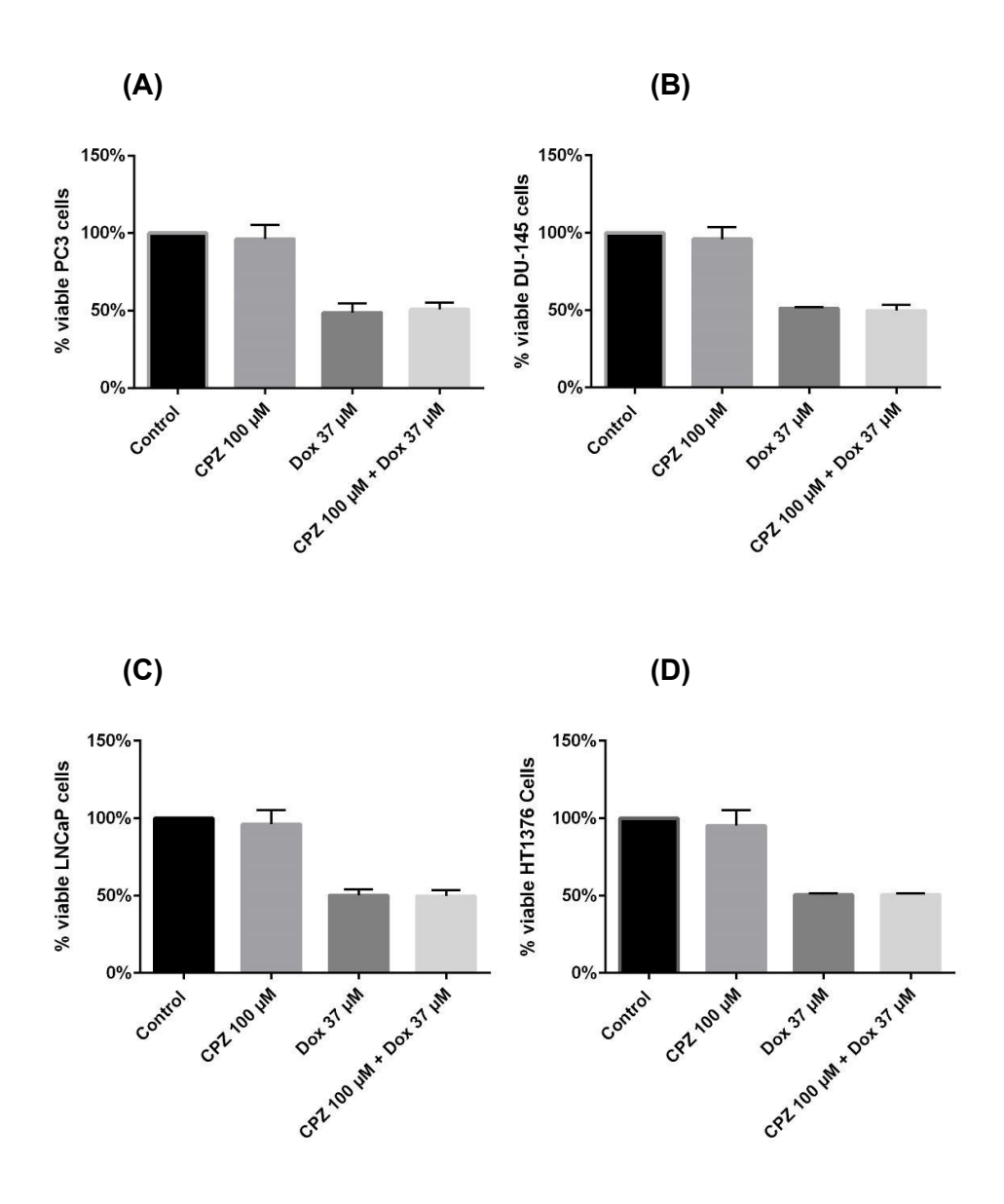


Figure 35: Effect of chlorpromazine (CPZ) on doxazosin (Dox)-induced cell death in the cell lines PC-3 (A), DU145 (B), LNCaP (C), and HT1376 (D). Pre-incubation with CPZ did not have a significant effect on cell death induced by $37 \mu M$ doxazosin.

5.7.2.9 Effect of doxazosin on PC-3 cells pre-incubated with dansylcadaverine:

When PC-3 cells were incubated with dansylcadaverine 75 μ M there was a small reduction in viable cells when compared to controls, though this difference was not statistically significant (p = 0.1437). Pre-incubation with dansylcadaverine 75 μ M for 4 h followed by doxazosin (37 μ M) for 72 h significantly reduced the cytotoxic action of doxazosin, (p = <0.0001).

5.7.2.10 Effect of doxazosin on DU145 cells pre-incubated with dansylcadaverine:

When DU-145 cells were incubated with dansylcadaverine 75 μ M there was a small reduction in viable cells when compared to controls and this difference was statistically significant (p = 0.0318). Pre-incubation with dansylcadaverine 75 μ M for 4 h followed by doxazosin (37 μ M) for 72 h significantly reduced the cytotoxic action of doxazosin, (p = <0.0001).

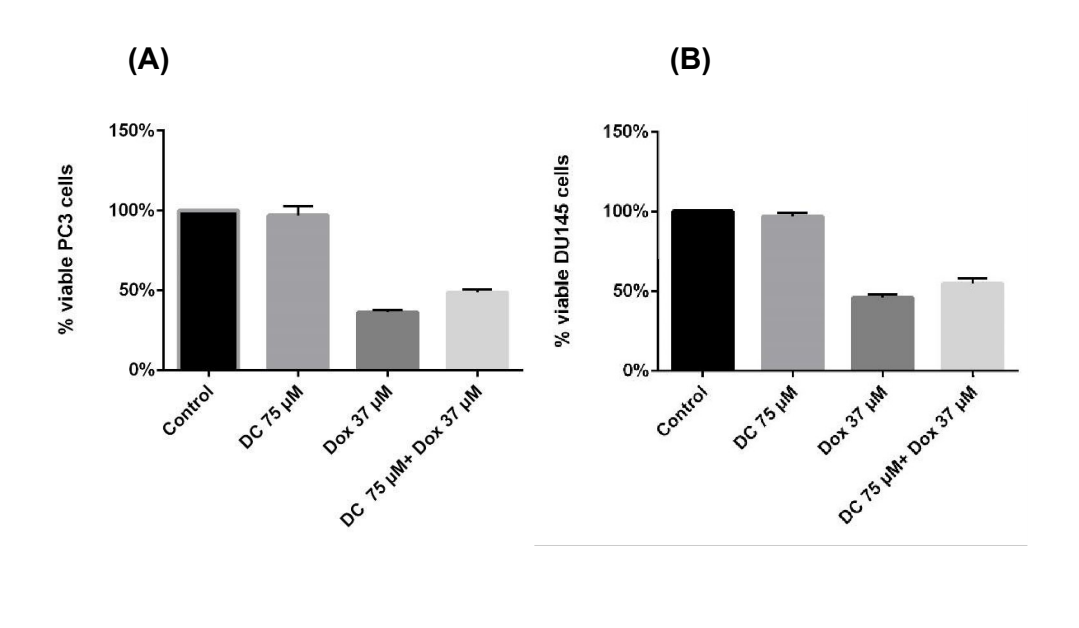
<u>5.7.2.11 Effect of doxazosin on LNCaP cells pre-incubated with</u> dansylcadaverine:

When LNCaP cells were incubated with dansylcadaverine 75 μ M there was a small reduction in viable cells when compared to controls, though this difference was not statistically significant (p = 0.5204). Pre-incubation with dansylcadaverine 75 μ M for 4 h followed by doxazosin (37 μ M) for 72 h significantly reduced the cytotoxic action of doxazosin, (p = <0.0002).

<u>5.7.2.12 Effect of doxazosin on HT1376 cells pre-incubated with</u> dansylcadaverine:

When HT1376 cells were incubated with dansylcadaverine 75 μ M there was a small reduction in viable cells when compared to controls, though this difference was not statistically significant (p = 0.7954). Pre-incubation with dansylcadaverine 75 μ M for

4 h followed by doxazosin (37 μ M) for 72 h significantly reduced the cytotoxic action of doxazosin, (p = <0.0001).



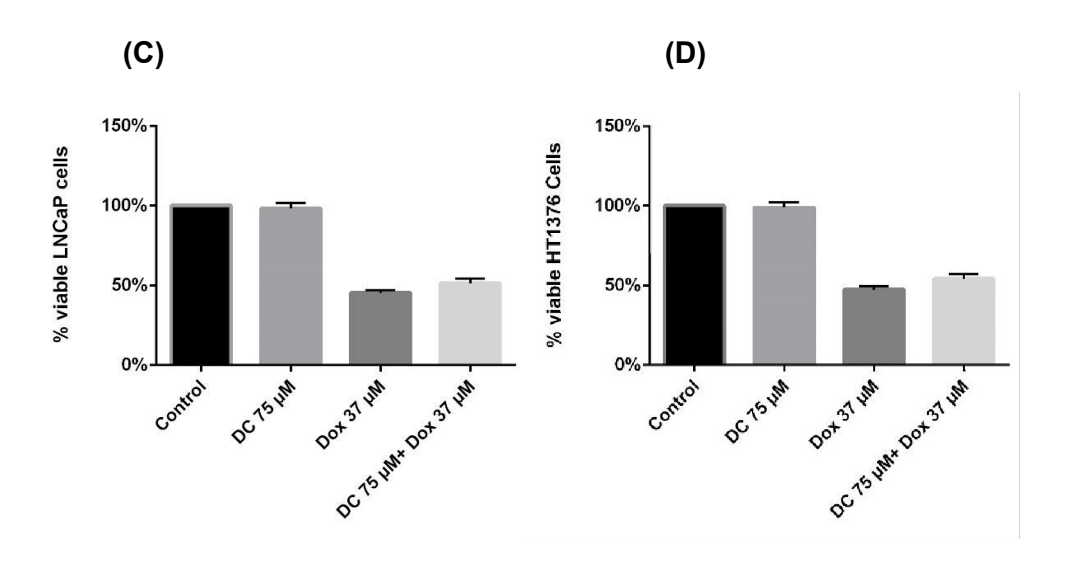


Figure 36: Effect of dansyl cadaverine (DC) on doxazosin (Dox)-induced cell death in the cell lines PC-3 (A), DU145 (B), LNCaP (C), and HT1376 (D). Pre-incubation with DC significantly attenuated cell death induced by 37 μ M doxazosin.

5.7.3 Inhibition of endocytosis using chemical inhibitors of caveolae-mediated (lipid raft) endocytic pathway:

5.7.3.1 Effect of doxazosin on PC-3 cells pre-incubated with mevastatin:

When PC-3 cells were incubated with mevastatin 20 μ M there was no significant difference in number of viable cells when compared to controls. Pre-incubation with mevastatin 20 μ M did not abrogate the cell death induced by doxazosin (37 μ M), (p = 0.1394).

5.7.3.2 Effect of doxazosin on DU145 cells pre-incubated with mevastatin:

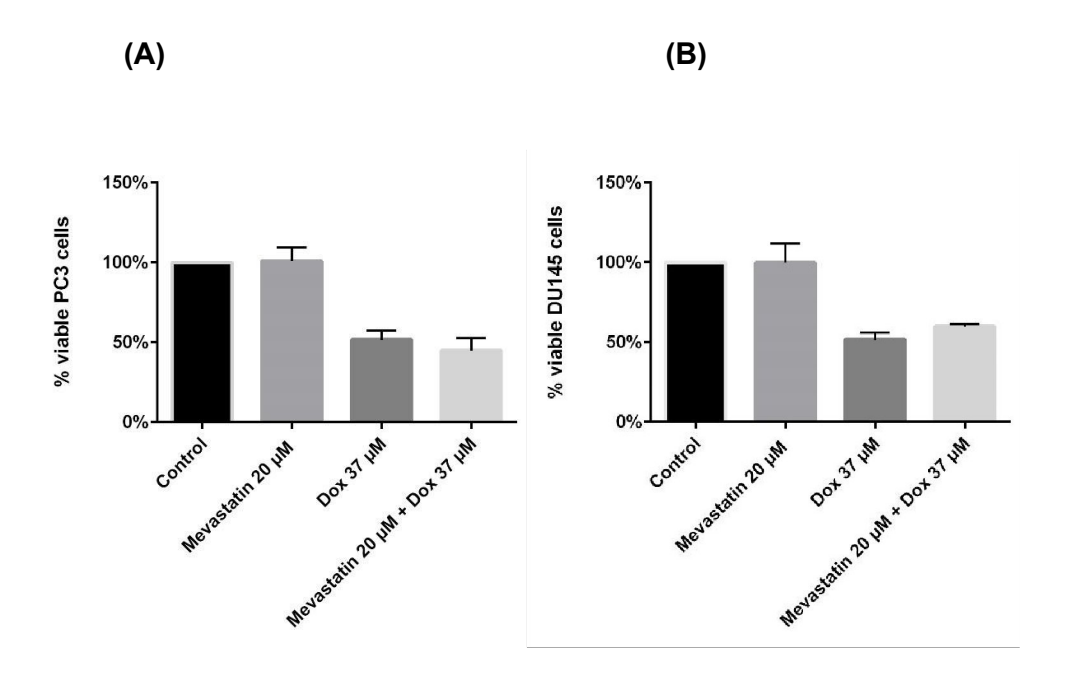
When DU145 cells were incubated with mevastatin 20 μ M there was no significant difference in number of viable cells when compared to controls. Pre-incubation with mevastatin 20 μ M attenuated the cell death induced by doxazosin 37 μ M though this was not significant (p = 0.0507).

5.7.3.3 Effect of doxazosin on LNCaP cells pre-incubated with mevastatin:

When LNCaP cells were incubated with mevastatin 20 μ M there was a small reduction in viable cells when compared to controls, though this difference was not statistically significant (p = 0.3947). Pre-incubation with mevastatin 20 μ M attenuated the cell death induced by doxazosin 37 μ M and this was significant (p = 0.0020).

5.7.3.4 Effect of doxazosin on HT1376 cells pre-incubated with mevastatin:

When HT1376 cells were incubated with mevastatin 20 μ M there was a small reduction in viable cells when compared to controls, though this difference was not statistically significant (p = 0.4464). Pre-incubation with mevastatin 20 μ M did not abrogate the cell death induced by doxazosin 37 μ M, (p = 0.4635).



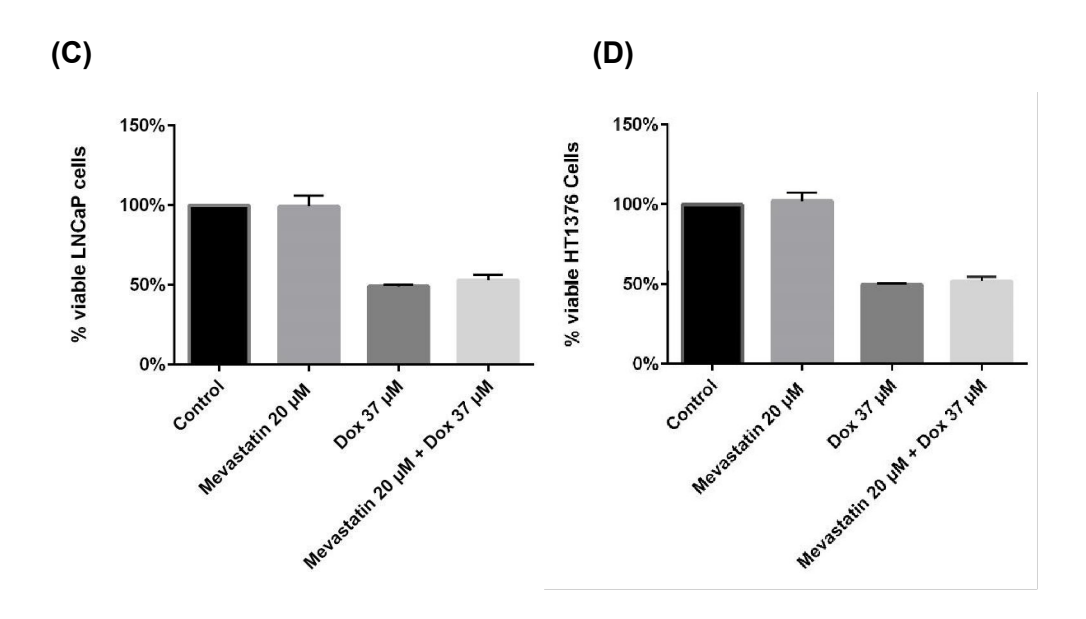


Figure 37: Effect of mevastatin on doxazosin (Dox)-induced cell death in the cell lines PC-3 (A), DU145 (B), LNCaP (C), and HT1376 (D). Pre-incubation with mevastatin significantly attenuated cell death induced by 37 μ M doxazosin in LNCaP cells but not in other cell lines.

5.7.3.5 Effect of doxazosin on PC-3 cells pre-incubated with MBCD:

When PC-3 cells were incubated with MBCD 1mM there was a small reduction in viable cells when compared to controls, though this difference was not statistically significant (p = 0.7960). Pre-incubation with MBCD 1mM did not abrogate the cell death induced by doxazosin 37 μ M, (p = 0.0975).

5.7.3.6 Effect of doxazosin on DU145 cells pre-incubated with MBCD:

When DU145 cells were incubated with MBCD 1mM there was a small reduction in viable cells when compared to controls, though this difference was not statistically significant (p = 0.7882). Pre-incubation with MBCD 1mM did not abrogate the cell death induced by doxazosin 37 μ M, (p = 0.2535).

5.7.3.7 Effect of doxazosin on LNCaP cells pre-incubated with MBCD:

When LNCaP cells were incubated with MBCD 1mM there was a reduction in viable cells when compared to controls, though this difference was statistically significant (p = 0.0002). However, pre-incubation with MBCD 1mM did not abrogate the cell death induced by doxazosin 37 μ M, (p = 0.0939).

5.7.3.8 Effect of doxazosin on HT1376 cells pre-incubated with MBCD:

When HT1376 cells were incubated with MBCD 1mM there was a small reduction in viable cells when compared to controls, though this difference was not statistically significant (p = 0.2859). Pre-incubation with MBCD 1mM did not abrogate the cell death induced by doxazosin 37 μ M, (p = 0.1630).

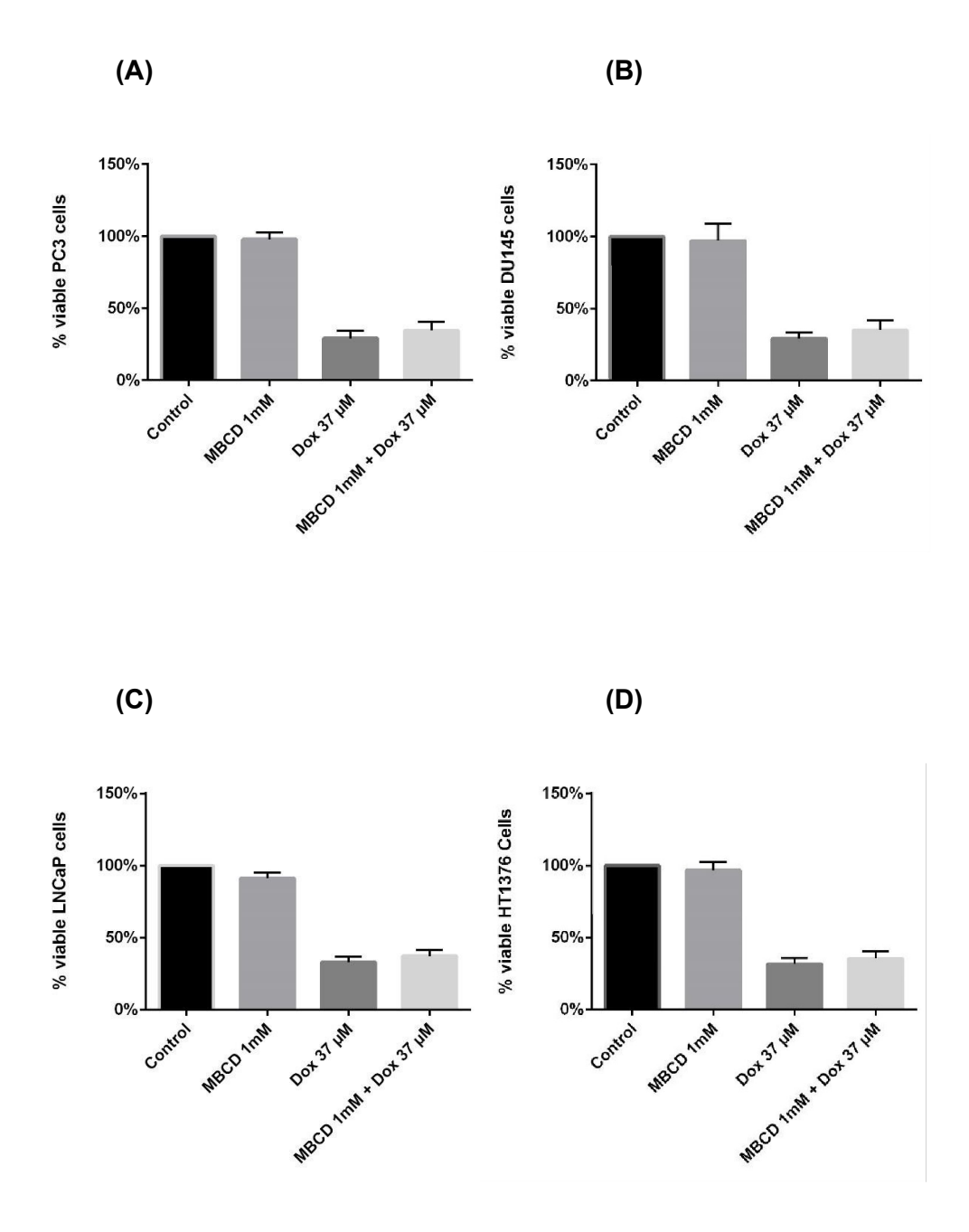


Figure 38: Effect of methyl beta cyclodextrin (MBCD) on doxazosin (Dox)-induced cell death in the cell lines PC-3 (A), DU145 (B), LNCaP (C), and HT1376 (D). Preincubation with MBCD did not significantly attenuate cell death induced by 37 μ M doxazosin in the above cell lines.

5.7.3.9 Effect of doxazosin on PC-3 cells pre-incubated with cholesterol oxidase:

When PC-3 cells were incubated with cholesterol oxidase 2 units/ml there was no significant difference in viable cells when compared to controls, (p = 0.5287). Pre-incubation with cholesterol oxidase 2 units/ml did not abrogate the cell death induced by doxazosin 37 μ M, (p = 0.8685).

5.7.3.10 Effect of doxazosin on DU145 cells pre-incubated with cholesterol oxidase:

When DU145 cells were incubated with cholesterol oxidase 2 units/ml there was no significant difference in viable cells when compared to controls, (p = 0.5012). Pre-incubation with cholesterol oxidase 2 units/ml did not abrogate the cell death induced by doxazosin 37 μ M, (p = 0.4894).

5.7.3.11 Effect of doxazosin on LNCaP cells pre-incubated with cholesterol oxidase:

When LNCaP cells were incubated with cholesterol oxidase 2 units/ml there was no significant difference in viable cells when compared to controls, (p = 0.1992). Pre-incubation with cholesterol oxidase 2 units/ml did not abrogate the cell death induced by doxazosin 37 μ M, (p = 0.5175).

5.7.3.12 Effect of doxazosin on HT1376 cells pre-incubated with cholesterol oxidase:

When HT1376 cells were incubated with cholesterol oxidase 2 units/ml there was no significant difference in viable cells when compared to controls, (p = 0.9352). Preincubation with cholesterol oxidase 2 units/ml did not abrogate the cell death induced by doxazosin 37 μ M, (p = 0.0673).

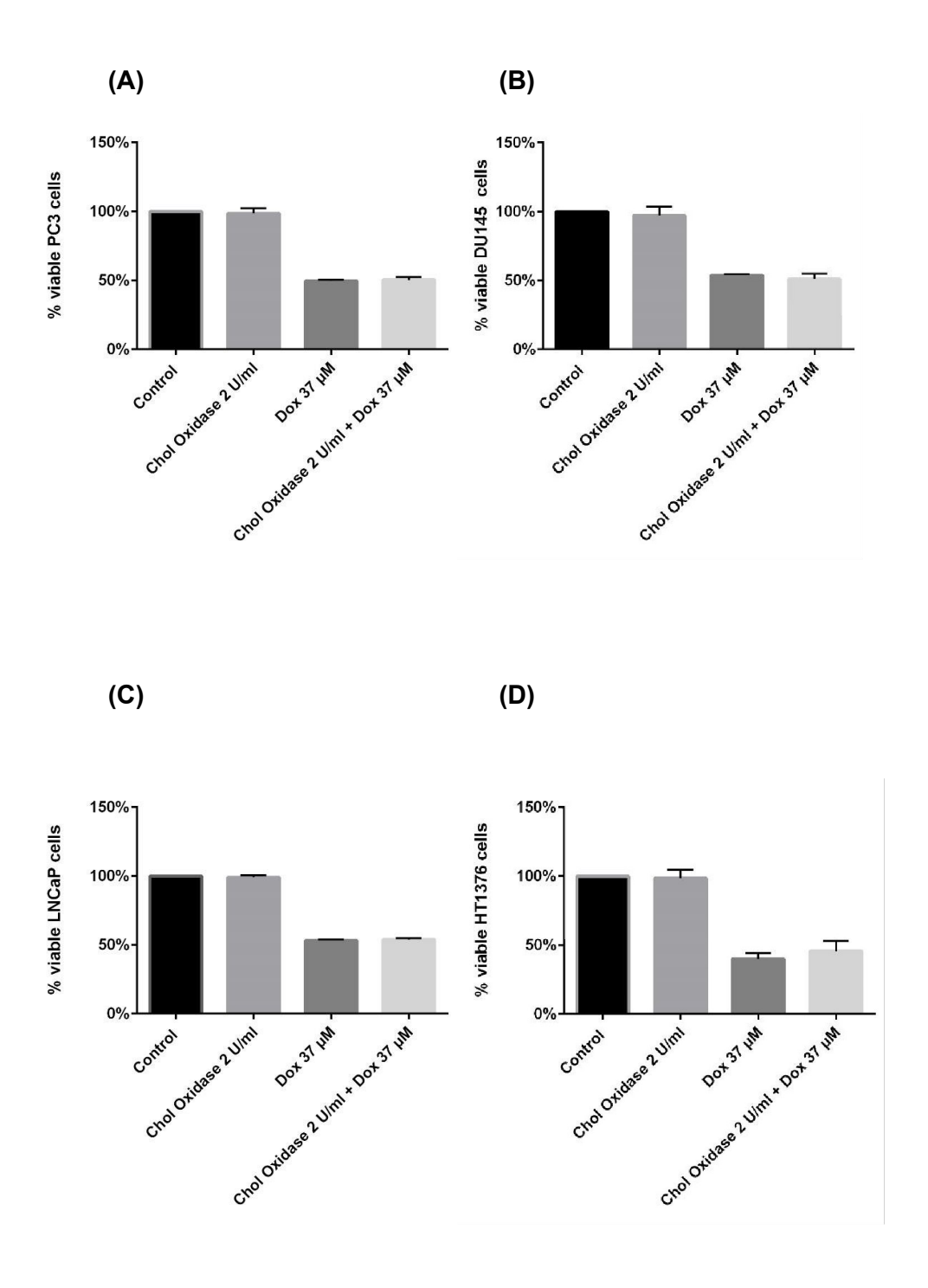


Figure 39: Effect of cholesterol oxidase (Chol oxidase) on doxazosin (Dox)-induced cell death in the cell lines PC-3 (A), DU145 (B), LNCaP (C), and HT1376 (D). Preincubation with cholesterol oxidase did not significantly attenuate cell death induced by 37 μ M doxazosin in the above cell lines.

5.7.4 Effect of inhibition of endocytosis using chemical inhibitors of micropinocytosis:

5.7.4.1 Effect of doxazosin on PC-3 cells pre-incubated with amiloride:

When PC-3 cells were incubated with amiloride 50 μ M there was no significant difference in viable cells when compared to controls (p = 0.5867). Pre-incubation with amiloride did not abrogate the cell death induced by doxazosin 37 μ M (p = 0.9985).

5.7.4.2 Effect of doxazosin on DU145 cells pre-incubated with amiloride:

When DU145 cells were incubated with amiloride 50 μ M there was no significant difference in viable cells when compared to controls (p = 0.7811). Pre-incubation with amiloride did not abrogate the cell death induced by doxazosin 37 μ M (p = 0.9504).

5.7.4.3 Effect of doxazosin on LNCaP cells pre-incubated with amiloride:

When LNCaP cells were incubated with amiloride 50 μ M there was no significant difference in viable cells when compared to controls (p = 0.3616). Pre-incubation with amiloride did not abrogate the cell death induced by doxazosin 37 μ M (p = 0.8920).

5.7.4.4 Effect of doxazosin on HT1376 cells pre-incubated with amiloride:

When HT1376 cells were incubated with amiloride 50 μ M there was no significant difference in viable cells when compared to controls (p =0.9724). Pre-incubation with amiloride did not abrogate the cell death induced by doxazosin 37 μ M (p = 0.5538).

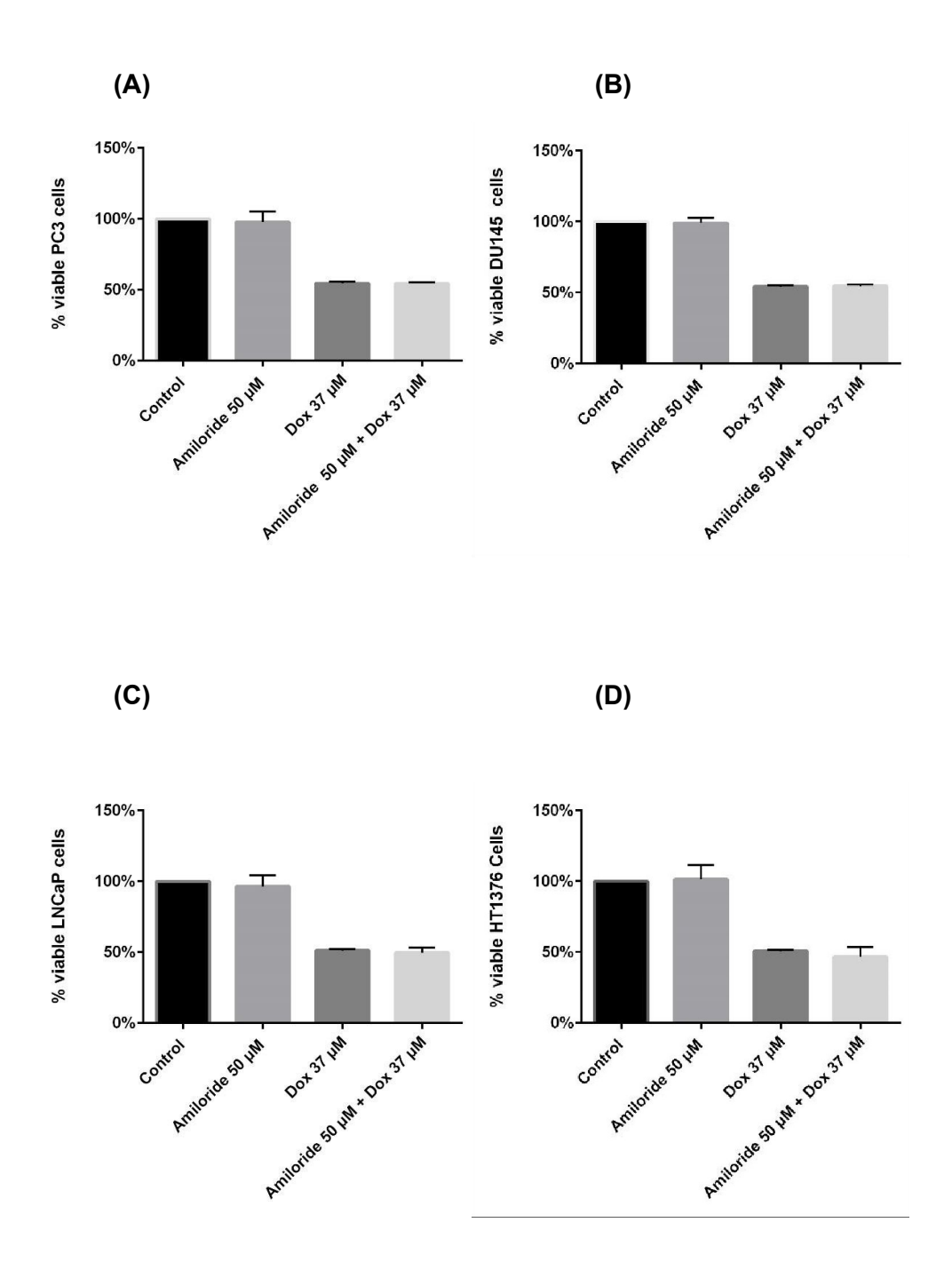


Figure 40: Effect of amiloride on doxazosin (Dox) induced cell death in the cell lines PC-3 (A), DU145 (B), LNCaP (C), and HT1376 (D). Pre-incubation with amiloride did not significantly attenuate cell death induced by 37 μ M doxazosin in the above cell lines.

5.7.5 Inhibition of endocytosis using chemical inhibitors of dynamin-mediated endocytic vesicle development:

5.7.5.1 Effect of doxazosin on PC-3 cells pre-incubated with dynasore:

When PC3 cells were incubated with dynasore 20 μ M there was a small reduction in viable cells when compared to controls though this difference was not statistically significant (p = 0.0940). Pre-incubation with dynasore 20 μ M attenuated the cell death induced by doxazosin 37 μ M and this was statistically significant (p = 0.0243). When the doxazosin concentration was 100 μ M this abrogation of the cytotoxicity of doxazosin by the dynasore was even more significant (p = <0.0001)

5.7.5.2 Effect of doxazosin on DU145 cells pre-incubated with dynasore:

When DU145 cells were incubated with dynasore 20 μ M there was a small reduction in viable cells when compared to controls though this difference was not statistically significant (p = 0.1860). Pre-incubation with dynasore 20 μ M attenuated the cell death induced by doxazosin 37 μ M and this was statistically significant (p = 0.0019). When the doxazosin concentration was 100 μ M this abrogation of the cytotoxicity of doxazosin by the dynasore was even more significant (p = <0.0001)

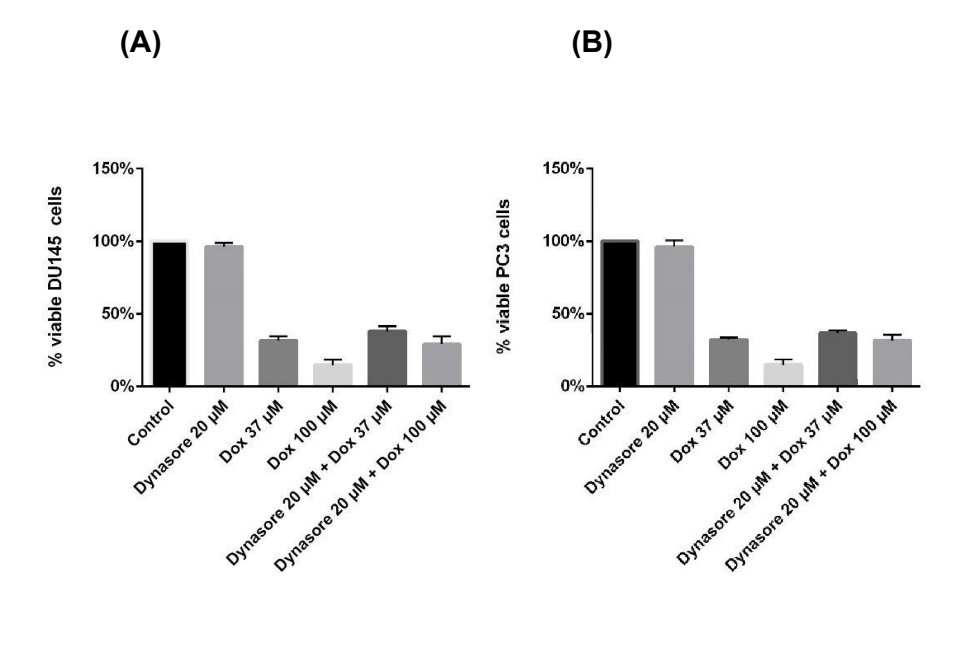
5.7.5.3 Effect of doxazosin on LNCaP cells pre-incubated with dynasore:

When LNCaP cells were incubated with dynasore 20 μ M there was a small reduction in viable cells when compared to controls though this difference was not statistically significant (p = 0.0669). Pre-incubation with dynasore 20 μ M attenuated the cell death induced by doxazosin 37 μ M but this was not statistically significant (p = 0.0766). However, when the doxazosin concentration was increased to 100 μ M this

abrogation of the cytotoxicity of doxazosin by the dynasore was significant (p = 0.0141)

5.7.5.4 Effect of doxazosin on HT1376 cells pre-incubated with dynasore:

When HT1376 cells were incubated with dynasore 20 μ M there was a small reduction in viable cells when compared to controls though this difference was not statistically significant (p = 0.1817). Pre-incubation with dynasore 20 μ M attenuated the cell death induced by doxazosin 37 μ M and this was statistically significant (p = 0.0007). When the doxazosin concentration was 100 μ M this abrogation of the cytotoxicity of doxazosin by the dynasore was even more significant (p = <0.0001).



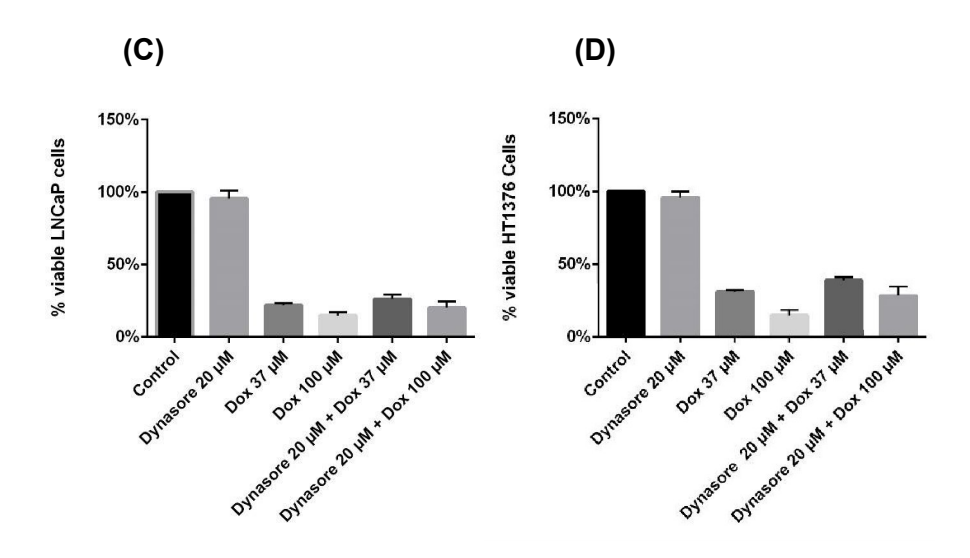


Figure 41: Effect of dynasore on doxazosin (Dox) induced cell death in the cell lines PC-3 (A), DU145 (B), LNCaP (C), and HT1376 (D). Pre-incubation with dynasore significantly attenuated cell death induced by 37 μ M and 100 μ M doxazosin in the above cell lines.

5.7.5.5 Effect of doxazosin on PC-3 cells pre-incubated with Mdivi-1:

Mdivi-1 50 μ M induced a significant inhibition of growth of PC-3 cells when compared to controls (p = <0.0001). Pre-incubation with Mdivi-1 50 μ M for 4 h followed by doxazosin (37 μ M) for 72 h significantly reduced the cytotoxic action of the latter (p = <0.0003).

5.7.5.6 Effect of doxazosin on DU145 cells pre-incubated with Mdivi-1:

Mdivi-1 50 μ M induced a significant inhibition of growth of PC-3 cells when compared to controls (p = <0.0001). Pre-incubation with Mdivi-1 50 μ M for 4 h followed by doxazosin (37 μ M) for 72 h significantly reduced the cytotoxic action of the latter (p = <0.0062).

5.7.5.7 Effect of doxazosin on LNCaP cells pre-incubated with Mdivi-1:

Mdivi-1 50 μ M induced a significant inhibition of growth of PC-3 cells when compared to controls (p = <0.0001). Pre-incubation with Mdivi-1 50 μ M for 4 h followed by doxazosin (37 μ M) for 72 h significantly reduced the cytotoxic action of the latter (p = <0.0009).

5.7.5.8 Effect of doxazosin on HT1376 cells pre-incubated with Mdivi-1:

Mdivi-1 50 μ M induced a significant inhibition of growth of PC-3 cells when compared to controls (p = <0.0001). Pre-incubation with Mdivi-1 50 μ M for 4 h followed by doxazosin (37 μ M) for 72 h significantly reduced the cytotoxic action of the latter (p = <0.0009).

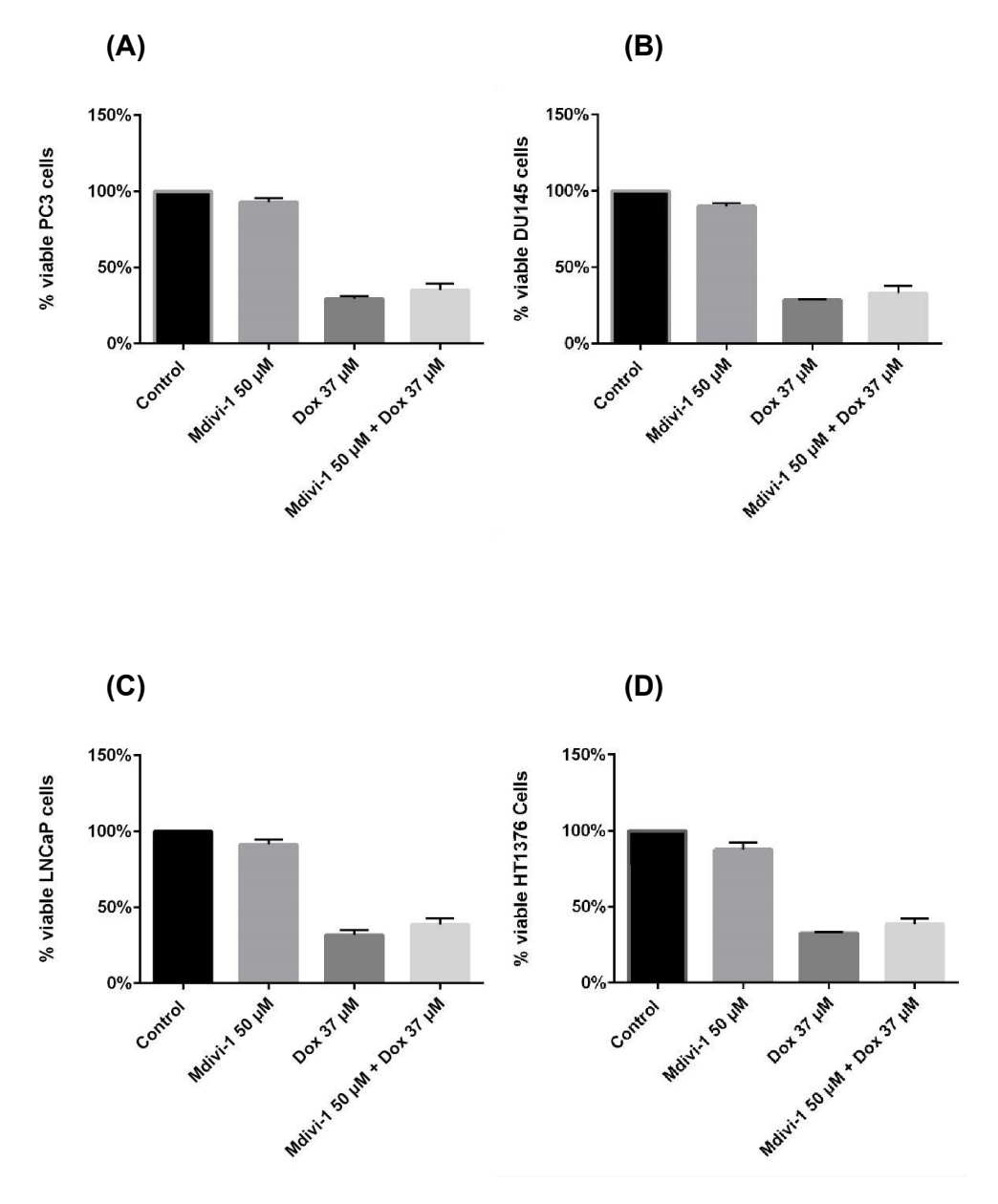


Figure 42: Effect of Mdivi-1 on doxazosin (Dox) induced cell death in the cell lines PC-3 (A), DU145 (B), LNCaP (C), and HT1376 (D). Pre-incubation with Mdivi-1 significantly attenuated cell death induced by 37 μ M of doxazosin in the above cell lines.

5.8 Discussion

Endocytosis is integrated with and necessary for the execution of a wide range of cellular programs (Di Fiore 2009). Endocytosis was considered to function primarily an attenuator of signalling, which can potentially serve as a tumour suppressor pathway (Polo, Pece et al. 2004, Di Fiore 2009). More recently, it has been shown that endocytic signalling persists throughout the signalling route giving rise to the concept of signalling endosomes (von Zastrow and Sorkin 2007, Di Fiore and von Zastrow 2014). Derailed endocytosis and its effects on the cellular processes is an emerging field of cancer research. Specifically, deranged endocytosis resulting in defective trafficking of growth factor receptors coupled with an unbalanced recycling of integrin –and –cadherin based adhesion complexes has become one of the hallmarks of malignant cells (Mosesson, Mills et al. 2008).

The mechanisms that govern the entry of macromolecules and regulate the subsequent trafficking within the cells via endocytosis are poorly understood. Once macromolecules enter the cells they are sorted to different cellular destinations in early/sorting endosomes.

Prazosin, a quinazoline derivative had been shown to inhibit the sorting process by an off-target perturbation of GPCR of which alpha-1 adrenergic receptors were a prime target (Zhang, Wang et al. 2012). Our results in agreement with others, have shown that the cytotoxic actions of doxazosin in PCa and BCa are independent of the alpha-adrenergic receptor (Benning and Kyprianou 2002, Pavithran and Thompson 2012, Pavithran, Shabbir et al. 2017). Therefore, the significance of the ability of prazosin to inhibit the sorting process of alpha-1 adrenergic receptors and its role in prazosin-induced cell death of cancer cells remained uncertain.

In this chapter, we had investigated the role of endocytosis in doxazosin-induced cell death in *In Vitro* cell cultures of PCa and BCa cell lines mainly using chemical inhibitors of endocytosis that target the clathrin-mediated, caveolae-mediated, dynamin-mediated and pinocytosis pathways. In brief, we observed that there was significant attenuation of doxazosin-induced cell death when clathrin-mediated pathways were inhibited.

Endocytosis is a temperature-dependent cellular process and at 10 C or below, the rate of endocytosis is negligible and between 10 to 20 C they increase proportionately to rise in temperature. Above 20 C this rise is at a much higher rate between 20 C to 41 C (Weigel and Oka 1981). Our results show that the cell death induced by doxazosin was attenuated when cells were incubated on ice as compared to positive controls at 37 C. We did not observe a significant effect of temperature at lower concentrations of doxazosin (10⁻⁷ and 10⁻⁶). However, at concentrations of 10⁻⁵ and 10⁻⁴, we observed that there was a significant attenuation of doxazosin-induced cell death when cells were cooled on ice, suggesting that the effects of doxazosin of cell viability was temperature dependent. At these temperatures, both clathrin -and -caveolae -mediated endocytic processes are inhibited and therefore does not provide information on the specific pathway that is inhibited. Moreover, the attenuation of cell death by cooling only provides indirect evidence of endocytic inhibition as the positive controls were not designed to show a direct inhibition of endocytosis but rather the consequence of such an effect on cell viability.

One of the caveats of using cell viability as a measure of end point was that cooling of cells has other unwarranted effects on the ability of the cells to remain adherent to the MP, and this was particularly more visible on LNCaP cells. Of the 4 cell lines

tested, under normal conditions LNCaP is the least adherent. We observed that cooling resulted in a marked inability of LNCaP cells to remain adherent. Androgen-independent cells (DU145 and PC-3) over express of α6β4 integrin, which results from the loss of AR, and increases cell adhesion (Baust, Klossner et al. 2010). This could likely explain the tolerance of androgen-resistant cells (DU145 and PC3) to lower temperatures whilst androgen-dependent LNCaP cells underwent significant anoikis at lower temperatures even after a relatively short duration (4 h) of incubation with doxazosin. Though this added to an unwarranted artefactual error (due to loss of cells) to the interpretation of results, particularly with LNCaP cells, they may possibly have some clinical significance in dissemination and subsequent establishment of metastasis of such tumours especially when cryotherapy is used as a mode of treatment. On the other hand, exploitation of the accelerated cell death processes involved in temperature dependent cell death of androgen-dependent tumours may be useful in planning novel option of treatments for androgen-dependent PCa (Baust, Klossner et al. 2010).

Our next experiments focussed on dissecting the role of clathrin-mediated endocytic pathways in doxazosin-induced cell death of PCa and BCa cell lines. These inhibitors, also besides interfering with specific steps of the endocytic pathway, are known to have several effects on other signalling processes within the cell thus confounding the validity of the results (Ivanov 2008). Chemical inhibitors of endocytosis serve as a preliminary step towards a broad understanding of the endocytic process (Ivanov 2008). Additionally, the different pathways of endocytosis are not clearly demarcated and there exists a significant overlap between the different endocytic pathways (Ivanov 2008). Moreover, endocytosis is linked to other unrelated cell processes such as apoptosis, autophagy and cell division and these

may have an influence on the results, especially when cell viability is considered as an end point of the experiments (Polo, Pece et al. 2004, von Zastrow and Sorkin 2007, Fielding, Willox et al. 2012, Di Fiore and von Zastrow 2014). Conversely, whilst visualizing of molecular trafficking by confocal studies can more reliably quantify the endocytic transport of a molecule (in this case doxazosin) (Ivanov 2008, Di Fiore and von Zastrow 2014), the results will still need to be corroborated with cell viability studies to ascribe relevance to those findings to doxazosin-induced cell death.

The chemical inhibitors we had chosen for inhibition of clathrin-mediated endocytosis included sucrose, chlorpromazine and dansylcadaverine using previously reported methods (Ostrom and Liu 2007, Ivanov 2008). We observed doxazosin-induced cell death in PC-3 was attenuated by pre-treatment with sucrose of 0.25 M and followed by exposure to doxazosin (10⁻⁵) significantly (p=0.0256). At a higher concentration of sucrose of 0.4 M, this effect was significant for two different concentrations of doxazosin (p=0.0122 for 10⁻⁵ and 0.0016 for 10⁻⁵ of doxazosin). Pre-treatment with sucrose 0.25 M and 0.4 M and followed by exposure to doxazosin (10⁻⁶) significantly (p=0.0147 and 0.0475, respectively) attenuated the cell death induced by doxazosin in DU145 cells. In HT1376 cells, the only significant (p=0.0004) attenuation of the doxazosin cytotoxicity was observed when pre-treatment with sucrose 0.25 M was followed by exposure to doxazosin (10⁻⁶). Sucrose had no significant effect on viability of at all the concentrations tested.

Sucrose inhibits clathrin-mediated endocytosis by trapping clathrin in micro cages (Malek, Xu et al. 2007, Dutta and Donaldson 2012). However, sucrose interferes with fluid phase micropinocytosis and therefore its effects are not limited to clathrin-mediated endocytosis (Carpentier, Sawano et al. 1989). Additionally, sucrose

induces vesicle accumulation and autophagy thereby limiting the ability to interpret the results on viability assays (Higuchi, Nishikawa et al. 2015).

In clathrin mediated endocytosis, the invagination of the cell membranes contains clathrin coated pits. These are polygonal lattice formations composed of a clathrin triskeleton and adaptor protein-2 subunits. Chlorpromazine inhibits clathrin coated pit formation by a reversible translocation of clathrin and adaptor protein-2 from plasma membrane to intracellular vesicles (Wang, Rothberg et al. 1993, Ivanov 2008, Vercauteren, Vandenbroucke et al. 2010, Dutta and Donaldson 2012). Chlorpromazine also decreased cell viability in concentrations required for inhibition of endocytosis (Vercauteren, Vandenbroucke et al. 2010). Not surprisingly, we noted a small but not significant reduction in cell populations exposed to doxazosin. However, chlorpromazine did not show any significant attenuation of doxazosin induced cell death in all the cell lines tested.

Dansylcadaverine stabilizes clathrin-coated vesicles and reversibly inhibits the uptake of ligands and this process is selective for receptor-mediated ligands (Schlegel, Dickson et al. 1982). Dansylcadaverine is also lysosomotropic and autofluorescent and selectively concentrates in autophagosomes making it a very useful marker of autophagy (Ivanov 2008, Klionsky, Abdalla et al. 2012). Our results show that dansylcadaverine had a significant effect in attenuation of doxazosin induced cell death (p = <0.0001 in PC3, DU145 and HT1376 cells and p = 0.0002 in LNCaP cells), suggesting that these may have been mediated by inhibitory of effects of dansylcadaverine on clathrin-mediated endocytosis.

To assess the caveolin-mediated endocytosis pathway on doxazosin-induced cell death we pre-treated PC-3, DU-145, LNCaP and HT1376 with mevastatin, MBCD or

cholesterol oxidase. Caveolin mediated endocytosis and lipid raft mediated endocytosis happen at the caveolae which are flask-shaped, 50-100 nm plasma membrane invaginations that are enriched in specific lipids such as cholesterol and glycolipids (Ostrom and Liu 2007, Sotgia, Martinez-Outschoorn et al. 2012). Caveolae are similar to lipid rafts in that they are both enriched with sphingolipid and cholesterol but caveolae also express a coat of caveolin proteins on the inner leaflet of the membrane bilayer; caveolin-1 is the predominant isoform of caveolin (Ostrom and Liu 2007).

Caveolin-1 dependent endocytosis enhances chemosensitivity of Herceptin-2 positive breast cancers to trastuzumab and emtansine (Chung, Kuo et al. 2015) and a loss of caveolin-1 has been implicated in the pathogenesis of human cancers (Sotgia, Martinez-Outschoorn et al. 2012). Caveolin-mediated endocytosis are clathrin-independent but dynamin-dependent and thus represent a parallel but distinct pathway from clathrin-coated pits for removal and destruction of plasma membrane receptors (Nabi and Le 2003). The caveolin –and –raft dependent pathways are characterized by their independence from the clathrin and a common sensitivity to cholesterol depletion and inhibition of dynamin function (Nabi and Le 2003).

Mevastatin is statin compound, which acts by inhibiting 3-hydroxy 3-methyl glutaryl coenzyme A (HMGCoA) reductase enzyme (Endo and Hasumi 1993). The HMG-CoA enzyme is essential for cholesterol biosynthesis in cells and controls the rate limiting required for intracellular production of cholesterol (Feher, Webb et al. 1993). Incubation of cells with 10- 100 μM concentration of statins (simvastatin, lovastatin, mevastatin, pravastatin etc), results in nearly 100 % blockage of intracellular cholesterol synthesis (Sidaway, Davidson et al. 2004, Ivanov 2008). Statins also

block the synthesis of franyl pyrophosphate and geranylgeranyl pyrophosphate, which are essential for post translation activation of intracellular proteins such as Ras, Rho and Rab families of small GTPases (de Toledo, Senic-Matuglia et al. 2003, Katoh and Katoh 2004, Liao and Laufs 2005). This results in accumulation of inactive GTPases and leads to profound and nonspecific disruption of the actin cytoskeleton (de Toledo, Senic-Matuglia et al. 2003, Liao and Laufs 2005, Ivanov 2008). In our experiments, we used mevastatin as a prototype statin given its well established role in preventing vesicle trafficking and disruption of caveolin mediated endocytic pathways (Hao, Mukherjee et al. 2004). Pre-incubating PC-3, DU145, LNCaP and HT-1376 with 20 µM of mevastatin for 4 h followed by exposure to doxazosin 37 µM had different effects on these cell lines. Whilst in PC-3 and HT1376 cell lines the inhibition of cell death by doxazosin were not significant (p = 0.1394 and p = 0.4635, respectively), this was not the case with DU145 cells where the p = 0.0507. Also, the attenuation of cell death by doxazosin by pre-incubation with mevastatin was significant (p = 0.002) in LNCaP cells. HMG-CoA inhibition and resultant inhibition of various cellular processes such as cholesterol synthesis, depletion of intermediates for small GTPase activation, disruption of vesicular trafficking and disruption of lipid rafts, actin cytoskeleton disruption (Endo and Hasumi 1993, Hao, Mukherjee et al. 2004, Sidaway, Davidson et al. 2004, Liao and Laufs 2005, Cheng, Ohsaki et al. 2006, Ivanov 2008). The results suggests that the cytotoxic effects of doxazosin may be dependent on the inter-dependency of these processes for cell viability, and that these may be variable for each cell line. The attenuation of cytotoxic effects of doxazosin in LNCaP cells could be attributed to be the androgen-sensitive status of these cell lines as androgen-resistant cells have an increased aberrant HMG-CoA reductase activity (Kong, Cheng et al. 2018).

MBCD is a water soluble compound with hydrophobic activity capable of sequestering cholesterol with a high affinity (Kilsdonk, Yancey et al. 1995). This property is used to deplete lipids and cholesterol from the caveolae and lipid rafts to inhibit this pathway of endocytosis (Ivanov 2008). In our experiments, we used MBCD at a concentration of 1 mM in serum free media to pre-treat PC3-, DU145, LNCaP and HT1376 to investigate if depletion of lipids and cholesterol from cells would result in an attenuation of cell death induced by doxazosin. We did not observe any significant attenuation of the effects of doxazosin following pre-treatment with MBCD.

Cholesterol oxidase converts cholesterol into 4-cholesten-3-one, which then gets enriched in the caveolae which dramatically changes its properties and result in disruption of caveolin-mediated internalization of endocytic vesicles (MacLachlan, Wotherspoon et al. 2000, Ivanov 2008). We did not observe a significant effect on doxazosin induced cell death any of the cell lines (PC-3, DU145, LNCaP and HT1376) were pre-incubated with cholesterol oxidase suggesting that caveolin mediated pathways were unlikely to have a significant role in intracellular trafficking of doxazosin.

Pinocytosis or micropinocytosis is the third major pathway of endocytosis and is an actin-dependent mechanism and functions in parallel to clathrin –and –caveolin mediated pathways (Thurn, Arora et al. 2011). Amiloride is a specific inhibitor of pinocytosis and acts by inhibiting the Na/K exchange at micromolar concentrations(Ivanov 2008). We did not observe any significant attenuation of the effects of doxazosin following pre-treatment with 50 µM of amiloride in any of the cell lines tested, suggesting that the actions of doxazosin were independent of pinocytosis.

We next examined if the actions of doxazosin were dependent on the actions of dynamin, which is a 100-kDa GTPase and a specific and essential component of vesicle formation in receptor-mediated endocytosis, synaptic vesicle recycling, caveolae internalization, and possibly vesicle trafficking in and out of Golgi bodies (Hinshaw 2000). Dynasore is a relatively specific, cell permeable inhibitor of dynamin (Macia, Ehrlich et al. 2006). In our experiments, we used dynasore at a concentration of 20 µM in serum free media to pre-treat PC3-, DU145, LNCaP and HT1376 to investigate if inhibition dynamin-dependent endocytosis would result in an attenuation of cell death induced by doxazosin. Dynasore had a small but not significant inhibitory action of all 4 cell lines (PC-3, DU145, LNCaP and HT1376 cells) tested. Our results showed that dynasore significantly attenuated the cell death induced by doxazosin. While pre-treatment with dynasore 20 µM for 4 h and followed by doxazosin 37 μ M for 72 h was significant (p=0.0243, p=0.0019, p=0.0766 and p=0.0007 for PC-3, DU145, LNCaP and HT1376 cell, respectively), this was more significant at higher concentration of doxazosin at 100 µM (p=<0.0001 for PC-3, DU145, HT1376 cells and p=0.0141 for LNCaP cells). These results indicate that the dynasore 20 µM resulted in greater attenuation of cell death at higher (100 µM) of doxazosin to that of a lower concentration (37 μM), suggesting a quantitative inhibition of intracellular trafficking of doxazosin by dynamin dependent process.

Chapter 6

The role of autophagy in doxazosin-induced cell death of hormone refractory prostate and bladder cancer cells

6.1 Introduction

In this chapter, we set out to characterize further the granularities that appeared within the PCa and BCa cells when they were exposed to doxazosin. We had previously stained these for lipofuscin using DAPS, which stains lipofuscin in magenta colour, and with Gomori's aldehyde fuchsin which demonstrates lipofuscin in deep purple. However, we were unable to demonstrate the presence of lipofuscin using these two techniques.

Our previous experiments had shown that the cell death induced by doxazosin is increased when the cells were grown is serum free media. We had also observed that the time of onset of these granulations were reduced in they were serum starved. Moreover, in our previous experiments, dansylcadaverine was shown to attenuate the cell death induced by doxazosin. Dansylcadaverine, in addition to its ability to inhibit clathrin-mediated endocytosis, also inhibits the autophagic pathway and accumulates in autophagic vacuoles (Munafo and Colombo 2001). These led us to hypothesize that these granulations may represent autophagy within the cells exposed to doxazosin.

We initially used two commonly used inhibitors of autophagy, namely, 3-MA and dansylcadaverine to explore if the chemical inhibition of autophagy had any effect on cell death induced by doxazosin. Dansylcadaverine is also autofluorescent and its accumulation in autophagic vacuoles can be demonstrated using fluorescent microscopy (Munafo and Colombo 2001). As a next step, we examined the presence of dansylcadaverine accumulation in cells exposed to doxazosin.

TEM is the gold standard for demonstration of autophagy. Moreover, the characteristic appearances of autophagy within cells when viewed using TEM are well described (Tabata, Hayashi-Nishino et al. 2013). In our next experiment, we examined the cells

that were exposed to doxazosin under TEM and compared the appearances to that of controls. Additionally, we also observed the cells using SEM to evaluate if the cell surface demonstrated any changes that would account for the granulations.

The detection of light chain 3-II (LC3-II) is a reliable marker of autophagy (Tanida, Ueno et al. 2008). LC3 is a soluble, microtubule-associated protein 1A/1B (with a molecular mass of approximately 17 KDa) is a ubiquitously distributed protein found in mammalian tissues and cultured cells. The cytosolic form of LC3 (LC3-I) is conjugated to phosphatidylethanolamine to form LC3-II, and these are recruited into the autophagosomal membranes (Wild, McEwan et al. 2014). In our next experiment, we investigated the presence of LC3-II using immunohistochemistry in cells exposed to doxazosin (Rosenfeldt, Nixon et al. 2012).

6.2 Chemical Inhibition of Autophagy

6.2.1 Evaluation of the effects of doxazosin on PC-3, DU145, LNCaP and HT1376 cells pre-incubated with dansylcadaverine:

PC-3, DU145, LNCaP and HT1376 cells were seeded into 96-well MP at 5000 cells in 100 μL/well and incubated overnight at 37 C in serum containing media. Subsequently, 10 μL was pipetted out of each well.

Test wells: 10 μ L each of solutions of dansylcadaverine [final concentration 75 μ M] was added to make up a total volume of 100 μ L. The plates were returned to the incubator for 4 h. Subsequently, 10 μ L was aspirated and replaced with doxazosin in 10 μ L (final concentration of 37 μ M). These were incubated for 72 and Cell-Titer 96® aqueous MTS assay performed.

Control wells: 10 μ L each of the solution used for preparing stock solutions of dansyl cadaverine [160 μ L of 1% acetic acid and 6160 μ L of sterile water] was added to make up a total volume of 100 μ L. The plates were returned to the incubator for 4 h. Subsequently, 10 μ L was aspirated and replaced with doxazosin in 10 μ L (final concentration of 37 μ M). These were incubated for 72 h and Cell-Titer 96® aqueous MTS assay performed.

For each cell line, the experiment was repeated three times each with triplicate samples. Data analysis was performed using GraphPad Prism 6 Software. Analysis by 2-way ANOVA was carried out between test and control groups.

6.2.2 Evaluation of the effects of doxazosin on PC-3, DU145, LNCaP and HT1376 cells pre-incubated with 3-MA:

PC-3, DU145, LNCaP and HT1376 cells were seeded into 96-well MT plates at 5000 cells in 100 μL/well and incubated overnight at 37 C in serum containing media. Subsequently, 10 μL was pipetted out of each well.

Test wells: 10 μ L each of solutions of 3 methyl adenine [final concentration 2 mM] was added to make up a total volume of 100 μ L. Stock solutions were prepared by dissolving in water at 40 C with agitation using sonification. The plates were returned to the incubator for 4 h. Subsequently, 10 μ L was aspirated and replaced with doxazosin in 10 μ L (final concentration of 37 μ M). These were incubated for 72 h and Cell-Titer 96® aqueous MTS assay performed.

Control wells: 10 μ L each of solutions of diluent [water] was added to make up a total volume of 100 μ L. The plates were returned to the incubator for 4 h. Subsequently, 10 μ L was aspirated and replaced with doxazosin in 10 μ L (final concentration of 37

μM). These were incubated for 72 h and Cell-Titer 96[®] aqueous MTS assay performed.

For each cell line, the experiment was repeated 3 times and done in triplicate each time (n = 9). Data analysis was performed using GraphPad Prism 6 Software.

Analysis using 2-way ANOVA was carried out between test and control groups.

6.3 Fluorescent Microscopic Studies Using Dansylcadaverine:

PC-3, DU145 and LNCaP cells were seeded (5000 cells per 100 μL; 1 ml per well) in 8-well chamber slides (Thermo Fischer Scientific, catalogue number T15434PK) and allowed to attach overnight. 100 μL was aspirated out and in test wells this was replaced with 100 μL solution of doxazosin (final concentration of 37 μM) whilst in control wells it was replaced with 100 μL of sterile water (solvent) and incubated for a further 48 h. Subsequently, dansylcadaverine was added to each well (final concentration of 100 μM) and incubated at room temperature for 30 minutes (Lee, Won et al. 2012). The wells were washed with PBS thrice and stained with DAPI blue fluorescent stained for nuclear staining and examined for green fluorescence under a fluorescent microscopy. Experiments were repeated two times, and each experiment was performed in triplicates.

6.4 TEM and SEM studies:

Low passage PC-3 cells, HT1376 cells and human skin fibroblasts were thawed from -80C, subjected to 2 passages at sub-confluence, harvested using (EDTA-trypsin), seeded in 25 cm² pre-labelled flasks and incubated overnight at 37C for 24 h. The

flasks were divided into test group (exposed to 37 µM doxazosin) and control group. Doxazosin was added to test flasks and an equal volume of sterile water added to controls and incubated for 24h, 48h and 72h, after which the cells were washed thrice with PBS, fixed with 2% glutaraldehyde, harvested using a cell scraper, centrifuged (800 rpm), and cell pellets stored at 4C. TEM and SEM of glutaraldehyde-fixed cell samples were carried out the next day in collaboration with the Dept. of Electron Microscopy Unit, Royal Free Hospital. The TEM samples and their matched controls at 24, 48 and 72 h were examined. Each TEM experiment was performed twice and in duplicates. The SEM was performed for PC-3 cell lines after exposure to doxazosin for 48 h and each experiment was also repeated twice and in duplicates.

6.5 Immunohistochemistry

Low passage PC-3 cells, DU145 cells and LNCaP cells and human skin fibroblasts were thawed from -80 C, subjected to 2 passages at sub-confluence, harvested using (EDTA-trypsin), seeded in 25 cm² pre-labelled flasks, and incubated overnight at 37C for 24 h. The flasks were divided into test group (exposed to 37 µM doxazosin) and control group; doxazosin was added to test flasks whilst an equal volume of sterile water added to controls and incubated for 24h, 48h and 72 h, after which the cells were washed thrice with PBS. The cells were harvested using EDTA-trypsin and pelleted by centrifugation (800 rpm). The pellets were used to prepare paraffin blocks to which LC3-II antibody (Abcam, UK; Catalogue Number ab51520 at 1/2000) was added. Breast cancer tissue known to demonstrate autophagy were used as positive controls. The experiment was performed in triplicate. All samples

(test samples, negative and positive controls) were examined under high power microscope for immunostaining by LC3-II antibody.

6.6 Results:

The effects of doxazosin on PC3 cells, DU145, LNCaP and HT-1376 cells pretreated with dansylcadaverine have already been detailed in the previous chapter (chapter 5):

6.6.1 Effect of doxazosin on PC3 cells pre-treated with 3-MA:

3-MA-1 at 2 mM induced a significant inhibition of growth of PC-3 cells when compared to controls (p= 0.0006). Pre-incubation with 3-MA-1 at 2 mM for 4 h followed by doxazosin (37 μ M) for 72 h significantly reduced the cytotoxic action of the latter (p = <0.0015).

6.6.2 Effect of doxazosin on DU-145 cells pre-treated with 3-MA:

3-MA-1 at 2 mM had no significant effect of growth of DU145 cells when compared to controls (p= 0.9871). Pre-incubation with 3-MA-1 at 2 mM for 4 h followed by doxazosin (37 μ M) for 72 h significantly reduced the cytotoxic action of the latter (p = <0.0.0001).

6.6.3 Effect of doxazosin on LNCaP cells pre-treated with 3-MA:

3-MA-1 2 at mM induced a significant inhibition of growth of LNCaP cells when compared to controls (p=<0.0001). Pre-incubation with 3-MA-1 at 2 mM for 4 h followed by doxazosin (37 μ M) for 72 h significantly reduced the cytotoxic action of the latter (p = <0.01).

6.6.4 Effect of doxazosin on HT1376 cells pre-treated with 3-MA:

3-MA-1 at 2 mM had no significant inhibition of growth of HT1376 cells when compared to controls (p=0.0579). Pre-incubation with 3-MA-1 at 2 mM for 4 h followed by doxazosin (37 μ M) for 72 h significantly reduced the cytotoxic action of the latter (p = <0.0001).

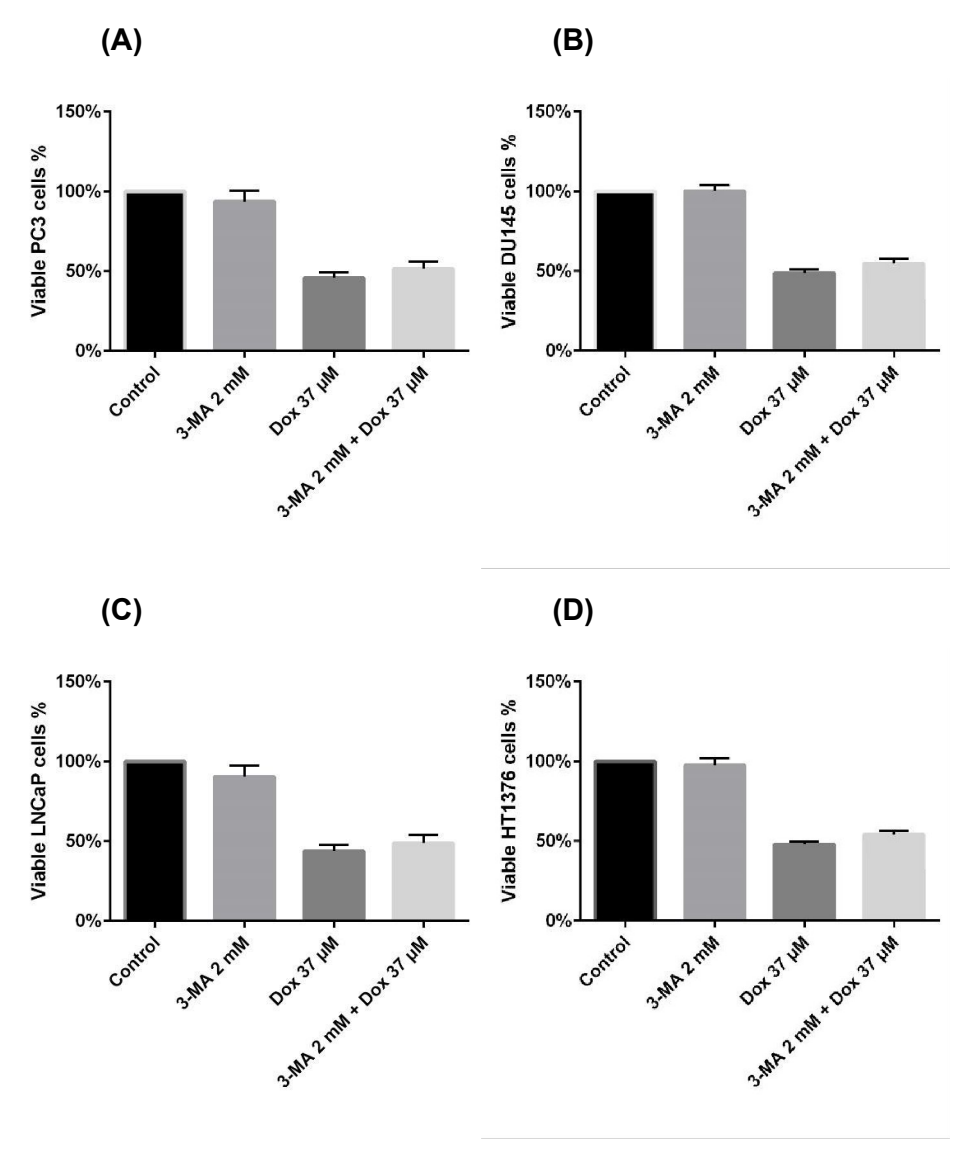


Figure 43: PC-3 (A), DU145 (B), LNCaP (C) and HT1376 cells (D) treated with vehicle (control); 3MA (2mM), doxazosin (37 μ M); and, pre-treated with 3MA (2mM) for 4h followed by doxazosin 37 μ M for 48h. Dox = doxazosin and 3-MA = 3-methyl adenine.

<u>6.6.5 Examination of PC-3, DU145 and LNCaP cells exposed to doxazosin</u> under fluorescent microscopy following incubation with dansyl cadaverine:

During the wash cycles, all cell lines underwent significant detachment. Nonetheless, there remained enough cell population to proceed with the experiment. There was significant concentration of dansylcadaverine in intracellular vesicles in doxazosin-exposed cells and these were absent in control group. The figure below shows PC-3 cells showing DAPI blue-fluorescent stained nucleus (DNA) and green dansylcadaverine (100 μ M) autofluorescence concentrated in the autophagosomes before (Figure 44, left) and after 37 μ M doxazocin for 48 h (Figure 44, right).

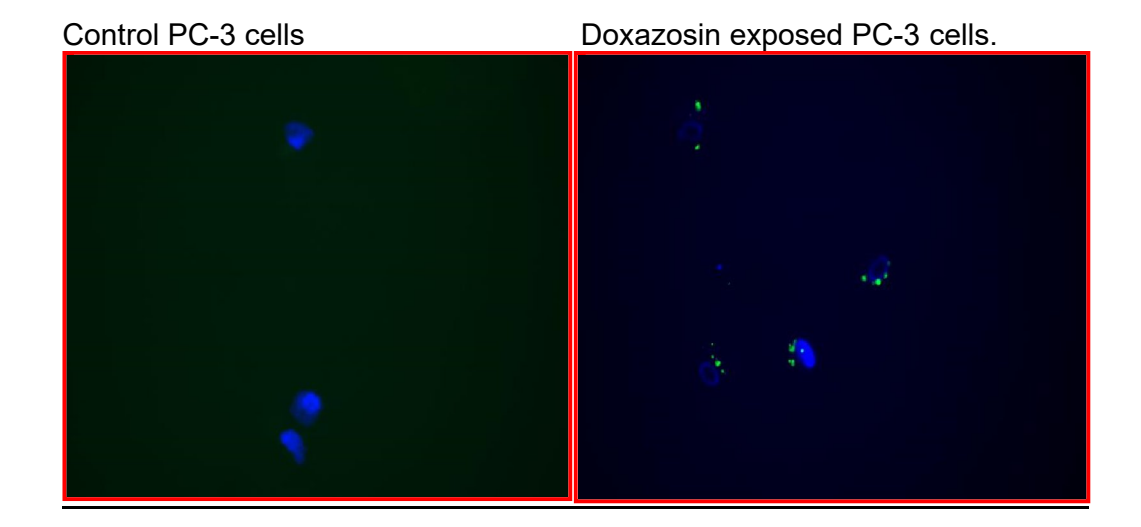


Figure 44: PC-3 cells showing DAPI blue-fluorescent stained nucleus (DNA) and green dansylcadaverine (100 μ M) autofluorescence concentrated in the autophagosome before (left) and after 37 μ M doxazocin for 48 h (right).

6.6.6 TEM studies:

Control PC-3 cells: Lower resolution images of cross sections of the control cell populations showed a large central nucleus, prominent nucleolus and cytoplasm containing long, ribbon like mitochondria and very few minute vacuoles. The edges of the cells revealed multiple, fine, short villous filamentous processes. The cytoplasm was granular, and the ER processes were seen within the cytoplasm. The ribbon like mitochondria were predominantly located around the nucleus of the cell. The nucleus was relatively characterless, granular and was less electron dense (compared to the cytoplasm) and contained one or two prominent electron dense nucleolus. Figure 45 below is a representative image of a control PC-3 cell after 48 h of incubation.

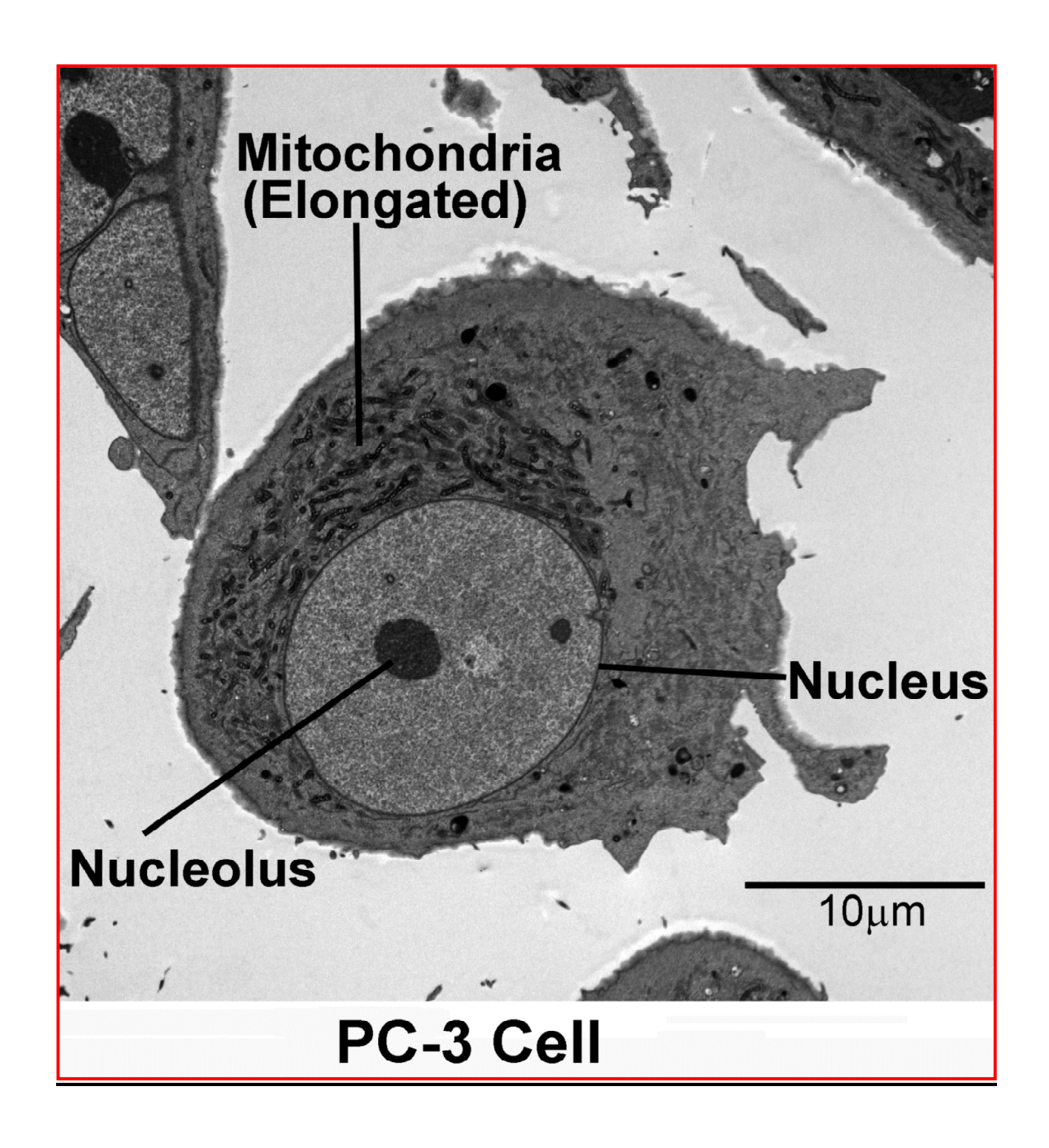


Figure 45: TEM image of PC-3 control cell treated with diluent (water) after 48 h of incubation. Note the large, homogeneous central nucleus with an electron-dense nucleolus, granular cytoplasm containing numerous perinuclear, elongated mitochondria.

Doxazosin treated PC-3 cells: The appearances of doxazosin-treated PC-3 cells were remarkably different from the control PC-3 cells. Moreover, the appearances changed over the duration of exposure.

After 48 h of exposure to 37 µM, the cytoplasm showed large electron-dense coalescent deposits resembling lipofuscin like material. Also, there appeared numerous, large vacuolations in the cytoplasm and some of these electron-dense deposits were contained within these vacuoles suggesting a process that resembled lysosomal digestion. The mitochondria had also changed from the long, ribbon structures to small and rounded.

Closer examination revealed that these lipofuscin-like material were in fact fragmented mitochondria and these fragmented mitochondria were also contained within the vacuoles. This led us to believe that the vacuoles were autophagosomes and the underlying process seen within these cells is that of mitophagy. The nucleus though less homogenous did not show clear evidence of dense chromatin condensation in them, suggesting that apoptosis was unlikely. Furthermore, even after 72 h of exposure to the doxazosin 37 µM, the appearances of the nucleus remained unchanged with a well demarcated nucleolus. However, the cells exposed to doxazosin 37 µM for 72 h had the entire cytoplasm filled with vacuolation and autophagosomes with fragmented mitochondria within them. Figure 46 and Figure 47 are representative images of a control PC-3 cell after 48 h and 72 h, respectively, following incubation with doxazosin 37 µM.

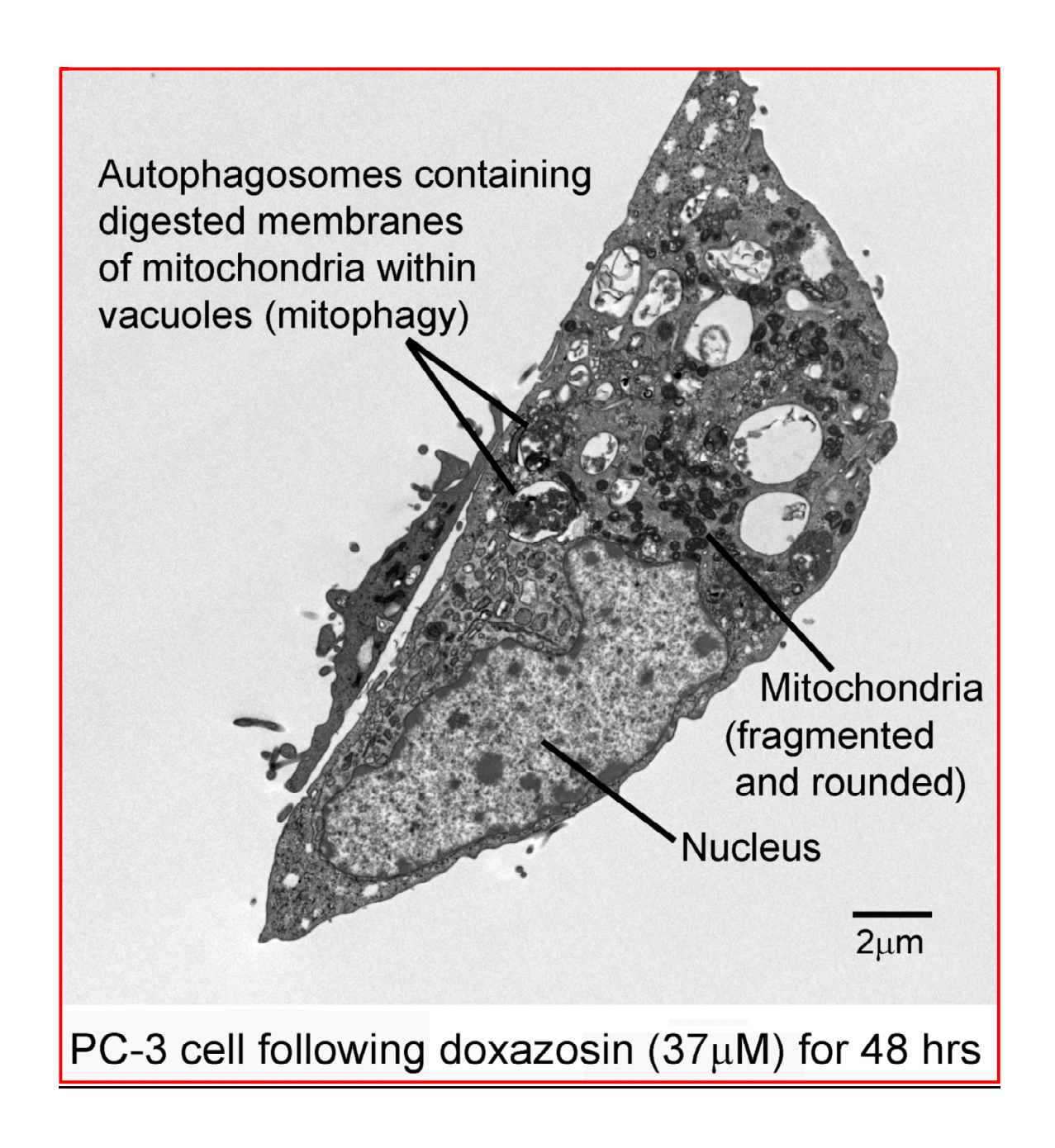


Figure 46: TEM image of a PC-3 cell that has been exposed to doxazosin 37 μ M for 48 h. Note the large vacuolation and fragmented mitochondria within the cytoplasm and within the vacuoles. The nucleus is less homogenous.

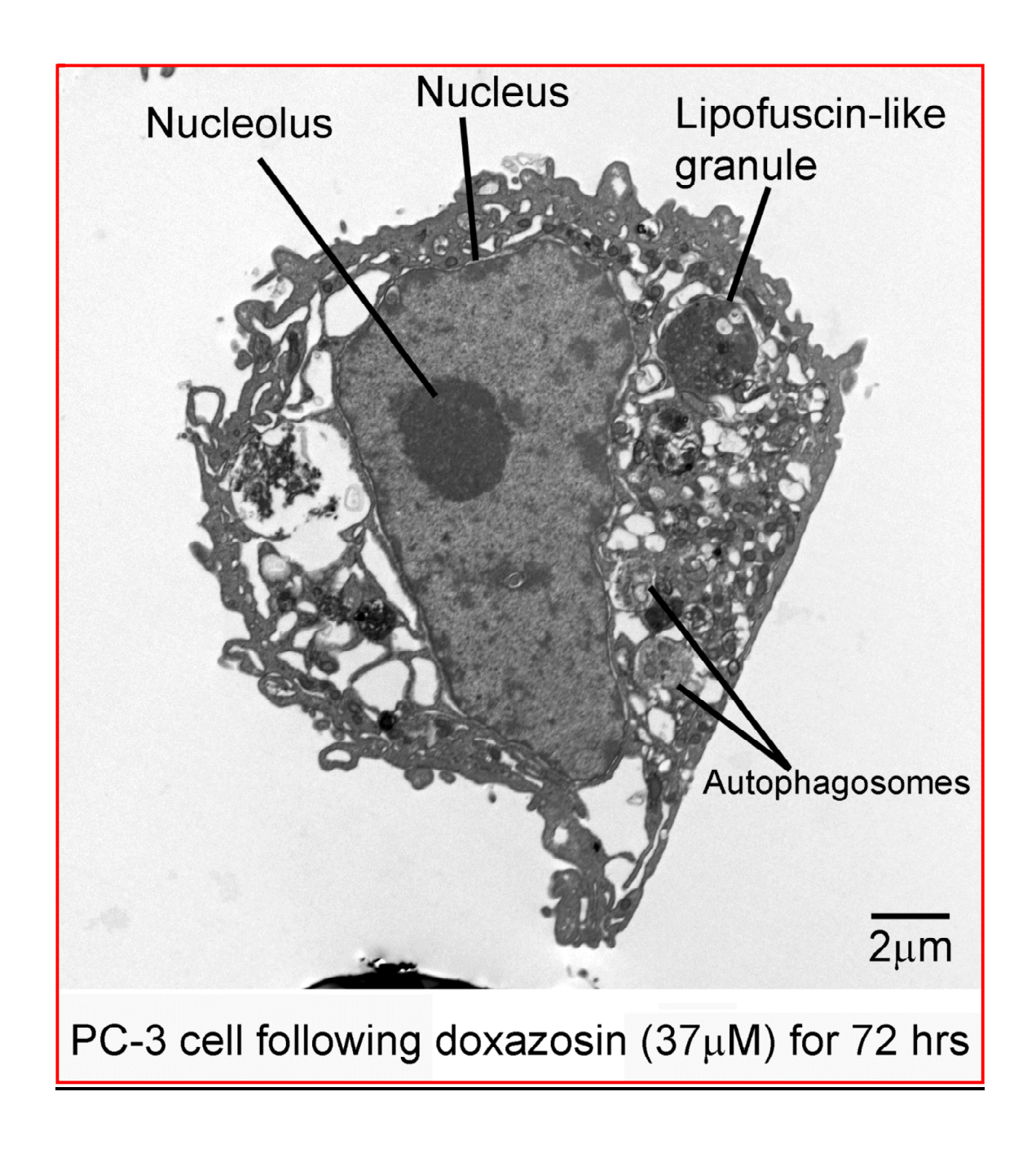
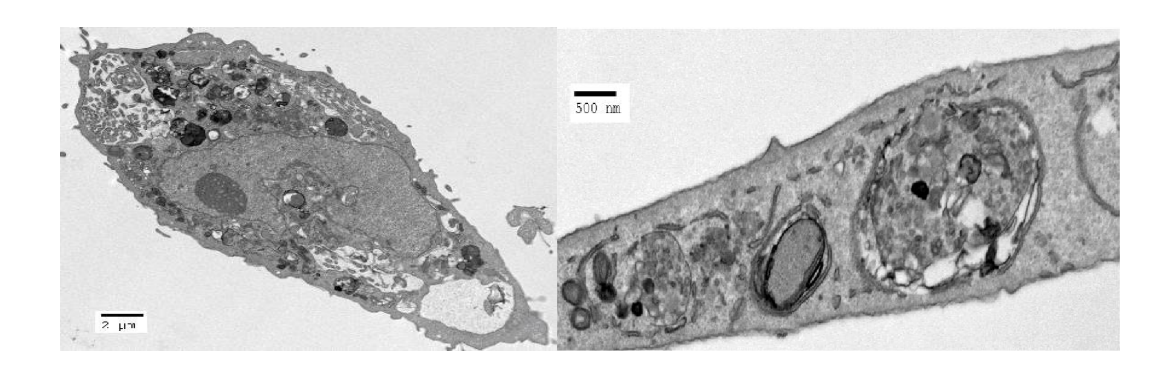


Figure 47: TEM image of a PC-3 cell that has been exposed to doxazosin 37 μ M for 72 h. Note the entire cytoplasm is filled with large vacuolation, fragmented mitochondria some of which have clumped into lipofuscin-like granules. The nucleus is less homogenous with a few electron-dense deposits at the periphery and a well-defined nucleolus.

Figure 48: TEM image of PC-3 cells exposed to doxazosin for 48 h showing mitophagy (left) and the stages of autophagic process (right).



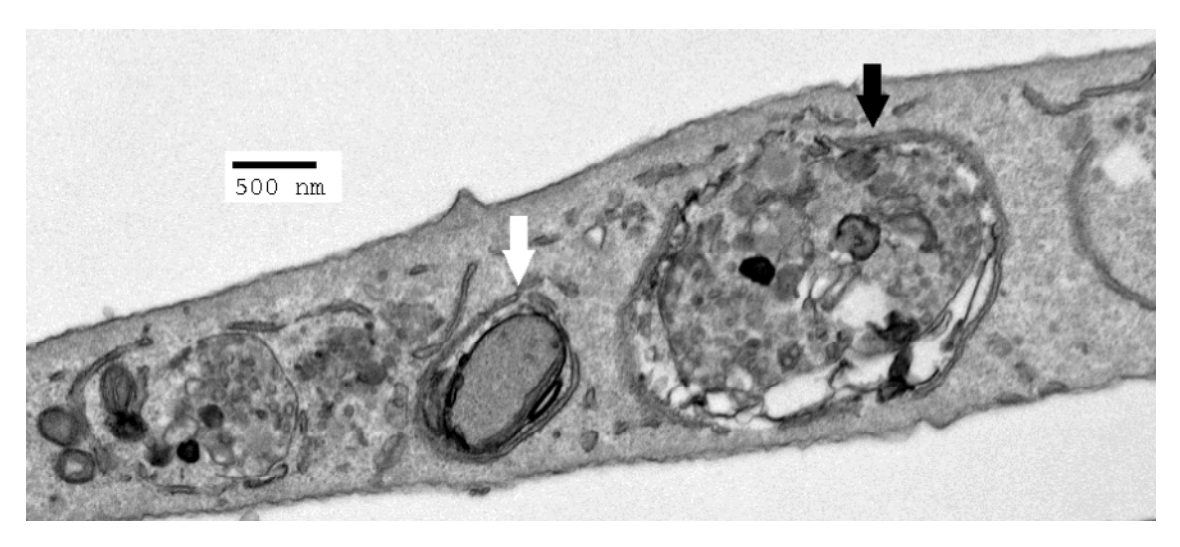


Figure 49: PC-3 cell exposed to doxazosin with early autophagosomes (white arrow) and late autophagosomes (black arrow).

6.6.6.1 TEM evaluation after exposure of fibroblasts skin cells to doxazosin:

The appearances of the skin fibroblast cells following exposure to doxazosin were comparable to those of PC-3 cells. After 48 h of exposure to doxazosin, the entire cytoplasm was filled with vacoulations and fragmented mitochondria. Thus, p53-null status of PC-3 cells could not be accounted for autophagy as the skin fibroblasts have p53 gene. Also, notable features of apoptosis and necrosis such as karyorrhexis and pyknosis were absent in the treated fibroblast cells.

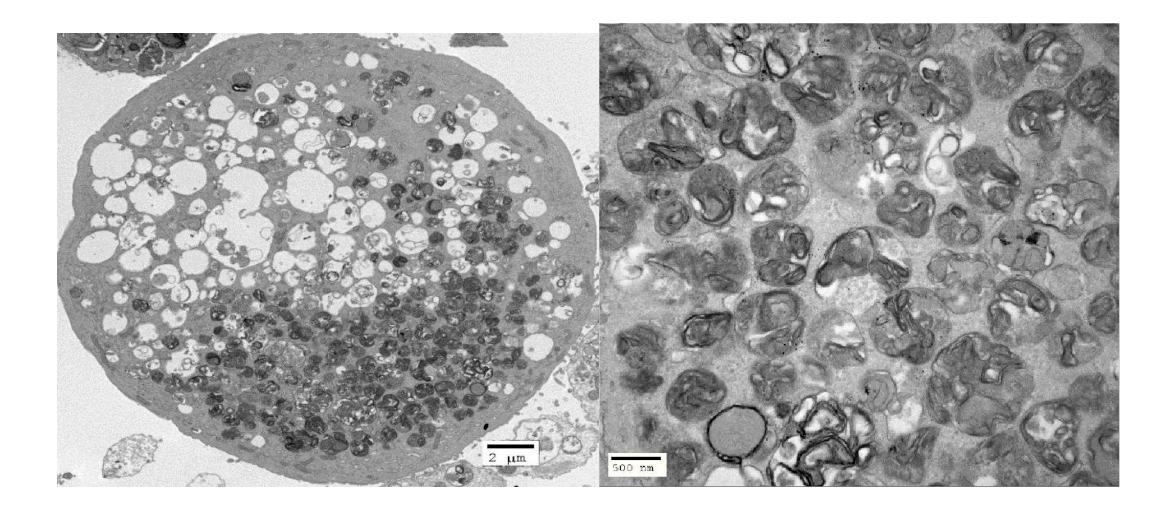


Figure 50: TEM image of skin fibroblast cells exposed to doxazosin for 48 h showing extensive vacuolation (left) and autophagosomes (right).

6.6.6.2 TEM evaluation after exposure of H1376 cells to doxazosin:

The appearances of the HT1376 cells following exposure to doxazosin were comparable to those of PC-3 cells. Doxazosin-treated cells demonstrated fragmentation of mitochondria with autophagosomes and these features progressed over the duration of exposure. In HT1376 cells, we also examined the cells at 24 h of eposure and found that changes consistent with autophagy were demonstrable within the cells within 24 h of exposure to 37 µM of doxazosin. Also, notable features of apoptosis and necrosis such as karyorrhexis and pyknosis were absent in the treated HT1376 cells during any of the three time points (24h, 48h and 72h) observed.

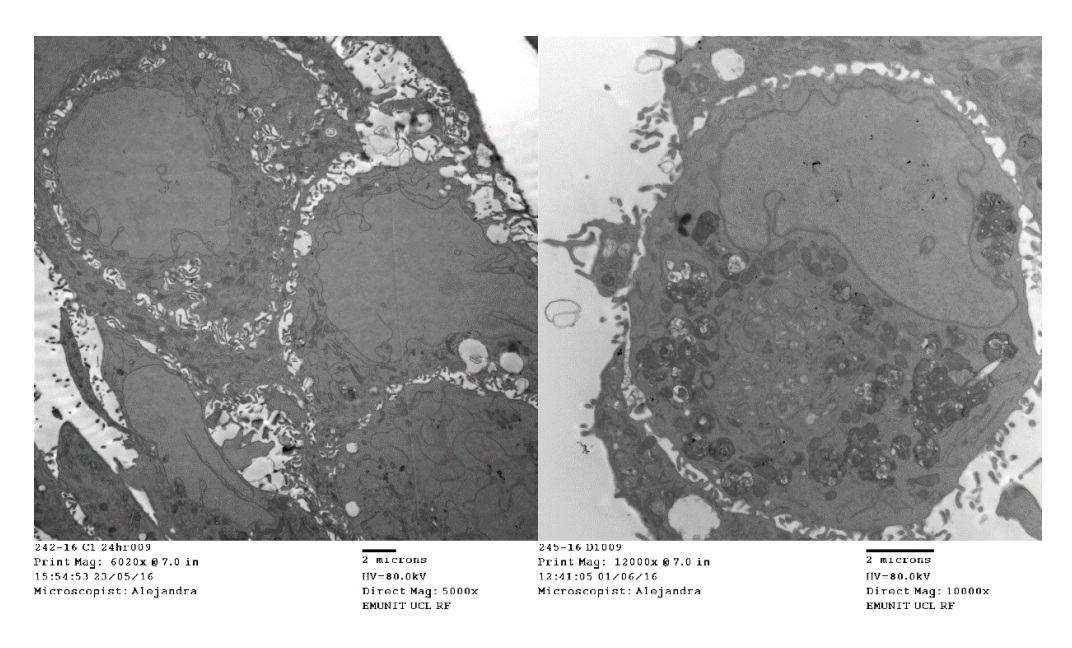
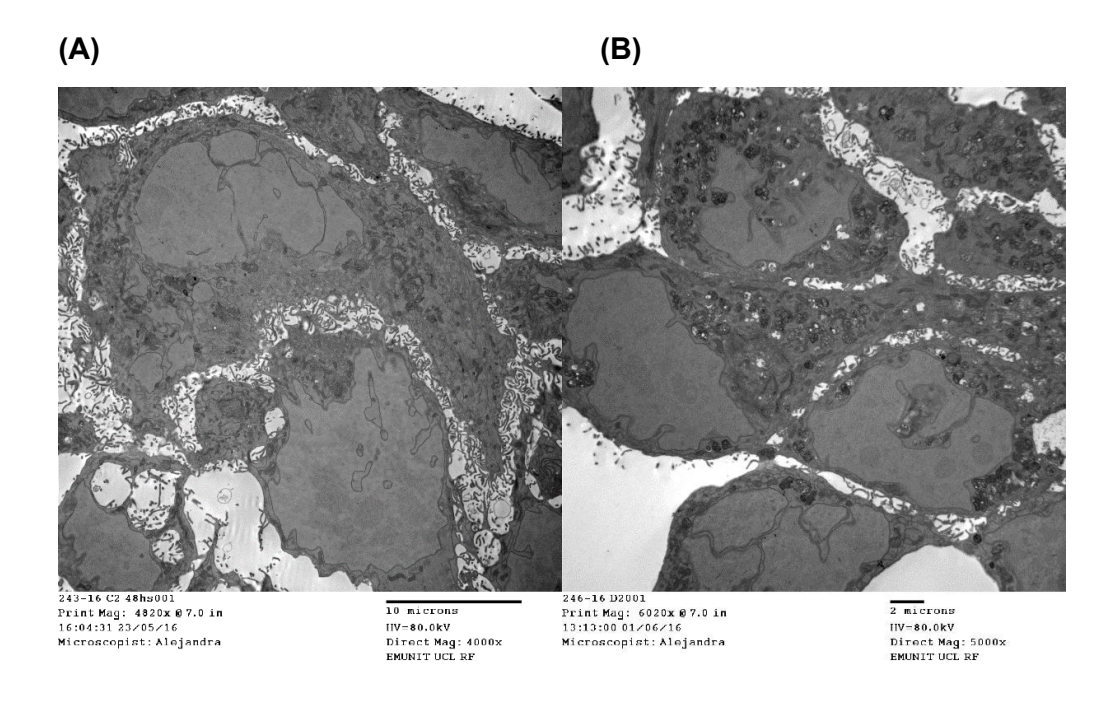


Figure 51: TEM image of HT1376 cells after exposure to doxazosin 37 μ M (right) for 24 h and control cells (left). Note the entire cytoplasm is filled with large vacuolation, fragmented mitochondria. The nucleus is homogenous in both control and treated cells.



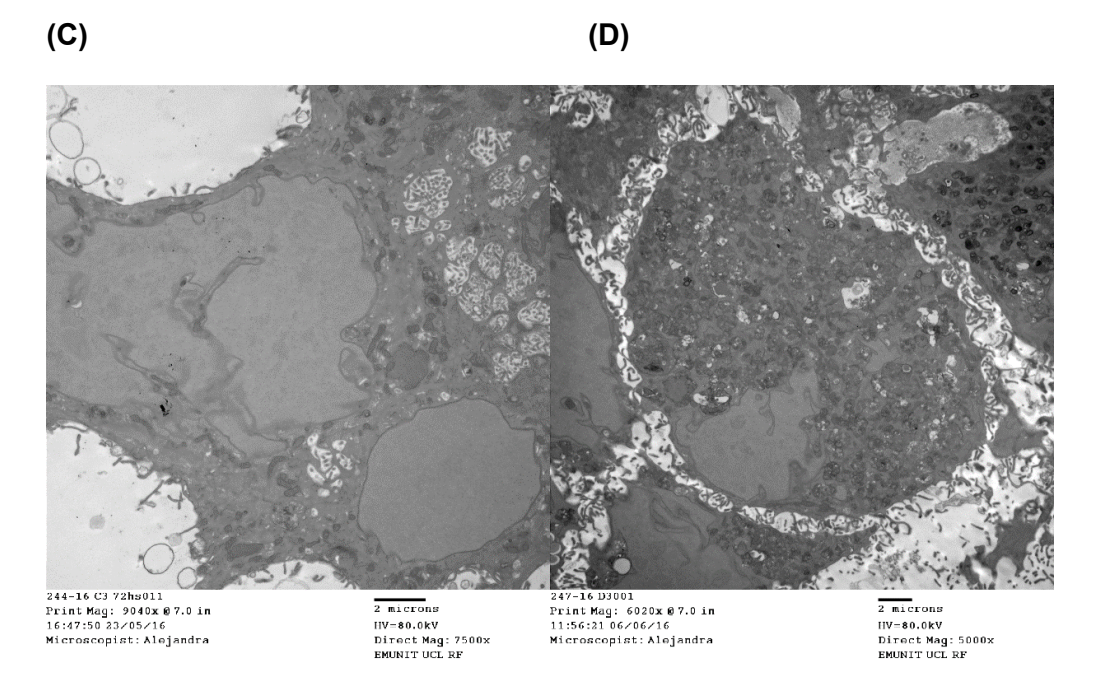


Figure 52: TEM image of HT1376 cells after exposure to doxazosin 37 μ M (A) for 48 h (B), and below are control cells (C) and after treatment for 72 h (D). Note the entire cytoplasm is filled with large vacuolation, fragmented mitochondria in treated cells at both time points. The nucleus is homogenous in both control and treated cells at both time points.

<u>6.6.7 Evaluation of surface characterisites of PC-3 cells exposed to doxazsoin</u> using SEM:

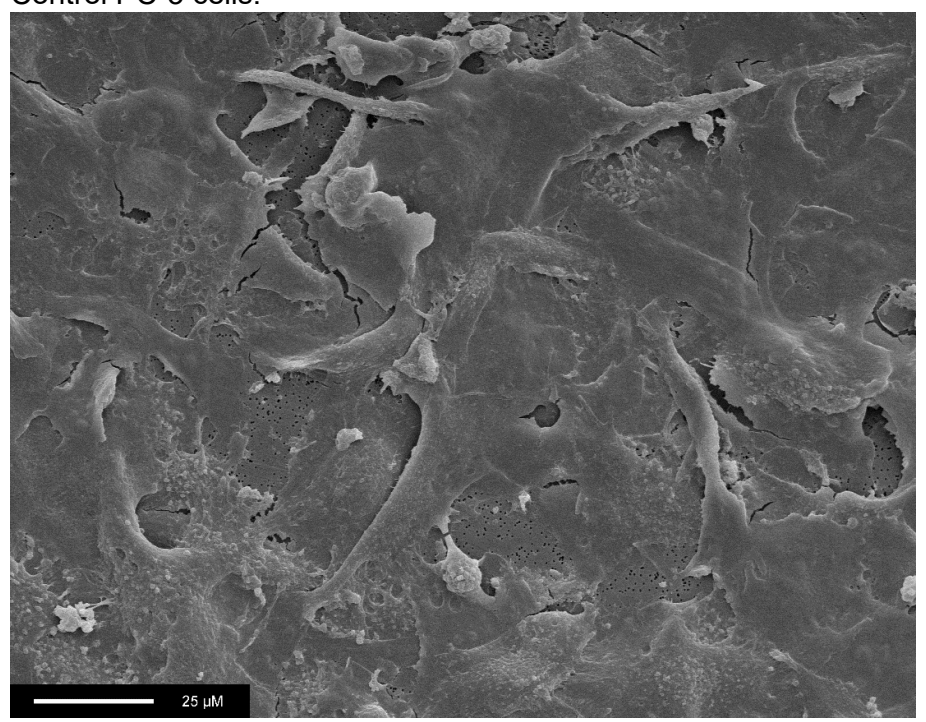
As these cells were not trypsanized and instead lifted carefully using cell scraper, they had maintained, to a certain extent, the spatial morphology they maintained in the flasks. Therfore the morphological differences were representative of the difference in morphological features seen in live cultures.

Not surprisingly, there were significant morphological differences between doxazosin exposed cells and control cell populations. A large part of the difference in the surface morphological appearance could be atributed to doxazosin exposed cell undergoing anoikis.

At lower resolutions, untreated (control) PC-3 cells appeared to form sheets of contigous growth and it was difficult to dileniate individual cells with the cell boundaries merging to one another. Doxazosin treated cells remained less contigous and several individual cells with distint borders could be visualized.

We then focused on a few individual cells exposed to doxazosin to understand further the morphological changes seen within these cells. It appeared that there were four distinct morphological stages in doxazosin-treated cells. These are described in the sections below (Figure 54 to 57).

Control PC-3 cells.



Doxazosin exposed PC-3 cells

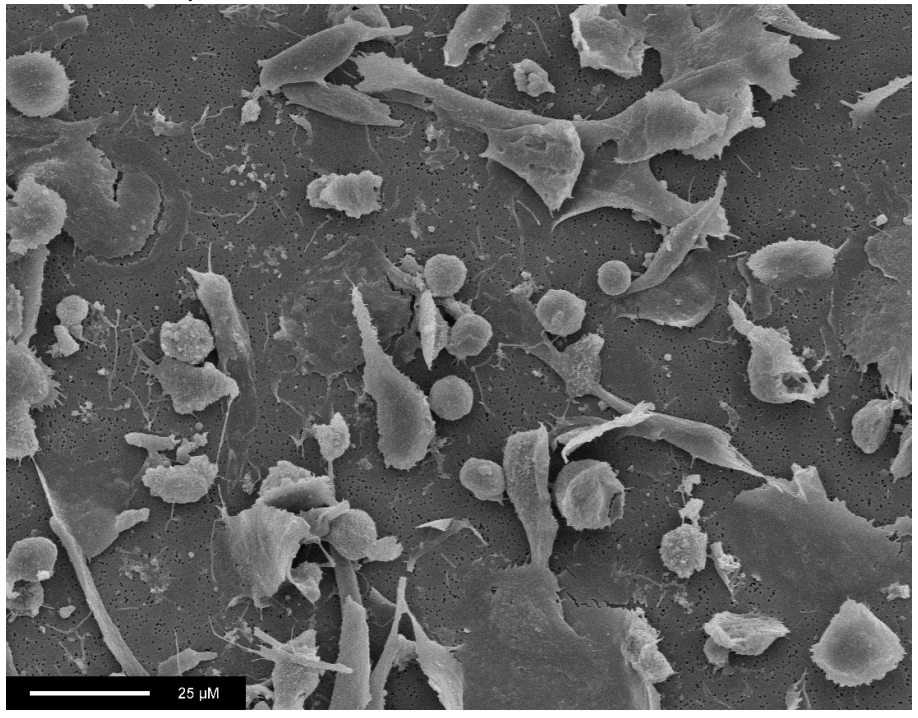


Figure 53: SEM imaging of PC-3 cells under low magnification showing contigous sheets of control cells (above) while cells exposed to doxazosin 37 μ M for 48 h (below) are in various stages of cell death, deatchment and anoikis.

Stage 1: The cells appeared hemispherical with the flattened surface representing its original site of attachment to the flask surface. The central part of the hemisphere had the bulk of the cytoplasm resembling a 3D bell curve. The outer surface of the cell showed minute bleb formations but was largely smooth and regular. The boundary of the cell was rougly circular with long villous processes at the periphery.

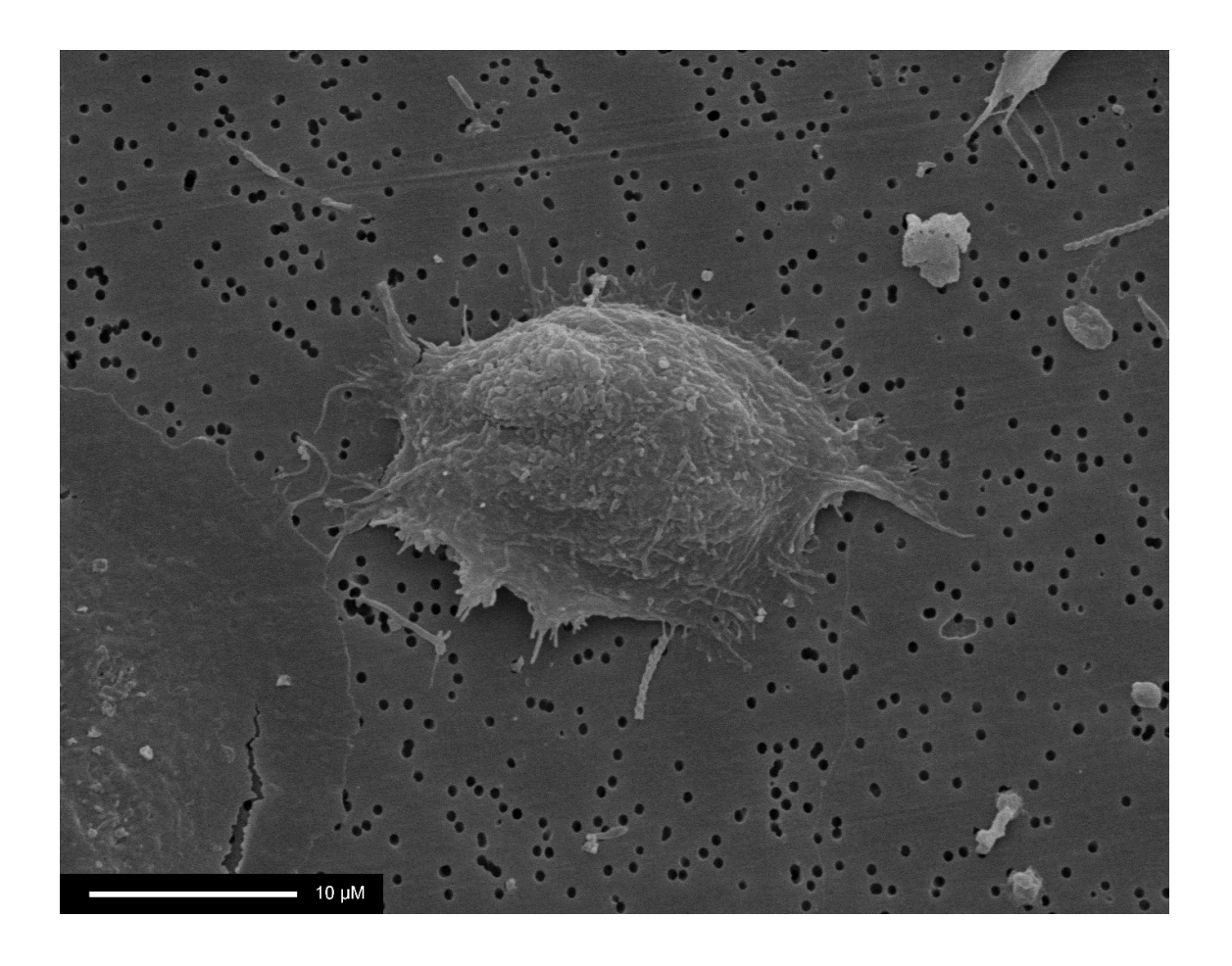


Figure 54: PC-3 cell treated with doxazosin 37 μ M for 48 h showing shwoing hemispherical shape with the bulk of the cytoplasm located centrally. There are very fine and elongted villous processes at the periphery.

Stage 2: The cell had an ellipsoid shape with a central and nearly spherical central mass that occupied half to two-third of the diameter of the cells; the outer periphery which was rougly a third of the diameter had flattened and consisted of several large villous extensions. The surface of the cell shower several large bleb formations. There were fewer blebs at the periphery though these were considerably larger. The central part of the cell had innumerable small blebs giving a blisetered appearance to the central part of the cell.

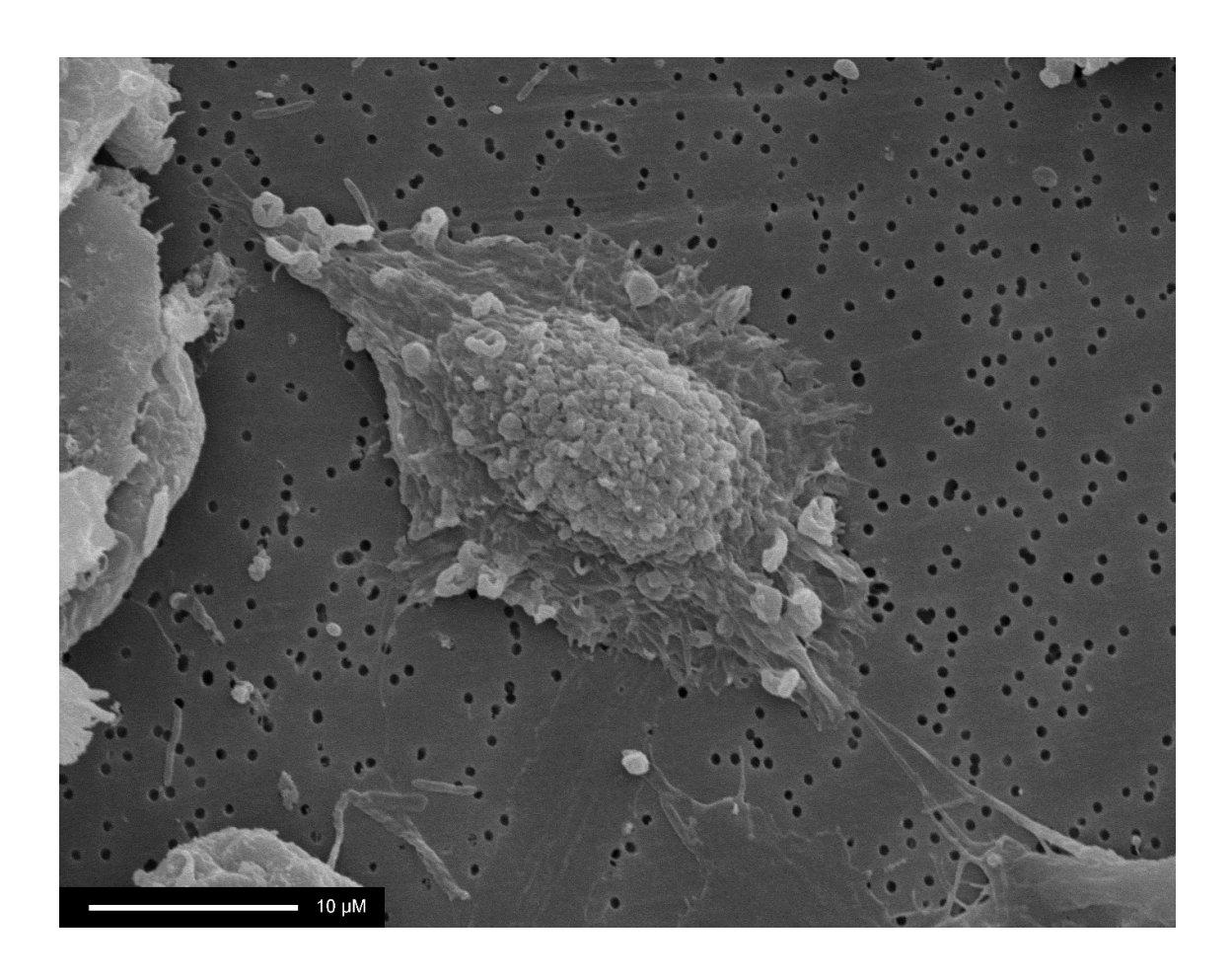


Figure 55: PC-3 cell treated with doxazosin 37 μ M for 48 h showing ellipsoid shape with centrally heaped mass and flattened peripheries, numerous fine villous attachment and the surface has multiple blebs.

Stage 3: The cell had become markedly smaller in size with the loss of the peripheral flattened zone. The surface also appeared smoother due to disappearance of the bleb formations. The most characterisitc feature was the coalescing of the innumerable smaller villi to a few large, bulky villi giving the appearance of the root of a tree.

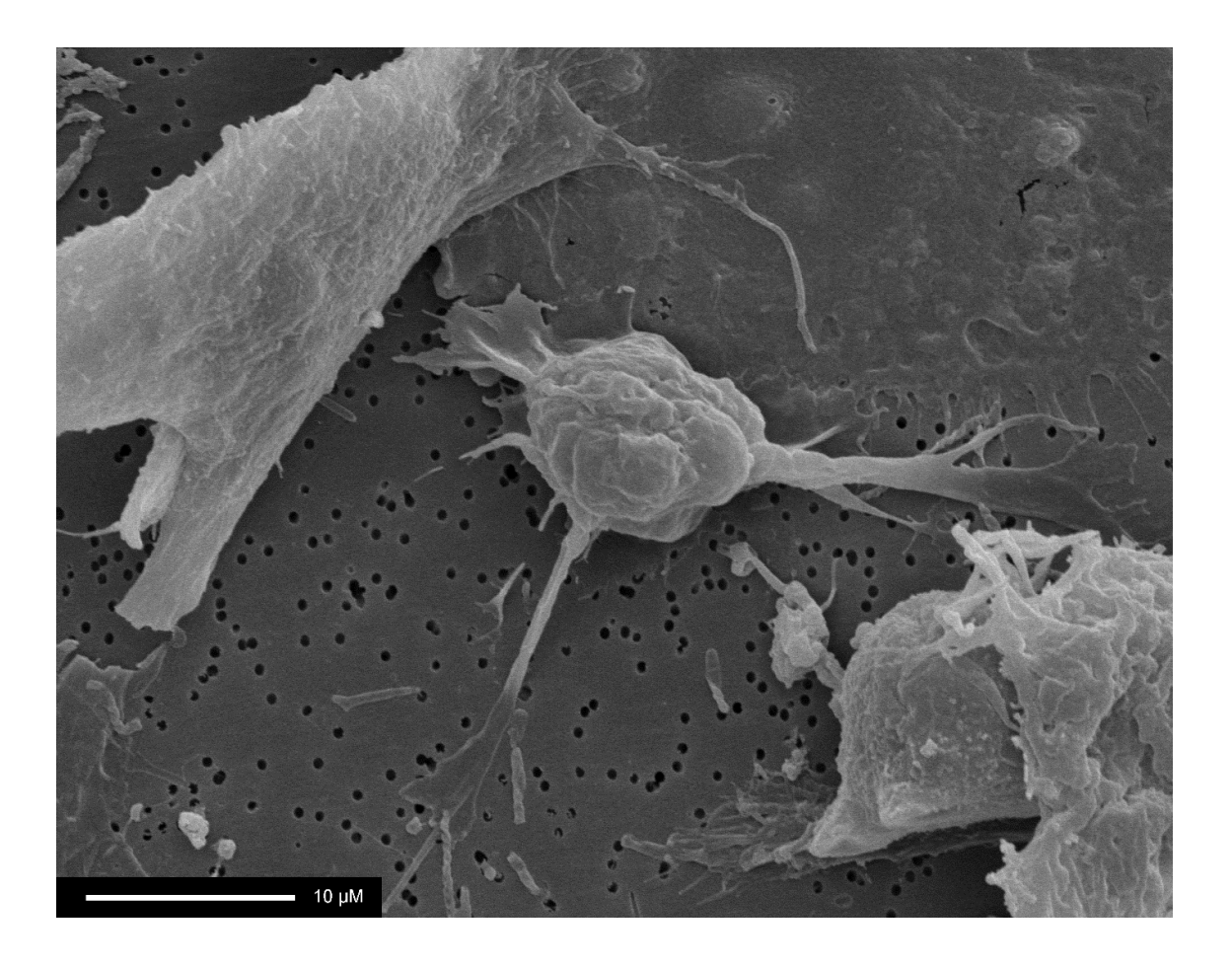


Figure 56: PC-3 cell treated with doxazosin 37 μ M for 48 h showing prominent, long villous attachment resembling tree-root and the surface is devoid of blebs.

Stage 4: The cell is spherical with no visible villi and appeared to have no attachment to the flask surface. The surface of the cells also was featureless and no bleb formations are seen. At this point the cell appeared to have been completely detached and consequenly assumed a rounded shape.

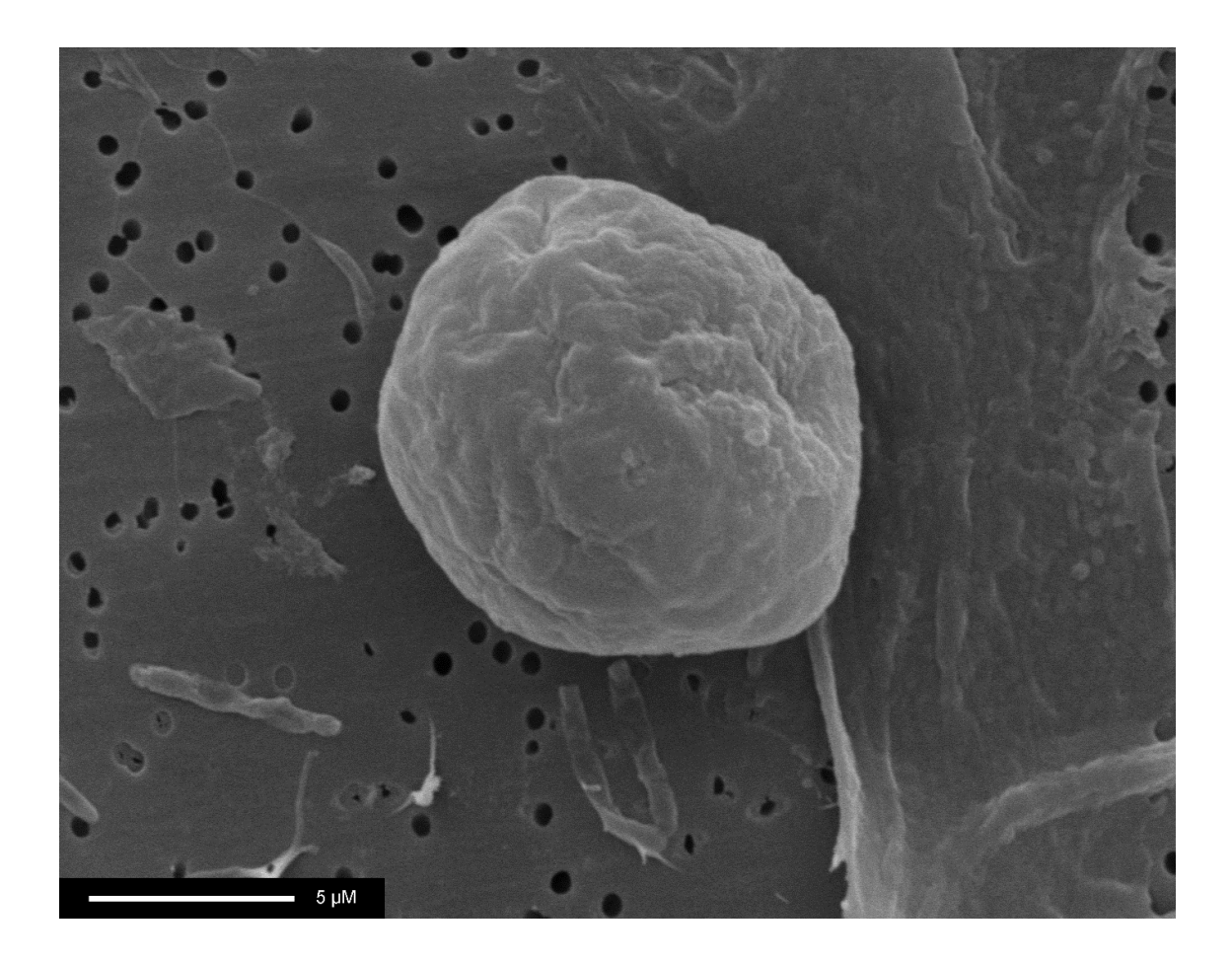
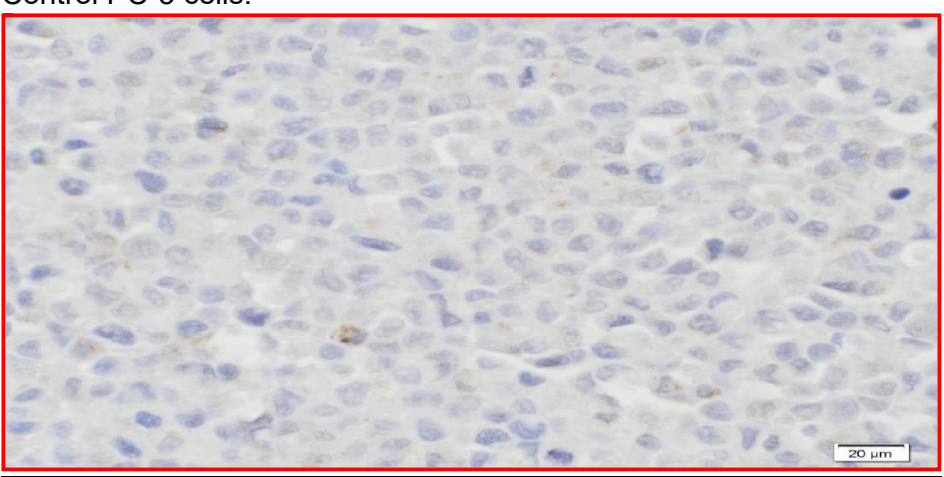


Figure 57: PC-3 cell treated with doxazosin for 48 h showing complete deatchment, loss of villi and unremarkable surface features.

6.6.8 Immunohistochemical labelling of PC-3, DU145 and LNCaP cells exposed to doxazosin with anti-LC3B antibody:

Immunohistochemically labelled sections revealed densely stained areas of LC3B (brown staining) in the cytoplasm of sections that had been exposed to doxazosin whilst this feature was absent in the control specimens. Three random fields were shown, and the figure below is from one of the randomly chosen views from PC-3 cell line as is also representative of views seen on the sections for other cells.

Control PC-3 cells.



Doxazosin exposed PC-3 cells

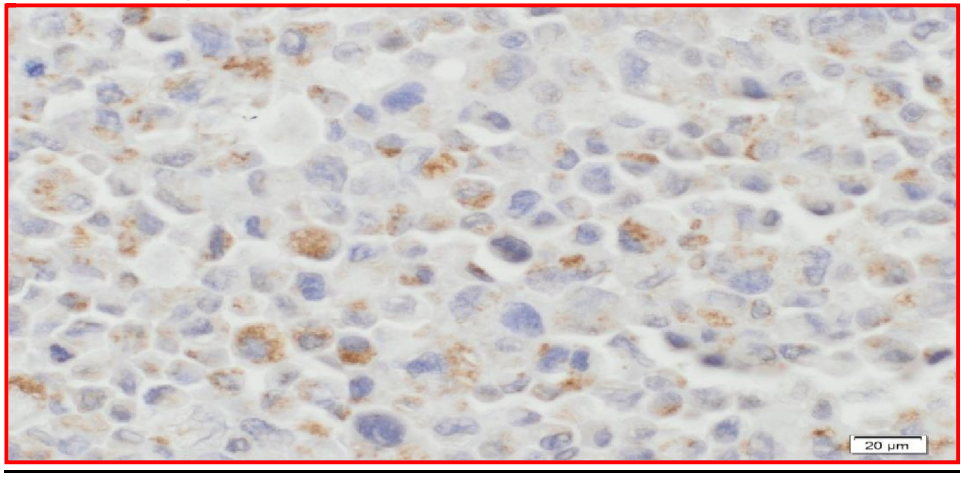


Figure 58: PC-3 cells in the absence (top) and presence of 37µm doxazocin after 48 h (bottom), labelled with anti-LC3B antibody a marker for autophagy.

6.7 Discussion

Autophagy is an evolutionarily highly conserved process of degradation of cytoplasm and organelles in the lysosomes for amino acid recycling and energy in eukaryotic cells (Klionsky, Abdalla et al. 2012). Mammalian cells exhibit 3 morphologically distinct types of autophagy: micro autophagy, macro autophagy (simply referred to as autophagy), and chaperone-mediated autophagy (Klionsky, Abdalla et al. 2012, Kim and Lee 2014). Dysregulation of autophagy has been implicated to be a causative role in several diseases including cancer (Mathew, Karantza-Wadsworth et al. 2007, Chen and Karantza-Wadsworth 2009, Choi 2012, Mah and Ryan 2012). Not surprisingly, several studies have suggested that autophagy can be a potentially useful target for treatment of cancers (Yang, Chee et al. 2011, Bhat, Kriel et al. 2018, Fulda 2018).

Structurally, the process of autophagy (macro autophagy) begins with *de novo* formation of double-membrane vesicles called phagophores which then sequesters the transport cargo by invagination and eventually fuse to form a double-membrane structure, the autophagosome. The exact origin of the phagophore membrane that leads to formation of the autophagosomes remains unresolved with ER-Golgi intermediate compartment and ER-mitochondria considered to be among the possible candidates (Rubinsztein, Shpilka et al. 2012, Chan and Tang 2013, Lamb, Yoshimori et al. 2013, Tooze 2013, Ge and Schekman 2014). The autophagosomes then fuse with the lysosome to form the autophagolysosome which then degrades the cargo (Parzych and Klionsky 2014).

Over 30 genes involved in autophagy have been identified in mammals of which 16 genes are involved in all types of autophagy (Klionsky, Abdalla et al. 2012, Pyo, Nah et al. 2012). The ubiquitin-like protein LC3 is a mammalian homolog of *ATG8* gene

and is essential for the formation of autophagosomes. LC3 is lipidated with phosphatidylethanolamine to form LC3-II which remains on the membranes of the autophagosomes until its fusion with the lysosomes (Burman and Ktistakis 2010, Pyo, Nah et al. 2012). The conversion of LC3 to LC3-II is therefore considered a reliable molecular indicator of autophagy (Klionsky, Abeliovich et al. 2008, Klionsky, Abdalla et al. 2012, Pyo, Nah et al. 2012). However, TEM is still considered to be the gold standard for detection of autophagy (Klionsky, Abdalla et al. 2012).

Chemical inhibitors of autophagy inhibitors serve as an initial tool to assess the presence or absence of autophagy; however, they are not specific in their actions (Yang, Hu et al. 2013, Vinod, Padmakrishnan et al. 2014, Pasquier 2016). This is compounded by the fact that autophagy is intrinsically linked to other cellular functions such as endocytosis (Lamb, Dooley et al. 2013).

Our experiments were designed to identify the causative factor for development of granulations within the cells when exposed to doxazosin when attempting to create doxazosin-resistant cells. We had previously looked at the possibility of these granules being lipofuscin granules but specific staining for these were negative and focussed out attention to autophagy. As a first step, we used 2 main chemical inhibitors of autophagy, namely, 3-MA and dansylcadaverine to evaluate their effects on doxazosin induced cell death.

3-MA is an inhibitor of autophagy and acts by its ability inhibit PI3K. Our experiments have shown that 3-MA significantly attenuated doxazosin-induced cell death in all the cell lines tested. However, 3-MA can also induce autophagy if the experimental conditions are varied and inhibit glycolytic enzymes and promote glycogen

breakdown and this is independent of its autophagy regulating abilities (Vinod, Padmakrishnan et al. 2014).

We had already shown that dansylcadaverine attenuates cell death induced by doxazosin in the previous chapter. Dansylcadaverine is an auto fluorescent, lysosomotropic compound which inhibits clathrin-mediated endocytosis as well as interfere with the maturation of autophagosome (Davies, Cornwell et al. 1984). Also, they concentrate in the autophagosomes and serve as a marker for the presence of autophagosomes (Davies, Cornwell et al. 1984, Pasquier 2016). Using fluorescent microscopy, we have been able to demonstrate that dansylcadaverine concentrates in autophagosome vesicles when cells were exposed to doxazosin. These observations suggests that the attenuation of cytotoxic actions of doxazosin is at least in part mediated by its action as an inhibitor of autophagosome maturation.

This study also was the first to report widespread autophagy by doxazosin in PCa

and BCa cell lines using TEM (Pavithran and Thompson 2012, Pavithran, Shabbir et al. 2017). Our experiment with TEM suggests that exposure to doxazosin 37 μM for 24 h to 72 h resulted in autophagy with a predominantly selective mitophagy in PC-3, fibroblasts and HT1376 cells. Furthermore, these autophagic changes were not accompanied by karyorrhexis and chromatin condensation in these cells.

Additionally, the autophagic process was independent of the independent of the *p53* gene as we were able to replicate these findings in PC-3 cells, which have a *p53-null* status. Moreover, immunohistochemically labelled sections revealed densely stained areas of LC3B (brown staining) in the cytoplasm of sections that had been exposed to doxazosin whilst this feature was absent in the control specimens (Pavithran, Shabbir et al. 2017). Taken together, these observations suggest that autophagy (especially mitophagy) plays an important role in the doxazosin-induced cell death in

the cell lines tested. The findings, however, cannot directly attribute the cell death from doxazosin to autophagy (Klionsky, Abdalla et al. 2012).

Other investigators have suggested that apoptosis and anoikis were the primary mode of cell death in doxazosin (Keledjian and Kyprianou 2003, Kyprianou 2003). Also, Yang at al reported that prazosin but not doxazosin induced *p53* mediated autophagy in H9C2 cells (Yang, Wu et al. 2011). We attribute the discrepancies in their findings as the duration of exposure to doxazosin (20 µM) was limited in their experiments to only 4 h and not 24 h (Yang, Wu et al. 2011). The rationale for using 24 h as the first time point for examination under TEM in our experiments was derived from our previous observations that granulations appeared within the cells in a time –and –concentration dependent manner.

Though autophagy and apoptosis appear to be divergent pathways in cell survival, several studies have shown that these are closely related and capable of switching from one pathway to the other (Bhutia, Dash et al. 2010, Bhutia, Das et al. 2011). Apoptosis signalling can regulate autophagy and conversely autophagy can regulate apoptosis (Yonekawa and Thorburn 2013). Given the extensive crosstalk between autophagy and apoptosis (and the existence of both these processes simultaneously), it is often difficult to attribute quantitatively the cell death to each of these two processes. Nonetheless, our results therefore suggests that autophagy is a predominant process involved in doxazosin-induced cell death.

Chapter 7

Measurement of gene expression changes in PC-3 cells following exposure to doxazosin

7.1 Introduction

At the time of conducting this study, there existed no previous data on the events that led to doxazosin-induced cell death of PCa lines at the transcriptome level.

A literature search revealed only one previously published work that looked at gene expression following doxazosin treatment in prostate pathology. This study had examined the prostate glands of male Sprague-Dawley rats following administration of doxazosin (4mg/kg/day subcutaneously and supplemented with 4mg/kg/day orally) (Yono, Foster et al. 2005). They had shown that when doxazosin is administered for 12 weeks in the doses mentioned above, it resulted in changes in expression of 625 genes of which 39 genes were related to cell death, necrosis, growth, proliferation, and GPCR signalling pathways (Yono, Foster et al. 2005). Interestingly, the highest fold-change observed in their experiment was that of the sulphated glycoprotein-2 gene clusterin which is an antiapoptotic mediator and known to be highly expressed in rat prostate involution following castration (Sensibar, Sutkowski et al. 1995).

In this study, our objective was to identify at a transcriptome level, using next generation sequencing, the events that lead to cell death in PC-3 cells following treatment with doxazosin. We hypothesised that the next generation sequencing data would reveal the relative changes between doxazosin treated cells (as compared to controls) in the activity levels of various genes groups responsible for autophagy, apoptosis, and key cell signalling proteins.

7.2 Material and Methods

7.2.1 Cell culture:

PC-3 cells were grown in 75 cm² flasks (n=12) with 20 ml of appropriate media to 50% confluence. Then the cells were washed with PBS and 18 ml of fresh media added. To the test flasks (labelled D1 to D6), 2ml of doxazosin solution (final concentration 37 µM) was added while 2 ml of sterile water was added to the control flasks (labelled C1 to C6). The test and control flasks were then incubated for 24 h (D1-D3 and C1-C3), or 48 h (D4-D6 and C4-C6). After the required incubation period (24 h or 48 h), the media was decanted, washed once with PBS and the flasks were immediately flash frozen to -80 C overnight.

The next day, 6 ml of EDTA-trypsin solution at 37 C was added and the flasks transferred to incubator at 37 C for 5 minutes. Once the cells had detached, 18 ml of fresh media at 37 C containing 10 % serum was added to the flask and the contents decanted to 50 ml aliquots. These were then centrifuged at 500 rpm for 5 minutes, the supernatant decanted, and the pellets were carefully washed 3 times with PBS solution.

7.2.2 RNA isolation for PC-3 cells using TRIzol®:

The washed cell pellets were homogenized in 1 ml of TRIzol[®] reagent. TRIzol[®] is monophasic solution of phenol, guanidine isothiocyanate and maintains the integrity of the RNA due to its highly effective inhibition of RNAse activity while simultaneously disrupting cells and dissolving cell components during sample homogenization. Also, TRIzol[®] allows the sequential precipitation of RNA, DNA & proteins from a single sample.

In our experiments, the RNA phase was separated by the addition of 200 μ L of chloroform followed by vigorous mixing for 15 seconds and centrifuging at 12,000 g for 15 minutes at 4 C. This separated the homogenate into 3 layers, namely, the clear, upper aqueous layer, a white interphase, and a red lower organic layer. The upper aqueous layer was transferred to a fresh tube whilst the lower layer was saved for DNA extraction. RNA was precipitated from the upper aqueous layer with the addition of 500 μ L of isopropanol. This was incubated at room temperature for 10 minutes and subsequently centrifuged at 12,000 g for 10 min at 4°C. After centrifuging, the supernatant was removed and the RNA pellet was washed with 1 ml of ethanol, vortex mixed, and centrifuged at 7500 g for 5 minutes at 4 C. This step was repeated twice after which the supernatant was discarded, and the tubes were dried out by placing them on heating blocks at 60 C to obtain pellets that were nearly dried. These were then dissolved in 50–100 μ L of RNAse-free water. The RNA solution was then aliquoted into 2 smaller tubes and stored at -80 °C overnight.



Figure 59: TRIzol® reagent separation showing the homogenate separated into 3 layers, namely, the clear upper aqueous layer, a white middle interphase layer and a red lower organic layer.

7.2.3 RNA quality control analysis:

We assessed the RNA preparation for the quantity and the integrity of the RNA preparation and its purity. For this we used absorption spectrometry to estimate the RNA quantitatively and to evaluate its purity. The integrity of the RNA was assessed using formaldehyde agarose gel electrophoresis. Also, prior to transcriptome sequencing the RNA quantity, purity and integrity were independently re-assessed by Genomics UCL by gel and spectrometric analysis of the individual samples.

7.2.4 Spectrophotometric analysis of RNA sample quality:

This is based on the estimation of light absorbed by the nucleic acids within a sample when light is passed through a solution containing them. The absorption is then converted to concentration based on the following conversion factors: An absorbance of 1.00 at 260 nm corresponds to approximately: 50 mg/ml for double-stranded DNA; 40 mg/ml for single-stranded DNA or RNA and 20 mg/ml for oligonucleotides. Pure preparations of DNA and RNA have an A₂₆₀/A₂₈₀ ratio of 1.8 to 2.0 respectively. Ratios significantly lower than this indicates protein or phenol contamination of the sample. The A₂₆₀/A₂₃₀ absorption ratio for pure nucleic acids are commonly in the range of 2.0-2.2. If this ratio is lower than 2, it indicates the presence of contaminants such as guanidine, EDTA, carbohydrates and phenol all of which absorb light near 230 nm.

We used the NanoDropTM (Thermo Scientific, UK), which allows for analysis of 1 μL of the sample solution. This solution placed directly on the pedestal of the NanoDropTM chamber, and the surface tension of the solution leads to the formation of a column of the sample through which light is directed to evaluate the absorption spectrum. Tables 8 and 9 shows the readings obtained and the representative graph obtained for an individual sample is shown in figure 60.

Table 8: Readings of the individual samples obtained using NanoDropTM for PC3 cells treated with doxazosin (D1-D3) 37 μ M for 24 h versus control (C1-C3) samples. The last row shows the calculated volumes for 2 μ g of RNA in 200 μ L.

| Sample ID | C1 | C2 | C3 | D1 | D2 | D3 |
|---------------------------------|--------|--------|--------|--------|-------|--------|
| RNA Concentration (ng/µL) | 534.2 | 564.1 | 691.7 | 400.1 | 308.9 | 433.6 |
| A260 (10 mm path) | 13.354 | 14.102 | 17.292 | 10.003 | 7.723 | 10.840 |
| A 280 (10 mm path) | 7.676 | 8.002 | 9.439 | 5.761 | 4.391 | 6.019 |
| 260/280 | 1.74 | 1.76 | 1.83 | 1.74 | 1.76 | 1.80 |
| 260/230 | 2.46 | 2.44 | 2.39 | 2.36 | 2.40 | 2.33 |
| Volume for 2 μg in 200 μL | 3.741 | 3.545 | 2.891 | 4.999 | 6.474 | 4.612 |

| Sample ID | C4 | C5 | C6 | D4 | D5 | D6 |
|-------------------|---------|----------|----------------|-------|--------|--------|
| RNA | 628.1 | 705.1 | 662.1 | 262.8 | 517.9 | 434.8 |
| Concentration | 627.8 | | | 264.9 | 371.5 | 313.5 |
| (ng/µL) | | | | | 298.5 | 279.8 |
| A260 (10 mm | 15.703 | 17.628 | 16.552 | 6.569 | 12.947 | 10.871 |
| path) | 15.695 | | | 6.622 | 9.287 | 7.837 |
| | | | | | 7.463 | 6.995 |
| A 280 (10 mm | 9.458 | 10.354 | 9.841 | 4.006 | 7.889 | 6.784 |
| path) | 9.185 | | | 4.067 | 5.726 | 4.861 |
| | | | | | 4.633 | 4.382 |
| 260/280 | 1.66 | 1.70 | 1.68 | 1.64 | 1.64 | 1.60 |
| | 1.71 | | | 1.63 | 1.62 | 1.61 |
| | | | | | 1.61 | 1.60 |
| 260/230 | 2.45 | 2.45 | 2.45 | 2.44 | 2.41 | 2.42 |
| | 2.46 | | | 2.46 | 2.42 | 2.44 |
| | | | | | 2.45 | 2.47 |
| Volume for 2 μg | 3.186 | 2.834 | 3.021 | 7.550 | 6.700 | 7.148 |
| in 180 to 200 μL. | (200µL) | (180 µL) | $(180 \mu L)$ | | | |

Table 9: Readings of the individual samples obtained using NanoDropTM for PC3 cells treated samples with doxazosin (D4-D6) 37 μ M for 48 h versus control samples (C4-C6). The last row shows the calculated volumes for 2 μ g of RNA in 180 or 200 μ L.

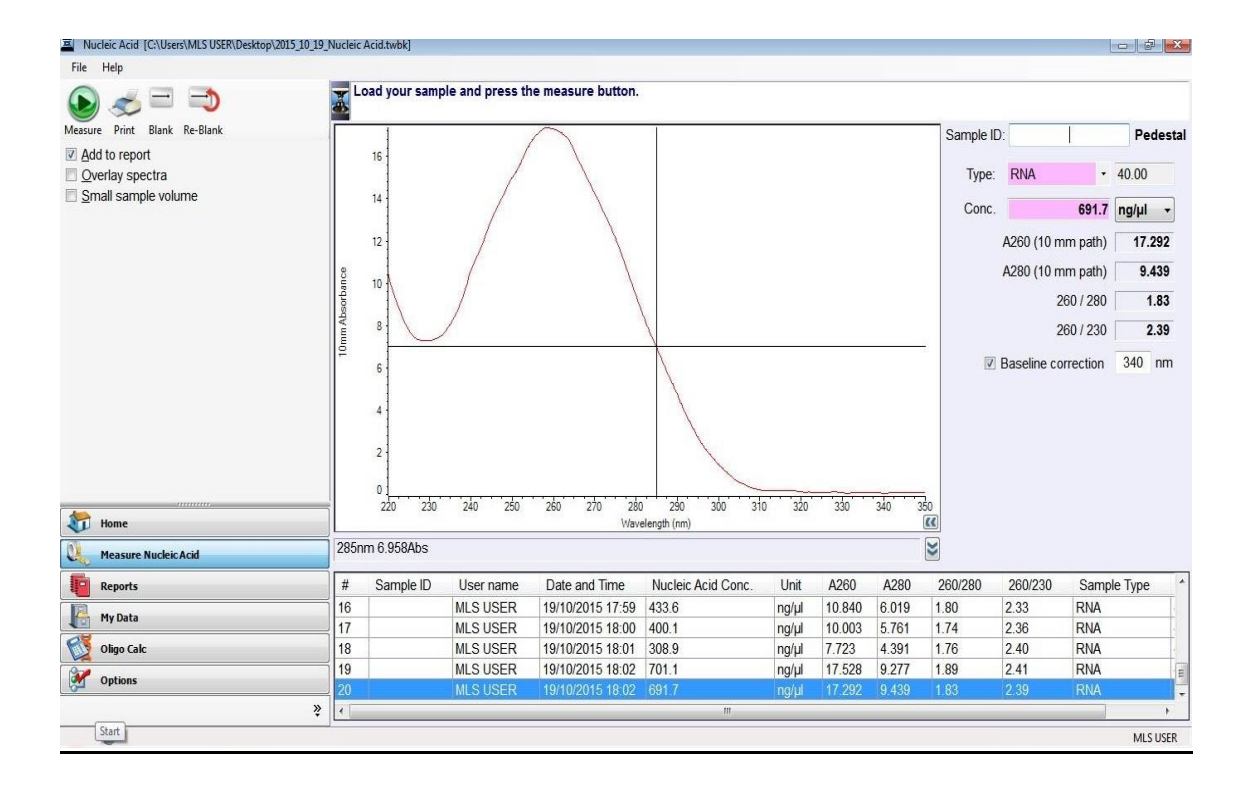


Figure 60: Screen capture of graph obtained (for a representative sample) using NanoDrop[™] quality control assessment of the purity and quantity of nucleic acid.

7.2.5 Formaldehyde agarose gel electrophoresis:

This involves the electrophoresis of the RNA preparation in 1.2% formaldehyde gel to separate the ribosomal bands to evaluate the integrity of the RNA. Intact total RNA shows 2 ribosomal bands; the upper 28S ribosomal band is approximately twice the intensity of the lower 18S rRNA band, whilst mRNA appears as a background smear. These bands are visualized from the gel following the electrophoresis using a transilluminator.

The first step is the preparation of the 1.2% formaldehyde gel. This involves mixing and dissolving 0.6 g of agarose in 5ml of 10x MOPS [3-N(morpholino) propane sulfonic acid] (MOPS) and 37 ml of distilled water by gentle heating until the agarose is completely dissolved. This this then allowed to cool until warm to touch and 8 ml of formaldehyde (37%) is added. This is mixed well and immediately poured into the preprepared gel moulds and allowed to solidify in them. The gel is then retrieved carefully from the mould, immersed in 1x MOPS in an electrophoresis tank and allowed to equilibrate for 30 minutes (Figure 61).

The second step is to load the RNA gels and a control ladder into the gel wells. The sample preparations (with 2 μ L of 100x Sybr Green®) are loaded into the wells and the gel run at 90 V until the dye has traversed two-thirds of the length of the gel. Finally, the gel is removed carefully and placed on the transilluminator to visualize the RNA (Figure 62).



Figure 61: Gel electrophoresis equipment with sample loaded and electrophoresis in progress.

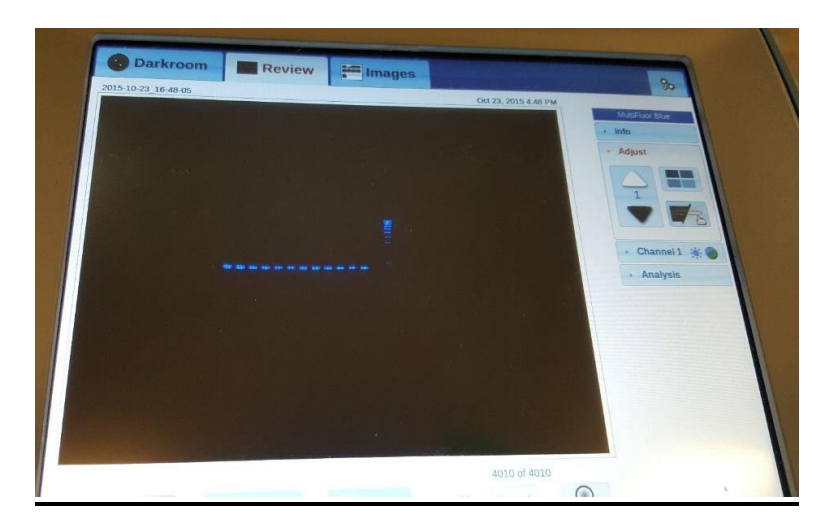


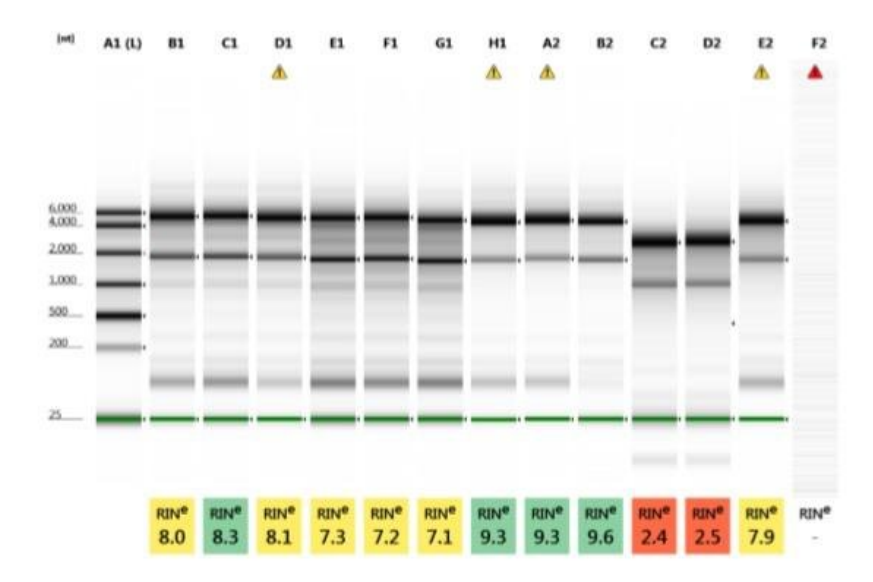
Figure 62: Visualization of RNA bands using transilluminator. The band on extreme right is the control.

7.2.6 RNA quality assessment using Agilent Tapestation™:

This quality control step was undertaken by the UCL Genomics, prior to transcriptome sequencing. This uses a screen tape gel matrix, where samples are automatically loaded into individually packaged lanes that prevents any cross contamination. Prior to loading, the samples are coated with an inter chelating dye and electrophoresed. The gels are imaged using a high-quality camera and a software generates a gel image electropherogram and peak tables (Figure 63).

It provided information about RNA integration number (RIN) equivalent, which is a ratio of the fast zone 18s RNA and the small RNAs (Table 10 and Figure 64).

Gel Images



Default image (Contrast 50%), Image is Scaled to Sample, Image is Scaled to view larger Molecular Weight range

Figure 63: Gel images obtained using Agilent Tape station showing the electropherogram and the RIN equivalents for each of the samples.

Sample Info

| Well | RINe | 28S/18S (Area) | Conc. [ng/µl] | Sample Description | Alert | Observations |
|------|------|----------------|---------------|--------------------|-------------|--|
| A1 | (*) | * | 162 | Ladder | | Ladder |
| B1 | 8.0 | 1.7 | 422 | D1 | | |
| C1 | 8.3 | 1.7 | 303 | D2 | | |
| DI | 8.1 | 2.3 | 504 | D3 | <u> </u> | RNA concentration outside recommended range for RINe |
| E1 | 7.3 | 1.4 | 256 | D4 | | |
| F1 | 7.2 | 1.4 | 308 | D5 | | |
| Gl | 7.1 | 1.2 | 282 | D6 | | |
| HI | 9.3 | 3.0 | 541 | Cl | \triangle | RNA concentration outside recommended range for RINe |
| A2 | 9.3 | 2.8 | 644 | C2 | A | RNA concentration outside recommended range for RINe |
| B2 | 9.6 | 2.2 | 258 | C3 | | |
| C2 | 2.4 | - | 174 | C4 | | |
| D2 | 2.5 | - | 181 | C5 | | |
| E2 | 7.9 | 2.3 | 728 | C6 | <u> </u> | RNA concentration outside recommended range for RINe |
| F2 | - | - | | | A | Marker(s) not detected |

Table 10: Peak table values obtained using Agilent Tape station showing the RIN equivalents for each of the samples.

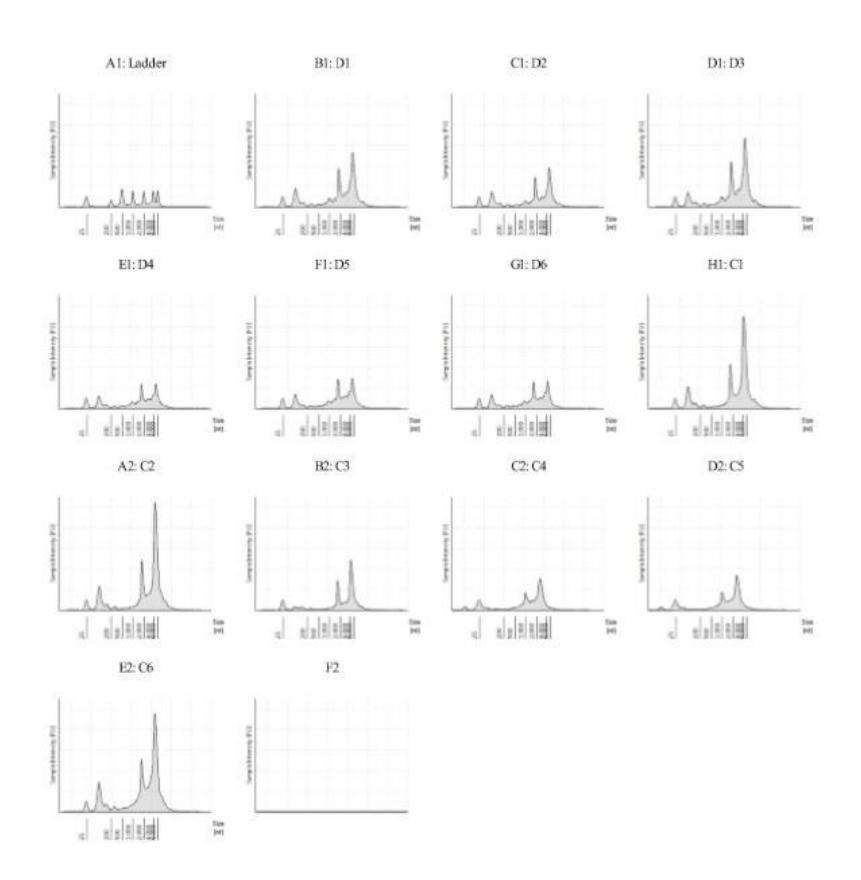


Figure 64: Peak table values as graphic representation of the RIN equivalents of the individual samples.

7.3 RESULTS

We looked at the transcriptome level changes in the control and doxazosin-treated samples for (a) fold changes in expression and (b) within gene families.

To identify the fold changes in expression we evaluated the 2x, 3x and over 4x fold changes between the control and treated samples at 24 h and 48 h. Also, we

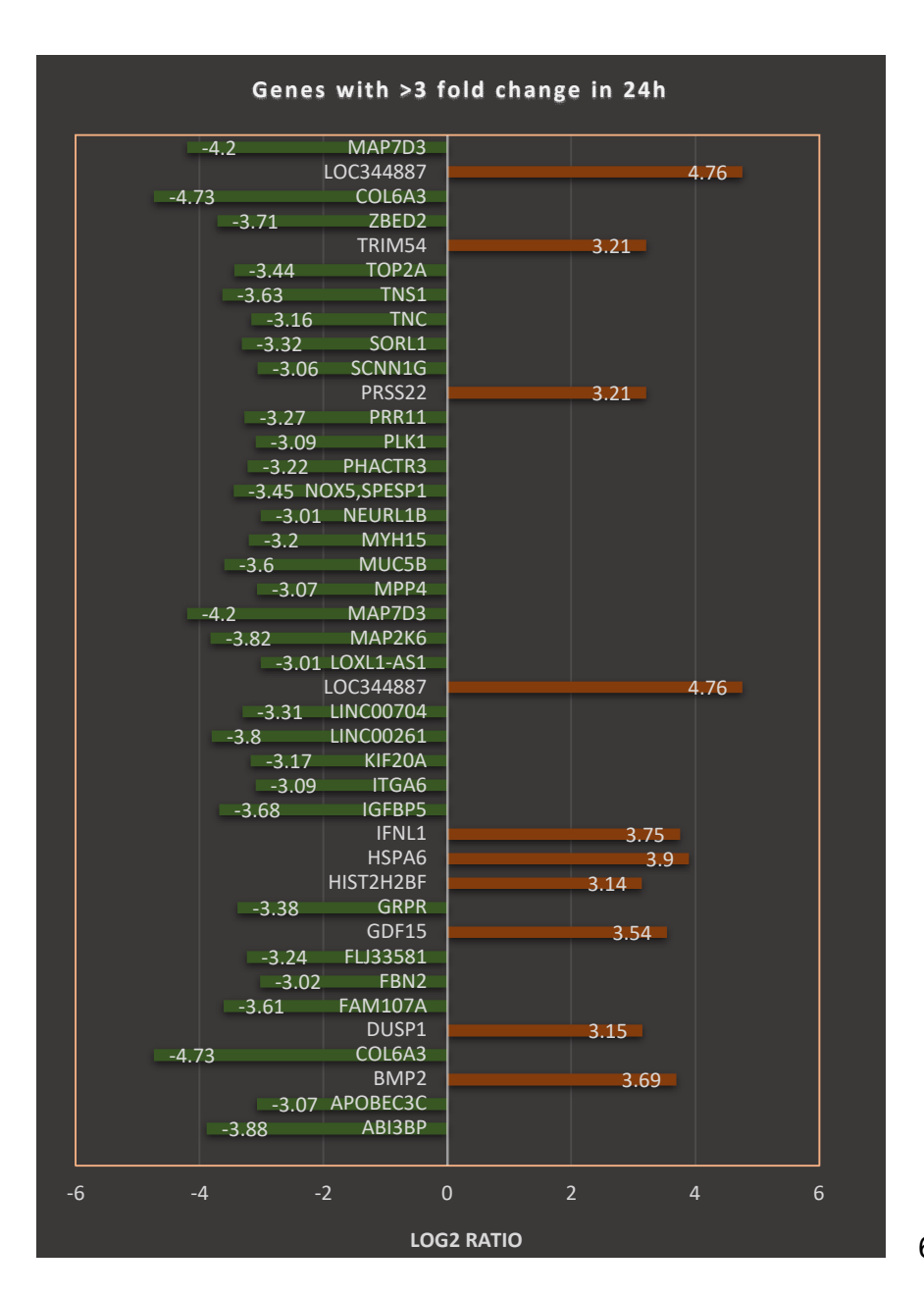
identified those genes which had the highest level of positive or negative fold changes in expression in samples at 24 h at 48 h and between samples at 24 h and 48 h.

7.3.1 Evaluation of fold changes in expression between control and test samples after 24 h of exposure to doxazosin:

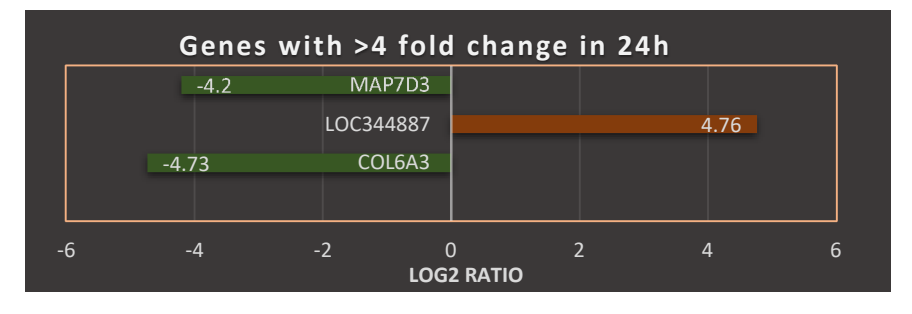
We assessed the data available at Basespace[™] (Illumina.com) to evaluate the log2 ratio of fold-changes in gene expression. The array was designed to assess the entire transcriptome accounting for over 30,000 genes.

Of these, we identified over 250 named-genes with a 2-fold increase in control versus 24-h doxazosin-treated group. When the parameters were set to 3-fold changes and 4-fold changes; there were 39 named genes and 3 other genes, respectively, within these groups (Figure 65). Interestingly, there were no named-genes that had a fold-change greater than 5 between control samples and test samples exposed to doxazosin for 24h.

Figure 65: The log2 values in PC3 following treatment with doxazosin for 24 h identifying genes with greater than 3-fold change (A, top) and over 4-fold change (B, bottom). Positive fold-changes in red (right) and negative fold-change in green (left)



66.A



66.B

7.3.2 Evaluation of fold changes in expression between control and test samples after 48 h of exposure to doxazosin:

We assessed the data available at Basespace[™] (Illumina.com) to evaluate the log2 ratio of fold-changes in gene expression. The array was designed to assess the entire transcriptome accounting for over 30,000 genes.

Of these, we identified 350 named-genes with a 2-fold increase in control versus 48-hour doxazosin-treated group. When the parameters were set to 3-fold changes and 4-fold changes; there were 85 named-genes (Figure 66) and 18 other genes (Figure 67), respectively, within these search parameters.

Above 5-fold expression values, the specific genes that were differentially over expressed included:

- (i) EGR1 and HSPA6 (x5 fold)
- (ii) LOC100271832 and MIR1256/SLC25A3 (x9 fold)
- (iii) CD3D (x10 fold)

There were no named-genes with a fold-change was greater than 10.

The genes that were identified to have an expression over 3-fold in PC3 cells treated with 37 μ M of doxazosin for 48 h is shown on figure 66; those with greater than 4-fold expression at 48 h with 37 μ M of doxazosin is shown on figure 67.

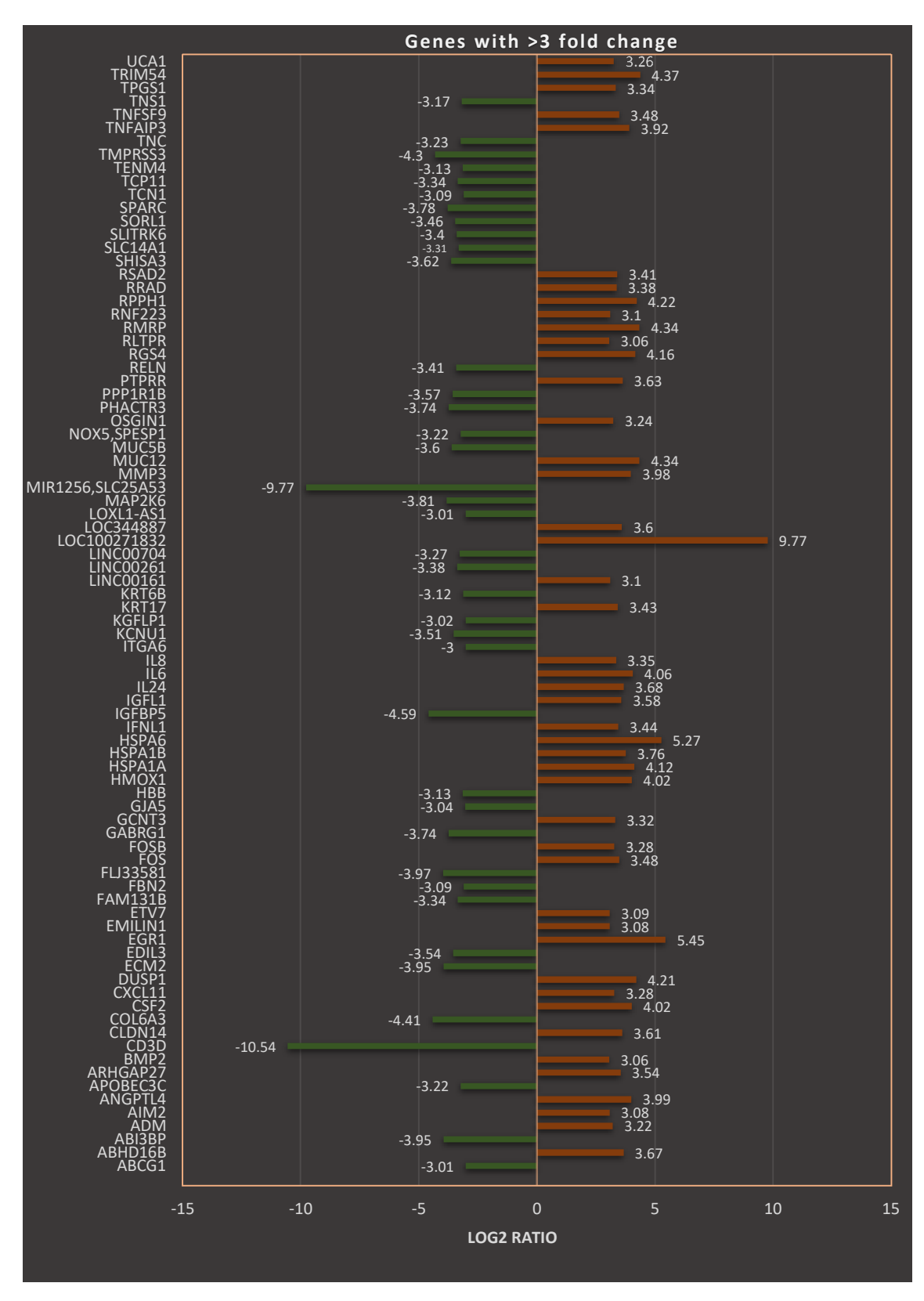


Figure 66: The log2 values in PC3 following treatment with doxazosin for 48h identifying genes with greater than 3-fold change. Positive fold-changes in red (right) and negative fold-change in green (left)

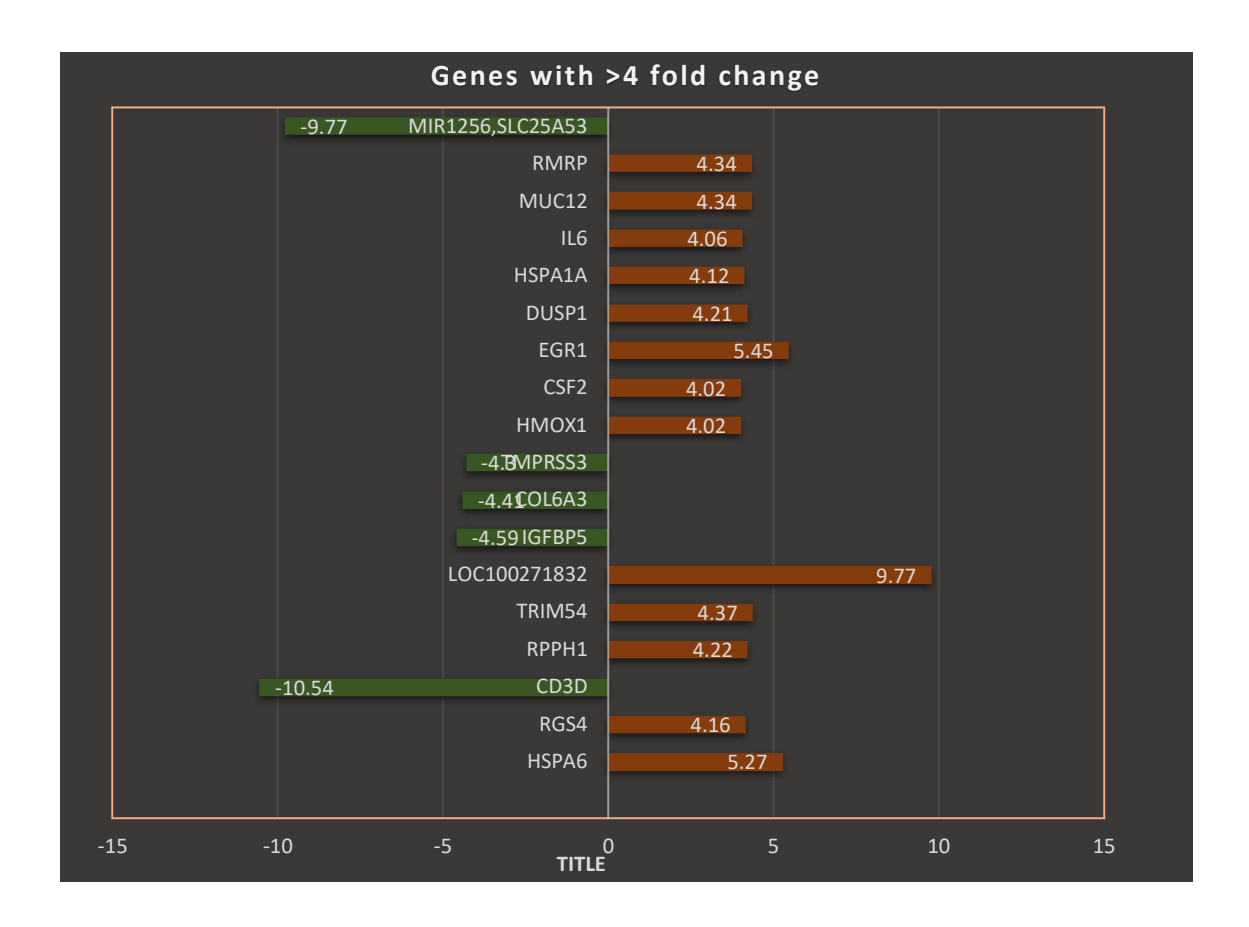


Figure 67: The log2 values in PC3 following treatment with doxazosin for 48h identifying genes with greater than 4-fold change. Positive fold-changes in red (right) and negative fold-change in green (left)

7.3.3. Comparison in fold-expression gene expression between 2 time points:

Using data sets available for the 2 time points, we compared the changes in gene expression between the 2 time points. For this we used the following comparisons:

- (a) Genes that had more than 2-fold change at 24h samples only (and not at 48h).
- (b) Genes that had over 2-fold-change only at 48 h samples only (and not at 24 h).
- (c) Genes that had more than 2-fold change in both time points (24 h and 48 h).
- (d) In group (c), we further identified the subgroups.

- a. Genes with an increase fold change expression from 24 h to 48 h
- b. Genes with a decrease in fold-change expression from 24 h to 48 h
- c. Genes where there was no variation in fold-change between two-time points.

Table 11: List of genes (n=108) that had over 2-fold change between test and control samples and were expressed at 24 h only.

| | | | log2 | log2 | | |
|--------------|------------------|-----------------------------|----------|-------------|-------------|-----------|
| | | | (control | (comparison | | |
| Test ID | Gene at 24h only | Locus | FPKM) | FPKM) | log2(Ratio) | q Value |
| | , | chr15:101420008- | , | , | , , | |
| XLOC_009476 | ALDH1A3 | 101456830 | 9.25 | 7.22 | -2.03 | 0.000166 |
| | | chr7:36363758- | | | | |
| XLOC_025566 | ANLN | 36493400 | 6.76 | 4.7 | -2.06 | 0.000166 |
| | | chr11:69924407- | | | | |
| XLOC_004807 | ANO1 | 70035652 | 5.88 | 3.74 | -2.14 | 0.000166 |
| | | chr17:33914281- | | | | |
| XLOC_011311 | AP2B1 | 34053436 | 6.45 | 4.36 | -2.09 | 0.000166 |
| | | chr4:57371374- | | | | |
| XLOC_020653 | ARL9 | 57390058 | -1.14 | 0.92 | 2.06 | 0.007198 |
| | | chr1:197053256- | | | | |
| XLOC_002730 | ASPM | 197115824 | 3.5 | 1.1 | -2.4 | 0.000166 |
| | | chr11:64755416- | | | | |
| XLOC_005566 | BATF2 | 64764517 | 0.13 | 2.83 | 2.69 | 0.000166 |
| | | chr7:97841565- | | | | |
| XLOC_025804 | BHLHA15 | 97881563 | -0.43 | 2.04 | 2.46 | 0.000166 |
| | | chr17:76210276- | | | | |
| XLOC_011724 | BIRC5 | 76221716 | 6.98 | 4.67 | -2.32 | 0.000166 |
| | | chr14:58470807- | | | | |
| XLOC_008714 | C14orf37 | 58618847 | 1.57 | -0.58 | -2.15 | 0.000166 |
| | | chr2:233734993- | | 0.10 | 2.22 | |
| XLOC_016055 | C2orf82 | 233741107 | -1.91 | 0.12 | 2.03 | 0.042664 |
| VI 06 000450 | CACCE | chr15:40886446- | 2.74 | 4.62 | 2.42 | 0.0004.66 |
| XLOC_009150 | CASC5 | 40954881 | 3.74 | 1.62 | -2.12 | 0.000166 |
| VI OC 031653 | CCND4 | chr5:68462836- | 6 77 | 4.60 | 2.00 | 0.000166 |
| XLOC_021653 | CCNB1 | 68474070 | 6.77 | 4.69 | -2.08 | 0.000166 |
| XLOC 009257 | CCNIDO | chr15:59397283- 59417244 | F 42 | 2 24 | 2.4 | 0.000166 |
| ALUC_009257 | CCNB2 | chr19:54976209- | 5.42 | 3.31 | -2.1 | 0.000166 |
| VI.OC 015007 | CDC43EDE | 54984422 | 2.05 | 0.01 | 2.00 | 0.027677 |
| XLOC_015007 | CDC42EP5 | | -2.05 | 0.01 | 2.06 | 0.037677 |
| XLOC 006734 | CDCA3 | chr12:6957971- 6960456 | 5.21 | 2.69 | -2.52 | 0.000166 |
| ALUC_006/34 | CDCAS | 0500430 | 5.21 | 2.09 | -2.52 | 0.000100 |

| | T | | | 1 | | |
|--------------|--------------|------------------|-------|-------|-------|-----------|
| VI OC 0104F8 | CDU1E | chr16:89238162- | 1.05 | 0.00 | 2.01 | 0.000222 |
| XLOC_010458 | CDH15 | 89261900 | -1.95 | 0.06 | 2.01 | 0.006223 |
| VIOC 035000 | CDUB3 | chr7:105603656- | 0.24 | 2.62 | 2.20 | 0.000166 |
| XLOC_025889 | CDHR3 | 105676877 | -0.34 | -2.63 | -2.29 | 0.000166 |
| VI OC 031303 | CENDE | chr4:104026962- | 2.02 | 1 11 | 2.72 | 0.0001.00 |
| XLOC_021283 | CENPE | 104119566 | 3.83 | 1.11 | -2.72 | 0.000166 |
| VI OC 001303 | CENDE | chr1:214776531- | 4.07 | 2.40 | 2.40 | 0.000166 |
| XLOC_001382 | CENPF | 214837914 | 4.97 | 2.48 | -2.49 | 0.000166 |
| VI OC 020145 | CURDI 1 | chrX:109917083- | 4.12 | 2.06 | 2.07 | 0.0001.00 |
| XLOC_030145 | CHRDL1 | 110039286 | 4.12 | 2.06 | -2.07 | 0.000166 |
| VI OC 007300 | CIT MID1170 | chr12:120123594- | 2.04 | 1.0 | 2.04 | 0.0001.00 |
| XLOC_007309 | CIT, MIR1178 | 120315095 | 3.94 | 1.9 | -2.04 | 0.000166 |
| VI 06 006774 | CLECZA | chr12:10269375- | 2.4 | 0.00 | 2.20 | 0.000000 |
| XLOC_006771 | CLEC7A | 10282868 | -2.4 | -0.02 | 2.39 | 0.000888 |
| VI 00 000000 | 0014344 | chr10:71561643- | 5.00 | 2.70 | 2.14 | 0.0004.66 |
| XLOC_003302 | COL13A1 | 71718904 | 5.89 | 3.78 | -2.11 | 0.000166 |
| VI 06 005645 | CTCF | chr11:66330934- | 2.56 | 0.04 | 2.52 | 0.0004.66 |
| XLOC_005615 | CTSF | 66336047 | 2.56 | 0.04 | -2.52 | 0.000166 |
| W 00 00000 | 0)/20044 | chr6:46517444- | 0.55 | 2.07 | 2.62 | 0.0004.66 |
| XLOC_023939 | CYP39A1 | 46620523 | 0.55 | -2.07 | -2.62 | 0.000166 |
| | | chr1:68939834- | | | | 0.0004.66 |
| XLOC_002116 | DEPDC1 | 68962799 | 4.29 | 2.27 | -2.02 | 0.000166 |
| W 00 00000 | D C V C | chr3:185864989- | 0.40 | 2.4 | 2.22 | 0.0004.66 |
| XLOC_020368 | DGKG | 186080023 | -0.18 | -2.4 | -2.23 | 0.000166 |
| | | chr14:55614833- | | 0.70 | | 0.000466 |
| XLOC_008692 | DLGAP5 | 55658396 | 6.74 | 3.76 | -2.97 | 0.000166 |
| W 00 000001 | D D)/4014 | chr7:34968492- | | 2.22 | 2.07 | 0.0004.66 |
| XLOC_026291 | DPY19L1 | 35077653 | 4.4 | 2.32 | -2.07 | 0.000166 |
| | 5.1.055 | chr10:112257624- | | | | 0.0004.66 |
| XLOC_003540 | DUSP5 | 112271302 | 4.67 | 6.91 | 2.24 | 0.000166 |
| W 00 045407 | 55000 | chr2:25264972- | 2.42 | 2.24 | 2.14 | 0.0004.66 |
| XLOC_015197 | EFR3B | 25382004 | 2.12 | 0.01 | -2.11 | 0.000166 |
| | | chr1:120839004- | 4.00 | 0.00 | | 0.0004.66 |
| XLOC_000832 | FAM72B | 120855681 | 1.92 | -0.09 | -2.01 | 0.000166 |
| | | chr20:37554954- | | | | |
| XLOC_017234 | FAM83D | 37581703 | 5.4 | 3.3 | -2.1 | 0.000166 |
| | 0.0000 | chr12:100967488- | 2.25 | 4.05 | | |
| XLOC_006483 | GAS2L3 | 101020721 | 3.25 | 1.25 | -2 | 0.000166 |
| | 0.100 | chr12:6949374- | 4.40 | 0.00 | | |
| XLOC_006732 | GNB3 | 6956557 | 1.18 | -0.82 | -2 | 0.007945 |
| | 0.100 | chr12:6949374- | | | 2.52 | |
| XLOC_006733 | GNB3 | 6956557 | 1.55 | -1.14 | -2.69 | 0.00267 |
| | | chr6:46965448- | | | | |
| XLOC_023942 | GPR110 | 47010372 | 5.9 | 3.51 | -2.39 | 0.000166 |
| W 00 000105 | CDD4273 | chr14:53019865- | 4.5- | | 2.22 | 0.000155 |
| XLOC_008126 | GPR137C | 53104431 | 1.67 | -1.25 | -2.92 | 0.000166 |
| | | chr1:222695601- | | | | |
| XLOC_002886 | HHIPL2 | 222721444 | 0.29 | -2.43 | -2.72 | 0.000468 |
| W 00 00055 | | chr6:26106542- | 4 | 2.5- | | 0.04.5005 |
| XLOC_023658 | HIST1H1T | 26108698 | -1.52 | 0.63 | 2.16 | 0.016298 |

| | LUCTALIZAD | ah #C+2C102202 | | | | |
|------------------|------------------|-----------------------------|-------|-------|-------|-----------|
| VI OC 022667 | HIST1H2AD, | chr6:26193202- | 0.7 | 2.25 | 2.64 | 0.0001.00 |
| XLOC_023667 | HIST1H3D | 26199521 | 0.7 | 3.35 | 2.64 | 0.000166 |
| VI OC 002276 | LUCTALIADE | chr1:149754244- | 1 1 5 | 1.00 | 2.14 | 0.022222 |
| XLOC_002376 | HIST2H2BF | 149783928 | -1.15 | 1.99 | 3.14 | 0.032233 |
| VI OC 021442 | LIDCD | chr4:175411327- | 2.20 | 1 2 4 | 2.05 | 0.000166 |
| XLOC_021443 | HPGD | 175444049 | 3.39 | 1.34 | -2.05 | 0.000166 |
| VI OC 010411 | 11004702 | chr16:82068857- | 2 11 | 0.50 | 2.52 | 0.0001.00 |
| XLOC_010411 | HSD17B2 | 82132139 | 3.11 | 0.59 | -2.52 | 0.000166 |
| VI OC 020C24 | IENID4 | chr9:21077103- | 1.00 | 1 22 | 2.20 | 0.001000 |
| XLOC_028634 | IFNB1 | 21077943 | -1.06 | 1.32 | 2.38 | 0.001809 |
| VI OC 010172 | ITCD2 | chr21:46305867- | 2 22 | 1 1 4 | 2.17 | 0.000166 |
| XLOC_018173 | ITGB2 | 46349595 | 3.32 | 1.14 | -2.17 | 0.000166 |
| VI 06 044602 | ITCD 4 | chr17:73717515- | F 76 | 2.46 | 2.2 | 0.0004.66 |
| XLOC_011693 | ITGB4 | 73753999 | 5.76 | 3.46 | -2.3 | 0.000166 |
| VI 00 047654 | 10113 | chr20:42735506- | 4.75 | 0.25 | 2.00 | 0.0004.66 |
| XLOC_017651 | JPH2 | 42816218 | 1.75 | -0.35 | -2.09 | 0.000166 |
| VI OC 02002C | V A I 1 | chrX:8496914- | 0.07 | 1 24 | 2 24 | 0.000166 |
| XLOC_029836 | KAL1 | 8700227 | 0.97 | -1.34 | -2.31 | 0.000166 |
| VI OC 017704 | I/CND4 | chr20:47988504- | 0.03 | 2.62 | 2.64 | 0.0001.00 |
| XLOC_017704 | KCNB1 | 48099181 | 0.02 | -2.62 | -2.64 | 0.000166 |
| VI OC 027012 | I/CNII I4 | chr8:36641841- | 0.26 | 2.24 | 2.00 | 0.00022 |
| XLOC_027012 | KCNU1 | 36793643 | -0.36 | -3.24 | -2.88 | 0.00032 |
| VI OC 003435 | IZIE44 | chr10:94352824- | 4 77 | 2.57 | 2.2 | 0.0001.00 |
| XLOC_003425 | KIF11 | 94415152 | 4.77 | 2.57 | -2.2 | 0.000166 |
| VI OC 002744 | 1/154.4 | chr1:200520624- | 2.72 | 1.4 | 2.22 | 0.0001.00 |
| XLOC_002744 | KIF14 | 200589862 | 3.72 | 1.4 | -2.32 | 0.000166 |
| XLOC 000436 | KIF2C | chr1:45205489- | 5.3 | 3.04 | -2.26 | 0.000166 |
| XLUC_000436 | NIFZC | 45233438 | 5.5 | 3.04 | -2.20 | 0.000166 |
| VI.O.C. 0204E.C. | IZIE 4 A | chrX:69509878- | 4.00 | 2.44 | 2.47 | 0.0001.00 |
| XLOC_029456 | KIF4A | 69640774 | 4.88 | 2.41 | -2.47 | 0.000166 |
| VI OC 007010 | KRT4 | chr12:53200326- 53207900 | 0.47 | 2.10 | 2.66 | 0.000166 |
| XLOC_007010 | KK14 | | 0.47 | -2.19 | -2.66 | 0.000166 |
| VI.O.C. 0170C0 | LINIC00310 | chr21:35552977- 35562220 | 2.02 | 0.00 | 2.07 | 0.014044 |
| XLOC_017868 | LINC00310 | | -3.03 | -0.06 | 2.97 | 0.014844 |
| VI 06 0030F6 | 11000707 | chr10:6821559- | 1 20 | 1.66 | 2.02 | 0.000166 |
| XLOC_003056 | LINC00707 | 6884868 | 1.28 | -1.66 | -2.93 | 0.000166 |
| VI.OC 010367 | 100153335 | chr3:101659702- | 1 74 | 0.67 | 2.41 | 0.00022 |
| XLOC_019267 | LOC152225 | 101716770 | 1.74 | -0.67 | -2.41 | 0.00032 |
| VI OC 004270 | 100255512 | chr11:1330937- | 2.10 | 0.17 | 2.01 | 0.024615 |
| XLOC_004279 | LOC255512 | 1331937 | -2.18 | -0.17 | 2.01 | 0.034615 |
| VI.O.C. 02.C722 | 100040330 | chr7:130565414- | 2.75 | F F2 | 2 77 | 0.000166 |
| XLOC_026733 | LOC646329 | 130598151 | 2.75 | 5.52 | 2.77 | 0.000166 |
| VI.O.C. 011030 | MAIDOO MAIDOOLLO | chr17:1614797- | 1.05 | 4 4 4 | 2.46 | 0.000100 |
| XLOC_011820 | MIR22, MIR22HG | 1619566 | 1.95 | 4.11 | 2.16 | 0.000166 |
| VI.OC 020722 | MIR29A, | chr7:130556555- | 0.33 | 2.40 | 2.25 | 0.000100 |
| XLOC_026732 | MIR29B1 | 130564945 | 0.23 | 2.48 | 2.25 | 0.000166 |
| VI.OC 004300 | NAVIC7 | chr10:129894924- | F 00 | 2.00 | 2.22 | 0.000166 |
| XLOC_004208 | MKI67 | 129924468 | 5.08 | 2.86 | -2.22 | 0.000166 |
| VIOC 01690C | MDD4 | chr2:202509596- | 0.1 | 2.07 | 2 07 | 0.000600 |
| XLOC_016806 | MPP4 | 202563417 | 0.1 | -2.97 | -3.07 | 0.000609 |

| VI.O.C. 01 F.C.C.4 | MAYO 7D | chr2:128293377- | 4 17 | 1 72 | 2.40 | 0.0001.00 |
|--------------------|----------|------------------------------|-------|-------|-------|-----------|
| XLOC_015664 | МҮО7В | 128395303 chr12:6603297- | 4.17 | 1.72 | -2.46 | 0.000166 |
| VI OC 006034 | NCADDO | 6641132 | г с | 2.07 | 2 52 | 0.000166 |
| XLOC_006024 | NCAPD2 | chr18:2571509- | 5.6 | 3.07 | -2.53 | 0.000166 |
| XLOC 012659 | NDC00 | 2616634 | 5.69 | 3.58 | 2 11 | 0.000166 |
| XLUC_012659 | NDC80 | chrX:43808023- | 5.09 | 3.36 | -2.11 | 0.000166 |
| XLOC_029911 | NDP | 43832921 | 0.42 | -2.11 | -2.54 | 0.000166 |
| XLOC_029911 | NDF | chr1:211831598- | 0.42 | -2.11 | -2.54 | 0.000100 |
| XLOC 002854 | NEK2 | 211848972 | 4.97 | 2.91 | -2.06 | 0.000166 |
| XLOC_00203+ | IVERZ | chr5:172068275- | 4.57 | 2.51 | 2.00 | 0.000100 |
| XLOC 022091 | NEURL1B | 172118533 | 0.04 | -2.97 | -3.01 | 0.000166 |
| X200_022031 | NEONEID | chr2:157180943- | 0.01 | 2.37 | 3.01 | 0.000100 |
| XLOC 016652 | NR4A2 | 157189287 | -1.13 | 0.98 | 2.11 | 0.000166 |
| <u> </u> | | chr20:61340188- | | 0.00 | | 0.000100 |
| XLOC 017356 | NTSR1 | 61394123 | 2.58 | 0.28 | -2.3 | 0.000166 |
| <u> </u> | | chr7:56182373- | | 0.20 | | 0.000100 |
| XLOC 026378 | NUPR1L | 56184090 | -0.26 | 1.87 | 2.13 | 0.002914 |
| _ | | chr15:41624862- | | | | |
| XLOC 009164 | NUSAP1 | 41673260 | 6.8 | 4.44 | -2.37 | 0.000166 |
| - | | chr1:100111430- | | | | |
| XLOC 000689 | PALMD | 100231349 | 1.3 | -1.02 | -2.32 | 0.000166 |
| - | | chr4:138440073- | | | | |
| XLOC_021348 | PCDH18 | 138453629 | 0.24 | -1.85 | -2.09 | 0.000166 |
| <u></u> | | chr7:31790790- | | | | |
| XLOC_026280 | PDE1C | 32338383 | 4.25 | 1.46 | -2.78 | 0.000166 |
| | | chr7:94285636- | | | | |
| XLOC_025796 | PEG10 | 94299006 | 5.83 | 3.76 | -2.06 | 0.000166 |
| | | chr9:70970108- | | | | |
| XLOC_028207 | PGM5 | 71145977 | 5.19 | 3.11 | -2.07 | 0.000166 |
| | | chr9:123617930- | | | | |
| XLOC_029005 | PHF19 | 123639606 | 5.77 | 3.42 | -2.35 | 0.000166 |
| | | chr2:217081611- | | | | |
| XLOC_015955 | PKI55 | 217084915 | 1.64 | -0.64 | -2.28 | 0.000166 |
| | | chr16:23690200- | | | | |
| XLOC_010132 | PLK1 | 23724821 | 5.71 | 2.62 | -3.09 | 0.000166 |
| | | chr4:82347549- | | | | |
| XLOC_021220 | RASGEF1B | 82393061 | -1.22 | 1.27 | 2.49 | 0.000166 |
| | | chr1:182567757- | | | | |
| XLOC_002699 | RGS16 | 182573548 | -2.21 | 0.03 | 2.24 | 0.000609 |
| VI 00 017015 | 5543 | chr20:35729628- | 0.00 | 5.00 | 2.4 | 0.0004.66 |
| XLOC_017215 | RPN2 | 35870028 | 8.02 | 5.92 | -2.1 | 0.000166 |
| VI.OC 034050 | DDACD | chr6:90074334- | 0.43 | 4.65 | 2.00 | 0.000166 |
| XLOC_024050 | RRAGD | 90121995 | -0.43 | 1.65 | 2.08 | 0.000166 |
| VI.OC 017425 | CIDDDO | chr20:1455235- | 1.00 | 0.72 | 2.44 | 0.000100 |
| XLOC_017425 | SIRPB2 | 1472233 | 1.68 | -0.73 | -2.41 | 0.000166 |
| VI.O.C. 019300 | CHCD3 | chr22:24577443- | 0.03 | 2 42 | 2.00 | 0.000166 |
| XLOC_018290 | SUSD2 | 24585074 | -0.03 | -2.12 | -2.09 | 0.000166 |
| XLOC 021897 | TGFBI | chr5:135364583- 135399507 | 0.53 | -2.01 | -2.54 | 0.000166 |
| VFOC_051931 | IUFDI | 10000000/ | 0.55 | -2.01 | -2.54 | 0.000100 |

| | | chr11:65122281- | | | | |
|----------------|----------|------------------|-------|-------|-------|----------|
| XLOC 004701 | TIGD3 | 65125082 | -2.47 | 0.08 | 2.55 | 0.001422 |
| X200_001701 | 11003 | chr3:12045861- | 2.17 | 0.00 | 2.33 | 0.001422 |
| XLOC 019682 | TIMP4 | 12233532 | 1.07 | -1.24 | -2.32 | 0.000888 |
| 7.12 0_010 001 | | chr15:102182048- | 2.07 | | | 0.00000 |
| XLOC 009912 | TM2D3 | 102192594 | 3.34 | 5.35 | 2.01 | 0.000166 |
| 7.100_000011 | 23 | chr12:72079877- | 0.0. | 3.00 | | 0.000200 |
| XLOC 006408 | TMEM19 | 72097839 | 2.97 | 0.88 | -2.09 | 0.000166 |
| | | chr2:220408744- | - | | | |
| XLOC 015994 | TMEM198 | 220415317 | -2.48 | -0.23 | 2.25 | 0.002304 |
| | | chr12:98906750- | | | | |
| XLOC 007195 | TMPO-AS1 | 98944157 | 2.07 | 0.01 | -2.06 | 0.001681 |
| _ | | chr6:30070673- | | | | |
| XLOC_023741 | TRIM31 | 30080867 | -2.34 | -0.26 | 2.08 | 0.005661 |
| | | chr2:27505296- | | | | |
| XLOC_015221 | TRIM54 | 27531130 | -2.83 | 0.38 | 3.21 | 0.000468 |
| | | chr17:3413795- | | | | |
| XLOC_011844 | TRPV3 | 3461289 | -1.57 | 0.47 | 2.04 | 0.000166 |
| | | chr2:239756672- | | | | |
| XLOC_016085 | TWIST2 | 239832237 | -0.32 | -2.67 | -2.35 | 0.031533 |
| | | chr22:24094929- | | | | |
| XLOC_018597 | VPREB3 | 24096630 | -1.67 | 1.11 | 2.78 | 0.027628 |
| | | chr3:111260925- | | | | |
| XLOC_020078 | ZBED2 | 111371206 | -0.4 | -4.11 | -3.71 | 0.047881 |
| | | chrX:152082983- | | | | |
| XLOC_029759 | ZNF185 | 152142025 | 6.58 | 4.23 | -2.35 | 0.000166 |
| | | chr19:58978292- | | | | |
| XLOC_015094 | ZNF324 | 58987404 | -1.01 | 1.53 | 2.54 | 0.001809 |
| | | chr19:52534651- | | | | |
| XLOC_013888 | ZNF432 | 52553195 | -1.06 | 1.38 | 2.43 | 0.018766 |
| | | chr16:88493878- | | | | |
| XLOC_010446 | ZNF469 | 88507165 | -0.26 | 2.04 | 2.3 | 0.000166 |
| | | chr19:58318449- | | | | |
| XLOC_014099 | ZNF552 | 58327343 | -2.09 | 0.63 | 2.72 | 0.045342 |

Table 12: List of genes (n= 206) that had over 2-fold change between test and control samples and were expressed at 48 h only.

| | | | log2 | log2 | | |
|------------------|------------|---------------------------|----------|-------------|-------------|-----------|
| | | | (control | (comparison | | |
| Test ID | Gene | Locus | FPKM) | FPKM) | log2(Ratio) | q Value |
| | 48H ONLY | | | | | |
| | | chr22:43088126- | | | | |
| XLOC 019550 | A4GALT | 43116876 | -1.78 | 0.61 | 2.39 | 0.000169 |
| | | chr21:43619798- | | | | |
| XLOC_018661 | ABCG1 | 43719917 | 3.01 | 0 | -3.01 | 0.000169 |
| | | chr20:62491519- | | | | |
| XLOC_018096 | ABHD16B | 62494341 | -1.8 | 1.87 | 3.67 | 0.000169 |
| | | chr10:72432558- | | | | |
| XLOC_003471 | ADAMTS14 | 72522195 | -2.63 | 0.37 | 2.99 | 0.000169 |
| | | chr11:10326641- | | | | |
| XLOC_004581 | ADM | 10328923 | 2.48 | 5.7 | 3.22 | 0.000169 |
| | | chr1:159032274- | | | | |
| XLOC_002682 | AIM2 | 159046647 | 0.08 | 3.17 | 3.08 | 0.000169 |
| | | chr1:77747661- | | | | |
| XLOC_000613 | AK5 | 78025654 | 1.31 | -1.05 | -2.37 | 0.000169 |
| | | chr4:186317839- | | | | |
| XLOC_021853 | ANKRD37 | 186347139 | -0.24 | 2 | 2.24 | 0.009826 |
| | | chr7:4815261- | | | | |
| XLOC_026508 | AP5Z1 | 4834083 | 1.46 | 3.47 | 2.02 | 0.000169 |
| | | chr22:39473009- | | | | |
| XLOC_019178 | APOBEC3G | 39483748 | 3.78 | 1.16 | -2.62 | 0.000169 |
| | | chr22:36649116- | 0.54 | 4.70 | | |
| XLOC_019138 | APOL1 | 36663577 | -0.61 | 1.79 | 2.41 | 0.000169 |
| VI OC 010467 | 40013 | chr22:36622254- | 2.04 | 4.00 | 2.04 | 0.0001.00 |
| XLOC_019467 | APOL2 | 36636000 | 2.84 | 4.88 | 2.04 | 0.000169 |
| VI.O.C. 01.2.C.4 | ADID2A | chr19:926036- | 1.0 | 0.50 | 2.16 | 0.0001.00 |
| XLOC_013664 | ARID3A | 972803 chr10:28101096- | -1.6 | 0.56 | 2.16 | 0.000169 |
| XLOC 003937 | ARMC4 | 28287977 | 1.91 | -0.68 | -2.59 | 0.000169 |
| XLUC_003937 | ANIVIC4 | chr7:97481428- | 1.91 | -0.08 | -2.59 | 0.000109 |
| XLOC 027696 | ASNS | 97501854 | 8.19 | 5.66 | -2.53 | 0.000169 |
| XLOC_027030 | 73113 | chr1:212738675- | 0.13 | 3.00 | 2.55 | 0.000103 |
| XLOC 001413 | ATF3 | 212794119 | 4.97 | 7.26 | 2.28 | 0.000169 |
| XLOC_001413 | Allo | chr15:35663169- | 4.57 | 7.20 | 2.20 | 0.000103 |
| XLOC 009507 | ATPBD4-AS1 | 36151202 | 1 | -1.6 | -2.6 | 0.030593 |
| | 554 7.51 | chr1:220321609- | | 1.0 | 2.0 | 3.00000 |
| XLOC 003013 | AURKAPS1 | 220445843 | -0.05 | 2.03 | 2.08 | 0.028053 |
| | | chr19:47724078- | 0.00 | | 2.50 | |
| XLOC 015391 | BBC3 | 47736023 | -0.8 | 1.26 | 2.07 | 0.000169 |
| | | chr2:60678301- | | | | |
| XLOC 016950 | BCL11A | 60780633 | -0.24 | -2.39 | -2.14 | 0.000169 |

| | C15orf48, | chr15:45722726- | | | | |
|-------------------|-----------|------------------|-------|-------|--------|-----------|
| XLOC_009595 | MIR147B | 45725647 | 2.73 | 5.29 | 2.56 | 0.000169 |
| | | chr19:3474404- | | | | |
| XLOC_014764 | C19orf77 | 3480540 | -0.04 | 2.24 | 2.28 | 0.000169 |
| | | chr4:2043719- | | | | |
| XLOC_021324 | C4orf48 | 2045697 | 0.9 | 3.45 | 2.55 | 0.000169 |
| | _ | chr5:179224597- | | | | |
| XLOC_023834 | C5orf45 | 179285840 | 4.56 | 6.71 | 2.15 | 0.00346 |
| | _ | chr9:112961845- | | | | |
| XLOC_030215 | C9orf152 | 112970413 | 1.69 | -0.93 | -2.61 | 0.000169 |
| | | chr11:104912052- | | | | |
| XLOC_006066 | CARD16 | 104916051 | -0.99 | 1.33 | 2.32 | 0.003217 |
| | | chr1:10696665- | | | | |
| XLOC_001761 | CASZ1 | 10856733 | -0.97 | 1.05 | 2.02 | 0.000169 |
| | | chr18:66382490- | | | | |
| XLOC_013387 | CCDC102B | 66722426 | 1.7 | -0.41 | -2.1 | 0.000169 |
| | | chr16:3077867- | | | | |
| XLOC_011009 | CCDC64B | 3089133 | -2.36 | -0.29 | 2.07 | 0.008211 |
| | | chr11:65657543- | | | | |
| XLOC_004947 | CCDC85B | 65659106 | 2.61 | 4.93 | 2.32 | 0.000169 |
| | | chr11:65657543- | | | | |
| XLOC_005844 | CCDC85B | 65659106 | 5.45 | 7.6 | 2.15 | 0.000169 |
| | | chr7:75398841- | | | | |
| XLOC_027612 | CCL26 | 75419064 | 3.28 | 5.83 | 2.55 | 0.000169 |
| | | chr17:34198495- | | | | |
| XLOC_012608 | CCL5 | 34207377 | -0.12 | 2.04 | 2.16 | 0.000169 |
| | | chr17:38710021- | | | 2.54 | |
| XLOC_012664 | CCR7 | 38721736 | -0.4 | -3.03 | -2.64 | 0.004627 |
| VII 0.0 00.04.0.4 | 6000 | chr11:118209788- | 0.54 | 10 | 40.54 | 0.00470 |
| XLOC_006134 | CD3D | 118213459 | 0.54 | -10 | -10.54 | 0.03472 |
| VI 00 000760 | CDE2 | chr1:111413820- | 0.20 | 2.6 | 2.24 | 0.044605 |
| XLOC_000769 | CD53 | 111442558 | -0.29 | -2.6 | -2.31 | 0.011685 |
| VI OC 01 4026 | CD70 | chr19:6585849- | 1.61 | 2.65 | 2.04 | 0.0001.00 |
| XLOC_014826 | CD70 | 6591163 | 1.61 | 3.65 | 2.04 | 0.000169 |
| VI 06 022600 | CD 7.4 | chr5:149781199- | 4.65 | 0.55 | 2.2 | 0.0004.60 |
| XLOC_023690 | CD74 | 149792499 | 1.65 | -0.55 | -2.2 | 0.000169 |
| VI OC 03C001 | CDK14 | chr7:90338711- | 2.40 | 1 40 | 2 | 0.0001.00 |
| XLOC_026881 | CDK14 | 90839904 | 3.49 | 1.49 | -2 | 0.000169 |
| VI OC 024100 | CED | chr6:31913720- | 1.00 | 1 20 | 2.20 | 0.0001.00 |
| XLOC_024108 | CFB | 31919861 | -1.09 | 1.29 | 2.38 | 0.000169 |
| VI OC 000330 | CLICA | chr1:25071759- | 7.64 | | 2.00 | 0.0001.00 |
| XLOC_000239 | CLIC4 | 25170815 | 7.64 | 5.55 | -2.09 | 0.000169 |
| VI.OC 0010E0 | COL16 4 1 | chr1:32117847- | 1 44 | 0.50 | 2.02 | 0.0001.00 |
| XLOC_001950 | COL16A1 | 32169768 | -1.44 | 0.59 | 2.03 | 0.000169 |
| VI.O.C. 00.C000 | CDVAD | chr11:111779349- | 0.53 | 2 02 | 2.20 | 0.0001.00 |
| XLOC_006098 | CRYAB | 111782473 | 0.53 | 2.82 | 2.28 | 0.000169 |
| VI.O.C. 000750 | CCE1 | chr1:110453232- | 0.00 | 2.46 | 2.50 | 0.0004.00 |
| XLOC_000758 | CSF1 | 110473616 | 0.88 | 3.46 | 2.58 | 0.000169 |
| VIOC 011042 | CCES | chr17:38171613- | 2.2 | 0.01 | 2 24 | 0.001042 |
| XLOC_011842 | CSF3 | 38174066 | -2.3 | 0.01 | 2.31 | 0.001842 |

| | | 1 4 450500654 | | | | |
|----------------|------------|------------------|-------|-------|-------|-----------|
| VI 00 003540 | CTCC | chr1:150702671- | 0.76 | 4 20 | 2.04 | 0.0004.00 |
| XLOC_002510 | CTSS | 150738433 | -0.76 | 1.28 | 2.04 | 0.000169 |
| VI 00 022400 | CVCL40 | chr4:76932332- | 4.2 | 1.46 | 2.66 | 0.002252 |
| XLOC_022100 | CXCL10 | 77033955 | -1.2 | 1.46 | 2.66 | 0.002352 |
| VI 00 022404 | CVCL44 | chr4:76932332- | 0.0 | 2.20 | 2.20 | 0.0004.60 |
| XLOC_022101 | CXCL11 | 77033955 | -0.9 | 2.39 | 3.28 | 0.000169 |
| VI OC 04 4776 | D A DIV2 | chr19:3958451- | 2.64 | 4.04 | 2.20 | 0.0004.60 |
| XLOC_014776 | DAPK3 | 3969826 | 2.64 | 4.94 | 2.29 | 0.000169 |
| VI OC 046644 | DANAM | chr2:228736326- | 0.24 | 2.00 | 2.20 | 0.0004.60 |
| XLOC_016644 | DAW1 | 228789026 | -0.21 | 2.08 | 2.28 | 0.000169 |
| VI 00 022200 | DAACDU | chr5:78293428- | 0.70 | 4.52 | 2.2 | 0.0004.60 |
| XLOC_023399 | DMGDH | 78365449 | 0.78 | -1.53 | -2.3 | 0.000169 |
| VI OC 047335 | DDD4 | chr2:162848754- | 4.52 | 2.46 | 2.00 | 0.0004.60 |
| XLOC_017335 | DPP4 | 162931052 | 4.52 | 2.46 | -2.06 | 0.000169 |
| VII 0.0 000000 | D D) (C) 4 | chr10:134000413- | 0.00 | 2 | 2.02 | 0.0004.60 |
| XLOC_003800 | DPYSL4 | 134019280 | 0.98 | 3 | 2.02 | 0.000169 |
| VI OC 043543 | DCC2 | chr18:28570051- | 2.46 | 4.00 | 2.00 | 0.0004.60 |
| XLOC_013512 | DSC3 | 28622781 | 3.16 | 1.08 | -2.08 | 0.000169 |
| VII 00 000100 | 50143 | chr9:95059639- | 0.10 | 2 77 | 2.05 | 0.040070 |
| XLOC_030128 | ECM2 | 95432547 | 0.19 | -3.77 | -3.95 | 0.043878 |
| VI 00 046040 | 50 AU 1014 | chr2:27301434- | 2.04 | 4.04 | 2.00 | 0.04.4400 |
| XLOC_016842 | EMILIN1 | 27309265 | -2.04 | 1.04 | 3.08 | 0.014403 |
| VII 00 00 4466 | END04 | chr6:132129155- | 4.40 | 0.60 | 2.02 | 0.0004.60 |
| XLOC_024466 | ENPP1 | 132216295 | 1.42 | -0.62 | -2.03 | 0.000169 |
| VII 00 011202 | 54011 | chr16:74746855- | 4.00 | | 2.50 | 0.0004.60 |
| XLOC_011393 | FA2H | 74808729 | 1.88 | 4.44 | 2.56 | 0.000169 |
| VII 00 0000F0 | 541840 | chr1:207070787- | 2.24 | 4.67 | 2.46 | 0.0004.60 |
| XLOC_002953 | FAIM3 | 207095378 | 2.21 | 4.67 | 2.46 | 0.000169 |
| VI OC 020252 | EAR4440D | chr8:58907112- | 4.26 | 4.02 | 2.27 | 0.0004.60 |
| XLOC_028252 | FAM110B | 59062277 | -1.26 | 1.02 | 2.27 | 0.000169 |
| VI OC 000E10 | FL 133447 | chr14:62037257- | 1.50 | 0.60 | 2.24 | 0.0001.00 |
| XLOC_008518 | FLJ22447 | 62121431 | 1.56 | -0.68 | -2.24 | 0.000169 |
| VI OC 016100 | F1.1422F4 | chr2:113399406- | 0.74 | 1 45 | 2.10 | 0.000634 |
| XLOC_016199 | FLJ42351 | 113402991 | 0.74 | -1.45 | -2.19 | 0.000621 |
| VI 06 003000 | FOVE | chr1:47900389- | 4.64 | 0.07 | 2.54 | 0.000534 |
| XLOC_002099 | FOXD2 | 47906363 | -1.64 | 0.87 | 2.51 | 0.008531 |
| VI OC 003000 | FOVD3 AC1 | chr1:47897806- | 0.46 | 1.04 | 2.4 | 0.0001.00 |
| XLOC_002098 | FOXD2-AS1 | 47900313 | -0.46 | 1.94 | 2.4 | 0.000169 |
| VI OC 000453 | EDNADC ACO | chr14:51921229- | 2.04 | | 2.50 | 0.006340 |
| XLOC_008453 | FRMD6-AS2 | 52197444 | 2.91 | 5.5 | 2.59 | 0.006248 |
| VI 00 000450 | EDNADC ACO | chr14:51921229- | 4.44 | 2.00 | 2.55 | 0.000634 |
| XLOC_008459 | FRMD6-AS2 | 52197444 | 1.44 | 3.99 | 2.55 | 0.000621 |
| VI OC 200455 | EDMARC ACC | chr14:51921229- | 2 75 | F 2.4 | 2.50 | 0.0001.00 |
| XLOC_008460 | FRMD6-AS2 | 52197444 | 2.75 | 5.34 | 2.59 | 0.000169 |
| VI 00 013013 | ECTL 2 | chr19:676388- | 2 27 | 4.00 | 2.42 | 0.0004.60 |
| XLOC_013648 | FSTL3 | 683392 | 2.87 | 4.99 | 2.12 | 0.000169 |
| VI 00 000015 | 570.4 | chr11:86656716- | | 2.25 | 2 = 2 | 0.0004.55 |
| XLOC_006016 | FZD4 | 86666440 | 4.54 | 2.01 | -2.53 | 0.000169 |
| VI 00 000015 | CARROL | chr4:46037786- | | 2.22 | 2 = 1 | 0.0001.00 |
| XLOC_022011 | GABRG1 | 46126082 | -0.2 | -3.93 | -3.74 | 0.000169 |

| VI OC 022018 | CARRCA | chr5:161494647- | 0.16 | 2.70 | 2.62 | 0.0001.00 |
|----------------|-----------|------------------|-------|-------|-------|-----------|
| XLOC_023018 | GABRG2 | 161582545 | -0.16 | -2.78 | -2.62 | 0.000169 |
| VI OC 000470 | CARRCA | chr15:27216428- | 2.24 | 0.15 | 2.00 | 0.0001.00 |
| XLOC_009478 | GABRG3 | 27779176 | 2.24 | 0.15 | -2.09 | 0.000169 |
| VI OC 0022C2 | CDD1 | chr1:89517986- | 2.22 | 4.01 | 2.50 | 0.0001.00 |
| XLOC_002263 | GBP1 | 89531043 | 2.23 | 4.81 | 2.58 | 0.000169 |
| VI.OC 000C40 | CDD1D1 | chr1:89873148- | 0.64 | 1 70 | 2.42 | 0.0001.00 |
| XLOC_000649 | GBP1P1 | 89890493 | -0.64 | 1.78 | 2.42 | 0.000169 |
| XLOC 020079 | CCCANA | chr3:111838228- | 0.60 | 2.04 | 2.26 | 0.0001.00 |
| XLUC_020079 | GCSAM | 111854678 | 0.68 | 2.94 | 2.26 | 0.000169 |
| VI OC 020020 | CENA | chr8:95261484- | 2.04 | E E 4 | 2.7 | 0.0001.00 |
| XLOC_029030 | GEM | 95274547 | 2.84 | 5.54 | 2.7 | 0.000169 |
| VI 00 002450 | CLAF | chr1:147228331- | 0.04 | 2.00 | 2.04 | 0.000335 |
| XLOC_002458 | GJA5 | 147245484 | -0.04 | -3.08 | -3.04 | 0.000325 |
| VI 06 046002 | CKNIS | chr2:69172363- | 0.02 | 2.07 | 2.02 | 0.0004.60 |
| XLOC_016993 | GKN2 | 69180102 | 0.03 | 2.07 | 2.03 | 0.000169 |
| VI OC 020000 | CNIAAA | chr9:80037994- | 0.42 | 2 24 | 2.00 | 0.000007 |
| XLOC_030080 | GNA14 | 80263232 | -0.42 | -3.31 | -2.89 | 0.003935 |
| VI OC 046720 | CDD25 | chr2:241544824- | 4.7 | 0.53 | 2.22 | 0.0004.00 |
| XLOC_016720 | GPR35 | 241570676 | -1.7 | 0.53 | 2.23 | 0.000169 |
| VI OC 01070C | 11463 | chr16:69139466- | 6.26 | 4.01 | 2.24 | 0.0001.00 |
| XLOC_010786 | HAS3 | 69166493 | 6.26 | 4.01 | -2.24 | 0.000169 |
| VI OC 0200E0 | LIEVA | chr8:80676244- | F 4F | 2.45 | 2.7 | 0.0001.00 |
| XLOC_028958 | HEY1 | 80680098 | 5.15 | 2.45 | -2.7 | 0.000169 |
| VI 00 002456 | LIKD C4 | chr10:70980058- | 4.02 | 4 44 | 2.42 | 0.0004.60 |
| XLOC_003456 | HKDC1 | 71027315 | -1.02 | 1.41 | 2.43 | 0.000169 |
| VI OC 024110 | III A DDA | chr6:32407618- | 2.00 | 0.61 | 2.7 | 0.0001.00 |
| XLOC_024119 | HLA-DRA | 32412826 | 2.09 | -0.61 | -2.7 | 0.000169 |
| VI 06 024020 | | chr6:29690988- | 2.44 | 4.62 | 2.40 | 0.0004.60 |
| XLOC_024038 | HLA-F | 29716826 | 2.44 | 4.63 | 2.19 | 0.000169 |
| VI OC 001440 | 11117 | chr1:221052742- | 0.17 | 2.22 | 2.00 | 0.0001.00 |
| XLOC_001449 | HLX | 221058400 | 0.17 | 2.23 | 2.06 | 0.000169 |
| VI.O.C. 005773 | LIDACICO | chr11:63014620- | 1 11 | 2.00 | 2.57 | 0.0001.00 |
| XLOC_005772 | HRASLS2 | 63330855 | 1.41 | 3.99 | 2.57 | 0.000169 |
| VI OC 040750 | 11004402 | chr16:67465035- | 4.27 | 4.02 | 2.4 | 0.0004.60 |
| XLOC_010758 | HSD11B2 | 67471454 | -1.37 | 1.03 | 2.4 | 0.000169 |
| VI OC 026047 | LICDD4 | chr7:75931874- | 6.20 | 0.20 | 2.01 | 0.0001.00 |
| XLOC_026847 | HSPB1 | 75933614 | 6.28 | 8.29 | 2.01 | 0.000169 |
| VI OC 000074 | HCDDO | chr12:119616594- | 4.40 | 4 47 | 2.05 | 0.0004.60 |
| XLOC_006871 | HSPB8 | 119632551 | -1.48 | 1.47 | 2.95 | 0.000169 |
| VI OC 04 4343 | 10514 | chr19:46720994- | 2.2 | 4 20 | 2.50 | 0.026050 |
| XLOC_014312 | IGFL1 | 46846690 | -2.2 | 1.38 | 3.58 | 0.036058 |
| VI 00 000570 | | chr7:22766765- | 2.7 | 7.76 | 4.00 | 0.0004.60 |
| XLOC_026572 | IL6 | 22771621 | 3.7 | 7.76 | 4.06 | 0.000169 |
| VI 00 000010 | 15.64.5 | chr1:948846- | 0.47 | 40.00 | 2.40 | 0.0004.00 |
| XLOC_000018 | ISG15 | 949919 | 8.47 | 10.96 | 2.49 | 0.000169 |
| VI 00 000451 | | chr1:59246462- | 2.54 | - 67 | 2.46 | 0.0004.00 |
| XLOC_002151 | JUN | 59249785 | 3.51 | 5.67 | 2.16 | 0.000169 |
| VI OC 04300C | ILIND | chr19:12902309- | 2 22 | E 0.4 | 2.52 | 0.0001.00 |
| XLOC_013896 | JUNB | 12904125 | 3.32 | 5.84 | 2.52 | 0.000169 |

| | | 1 0 0 0 0 0 4 4 0 4 4 | | | | <u> </u> |
|--------------|--------------|-----------------------------|-------|-------|-------|-----------|
| VI OC 020100 | I/CNII.14 | chr8:36641841- | 0.04 | 2.67 | 2.54 | 0.0001.00 |
| XLOC_028180 | KCNU1 | 36793974 | 0.84 | -2.67 | -3.51 | 0.000169 |
| XLOC 029434 | KGFLP1 | chr9:46687556- 46746820 | 0.89 | 2 12 | 2.02 | 0.000160 |
| XLUC_029434 | KGFLFI | chr15:81071711- | 0.89 | -2.13 | -3.02 | 0.000169 |
| XLOC 009771 | KIAA1199 | 81243999 | 0.24 | -2.31 | -2.54 | 0.000169 |
| XLOC_003771 | KIAA1199 | chr1:6650783- | 0.24 | -2.31 | -2.34 | 0.000109 |
| XLOC 001742 | KLHL21 | 6662929 | 4.06 | 6.09 | 2.04 | 0.000169 |
| X200_001742 | KLITEZI | chrX:86772714- | 4.00 | 0.03 | 2.01 | 0.000103 |
| XLOC 030775 | KLHL4 | 86925050 | 2.98 | 0.6 | -2.38 | 0.000169 |
| | | chr7:98771196- | | | | 0.0000 |
| XLOC 027704 | KPNA7 | 98805089 | -1.12 | 0.93 | 2.05 | 0.000169 |
| _ | | chr17:39775691- | | | | |
| XLOC_012717 | KRT17 | 39780882 | -1.04 | 2.39 | 3.43 | 0.000169 |
| | | chr12:52840434- | | | | |
| XLOC_006537 | KRT6B | 52845910 | -0.13 | -3.25 | -3.12 | 0.028513 |
| | | chr1:31205314- | | | | |
| XLOC_001937 | LAPTM5 | 31230683 | 0.98 | -1.28 | -2.26 | 0.000169 |
| | | chr17:25958173- | | | | |
| XLOC_011715 | LGALS9 | 25976586 | -0.46 | 1.54 | 2.01 | 0.000169 |
| | | chr6:133409218- | | | | |
| XLOC_024475 | LINC00326 | 133427717 | -0.02 | -2.55 | -2.53 | 0.017108 |
| VI OC 042404 | 1111000402 | chr17:79276623- | 2.6 | 0.45 | 2.45 | 0.000474 |
| XLOC_013101 | LINC00482 | 79283048 | -2.6 | -0.45 | 2.15 | 0.000474 |
| XLOC 009076 | LINC00520 | chr14:56247852- 56263392 | 1.14 | 3.93 | 2.8 | 0.000169 |
| XLOC_009076 | LINCOUSZU | chr18:36786887- | 1.14 | 5.95 | 2.0 | 0.000109 |
| XLOC 013538 | LINC00669 | 37331959 | 1.58 | -1.16 | -2.74 | 0.000169 |
| X200_013330 | Liiveoooos | chr1:3816967- | 1.50 | 1.10 | 2.,7 | 0.000103 |
| XLOC 000070 | LOC100133612 | 3833913 | -1.29 | 1.06 | 2.35 | 0.000169 |
| | | chr2:33050509- | | | | 0.0000 |
| XLOC_015856 | LOC100271832 | 33171202 | -10 | -0.23 | 9.77 | 0.033882 |
| | | chr10:105353783- | | | | |
| XLOC_003696 | LOC100505839 | 105615164 | 0.17 | -2.81 | -2.98 | 0.028336 |
| | | chr7:22602955- | | | | |
| XLOC_026571 | LOC100506178 | 22613617 | -1.79 | 0.31 | 2.1 | 0.000169 |
| | | chr3:156799455- | | | | |
| XLOC_021115 | LOC339894 | 156840791 | -1.9 | 0.28 | 2.18 | 0.000903 |
| | | chr11:9776316- | | | | |
| XLOC_005516 | LOC440028 | 10315754 | -0.92 | 1.33 | 2.24 | 0.036312 |
| VI OC 045334 | I DENIA | chr19:39797456- | 1.65 | 0.45 | 2.4 | 0.0001.00 |
| XLOC_015234 | LRFN1 | 39805976 | -1.65 | 0.45 | 2.1 | 0.000169 |
| XLOC 004973 | LRFN4 | chr11:66615996- 66725847 | 2.29 | 4.5 | 2.21 | 0.000160 |
| 7100_004973 | LINI IN4 | chr10:94178417- | 2.23 | 4.5 | 2.21 | 0.000169 |
| XLOC 003593 | MARK2P9 | 94179363 | -2.5 | -0.2 | 2.3 | 0.047518 |
| | | chr17:81037566- | 2.3 | 0.2 | 2.3 | 5.547510 |
| XLOC 012301 | METRNL | 81052591 | -0.87 | 1.24 | 2.11 | 0.000169 |
| | MGC16121, | chrX:133677207- | | | | |
| XLOC_031527 | MIR424 | 133680741 | 3.7 | 1.42 | -2.29 | 0.000169 |
| | • | | | I | | • |

| | NAID43EC | ab av. 102120054 | | | | |
|---------------|----------|------------------|-------|-------|-------|-----------|
| VI OC 021420 | MIR1256, | chrX:103139054- | 0.4 | 0.27 | 0.77 | 0.0001.00 |
| XLOC_031420 | SLC25A53 | 103401708 | 9.4 | -0.37 | -9.77 | 0.000169 |
| | MIR205, | chr1:209602167- | | 0.45 | 0.50 | 0.004.00 |
| XLOC_001390 | MIR205HG | 209605973 | 3.08 | 0.45 | -2.63 | 0.000169 |
| | | chr11:565656- | | | | |
| XLOC_005377 | MIR210HG | 568457 | 1.22 | 3.32 | 2.1 | 0.000169 |
| | | chr1:1103530- | | | | |
| XLOC_000028 | MIR429 | 1105715 | -0.42 | 1.83 | 2.25 | 0.000169 |
| | | chr10:27961802- | | | | |
| XLOC_003936 | MKX | 28034778 | 2.85 | 0.71 | -2.14 | 0.000169 |
| | | chr11:102654406- | | | | |
| XLOC_006056 | MMP3 | 102714342 | -2.75 | 1.23 | 3.98 | 0.032948 |
| | | chr16:56716381- | | | | |
| XLOC_010705 | MT1X | 56718108 | 6.09 | 8.21 | 2.12 | 0.000169 |
| | | chr8:125563027- | | | | |
| XLOC_028508 | MTSS1 | 125740730 | -0.6 | 1.79 | 2.39 | 0.01654 |
| | | chr7:100612903- | | | | |
| XLOC_026957 | MUC12 | 100662230 | -4.48 | -0.14 | 4.34 | 0.007683 |
| | | chr12:44902057- | | | | |
| XLOC_007207 | NELL2 | 45307711 | 0.27 | -2.02 | -2.29 | 0.000169 |
| _ | | chr14:35870715- | | | | |
| XLOC 008975 | NFKBIA | 35873960 | 5.52 | 7.66 | 2.13 | 0.000169 |
| _ | | chr11:65554504- | | | | |
| XLOC 004943 | OVOL1 | 65564690 | -1.75 | 1.02 | 2.77 | 0.000169 |
| _ | | chr13:25670275- | | | | |
| XLOC 007764 | PABPC3 | 25672704 | 1.46 | -0.81 | -2.27 | 0.000169 |
| | | chr22:50609159- | | 0.00 | | 0.00000 |
| XLOC 019273 | PANX2 | 50618724 | -1.54 | 0.66 | 2.21 | 0.000169 |
| 7.10 0_010170 | . , , | chr1:176432306- | | 0.00 | | 0.000 |
| XLOC 001209 | PAPPA2 | 176814727 | 0.39 | -2.01 | -2.4 | 0.000169 |
| X200_001203 | 17111712 | chr14:24563482- | 0.03 | 2.01 | | 0.000103 |
| XLOC 008348 | PCK2 | 24573339 | 5.54 | 3.01 | -2.53 | 0.000169 |
| X200_0000 10 | T CKL | chr17:62396776- | 3.3 . | 3.01 | 2.33 | 0.000103 |
| XLOC_012974 | PECAM1 | 62407083 | 0.51 | -1.75 | -2.26 | 0.000169 |
| XLOC_012374 | TECAIVIT | chrX:22050920- | 0.51 | 1.73 | 2.20 | 0.000103 |
| XLOC 030536 | PHEX | 22269420 | -0.04 | -2.17 | -2.13 | 0.000169 |
| XLOC_030330 | FIILX | chr1:120254418- | -0.04 | -2.17 | -2.13 | 0.000103 |
| XLOC 000849 | PHGDH | 120286849 | 7.65 | 5.51 | -2.14 | 0.000169 |
| XLOC_000849 | FIIGDII | chr1:201433345- | 7.03 | 3.31 | -2.14 | 0.000103 |
| XLOC 002878 | PHLDA3 | 201438510 | 4.79 | 6.79 | 2.01 | 0.000169 |
| XLUC_002878 | PHLDAS | | 4.79 | 0.79 | 2.01 | 0.000109 |
| VI OC 015402 | PLA2G4C | chr19:48551099- | 0.51 | 1 67 | 2.18 | 0.000160 |
| XLOC_015402 | PLAZG4C | 48614109 | -0.51 | 1.67 | 2.10 | 0.000169 |
| VIOC 017750 | DI CD1 | chr20:8113295- | 0.05 | 1.00 | 2.02 | 0.0001.00 |
| XLOC_017758 | PLCB1 | 8865547 | 0.95 | -1.08 | -2.03 | 0.000169 |
| VI OC 045434 | DIEKLAA | chr19:49340353- | | 4.6 | _ | 0.0004.00 |
| XLOC_015421 | PLEKHA4 | 49371884 | -0.41 | 1.6 | 2 | 0.000169 |
| W 00 00==== | D1 46:: | chr12:102513955- | | | | 0.0005== |
| XLOC_007525 | PMCH | 102591614 | 2.49 | 0.41 | -2.08 | 0.002352 |
| | | chr1:203020310- | | | | 0.000:00 |
| XLOC_001335 | PPFIA4 | 203047864 | -1.71 | 0.85 | 2.55 | 0.000169 |

| | | 1 10 01107010 | | | | |
|---------------|----------|-----------------------------|-------|-------|-------|-----------|
| XLOC 003525 | PPIF | chr10:81107219- 81115089 | 7.45 | 9.56 | 2.11 | 0.000169 |
| XLUC_003323 | PPIF | chr17:37783176- | 7.45 | 9.50 | 2.11 | 0.000109 |
| XLOC 011831 | PPP1R1B | 37792878 | 0.45 | -3.12 | -3.57 | 0.00223 |
| VFOC_011921 | PALTITIE | chr6:106534194- | 0.43 | -3.12 | -3.37 | 0.00223 |
| XLOC 024375 | PRDM1 | 106557814 | -2.25 | 0.31 | 2.56 | 0.000169 |
| XLUC_024373 | PRDIVIT | | -2.25 | 0.31 | 2.50 | 0.000169 |
| XLOC 007201 | PRICKLE1 | chr12:42850967- 42983572 | 4.12 | 1.97 | -2.15 | 0.000169 |
| XLOC_007201 | PRICKLET | | 4.12 | 1.57 | -2.13 | 0.000109 |
| XLOC 022117 | DDVC3 | chr4:82009155- | 0.13 | 2 11 | 2 22 | 0.000160 |
| XLUC_022117 | PRKG2 | 82126215 | 0.12 | -2.11 | -2.23 | 0.000169 |
| VI.OC 009607 | DDOV2 | chr14:75319735- | 1 24 | 1 26 | 2.7 | 0.00725 |
| XLOC_008607 | PROX2 | 75330537 | 1.34 | -1.36 | -2.7 | 0.00735 |
| VI OC 024225 | DDCC2F | chr6:84222193- | 2.1 | 0.47 | 2.50 | 0.0001.00 |
| XLOC_024335 | PRSS35 | 84235421 | 2.1 | -0.47 | -2.58 | 0.000169 |
| VI OC 020472 | DC AT1 | chr9:80912058- | 7.66 | F 24 | 2.45 | 0.0001.00 |
| XLOC_029472 | PSAT1 | 80945009 | 7.66 | 5.21 | -2.45 | 0.000169 |
| VI OC 000C27 | DTCED | chr1:78956727- | 2.65 | 1 20 | 2.20 | 0.0001.00 |
| XLOC_000627 | PTGFR | 79006386 | 3.65 | 1.29 | -2.36 | 0.000169 |
| VI OC 001300 | DTDDC | chr1:198608097- | 0.43 | 2.55 | 2.12 | 0.0001.00 |
| XLOC_001288 | PTPRC | 198726605 | -0.43 | -2.55 | -2.12 | 0.000169 |
| VI OC 031660 | DADZOD | chrX:154487525- | 0.40 | 4 75 | 2.24 | 0.0001.00 |
| XLOC_031669 | RAB39B | 154493852 | 0.49 | -1.75 | -2.24 | 0.000169 |
| VI 06 002400 | DEC 4 | chr1:120336640- | 4 20 | 0.77 | 2.46 | 0.0004.60 |
| XLOC_002408 | REG4 | 120354203 | 1.39 | -0.77 | -2.16 | 0.000169 |
| VI 06 04 4204 | DELD | chr19:45504706- | 2.02 | 4.04 | 2.04 | 0.0004.60 |
| XLOC_014291 | RELB | 45541456 | 2.03 | 4.04 | 2.01 | 0.000169 |
| VI OC 027770 | DELM | chr7:103112230- | 2.02 | 1 20 | 2.44 | 0.0001.00 |
| XLOC_027770 | RELN | 103629963 | 2.02 | -1.39 | -3.41 | 0.000169 |
| VI 06 005040 | DELT | chr11:73087404- | 0.60 | 2.50 | 2.00 | 0.0004.60 |
| XLOC_005048 | RELT | 73108519 | 0.69 | 3.58 | 2.89 | 0.000169 |
| VI OC 015770 | DUOD | chr2:20646834- | 2.27 | 4.4 | 2.02 | 0.0001.00 |
| XLOC_015779 | RHOB | 20649201 | 2.37 | 4.4 | 2.03 | 0.000169 |
| VI 06 040763 | DITOD | chr16:67679029- | 4.25 | 4 72 | 2.00 | 0.0004.60 |
| XLOC_010763 | RLTPR | 67694718 | -1.35 | 1.72 | 3.06 | 0.000169 |
| VI 06 022042 | DNE402 | chr6:13924676- | F 60 | 2.64 | 2.04 | 0.0004.60 |
| XLOC_023912 | RNF182 | 13980240 | 5.68 | 3.64 | -2.04 | 0.000169 |
| VI OC 000503 | DDECE | chr1:68894506- | F 16 | 2.02 | 2.22 | 0.0001.00 |
| XLOC_000583 | RPE65 | 68917732 | 5.16 | 2.93 | -2.23 | 0.000169 |
| VI 06 040306 | DDD35 | chr15:75247442- | 4.2 | 2.54 | 2.24 | 0.0004.60 |
| XLOC_010206 | RPP25 | 75249775 | 1.2 | 3.51 | 2.31 | 0.000169 |
| VI OC 000075 | DDD114 | chr14:20811229- | 4 44 | F 63 | 4 22 | 0.0004.00 |
| XLOC_008875 | RPPH1 | 20811570 | 1.41 | 5.63 | 4.22 | 0.000169 |
| VII 00 040000 | DTNIAD | chr22:20228937- | 0.00 | 2.24 | 2.47 | 0.0004.60 |
| XLOC_019326 | RTN4R | 20255816 | 0.08 | 2.24 | 2.17 | 0.000169 |
| VI 06 02025 | DTD 4 | chr3:187086167- | 0.55 | 4.00 | 2 | 0.0004.60 |
| XLOC_020389 | RTP4 | 187089369 | -0.66 | 1.92 | 2.57 | 0.000169 |
| VI 00 000707 | 664545 | chr8:27727398- | 0.00 | | 2 2= | 0.0004.55 |
| XLOC_028764 | SCARA5 | 27850369 | 0.98 | -1.1 | -2.07 | 0.000169 |
| VI OC 000400 | SCCE | chr15:32933869- | 0.00 | 2 27 | 2.20 | 0.0004.00 |
| XLOC_009499 | SCG5 | 32989298 | 0.98 | 3.37 | 2.39 | 0.000169 |

| | 1 | | | | | |
|-----------------|-----------|-----------------------------|-------|-------|-------|--------------|
| VI.O.C. 022.C72 | SCCD2A2 | chr5:147257048- | 1.1 | 1 17 | 2 27 | 0.0001.00 |
| XLOC_023673 | SCGB3A2 | 147261756 | 1.1 | -1.17 | -2.27 | 0.000169 |
| VI OC 002764 | CELL | chr1:169659805- | 0.00 | 2.1 | 2.01 | 0.000634 |
| XLOC_002764 | SELL | 169680843 | -0.08 | -2.1 | -2.01 | 0.000621 |
| VI OC 027642 | CENANDO | chr7:84624871- | 1.12 | 1.50 | 2.60 | 0.0001.00 |
| XLOC_027642 | SEMA3D | 84751247 | 1.13 | -1.56 | -2.69 | 0.000169 |
| VI OC 00030C | CEDDINIAA | chr14:94843083- | 2.25 | 0.22 | 2.02 | 0.0001.00 |
| XLOC_009286 | SERPINA1 | 94857029 | 2.25 | 0.22 | -2.03 | 0.000169 |
| VI OC 035335 | CCK1 | chr6:134490383- | 2.10 | 4 24 | 2.12 | 0.0001.00 |
| XLOC_025225 | SGK1 | 134639196 | 2.19 | 4.31 | 2.12 | 0.000169 |
| VI OC 021402 | CLUCAS | chr4:42399855- | F 02 | 2.20 | 2.62 | 0.0001.00 |
| XLOC_021483 | SHISA3 | 42404504 | 5.92 | 2.29 | -3.62 | 0.000169 |
| XLOC 005720 | SLC15A3 | chr11:60691912- | -0.14 | 2.20 | 2.51 | 0.0001.00 |
| XLUC_005720 | SLCISAS | 60719257 | -0.14 | 2.38 | 2.51 | 0.000169 |
| XLOC 016015 | SICAAE | chr2:74442995- 74570534 | 4.86 | 2.41 | 2.46 | 0.000169 |
| XFOC_019012 | SLC4A5 | | 4.80 | 2.41 | -2.46 | 0.000169 |
| XLOC 018005 | SNAI1 | chr20:48599512- 48605420 | -0.35 | 1.78 | 2.13 | 0.000169 |
| VFOC_019002 | SIVALL | chr9:139270025- | -0.55 | 1.78 | 2.13 | 0.000169 |
| XLOC 030397 | CNIADC4 | 139292889 | 0.17 | 2.49 | 2.33 | 0.000160 |
| XLUC_030397 | SNAPC4 | | 0.17 | 2.49 | 2.33 | 0.000169 |
| XLOC 010394 | CNIHCO | chr16:2014996- 2015505 | 4.29 | 6.5 | 2.21 | 0.000169 |
| XLUC_010394 | SNHG9 | | 4.29 | 0.5 | 2.21 | 0.000169 |
| XLOC 010375 | SOX8 | chr16:1031807- 1036979 | -2.23 | -0.14 | 2.09 | 0.000169 |
| XLOC_010373 | 3070 | chr5:151040656- | -2.23 | -0.14 | 2.09 | 0.000103 |
| XLOC 023708 | SPARC | 151066615 | 1.17 | -2.6 | -3.78 | 0.000169 |
| XLUC_023708 | SPARC | chr17:74380672- | 1.17 | -2.0 | -3.76 | 0.000109 |
| XLOC 012191 | SPHK1 | 74383941 | 2.48 | 5.21 | 2.73 | 0.000169 |
| XLOC_012191 | SFIIKI | chr5:147204142- | 2.40 | 5.21 | 2.73 | 0.000103 |
| XLOC 023672 | SPINK1 | 147211260 | 1.75 | 3.85 | 2.1 | 0.000169 |
| XLOC_023072 | JI IIVKI | chr5:147582356- | 1.75 | 3.03 | 2.1 | 0.000103 |
| XLOC 022936 | SPINK6 | 147594700 | -1.78 | 1 | 2.78 | 0.011481 |
| XLOC_022330 | 31 IIVIO | chr1:32256024- | 1.70 | | 2.70 | 0.011401 |
| XLOC 001953 | SPOCD1 | 32281580 | -0.2 | 2 | 2.2 | 0.000169 |
| XLOC_001333 | 31 0001 | chr16:1114081- | 0.2 | | 2.2 | 0.000103 |
| XLOC 010957 | SSTR5-AS1 | 1131454 | 2.84 | 0.77 | -2.07 | 0.000169 |
| XLOC_010337 | 331N3 A31 | chr8:23699433- | 2.04 | 0.77 | 2.07 | 0.000103 |
| XLOC 028745 | STC1 | 23712320 | 0.35 | 2.84 | 2.49 | 0.000169 |
| <u> </u> | 0.02 | chr5:146614578- | 0.55 | 2.0 . | 25 | 0.000103 |
| XLOC 022931 | STK32A | 146767405 | 3.63 | 1.33 | -2.3 | 0.000169 |
| <u> </u> | 01113271 | chr4:5053526- | 3.03 | 1.00 | | 0.000103 |
| XLOC_021344 | STK32B | 5502725 | 1.4 | -0.84 | -2.24 | 0.000169 |
| | | chr6:125229391- | | | | |
| XLOC 024440 | STL | 125285041 | -0.82 | 1.33 | 2.16 | 0.002971 |
| <u>-</u> | | chr6:144471653- | | , | | . |
| XLOC 024508 | STX11 | 144513076 | -2.08 | -0.03 | 2.05 | 0.000169 |
| _: :::0 | | chr20:46286149- | | 3.00 | | |
| XLOC 018433 | SULF2 | 46415360 | 6.26 | 4 | -2.26 | 0.000169 |
| | | chr7:48026745- | | | | |
| XLOC_027492 | SUN3 | 48068716 | -1.4 | 1.11 | 2.51 | 0.000169 |
| | 1 | 1 | 1 | | | |

| | | chr6:35085848- | | | | |
|-------------|---------|-----------------|-------|-------|-------|----------|
| XLOC_024900 | TCP11 | 35109187 | -0.24 | -3.58 | -3.34 | 0.000325 |
| | | chr19:362056- | | | | |
| XLOC_014703 | THEG | 376013 | -2.11 | 0.06 | 2.16 | 0.007464 |
| | | chr19:4815935- | | | | |
| XLOC_014793 | TICAM1 | 4831754 | 3.42 | 5.68 | 2.26 | 0.000169 |
| | | chr12:29653745- | | | | |
| XLOC_007171 | TMTC1 | 29937692 | 1.62 | -0.43 | -2.05 | 0.000169 |
| | | chr19:507496- | | | | |
| XLOC_013642 | TPGS1 | 519654 | -2.67 | 0.66 | 3.34 | 0.011386 |
| | | chr17:18625401- | | | | |
| XLOC_011686 | TRIM16L | 18639431 | 1.26 | 3.55 | 2.29 | 0.000169 |
| | | chr2:27505296- | | | | |
| XLOC_015813 | TRIM54 | 27531130 | -2.75 | 1.62 | 4.37 | 0.000169 |
| | | chr19:19625027- | | | | |
| XLOC_015082 | TSSK6 | 19626469 | -2.28 | -0.07 | 2.21 | 0.007894 |
| | | chr19:15939756- | | | | |
| XLOC_013948 | UCA1 | 15947131 | 1.57 | 4.83 | 3.26 | 0.000169 |
| | | chr16:4390251- | | | | |
| XLOC_010457 | VASN | 4466962 | -1.34 | 0.84 | 2.18 | 0.002352 |
| | | chr13:21872263- | | | | |
| XLOC_008026 | ZDHHC20 | 22033508 | 4.11 | 1.89 | -2.22 | 0.000169 |

Table 13: List of genes that expressed a fold-change at 24 h and 48 h, listed in order from the highest positive fold-change to highest negative fold-change.

| Test ID | Gene | Locus | log2 (Ratio) 24h | log2 Ratio 48h | q2-q1 | Gene fold change from 24h to 48h |
|-------------|-----------------|--------------------------|------------------------|----------------------|------------|---|
| XLOC_021907 | EGR1 | chr5:137801180-137805004 | 2.55 | 5.45 | 0.00045451 | 2.9 |
| XLOC_028723 | RMRP | chr9:35657747-35658015 | 2.05 | 4.34 | -0.0046599 | 2.29 |
| XLOC_021868 | CSF2 | chr5:131409484-131411863 | 2.2 | 4.02 | 0.00000309 | 1.82 |
| XLOC_023458 | TNFAIP3 | chr6:138144806-138204451 | 2.32 | 3.92 | 0.00000309 | 1.6 |
| XLOC_023095 | HSPA1A | chr6:31783290-31785719 | 2.58 | 4.12 | 0.00000309 | 1.54 |
| XLOC_007127 | PTPRR | chr12:71031852-71314584 | 2.12 | 3.63 | 0.00000309 | 1.51 |
| XLOC_023096 | HSPA1B | chr6:31795511-31798031 | 2.32 | 3.76 | 0.00000309 | 1.44 |
| XLOC_001092 | HSPA6 | chr1:161494035-161496687 | 3.9 | 5.27 | 0.00000309 | 1.37 |
| XLOC_008257 | FOS | chr14:75745480-75748937 | 2.12 | 3.48 | 0.00000309 | 1.36 |
| XLOC_010839 | RRAD | chr16:66955581-66959439 | 2.02 | 3.38 | -0.0001506 | 1.36 |
| XLOC_018101 | CLDN14 | chr21:37832584-37948867 | 2.34 | 3.61 | 0.00000309 | 1.27 |
| XLOC_001342 | IL24 | chr1:207070787-207095378 | 2.43 | 3.68 | 0.00000309 | 1.25 |
| XLOC_030246 | MAP7D3 | chrX:135295378-135338641 | -4.2 | -2.97 | 0.00000309 | 1.23 |
| XLOC_012292 | ARHGAP27 | chr17:43506717-43510282 | 2.33 | 3.54 | 0.00357035 | 1.21 |
| XLOC_001109 | RGS4 | chr1:163038395-163046592 | 2.97 | 4.16 | 0.00000309 | 1.19 |
| XLOC_020701 | IL8 | chr4:74606222-74609433 | 2.2 | 3.35 | 0.00000309 | 1.15 |
| XLOC_012151 | TOP2A | chr17:38544772-38574202 | -3.44 | -2.35 | 0.00000309 | 1.09 |
| XLOC_022779 | DUSP1 | chr5:172195092-172198203 | 3.15 | 4.21 | 0.00000309 | 1.06 |
| XLOC_019953 | FAM107A | chr3:58549844-58563491 | -3.61 | -2.57 | 0.00000309 | 1.04 |
| XLOC_018371 | HMOX1 | chr22:35777059-35790207 | 2.98 | 4.02 | 0.00000309 | 1.04 |
| XLOC_021903 | KIF20A | chr5:137475458-137549032 | -3.17 | -2.14 | 0.00015897 | 1.03 |
| XLOC_013241 | ANGPTL4 | chr19:8429010-8439257 | 2.97 | 3.99 | 0.00000309 | 1.02 |
| XLOC_010126 | SCNN1G | chr16:23194039-23228200 | -3.06 | -2.04 | 0.00000309 | 1.02 |
| XLOC_009260 | GCNT3 | chr15:59903981-59912210 | 2.37 | 3.32 | 0.00000309 | 0.95 |
| XLOC_001619 | RNF223 | chr1:1006348-1009687 | 2.16 | 3.1 | 0.00000309 | 0.94 |
| XLOC_011586 | PRR11 | chr17:57232859-57284070 | -3.27 | -2.37 | 0.00000309 | 0.9 |
| XLOC_023160 | CDKN1A | chr6:36644236-36655116 | 2.01 | 2.9 | 0.00000309 | 0.89 |
| XLOC_006947 | RND1 | chr12:49250915-49259653 | 2 | 2.85 | 0.00000309 | 0.85 |
| XLOC_016136 | RNF144A- AS1 | chr2:7052406-7184309 | 2.03 | 2.88 | -0.0004402 | 0.85 |
| XLOC_013207 | TNFSF9 | chr19:6531009-6535939 | 2.64 | 3.48 | 0.00000309 | 0.84 |
| XLOC_023856 | ETV7 | chr6:36321997-36355577 | 2.26 | 3.09 | 0.00000309 | 0.83 |
| XLOC_019288 | C3orf52 | chr3:111805181-111837073 | 2.16 | 2.97 | 0.00000309 | 0.81 |
| XLOC_002885 | DUSP10 | chr1:221874763-221915516 | 2.01 | 2.81 | 0.00000309 | 0.8 |
| XLOC_015141 | RSAD2 | chr2:7016846-7038987 | 2.63 | 3.41 | 0.00000309 | 0.78 |
| XLOC_027285 | FAM83A | chr8:124194751-124222318 | -2.89 | -2.21 | 0.00000309 | 0.68 |
| XLOC_017830 | LINC00161 | chr21:29911639-29912677 | 2.43 | 3.1 | 0.00000309 | 0.67 |

| XLOC_029258 | GRPR | chrX:16141423-16173308 | -3.38 | -2.72 | 0.00000309 | 0.66 |
|-----------------|-----------|---------------------------|-------|-------|------------|------|
| XLOC 022071 | HMMR | chr5:162887516-162918953 | -2.86 | -2.2 | 0.00000309 | 0.66 |
| XLOC 010416 | OSGIN1 | chr16:83986826-83999937 | 2.61 | 3.24 | 0.00000309 | 0.63 |
| XLOC_010127 | SCNN1B | chr16:23313590-23392620 | -2.61 | -2.02 | 0.00000309 | 0.59 |
| XLOC 013630 | ZFP36 | chr19:39897486-39900052 | 2.08 | 2.67 | 0.00000309 | 0.59 |
| XLOC 027031 | IDO1 | chr8:39771327-39786309 | 2.14 | 2.68 | 0.00000309 | 0.54 |
| XLOC 020068 | MYH15 | chr3:108099215-108248169 | -3.2 | -2.66 | 0.00000309 | 0.54 |
| XLOC_030138 | COL4A6 | chrX:107398836-107682704 | -2.59 | -2.06 | 0.00000309 | 0.53 |
| XLOC_011378 | KRTAP4-9 | chr17:39261640-39262740 | -2.81 | -2.3 | -0.0066149 | 0.51 |
| XLOC_022159 | SQSTM1 | chr5:179224597-179285840 | 2.05 | 2.56 | 0.00000309 | 0.51 |
| XLOC_013741 | FOSB | chr19:45971252-45978437 | 2.82 | 3.28 | 0.00000309 | 0.46 |
| XLOC_016858 | TNS1 | chr2:218664511-218808796 | -3.63 | -3.17 | 0.00000309 | 0.46 |
| XLOC_029693 | FHL1 | chrX:135228860-135293518 | -2.65 | -2.22 | 0.00000309 | 0.43 |
| XLOC_007298 | HRK | chr12:117296434-117319232 | 2.09 | 2.51 | 0.00000309 | 0.42 |
| XLOC_017519 | LINC00261 | chr20:22541191-22559280 | -3.8 | -3.38 | 0.00000309 | 0.42 |
| XLOC_005627 | CLCF1 | chr11:67085309-67159158 | 2.13 | 2.54 | 0.00000309 | 0.41 |
| XLOC_026762 | ZC3HAV1 | chr7:138728265-138794465 | 2.07 | 2.45 | 0.00000309 | 0.38 |
| XLOC_006241 | NR4A1 | chr12:52416615-52453291 | 2.21 | 2.59 | 0.00000309 | 0.38 |
| XLOC_001111 | PBX1 | chr1:164528596-164821060 | -2.69 | -2.32 | 0.00000309 | 0.37 |
| XLOC_003040 | AKR1C1 | chr10:5005453-5020158 | 2.07 | 2.42 | 0.00000309 | 0.35 |
| XLOC_016021 | CCL20 | chr2:228678557-228682280 | 2.48 | 2.83 | 0.00000309 | 0.35 |
| XLOC_010164 | LAT | chr16:28996146-29002104 | 2.08 | 2.43 | 0.00000309 | 0.35 |
| XLOC_007326 | OASL | chr12:121458094-121477045 | 2.29 | 2.64 | 0.00000309 | 0.35 |
| XLOC_007443 | RASL11A | chr13:27844463-27847827 | -2.9 | -2.55 | 0.00000309 | 0.35 |
| XLOC_009967 | SPSB3 | chr16:1826712-1832581 | 2.39 | 2.72 | 0.00000309 | 0.33 |
| XLOC_019952 | ACOX2 | chr3:58490862-58522929 | -2.6 | -2.28 | 0.00000309 | 0.32 |
| XLOC_016960 | COL6A3 | chr2:238232654-238322850 | -4.73 | -4.41 | 0.00000309 | 0.32 |
| XLOC_025892 | PRKAR2B | chr7:106685177-106802256 | -2.45 | -2.16 | 0.00000309 | 0.29 |
| XLOC_008840 | LTBP2 | chr14:74964885-75079034 | -2.41 | -2.14 | 0.00000309 | 0.27 |
| XLOC_005500 | RAB3IL1 | chr11:61664767-61687741 | 2.03 | 2.29 | 0.00000309 | 0.26 |
| XLOC_019794 | TMEM158 | chr3:45265955-45267814 | 2 | 2.26 | 0.00000309 | 0.26 |
| XLOC_014911 | KLK5 | chr19:51446558-51456344 | -2.75 | -2.5 | 0.00000309 | 0.25 |
| W. 0.0. 00000.5 | NOX5, | | 2.45 | 2 22 | | 0.00 |
| XLOC_009296 | SPESP1 | chr15:69116302-69564544 | -3.45 | -3.22 | 0.00000309 | 0.23 |
| XLOC_023940 | PLA2G7 | chr6:46655611-46703430 | -2.27 | -2.05 | -0.0005801 | 0.22 |
| XLOC_021191 | CXCL2 | chr4:74962750-74964997 | 2.07 | 2.28 | 0.00000309 | 0.21 |
| XLOC_019497 | IL12A | chr3:159706622-159713806 | 2.43 | 2.63 | 0.00000309 | 0.2 |
| XLOC_026615 | RELN | chr7:103112230-103629963 | -2.59 | -2.45 | 0.00030811 | 0.14 |
| XLOC_015891 | AOX1 | chr2:201450730-201536217 | -2.87 | -2.74 | 0.00000309 | 0.13 |
| XLOC_021189 | CXCL3 | chr4:74902311-74904490 | 2.67 | 2.8 | 0.00000309 | 0.13 |
| XLOC_009624 | PATL2 | chr15:44957929-44969086 | 2.1 | 2.23 | 0.00000309 | 0.13 |
| XLOC_018029 | ADAMTS1 | chr21:28208605-28217728 | 2.68 | 2.79 | 0.00000309 | 0.11 |
| XLOC_017897 | ETS2 | chr21:40177230-40196878 | 2 22 | 2.1 | 0.00000309 | 0.1 |
| XLOC_015783 | ITGA6 | chr2:173292313-173371181 | -3.09 | -3 | 0.00000309 | 0.09 |
| XLOC_007879 | SOX21 | chr13:95361878-95364389 | -2.56 | -2.47 | 0.00000309 | 0.09 |

| VI OC 022200 | CD100 | ch =C.7440FF07 74F29041 | 2.4 | 2 22 | 0.00000300 | 0.00 |
|--------------|-----------|---------------------------|-------|-------|------------|-------|
| XLOC_023300 | CD109 | chr6:74405507-74538041 | -2.4 | -2.32 | 0.00000309 | 0.08 |
| XLOC_003409 | IFIT3 | chr10:91087601-91100725 | 2.1 | 2.18 | 0.00000309 | 0.08 |
| XLOC_016974 | FLJ43879 | chr2:239840997-239847965 | -2.98 | -2.91 | 0.00000309 | 0.07 |
| XLOC_023798 | TNXB | chr6:32006092-32077151 | -2.82 | -2.75 | 0.00000309 | 0.07 |
| XLOC_019293 | GCSAM | chr3:111838247-111854589 | 2.03 | 2.09 | 0.00000309 | 0.06 |
| XLOC_014912 | KLK6 | chr19:51461886-51472929 | -2.26 | -2.2 | 0.00000309 | 0.06 |
| XLOC_002123 | NEGR1 | chr1:71868624-72748277 | -2.64 | -2.59 | 0.00000309 | 0.05 |
| XLOC_018147 | SIK1 | chr21:44834397-44847002 | 2.15 | 2.2 | 0.00000309 | 0.05 |
| XLOC_027603 | PLAT | chr8:42032235-42065194 | -2.54 | -2.49 | 0.00000309 | 0.05 |
| XLOC_003664 | LINC00704 | chr10:4692376-4720262 | -3.31 | -3.27 | 0.00000309 | 0.04 |
| XLOC_016849 | FN1 | chr2:216225178-216300849 | -2.56 | -2.54 | 0.00000309 | 0.02 |
| XLOC_022325 | PLCXD3 | chr5:41307047-41510730 | -2.19 | -2.17 | 0.00000309 | 0.02 |
| XLOC_011650 | MAP2K6 | chr17:67410837-67538470 | -3.82 | -3.81 | 0.00015897 | 0.01 |
| XLOC_009776 | LOXL1-AS1 | chr15:74208370-74244478 | -3.01 | -3.01 | 0.00000309 | 0 |
| XLOC_004278 | MUC5B | chr11:1244294-1283406 | -3.6 | -3.6 | 0.00000309 | 0 |
| XLOC_005827 | KDELC2 | chr11:108342832-108369159 | -2.19 | -2.2 | 0.00000309 | -0.01 |
| XLOC_018148 | LINC00313 | chr21:44881973-44898103 | 2.56 | 2.55 | 0.0016492 | -0.01 |
| XLOC_017482 | TMX4 | chr20:7960296-8000393 | -2.13 | -2.14 | 0.00000309 | -0.01 |
| XLOC_007580 | SCEL | chr13:78109808-78219420 | -2.49 | -2.53 | 0.00000309 | -0.04 |
| XLOC_026189 | ETV1 | chr7:13930855-14031050 | -2.05 | -2.1 | 0.00000309 | -0.05 |
| XLOC_009043 | IPW | chr15:25361691-25367623 | -2.05 | -2.11 | 0.00000309 | -0.06 |
| XLOC_022572 | FBN2 | chr5:127593600-127873877 | -3.02 | -3.09 | 0.00000309 | -0.07 |
| XLOC_028995 | TNC | chr9:117781853-117880536 | -3.16 | -3.23 | 0.00000309 | -0.07 |
| XLOC_020022 | ABI3BP | chr3:100468082-100712334 | -3.88 | -3.95 | 0.00000309 | -0.07 |
| XLOC_012021 | ALDH3A1 | chr17:19641297-19651746 | -2.69 | -2.78 | 0.00000309 | -0.09 |
| XLOC_021218 | ANTXR2 | chr4:80822770-80994477 | -2.04 | -2.13 | 0.00000309 | -0.09 |
| XLOC_015263 | LTBP1 | chr2:33172368-33624575 | -2.17 | -2.29 | 0.00000309 | -0.12 |
| XLOC_029650 | GRIA3 | chrX:122318095-122624766 | 2.24 | 2.11 | 0.00000309 | -0.13 |
| XLOC_005053 | SORL1 | chr11:121322911-121504471 | -3.32 | -3.46 | 0.00000309 | -0.14 |
| XLOC_018408 | APOBEC3C | chr22:39410168-39416393 | -3.07 | -3.22 | 0.00000309 | -0.15 |
| XLOC_016637 | RND3 | chr2:151324706-151344209 | 2.61 | 2.43 | 0.00000309 | -0.18 |
| XLOC_004703 | NEAT1 | chr11:65190268-65194003 | 2.72 | 2.53 | 0.00000309 | -0.19 |
| XLOC_028049 | DOCK8 | chr9:213107-465259 | -2.41 | -2.61 | 0.00000309 | -0.2 |
| XLOC_020135 | MUC13 | chr3:124624288-124653595 | 2.29 | 2.09 | 0.00000309 | -0.2 |
| XLOC_013268 | ICAM5 | chr19:10400654-10407454 | 2.36 | 2.15 | 0.00000309 | -0.21 |
| XLOC_006854 | BCAT1 | chr12:24962957-25102393 | -2 | -2.29 | 0.00000309 | -0.29 |
| XLOC_020923 | СРЕ | chr4:166300096-166419482 | -2.01 | -2.3 | 0.00000309 | -0.29 |
| XLOC_013627 | IFNL1 | chr19:39786964-39789312 | 3.75 | 3.44 | -0.0078816 | -0.31 |
| XLOC_020282 | LXN | chr3:158362316-158410360 | -2.16 | -2.52 | 0.00000309 | -0.36 |
| XLOC_026736 | PLXNA4 | chr7:131808090-132333447 | -2.59 | -2.95 | 0.00000309 | -0.36 |
| XLOC_022562 | ALDH7A1 | chr5:125877532-125931082 | -2.08 | -2.46 | 0.00000309 | -0.38 |
| XLOC_018410 | APOBEC3F | chr22:39436672-39451975 | -2.19 | -2.58 | 0.00000309 | -0.39 |
| XLOC_023472 | GPR126 | chr6:142623055-142767403 | -2.02 | -2.45 | 0.00000309 | -0.43 |
| XLOC_005483 | TCN1 | chr11:59620280-59634041 | -2.63 | -3.09 | -0.0069746 | -0.46 |

| XLOC_003408 | IFIT2 | chr10:91061705-91069033 | 2.62 | 2.15 | 0.00000309 | -0.47 |
|-------------|-----------|---------------------------|-------|-------|------------|-------|
| XLOC_017340 | PHACTR3 | chr20:58152563-58422766 | -3.22 | -3.74 | 0.00000309 | -0.52 |
| XLOC_005214 | НВВ | chr11:5246695-5248301 | -2.6 | -3.13 | 0.00117579 | -0.53 |
| XLOC_013438 | GDF15 | chr19:18496967-18499986 | 3.54 | 2.99 | 0.00000309 | -0.55 |
| XLOC_005005 | NNMT | chr11:114166534-114183238 | -2.36 | -2.97 | 0.00000309 | -0.61 |
| XLOC_017071 | BMP2 | chr20:6748744-6760910 | 3.69 | 3.06 | 0.00015897 | -0.63 |
| XLOC_006722 | IFFO1 | chr12:6648693-6665249 | 2.92 | 2.26 | 0.00000309 | -0.66 |
| XLOC_015754 | CSRNP3 | chr2:166326156-166545917 | -2.15 | -2.82 | 0.00000309 | -0.67 |
| XLOC_017128 | FLJ33581 | chr20:24180402-24205224 | -3.24 | -3.97 | 0.00000309 | -0.73 |
| XLOC_007868 | SLITRK6 | chr13:86366921-86373483 | -2.67 | -3.4 | 0.00000309 | -0.73 |
| XLOC_005730 | TENM4 | chr11:78364327-79151695 | -2.38 | -3.13 | 0.00000309 | -0.75 |
| XLOC_016855 | IGFBP5 | chr2:217536827-217560272 | -3.68 | -4.59 | 0.00000309 | -0.91 |
| XLOC_012794 | SLC14A1 | chr18:43304091-43332485 | -2.28 | -3.31 | 0.00000309 | -1.03 |
| XLOC_010555 | PRSS22 | chr16:2902727-2908171 | 3.21 | 2.06 | -0.0007188 | -1.15 |
| XLOC_019577 | LOC344887 | chr3:185677757-185698753 | 4.76 | 3.6 | 0.00000309 | -1.16 |
| XLOC_022467 | EDIL3 | chr5:83236288-83680611 | -2.31 | -3.54 | 0.00000309 | -1.23 |
| XLOC_026792 | FAM131B | chr7:143050492-143059840 | -2.01 | -3.34 | 0.00000309 | -1.33 |
| XLOC_018138 | TMPRSS3 | chr21:43791995-43816955 | -2.45 | -4.3 | -0.0001506 | -1.85 |

7.3.4 Identification of transcriptome expression within gene families:

Next, we looked at the gene families that were associated with autophagy, apoptosis, anoikis and cell adhesion, endocytosis, and lipid-like receptors, to name a few.

The genes within these families were identified from available databases that have attributed these to specific family of genes. We investigated if specific genes were expressed differently within these families and how these differential expressions related to the duration of exposure to doxazosin. A non-significant expression at both time points were assigned green, a significant expression was assigned brown, and a change in significance at either time point was assigned yellow and indeterminate significance as blue.

Table 14: Evaluation of fold changes within autophagy gene family at 24 h and 48 h and the change in fold-expression between the two time points: Green – false at both time points; Yellow – transition from true to false (or vice versa) between time points; Orange – True at both time points.

| | Log2 | | | log2 ratio | | | Fold change 24h to |
|-----------|-------|----------|--------------|---------------|----------|--------------|--------------------|
| Gene | 24h | q1 24h | significance | 48h | q2 48h | significance | 48h |
| ULK1 | -0.25 | 0.054864 | FALSE | 0.21 | 0.110383 | FALSE | 0.46 |
| ULK2 | -0.35 | 0.064051 | FALSE | -0.13 | 0.530799 | FALSE | 0.22 |
| ATG10 | -0.58 | 0.000166 | TRUE | -0.84 | 0.000169 | TRUE | -0.26 |
| ATG12 | -0.1 | 0.367662 | FALSE | -0.1 | 0.388466 | FALSE | 0 |
| ATG13 | -0.53 | 0.000166 | TRUE | -0.42 | 0.000169 | TRUE | 0.11 |
| ATG14 | 0.26 | 0.020512 | TRUE | 0.2 | 0.092812 | FALSE | -0.06 |
| ATG16L1 | -1.14 | 0.000166 | TRUE | -1.1 | 0.000169 | TRUE | 0.04 |
| ATG16L2 | 0.03 | 0.873935 | FALSE | 0.29 | 0.147515 | FALSE | 0.26 |
| ATG2A | -0.41 | 0.001157 | TRUE | 0.56 | 0.000169 | TRUE | 0.97 |
| ATG2B | -0.61 | 0.000166 | TRUE | -0.63 | 0.000169 | TRUE | -0.02 |
| ATG3 | 0.2 | 0.065295 | FALSE | -0.07 | 0.53539 | FALSE | -0.27 |
| ATG4A | 0.26 | 0.046492 | TRUE | 0.73 | 0.000169 | TRUE | 0.47 |
| ATG4B | 0.49 | 0.000166 | TRUE | 0.91 | 0.000169 | TRUE | 0.42 |
| ATG4C | -0.2 | 0.179178 | FALSE | -0.47 | 0.001177 | TRUE | -0.27 |
| ATG4D | 0.44 | 0.19043 | FALSE | 0.95 | 0.001712 | TRUE | 0.51 |
| ATG5 | -0.15 | 0.232 | FALSE | -0.13 | 0.302037 | FALSE | 0.02 |
| ATG7 | -0.58 | 0.009186 | TRUE | -0.67 | 0.011481 | TRUE | -0.09 |
| ATG9A | -0.24 | 0.03954 | TRUE | 0.38 | 0.001177 | TRUE | 0.62 |
| BECN1 | -0.74 | 0.000166 | TRUE | -0.45 | 0.000169 | TRUE | 0.29 |
| GABARAP | -0.13 | 0.259205 | FALSE | -0.01 | 0.93661 | FALSE | 0.12 |
| GABARAPL1 | 1.32 | 0.000166 | TRUE | 1.6 | 0.000169 | TRUE | 0.28 |
| GABARAPL2 | -0.24 | 0.039691 | TRUE | 0.05 | 0.711026 | FALSE | 0.29 |
| MAP1LC3A | 0.87 | 0.10881 | FALSE | 1.12 | 0.024193 | TRUE | 0.25 |
| MAP1LC3B | 0.23 | 0.029783 | TRUE | 0.24 | 0.032786 | TRUE | 0.01 |
| MAP1LC3B2 | -0.02 | 0.950189 | FALSE | 0.68 | 0.004284 | TRUE | 0.7 |
| RB1CC1 | -0.8 | 0.000166 | TRUE | -0.98 | 0.000169 | TRUE | -0.18 |
| WIPI1 | 0.22 | 0.12524 | FALSE | -0.17 | 0.200884 | FALSE | -0.39 |
| WIPI2 | -0.15 | 0.191622 | FALSE | 0.18 | 0.145801 | FALSE | 0.33 |
| SNX4 | 0.56 | 0.000166 | TRUE | 0.59 | 0.000169 | TRUE | 0.03 |
| SNX30 | -0.54 | 0.000166 | TRUE | -0.66 | 0.000169 | TRUE | -0.12 |

Table 15: Evaluation of fold changes within adrenoceptor gene family at 24 h and 48 h and the change in fold-expression between the two time points: Green – false at both time points; Orange – True at both time points; blue – data not available.

| Gene | Log2 ratio 24h | q1 | significance | log2 ratio 48h | q2 value | significance | Fold change | e 24h to |
|-------|----------------------|---------|--------------|----------------------|-------------|--------------|-------------|----------|
| | | | | ADRA1 | | | | |
| na | na | na | na | D | -0.98 | 0.007127 | TRUE | NA |
| | | 0.23109 | | | | | | |
| ADRB2 | -0.16 | 2 | FALSE | ADRB2 | 0.18 | 0.190795 | FALSE | 0.34 |

| Gene | Log2 ratio 24h | q1 | significance | log2 ratio 48h | q2 | significance | Fold change 24h to 48h |
|-------|----------------------|----------|--------------|----------------------|----------|--------------|------------------------------|
| APAF1 | -0.83 | 0.000166 | TRUE | -0.36 | 0.03717 | TRUE | 0.47 |
| CASP9 | 0.08 | 0.679066 | FALSE | -0.11 | 0.545993 | FALSE | -0.19 |
| CYC1 | 0.11 | 0.30238 | FALSE | -0.05 | 0.678825 | FALSE | -0.16 |

Table 16: Evaluation of fold changes within apoptosome gene family at 24 h and 48 h and the change in fold-expression between the two time points: Green – false at both time points; Orange – True at both time points.

| Gene | Log2 ratio 24h | q1 | significance | log2 ratio 48h | q2 value | significance | Fold change 24h to 48h |
|--------|----------------------|----------|--------------|----------------------|----------|--------------|---------------------------------|
| CASP1 | 0.86 | 0.000888 | TRUE | 1.12 | 0.000169 | TRUE | 0.26 |
| CASP2 | -0.39 | 0.000749 | TRUE | -0.47 | 0.000169 | TRUE | -0.08 |
| CASP3 | -0.1 | 0.456311 | FALSE | 0.34 | 0.011883 | TRUE | 0.44 |
| CASP4 | 0.97 | 0.000166 | TRUE | 0.75 | 0.000169 | TRUE | -0.22 |
| CASP6 | -0.33 | 0.028034 | TRUE | -0.55 | 0.000169 | TRUE | -0.22 |
| CASP7 | 1.03 | 0.000166 | TRUE | 1.16 | 0.000169 | TRUE | 0.13 |
| CASP8 | 0.72 | 0.000166 | TRUE | 0.71 | 0.000169 | TRUE | -0.01 |
| CASP10 | -0.56 | 0.000166 | TRUE | -0.3 | 0.021582 | TRUE | 0.26 |
| CASP14 | -1.19 | 0.000166 | TRUE | 0.5 | 0.022436 | TRUE | 1.69 |

Table 17: Evaluation of fold changes within caspase gene family at 24 h and 48 h and the change in fold-expression between the two time points: Yellow – transition from true to false (or vice versa) between time points; Orange – True at both time points.

Table 18: Evaluation of fold changes within the *Bcl-2* gene family at 24 h and 48 h and the change in fold-expression between the two time points: Green – false at both time points; Yellow – transition from true to false (or vice versa) between time points; Orange – True at both time points.

| | Log2 ratio | | | log2 ratio | | | Fold change |
|---------|---------------|----------|--------------|---------------|----------|--------------|-------------|
| Gene | 24h | q1 | significance | 48h | q2 value | significance | 24h to 48h |
| BCL2 | -0.14 | 0.57646 | FALSE | -0.32 | 0.337698 | FALSE | -0.18 |
| BCL2L1 | -0.52 | 0.000166 | TRUE | -0.58 | 0.000169 | TRUE | -0.06 |
| BCL2L2 | 0.18 | 0.104845 | FALSE | 0.28 | 0.01608 | TRUE | 0.1 |
| BCL2A1 | -0.69 | 0.00032 | TRUE | -0.12 | 0.591776 | FALSE | 0.57 |
| BCL10 | -0.06 | 0.690189 | FALSE | -0.38 | 0.002352 | TRUE | -0.32 |
| BCL2L12 | -0.16 | 0.442568 | FALSE | 0.44 | 0.027234 | TRUE | 0.6 |
| BCL2L13 | 0.21 | 0.073013 | FALSE | -0.02 | 0.885195 | FALSE | -0.23 |
| MCL1 | 0.85 | 0.000166 | TRUE | 0.85 | 0.000169 | TRUE | 0 |
| BAK1 | 0.49 | 0.000166 | TRUE | 0.12 | 0.33937 | FALSE | -0.37 |
| ВОК | 0.02 | 0.895133 | FALSE | 0.57 | 0.000169 | TRUE | 0.55 |
| BNIP2 | 0.11 | 0.383171 | FALSE | 0.08 | 0.531462 | FALSE | -0.03 |

Table 19: Evaluation of fold changes within *Bcl-2* homology region 3 (BH3) subset of the *Bcl-2* gene family at 24 h and 48 h and the change in fold-expression between the two time points: Green – false at both time points; Yellow – transition from true to false (or vice versa) between time points; Orange – True at both time points.

| | Log2 ratio | | | log2 ratio | | | Fold change |
|---------|---------------|----------|--------------|---------------|----------|--------------|-------------|
| Gene | 24h | q1 | significance | 48h | q2 value | significance | 24h to 48h |
| BAD | -0.07 | 0.698637 | FALSE | 0.74 | 0.000169 | TRUE | 0.81 |
| ВВС3 | 1.4 | 0.008048 | TRUE | 2.07 | 0.000169 | TRUE | 0.67 |
| BCL2L11 | 0.36 | 0.138562 | FALSE | 0.58 | 0.003821 | TRUE | 0.22 |
| BID | -0.72 | 0.282102 | FALSE | -1.28 | 0.08974 | FALSE | -0.56 |
| BID | 0.41 | 0.00396 | TRUE | 0.81 | 0.000169 | TRUE | 0.4 |
| BIK | 1.31 | 0.000166 | TRUE | 1.34 | 0.000169 | TRUE | 0.03 |
| BMF | 1.06 | 0.000166 | TRUE | 1.71 | 0.000169 | TRUE | 0.65 |
| BNIP1 | 0.46 | 0.000609 | TRUE | 0.45 | 0.000763 | TRUE | -0.01 |
| BNIP3 | 0.27 | 0.009496 | TRUE | 1.36 | 0.000169 | TRUE | 1.09 |
| HRK | 2.09 | 0.000166 | TRUE | 2.51 | 0.000169 | TRUE | 0.42 |
| PMAIP1 | 1.88 | 0.000166 | TRUE | 1.49 | 0.000169 | TRUE | -0.39 |

Table 20: Evaluation of fold changes within cyclin-dependent kinase gene family at 24 h and 48 h and the change in fold-expression between the two time points: Green – false at both time points; Yellow – transition from true to false (or vice versa) between time points; Orange – True at both time points; blue – data not available.

| | Log2 ratio | | | log2 ratio | _ | | Fold change |
|---------|---------------|----------|--------------|---------------|----------|--------------|-------------|
| Gene | 24h | q1 | significance | 48h | q2 value | significance | 24h to 48h |
| CDK1 | -1.85 | 0.000166 | TRUE | -0.72 | 0.000169 | TRUE | 1.13 |
| CDK2 | -0.46 | 0.000166 | TRUE | 0.13 | 0.298313 | FALSE | 0.59 |
| CDK2AP1 | -1.29 | 0.000166 | TRUE | -1.11 | 0.000169 | TRUE | 0.18 |
| CDK2AP2 | 0 | 0.978638 | FALSE | 0.62 | 0.000169 | TRUE | 0.62 |
| CDK3 | 0.76 | 0.014844 | TRUE | 1.08 | 0.000621 | TRUE | 0.32 |
| CDK4 | -0.87 | 0.000166 | TRUE | -0.63 | 0.000169 | TRUE | 0.24 |
| CDK5 | -0.72 | 0.000166 | TRUE | -0.48 | 0.000325 | TRUE | 0.24 |
| CDK6 | -0.24 | 0.057657 | FALSE | -0.47 | 0.000169 | TRUE | -0.23 |
| CDK7 | 0.11 | 0.433544 | FALSE | -0.17 | 0.171668 | FALSE | -0.28 |
| CDK8 | 0.4 | 0.004305 | TRUE | 0.18 | 0.213693 | FALSE | -0.22 |
| CDK9 | 0.13 | 0.326383 | FALSE | 0.17 | 0.207234 | FALSE | 0.04 |
| CDK10 | 0.18 | 0.256291 | FALSE | 0.4 | 0.004397 | TRUE | 0.22 |
| CDK11A, | | | | | | | |
| В | -0.01 | 0.957187 | FALSE | 0 | 0.98372 | FALSE | 0.01 |
| CDK12 | -0.02 | 0.855399 | FALSE | -0.11 | 0.390567 | FALSE | -0.09 |
| CDK13 | -0.04 | 0.763476 | FALSE | -0.22 | 0.076688 | FALSE | -0.18 |
| CDK14 | -1.53 | 0.000166 | TRUE | -2 | 0.000169 | TRUE | -0.47 |
| CDK16 | -0.69 | 0.000166 | TRUE | -0.52 | 0.000169 | TRUE | 0.17 |
| CDK17 | 0.71 | 0.000166 | TRUE | 0.58 | 0.000169 | TRUE | -0.13 |
| CDK18 | 0.51 | 0.000609 | TRUE | 0.33 | 0.025849 | TRUE | -0.18 |
| CDK19 | -0.96 | 0.000166 | TRUE | -1.13 | 0.000169 | TRUE | -0.17 |
| CDK20 | 0.85 | 0.00032 | TRUE | 0.47 | 0.022627 | TRUE | -0.38 |
| CDKL1 | 0.21 | 0.542026 | FALSE | 1 | 0.001446 | TRUE | 0.79 |
| CDKL3 | -0.25 | 0.420623 | FALSE | -0.02 | 0.93435 | FALSE | 0.23 |
| CDKL5 | 0.35 | 0.102263 | FALSE | na | na | na | na |

Table 21: Evaluation of fold changes within cyclin gene family at 24 h and 48 h and the change in fold-expression between the two time points: Green – false at both time points; Yellow – transition from true to false (or vice versa) between time points; Orange – True at both time points.

| Gene | Log2 ratio 24h | q1 24h | significance | log2 ratio 48h | q2 48h | significance | Fold change 24h to 48h |
|----------|----------------------|----------|--------------|----------------------|----------|--------------|---------------------------|
| CCNA1 | -0.74 | 0.000166 | TRUE | -0.81 | 0.000169 | TRUE | -0.07 |
| CCNA2 | -1.75 | 0.000166 | TRUE | -1.24 | 0.000169 | TRUE | 0.51 |
| CCNB1 | -2.08 | 0.000166 | TRUE | -1.42 | 0.000169 | TRUE | 0.66 |
| CCNB1IP1 | -0.1 | 0.467954 | FALSE | -0.63 | 0.000169 | TRUE | -0.53 |
| CCNB2 | -2.1 | 0.000166 | TRUE | -1.65 | 0.000169 | TRUE | 0.45 |
| CCNC | -0.05 | 0.688475 | FALSE | 0.12 | 0.375196 | FALSE | 0.17 |
| CCND1 | -0.3 | 0.001681 | TRUE | 0 | 0.999068 | FALSE | 0.3 |
| CCND3 | 0.25 | 0.043051 | TRUE | 0.58 | 0.000169 | TRUE | 0.33 |
| CCNDBP1 | -0.05 | 0.734513 | FALSE | 0.13 | 0.315677 | FALSE | 0.18 |
| CCNE1 | 0.99 | 0.000166 | TRUE | 1.08 | 0.000169 | TRUE | 0.09 |
| CCNE2 | 0.51 | 0.004867 | TRUE | 0.99 | 0.000325 | TRUE | 0.48 |
| CCNF | -1.63 | 0.000166 | TRUE | -0.4 | 0.021492 | TRUE | 1.23 |
| CCNG1 | -0.65 | 0.000166 | TRUE | -0.85 | 0.000169 | TRUE | -0.2 |
| CCNG2 | -0.49 | 0.001809 | TRUE | -0.74 | 0.000169 | TRUE | -0.25 |
| CCNH | 0.56 | 0.001023 | TRUE | -0.82 | 0.686968 | FALSE | -1.38 |
| CCNI | -0.88 | 0.000166 | TRUE | -1.2 | 0.000169 | TRUE | -0.32 |
| CCNJ | 0.72 | 0.00032 | TRUE | 0.26 | 0.234475 | FALSE | -0.46 |
| CCNJL | 0.29 | 0.058445 | FALSE | -0.02 | 0.881535 | FALSE | -0.31 |
| CCNK | 0.42 | 0.008774 | TRUE | 0.51 | 0.001177 | TRUE | 0.09 |
| CCNL1 | 1.03 | 0.000166 | TRUE | 0.98 | 0.000169 | TRUE | -0.05 |
| CCNL2 | 0.77 | 0.000166 | TRUE | 0.48 | 0.000325 | TRUE | -0.29 |
| CCNO | 0.79 | 0.000749 | TRUE | 0.87 | 0.000325 | TRUE | 0.08 |
| CCNT1 | 0.28 | 0.014052 | TRUE | -0.01 | 0.960707 | FALSE | -0.29 |
| CCNT2 | 0.63 | 0.002063 | TRUE | 0.46 | 0.088135 | FALSE | -0.17 |
| CCNY | -0.16 | 0.145003 | FALSE | -0.42 | 0.000169 | TRUE | -0.26 |
| CCNYL1 | -0.38 | 0.011225 | TRUE | 0.07 | 0.657931 | FALSE | 0.45 |

Table 22: Evaluation of fold changes within death inducing signal complex gene family at 24 h and 48 h and the change in fold-expression between the two time points: Green – false at both time points; Orange – True at both time points.

| Gene | Log2 ratio 24h | q1 | significance | log2 ratio 48h | q2 value | significance | Fold change 24h to 48h |
|--------|----------------------|-----------|--------------|----------------------|----------|--------------|---------------------------|
| CASP8 | 0.72 | 0.000166 | TRUE | 0.71 | 0.000169 | TRUE | -0.01 |
| CASP10 | -0.56 | 0.000166 | TRUE | -0.3 | 0.021582 | TRUE | 0.26 |
| CFLAR | 0.12 | 0.567961 | FALSE | 0.2 | 0.365671 | FALSE | 0.08 |
| FADD | 0.35 | 0.00218 | TRUE | 0.5 | 0.000169 | TRUE | 0.15 |
| FAS | 0.49 | 0.002425 | TRUE | 0.91 | 0.000169 | TRUE | 0.42 |

Table 23: Evaluation of fold changes within EARP gene family at 24 h and 48 h and the change in fold-expression between the two time points: Green – false at both time points; Yellow – transition from true to false (or vice versa) between time points; Orange – True at both time points.

| Gene | Log2 ratio 24h | q1 | significance | log2 ratio 48h | q2 value | significance | Fold change 24h to 48h |
|---------|----------------------|----------|--------------|----------------------|----------|--------------|---------------------------------|
| VPS50, | | | | | | | |
| CCDC132 | -0.44 | 0.046721 | TRUE | 0.01 | 0.966327 | FALSE | 0.45 |
| VPS51, | | | | | | | |
| TM7SF2 | -0.71 | 0.000166 | TRUE | -0.63 | 0.000169 | TRUE | 0.08 |
| VPS52 | -0.97 | 0.000166 | TRUE | -0.93 | 0.000169 | TRUE | 0.04 |
| VPS53 | -0.1 | 0.638006 | FALSE | 0.08 | 0.726421 | FALSE | 0.18 |

Table 24: Evaluation of fold changes within MTORC 1 and 2 gene families at 24 h and 48 h and the change in fold-expression between the two time points: Green – false at both time points; Yellow – transition from true to false (or vice versa) between time points; Orange – True at both time points.

| | Log2 ratio | | | log2 ratio | | | Fold change |
|----------|---------------|-----------|--------------|---------------|----------|--------------|-------------|
| Gene | 24h | q1 | significance | 48h | q2 value | significance | 24h to 48h |
| AKT1 | -0.72 | 0.000166 | TRUE | -0.4 | 0.000474 | TRUE | 0.32 |
| AKT1S1 | -0.16 | 0.187516 | FALSE | 0.22 | 0.08479 | FALSE | 0.38 |
| MLST8 | -0.1 | 0.536227 | FALSE | 0.23 | 0.11513 | FALSE | 0.33 |
| MTOR | -0.76 | 0.000166 | TRUE | -0.75 | 0.000169 | TRUE | 0.01 |
| RPTOR | 0.15 | 0.242811 | FALSE | 0.7 | 0.000169 | TRUE | 0.55 |
| MAPKAP1 | -0.65 | 0.000166 | TRUE | -0.51 | 0.000169 | TRUE | 0.14 |
| ARHGAP8, | | | | | | | |
| PRR5, | 0.61 | 0.001937 | TRUE | 0.77 | 0.000763 | TRUE | 0.16 |
| RICTOR | 0.59 | 0.000166 | TRUE | 0.26 | 0.023464 | TRUE | -0.33 |

Table 25: Evaluation of fold changes within PIK3C3 gene families at 24 h and 48 h and the change in fold-expression between the two time points: Green – false at both time points; Yellow – transition from true to false (or vice versa) between time points; Orange – True at both time points.

| | Log2 ratio | | | log2 ratio | | | Fold change |
|--------|---------------|----------|--------------|---------------|----------|--------------|-------------|
| Gene | 24h | q1 | significance | 48h | q2 value | significance | 24h to 48h |
| ATG14 | 0.26 | 0.020512 | TRUE | 0.2 | 0.092812 | FALSE | -0.06 |
| BECN1 | -0.74 | 0.000166 | TRUE | -0.45 | 0.000169 | TRUE | 0.29 |
| NRBF2 | 0.59 | 0.000166 | TRUE | 0.31 | 0.005094 | TRUE | -0.28 |
| PIK3C3 | -0.2 | 0.129148 | FALSE | -0.15 | 0.273223 | FALSE | 0.05 |
| PIK3R4 | 0.1 | 0.475573 | FALSE | -0.08 | 0.559314 | FALSE | -0.18 |
| RUBCN | 0.76 | 0.002914 | TRUE | 0.81 | 0.001579 | TRUE | 0.05 |
| UVRAG | 0.74 | 0.000166 | TRUE | 0.42 | 0.000169 | TRUE | -0.32 |

Table 26: Evaluation of fold changes within SNARE gene families at 24 h and 48 h and the change in fold-expression between the two time points. Green – false at both time points; Yellow – transition from true to false (or vice versa) between time points; Orange – True at both time points.

| | Log2 ratio | | | log2 ratio | | | Fold change |
|--------|---------------|----------|--------------|---------------|----------|--------------|-------------|
| Gene | 24h | q1 | significance | 48h | q2 value | significance | 24h to 48h |
| BET1 | 0.13 | 0.363005 | FALSE | -0.13 | 0.330423 | FALSE | -0.26 |
| BET1L | 0.26 | 0.028034 | TRUE | -0.06 | 0.667444 | FALSE | -0.32 |
| BNIP1 | 0.46 | 0.000609 | TRUE | 0.45 | 0.000763 | TRUE | -0.01 |
| GOSR1 | 0.12 | 0.320609 | FALSE | 0.23 | 0.059113 | FALSE | 0.11 |
| GOSR2 | 0.52 | 0.000166 | TRUE | 0.34 | 0.0069 | TRUE | -0.18 |
| SEC22A | 0.48 | 0.000166 | TRUE | 0.38 | 0.001446 | TRUE | -0.1 |
| SEC22B | -0.07 | 0.586878 | FALSE | 0.11 | 0.387971 | FALSE | 0.18 |
| SEC22C | -0.65 | 0.011425 | TRUE | -0.96 | 0.000169 | TRUE | -0.31 |
| SNAP23 | -0.45 | 0.000166 | TRUE | -0.24 | 0.054667 | FALSE | 0.21 |
| SNAP29 | -0.31 | 0.010204 | TRUE | -0.3 | 0.017301 | TRUE | 0.01 |
| USE1 | 0.31 | 0.045002 | TRUE | 0.33 | 0.042264 | TRUE | 0.02 |
| VTI1A | -0.12 | 0.393315 | FALSE | 0.22 | 0.146143 | FALSE | 0.34 |
| VTI1B | -0.49 | 0.000166 | TRUE | -0.31 | 0.028779 | TRUE | 0.18 |
| YKT6 | -0.29 | 0.004982 | TRUE | -0.03 | 0.778435 | FALSE | 0.26 |

Table 27: Evaluation of fold changes within TNF gene families at 24h and 48h and the change in fold-expression between the two time points: Green – false at both time points; Yellow – transition from true to false (or vice versa) between time points; Orange – True at both time points; blue – data not available.

| | Log2 | | | log2 | | | |
|-------|-------|----------|--------------|-------|----------|--------------|-------------|
| | ratio | | | ratio | | | Fold change |
| Gene | 24h | q1 | significance | 48h | q2 value | significance | 24h to 48h |
| na | na | na | na | 1.24 | 0.000169 | TRUE | na |
| TRAF2 | 0.6 | 0.000166 | TRUE | 1.28 | 0.000169 | TRUE | 0.68 |
| TRAF3 | -0.1 | 0.43044 | FALSE | 0.41 | 0.001579 | TRUE | 0.51 |
| TRAF4 | 0.63 | 0.000166 | TRUE | 0.99 | 0.000169 | TRUE | 0.36 |
| TRAF5 | 1.08 | 0.000166 | TRUE | 0.91 | 0.000169 | TRUE | -0.17 |
| TRAF6 | 0.48 | 0.000166 | TRUE | 0.58 | 0.000169 | TRUE | 0.1 |
| TRAF7 | -0.86 | 0.000166 | TRUE | -0.66 | 0.000169 | TRUE | 0.2 |

7.4 Discussion

Next generation transcriptome sequencing can identify the changes for the entire genome, however, a vast amount of data is generated (Akhoundova, Feng et al. 2022). Moreover, it is also difficult to ascertain if the change in expression is of significance and if these would translate to clinically relevant outcomes. Therefore, the findings are verified to confirm if the gene expression level changes are indeed translated into the transcription of proteins. As it is impractical to test for all the proteins that would have a fold changes, it is necessary to identify the subgroups that are of relevance.

Our initial approach was to identify, using log2 ratio data, the genes that exhibited greatest fold changes in PC-3 cell lines when there were exposed to 37 μ M for 24 h or 48 h. As an initial screening step, we compared the fold-change in gene expression of those genes (to that of controls) that were expressed at both 24 h and 48 h when treated with 37 μ M of doxazosin.

A total of 250 genes showed a fold change of greater than at 24 h, and after 48 h this increased to 350. Among these, 41 showed a fold change of greater than 3 at 24 h and this increased to 85 at 48 h. The number of genes that had a greater than 4-fold increase was 3 at 24 h, increasing to 18 at 48 h. At 24 h, the fold increase was consistently less than 5 and this might reflect the short time to which cells were exposed to doxazosin. At 48 h of exposure to doxazosin, 5 genes had a greater than 5-fold change – of these both LOC100271832 and MR1256/SLC25A3 genes had a 9-fold increase. Among all time periods, the highest fold change was seen in CD3D gene which was the only gene to exhibit a fold change of greater than 10.

In the case of CD3D gene, there was a 10.54-fold reduction in the log2 ratio; hence, this gene was supressed in the presence of doxazosin. The CD3D gene is also known as the CD3-Delta unit of the T-cell receptor complex as they were initially identified in T cell lymphocytes; subsequently, they were found to be expressed in benign as well as malignant prostate tissues (Essand, Vasmatzis et al. 1999). CD3D expression levels is known to be a prognostic marker for a wide range of cancers or their response to treatment including muscle-invasive BCa (Shi, Meng et al. 2019), gastric cancer (Yuan, Xu et al. 2022), colon cancer (Yang, Zang et al. 2020), and is a marker for response to radiotherapy in PCa (Fortis, Goulielmaki et al. 2022). To our knowledge, no previous studies has previously examined the relationship between CD3D gene expression and PCa cells.

The LOC100271832 is an uncharacterized gene that is expressed at low levels in several tissues in humans (Fagerberg, Hallstrom et al. 2014). Therefore, an increase in fold change by a factor of 9.77 in our data is intriguing. Further studies into understanding the functions of this gene and the protein expressed by this gene could shed light into novel pathways that are involved in androgen-resistant PCa.

The SLC25A3 gene, which demonstrated a 9.77-fold reduction and belongs to a family of mitochondrial transport proteins that is involved in transport of copper ions, which is need for cytochrome oxidase for cytochrome-*c* release – this recently described pathway sometimes referred to as cuproptosis (Wang, Zhang et al. 2022). There have been no previous studies that have examined the relationship between adrenergic receptors or its antagonists with cuproptosis. Whilst suppression of cuproptosis could be a possible pathway in doxazosin induced cell death, further studies will be needed to clarify this. Moreover, the reduction in expression could be reflection of disruption to the mitochondrial membrane and subsequent autophagy.

Separately, there also exists a recently reported copper-dependent macro autophagic process mediated by glutathione peroxidase 4 (Xue, Yan et al. 2023).

Therefore, further studies would be needed to understand the role of SLC25A3 gene in PCa and to delineate the relationship between cuproptosis and doxazosin-induced cell death.

Among the genes which had a fold change of over 2, we then identified that 143 genes underwent the greatest fold changes between the two time points of 24 h and 48 h. These fold changes were more likely to be from exposure to doxazosin rather than the cell conditions. However, the control flasks significantly have higher population of cells that in those exposed to doxazosin. It is therefore possible that these fold changes between control and doxazosin treated group might arise from the discrepancy in the population of the cells, which in turn can influence several factors including those that involve cell-cell adhesion and nutrition depletion.

Our next approach was to look at specific gene families to identify which genes in the groups underwent fold changes (Tables 14 to 27). We looked at the fold expression within individual genes that are classed under the following gene families, namely: autophagy, adrenoreceptor gene family, apoptosome gene family, caspase gene family, Bcl-2 gene family, BH3 subset of Bcl-2 gene family, cyclin-dependent kinase gene family, the cyclin gene family, death inducing signal complex gene family, EARP gene family, MTORC 1 and 2 gene families, PIK3C3 gene families, SNARE gene families and TNF gene families. The selection of these gene families was based on the hypothesis that the cell death induced by doxazosin would involve one or more of the pathways (namely autophagy, apoptosis and anoikis) and such gene

fold changes would be reflected at a transcriptome level which can be identified using next generation sequence analysis.

Table 28: Summary table of changes in gene expression in the various gene families in PC-3 cells exposed to doxazosin compared to control. The colour schematic below is also replicated on figure 66 for easier correlation.

| Gene Family | Total Genes | Significant at both time points (%) | Not significant at both time points (%) | Significance changes between time points (%) | Uncertain |
|----------------|-------------|-------------------------------------|---|--|-----------|
| | | | | | |
| Autophagy | 30 | 15 (50%) | 9 (30%) | 6 (20%) | 0 |
| Adrenoreceptor | 2 | 0 | 1(50%) | 0 | 1 |
| Apoptosome | 3 | 1 (33%) | 2 (66%) | 0 | 0 |
| Caspase | 9 | 8 (88%) | 0 | 1 (12%) | 0 |
| Bcl-2 | 11 | 2 (18%) | 3 (27%) | 6 (54%) | 0 |
| BH3 subset | 11 | 8 (72%) | 1 (9%) | 2 (18%) | 0 |
| CDK GF | 24 | 11 (45%) | 6 (25%) | 6 (25%) | 1 |
| Cyclin GF | 26 | 15 (58%) | 3 (11%) | 8 (31%) | 0 |
| DISC | 5 | 4 (80%) | 1 (20%) | 0 | 0 |
| EARP | 4 | 2 (50%) | 1 (25%) | 1 (25%) | 0 |
| MTORC 1 & 2 | 8 | 5 (63%) | 2 (25%) | 1 (12%) | 0 |
| PIK3C3 | 7 | 4 (57%) | 2 (29%) | 1 (14%) | 0 |
| SNARE | 14 | 7 (50%) | 4 (29%) | 3 (21%) | 0 |
| TNF | 7 | 5 (72%) | 0 | 1(14%) | 1 |

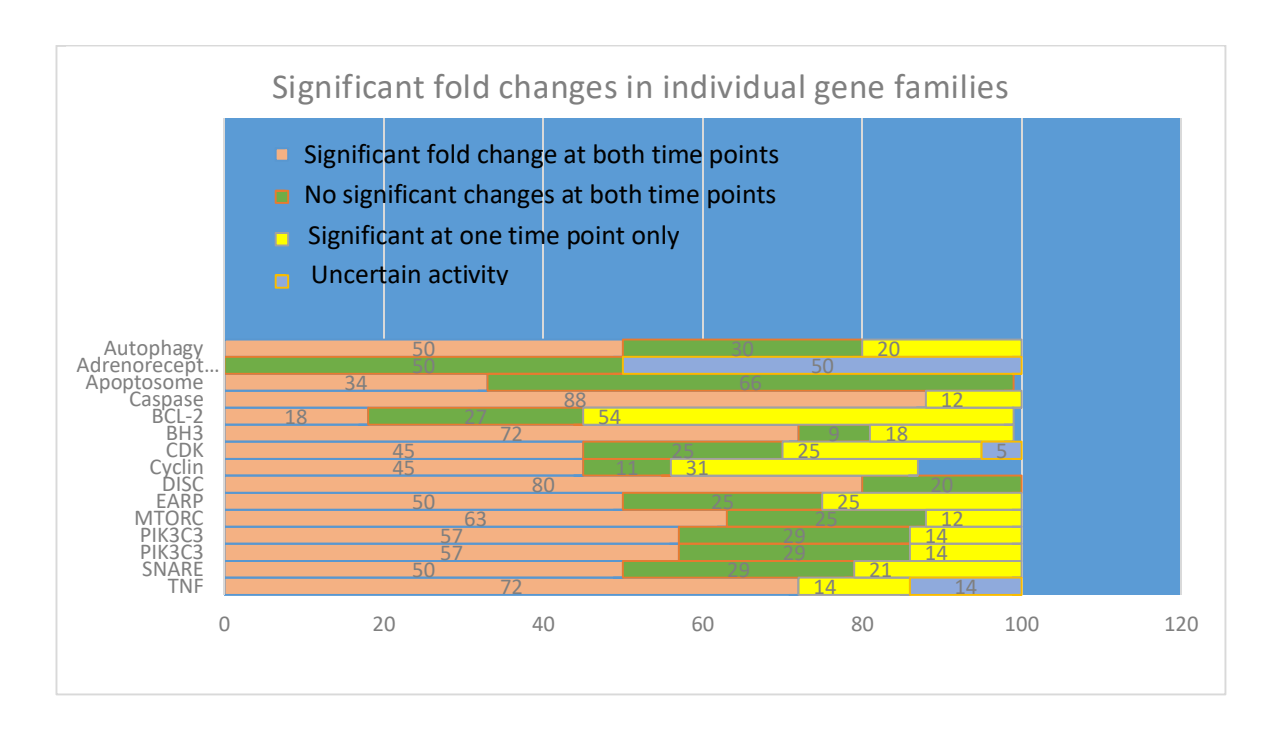


Figure 66: Data from Table 28 shown as a graphical representation to highlight the changes in gene expression in the various gene families in PC-3 cells exposed to doxazosin compared to control.

Next, we assessed the first 17 genes in the table 13 to identify if these changes in expression could be related to an increased duration of exposure to doxazosin or to a discrepancy from the reduced cell population in doxazosin-treated group as compared to the control group as the latter has a higher population density and more confluent.

EGR1, also known as early growth response-1 gene, encodes zinc finger nuclear proteins as functions as a transcriptional regulator (Cao, Mahendran et al. 1993, Arora, Wang et al. 2008). Interestingly, it is also a cancer suppressor gene and involves the induction of *TGF-β1* in its tumour suppression activity (Liu, Calogero et al. 1996).

RMRP gene (also known as RNA component of mitochondrial RNA processing endoribonuclease) encodes the RNA component of mRNA processing endoribonuclease, which cleaves mRNA at the priming site of mitochondrial DNA replication (van Eenennaam, Jarrous et al. 2000). They can also interact with telomerase reverse transcriptase catalytic subunit to form RNA-protein complex and double stranded RNA that can be processed into siRNA (Maida, Kyo et al. 2013). Pathway analysis of *RMRP* gene activity have shown to down regulate several genes including those associated with cell proliferation and differentiation (Rogler, Kosmyna et al. 2014).

TNFAIP3 gene encodes for TNF alpha-induced protein 3 (also known as A20 protein), which is a zinc finger protein that inhibits NF-kappa-β activation as well as TNF-mediated apoptosis (Van Antwerp, Martin et al. 1998, Hsu, Young et al. 2000). Additionally overexpression of A20 has been postulated to play a role in resistance to chemotherapy (da Silva, Minussi et al. 2014).

Several *HSP* genes, also called heat shock protein genes, have been upregulated with >1 fold-change and these included *HSPA1A* (also known as *HSP70*), *HSPA1B*, and *HSPA6*.

These 3 genes encodes for the family of proteins called HSP70, which consists of adenosine triphosphatase molecular chaperones of 70 KDa size that play a critical role in unfolding misfolded or denatured proteins and maintain such proteins in a folding-competent state (Murphy 2013). The chaperone proteins thus improve cellular survival in conditions of proteotoxic stress by facilitating protein damage repair (Radons 2016). HSP70 has also been shown to confer resistance to stress-induced apoptosis and improve survival to radiation induced damage (Kennedy,

Jager et al. 2014, Radons 2016). Therefore, the increased expression of genes encoding for the HSP70 family of chaperone proteins may suggest that it may play a role in supressing the apoptosis machinery following exposure to doxazosin.

Alternatively, doxazosin could lead to a proteotoxic response within the cells and the *HSP70* over expression may reflect the augmented response to protein damage.

When protein damage occurs, the balance between protein folding and degradation (proteostasis) is controlled by heat shock proteins, ubiquitin proteasome system, autophagy, and lysosome dependent systems (Dokladny, Myers et al. 2015). An elevated HSP70 can therefore be a reflection of increased repair as well as recycling, vesicle trafficking and repair. Not surprisingly, an upregulation of *HSP70* is a marker of increased endocytosis, especially the clathrin-mediated pathway (Vega, Charles et al. 2010, Sousa and Lafer 2015). Overexpression, of *HSP70* may thus facilitate proteostasis on one hand, whilst on the other hand increase clathrin-mediated doxazosin trafficking into cells, supress apoptosis and lead to an autophagic response.

FOS gene encodes leucine zipper nuclear phosphoproteins that can dimerize with proteins in the JUN family, to form the transcription factor complex activator protein-1 (AP-1) (Neuberg, Adamkiewicz et al. 1989, Steinmuller, Cibelli et al. 2001). The latter controls a wide range of cellular processes including differentiation, cell proliferation, endothelial cell migration, cell adhesion and apoptosis (Galvagni, Orlandini et al. 2013, Jia, Ye et al. 2016). Additionally, inhibition of dynamin 2 is a strong stimulator of the AP-1 pathway (Szymanska, Skowronek et al. 2016). *DNM2* mutations using dominant-negative *Dyn2 K44*A mutations lead to an increased phosphorylation of several receptor tyrosine kinases, which initiated JNK-dependent signalling cascades that resulted in stimulation of AP-1 target genes (Szymanska, Skowronek

et al. 2016). Our previous results have shown that doxazosin induced cell death was a dynamin-dependent process and that chemical inhibition of dynamin using dynasore attenuated these effects of doxazosin in PC-3, DU-145, LNCaP and HT-1376 cell lines. The expression of *DNM2*, the gene encoding for dynamin 2, is downregulated when exposed to doxazosin over 24 h. The log2 ratio for DNM2 was 0.31 after exposure to doxazosin for 24 h, and this was downregulated to -0.27 over 48 h exposure. Therefore, reduced dynamin 2 following exposure to doxazosin for 48 h could at least in part account for upregulation of AP-1 between the two time points in our experiment.

Ras related glycolysis inhibitor and calcium channel regulator is a suppressor of voltage gated calcium channels and has been shown to inhibit cardiac hypertrophy through its interaction with calmodulin-dependent kinase II (Chang, Zhang et al. 2007). It also acts as a positive regulator of EGFR pathway by enhancing the endosome-associated nuclear translocation of EGFR (Yeom, Nam et al. 2014). Nonetheless, the increased expression of this gene when exposed to doxazosin remains unclear.

CLDN14 encodes for claudin family of proteins that are exclusively responsible for the formation of tight junction strands and are also a critical component in the coat complex II mediated vesicle transport system required for entry of hepatitis C virus into the cell (Sawada, Murata et al. 2003, Yin, Li et al. 2017). Doxazosin has been shown to induce anoikis and this results in detachment from the surface; additionally, cell-to-cell adhesion is also lost (Keledjian and Kyprianou 2003). A recently synthesized quinazoline compound DZ-50, which is a doxazosin based derivative have been shown to downregulate the expression of claudin (by downregulation of CLDN11) and other genes involved in focal adhesion integrity in DU-145 PCa cells

(Hensley, Desiniotis et al. 2014). In agreement with the above findings, our results also show that *CLDN11* is downregulated (log2 ratio of -1.82 and -1.94 at 24h and 48h, respectively) in PC-3 cell lines. On the other hand, *CLDN9* was not expressed at 24 h and was significantly upregulated (log2 ratio of +1.86) at 48 h. These suggest that interpretation of the results of claudin family gene expression are difficult as they may vary greatly between the individual genes as well as the duration of exposure of doxazosin.

IL24 and *IL8* genes encodes for the IL10, also known as interleukin 10, family of cytokines (Piazzon, Lutfalla et al. 2016). Overexpression of these genes have been postulated to increase expression of *GADD* genes (encodes for growth arrest and DNA damage proteins) which induces growth arrest and induces apoptotic cell death (Fornace, Jackman et al. 1992, Zhan, Lord et al. 1994). These findings suggest that doxazosin may be genotoxic to the PC-3 cell lines and that growth suppression from doxazosin maybe mediated by IL10 subfamily.

MAP7D3 gene (also known as microtubule associated protein containing domain 3) encodes for microtubule associated protein 7 (MAP7) promotes the assembly and stability of microtubules. (Ramkumar, Jong et al. 2018). Another significant MAP is LC3 which is a molecular marker of autophagosomes and is encoded by the MAPLC3 gene family (Tanida, Ueno et al. 2008, Liu, Xu et al. 2013, Wild, McEwan et al. 2014). The MAPLC3 gene family includes MAPLC3A, MAPLC3B, MAPLCB2 and MAPLC3C (Kar, Singha et al. 2009). Our results show that MAP1LC3A, MAP1LCB and MAP1LC3B2 were significantly upregulated (log2 ratios 0.66, 0.24 and 0.68, respectively) in the PC-3 cell lines after 48h of exposure to doxazosin. MAP1LC3C was not expressed in PC-3 cell lines at any of the time points tested.

ARHGAP27 gene (also known as Rho-GTPase activating protein 27) encodes for a large family of proteins that activate Rho GTPases, which play a critical role in clathrin-mediated endocytosis(de Toledo, Senic-Matuglia et al. 2003, Katoh and Katoh 2004). Another gene that has been upregulated is the RGS4 gene (also known as regulator of G protein signalling 4) and are located within the cytoplasm and involved in deactivating G-protein signalling (Tamirisa, Blumer et al. 1999). Additionally, the RGS4 gene is known to interact with the COPB2 gene which encodes for the protein coatomer subunit beta 2, which is an integral part of clathrin scaffolds and also essential for budding of non-clathrin coated vesicles from Golgi complex for transport to ER (Waters, Serafini et al. 1991, McMahon and Mills 2004, Antonny 2006, Beck, Rawet et al. 2009, Yu, Lin et al. 2009).

TOP2A gene (also known as topoisomerase 2 alpha) encodes for TOP liα, a nuclear enzyme that controls the DNA coiling and thereby the topological structure and is a marker of cell cycle progression (Smith 1981, de Resende, Vieira et al. 2013). Several chemotherapeutic agents such as etoposide, doxorubicin and ICRF-193 are inhibitors of TOP2A (Ishida, Sato et al. 1994, Maede, Shimizu et al. 2014). In PCa, higher levels of TOP liα has been correlated with higher Gleason scores and preoperative PSA levels and TOP liα inhibitors block androgen signalling (de Resende, Vieira et al. 2013, Li, Xie et al. 2015). The upregulation of *TOP2A* with increasing exposure to doxazosin remains unclear and may possibly be related in part to the toxic effects of doxazosin on nuclear chromatin and microtubules, and in part the elevation may reflect the androgen-resistant profile of PC-3 cells (de Resende, Vieira et al. 2013).

Our preliminary analysis showed that several gene families are involved in the process of doxazosin-induced cell death. Several genes in the autophagy and apoptosis gene families underwent wide variations in expressions suggesting that both these processes are involved in doxazosin-induced cell death. Nonetheless, our results would need to be confirmed on other cell lines and further verified to confirm protein analysis and this would be a subject of further studies.

Chapter 8

Effect of doxazosin on the growth of high-grade bladder cancer *In Vivo*

8.1 Introduction

Doxazosin-induced cell death, observed in *In Vitro* studies, have been replicated *In Vivo* studies using PCa cells (Tahmatzopoulos and Kyprianou 2004). Our previous experiments have established that doxazosin also induced dosedependent cell death in high grade BCa cell line, HT-1376. We investigated if these *In Vitro* effects of doxazosin on BCa cells can also be replicated *In Vivo*, and if doxazosin can reduce the growth of bladder tumours *In Vivo*. For this, we chose HT-1376 as they are a well characterized cell line and our team had experience of this cell line in nude athymic mice (Shabbir, Ryten et al. 2008, Shabbir, Thompson et al. 2008). Additionally, it is difficult to obtain tissue form human BCa cells and is expensive to characterize their individual properties fully.

Several established animal models of cancer exist within the literature (Sharkey and Fogh 1984, van Weerden and Romijn 2000, Roy-Burman, Wu et al. 2004, Ittmann, Huang et al. 2013, Cekanova and Rathore 2014, Grabowska, DeGraff et al. 2014, Szadvari, Krizanova et al. 2016). The majority of these involve inoculation of human cancer cells (obtained from patient or from established cell lines) into immunocompromised mice. More recently, genetically engineered mice (Shappell, Thomas et al. 2004) have also been described and are gaining in popularity due to their ability to replicate the physiological and pathological characteristics of the disease process being studied (Roy-Burman, Wu et al. 2004, Seager, Puzio-Kuter et al. 2010, Ahmad, Sansom et al. 2012, Ding, Xu et al. 2014, John and Said 2017).

cell deficient. The SCID mice are expensive to use in larger numbers and their severe immune deficiency status render them very vulnerable and at risk of sepsis and death; nonetheless, they are more effective in reproducing reliable metastatic event (Shibayama, Tachibana et al. 1991).

In the present study, we used nude athymic mice in all the experiments.

8.2 Methods:

8.2.1 Ethical considerations:

All experiments were conducted according to Home Office Guidelines and under a Home Office of United Kingdom license granted to Dr Cecil Thompson and with local ethical committee approval.

The study was conducted under the guidance of animal welfare team under the guidance of Dr Cecil Thompson at the UCL Animal Research House and in accordance with the Animals (Scientific Procedures) Act 1986. Specialized individually ventilated cages were used to house the immunodeficient mice in a pathogen free environment. The mice were acclimatised for 5 days before experiments were commenced. The Well Being Score Assessment was used to evaluate the wellbeing of the mice (Table 8.1) and the overall score calculated once weekly or more frequently if mice appeared to be distressed. A pre-formulated strategy protocol (Table 8.2) was then adhered to and it was based on the overall wellbeing score of each mouse.

Table 8.1: Assessment to calculate the 'Wellbeing score' of nude athymic mice based on appearance, change in body weight, behaviour and tumour characteristics.

| Para | Score | |
|------------------------|--|---|
| | Normal | 0 |
| (A) Appearance | Decreased grooming | 1 |
| | Piloerection | 2 |
| | Hunched posture | 3 |
| | 0-4% | 0 |
| (B) % Loss of Body | 5-9% | 1 |
| Weight | 10-14% | 2 |
| | 15-20% | 3 |
| | Normal | 0 |
| (C) Provoked Behaviour | Agitated | 1 |
| | Isolated | 2 |
| | Lethargic | 3 |
| (D) Clinical signs for | Tumour < 0.5 cm | 0 |
| subcutaneous tumour | Tumour 0.5 – 1.0 cm | 1 |
| models | Tumour 1.1 to 2.0 cm | 2 |
| | Tumour > 2.0 cm | 3 |
| | Any evidence of ulceration over tumour | 4 |

Note: For sections A-C, consecutive readings of maximum score (3) add a score of +1 per section. Overall score is the sum of score from sections A-D and maximum overall score is 16.

Table 8.2: Protocol for strategies to be adopted on the basis of final overall wellbeing scores

| Score | Strategy |
|-------|--|
| 0-4 | Normal animal |
| 5-8 | Increased monitoring: analgesia required |
| 9-12 | Increased monitoring: Analgesia is required. If animal is in treatment group, all therapy to be stopped. Involve and seek help of named veterinary surgeon |
| 13-16 | Kill animal by method outlined in schedule 1 without delay |

8.2.2 Subcutaneous tumour cell inoculation:

HT-1376 cells (1 x 10^6 cells with over 90% viability) were suspended in matrigel (total inoculation volume of 150 μ L in a ratio of 1:1), as per protocol previously described (Sato, Gleave et al. 1997).

Matrigel facilitates the uniformed and localized tumour growth and retains the inoculated cells in the discrete area at the site of inoculation (Benton, Arnaoutova et al. 2014). This allows the assessment of correct tumour cell placement in the subcutaneous tissue and subsequent monitoring of its growth. Matrigel is composed of an extract of basement membrane proteins and remains in liquid state at 4 C but rapidly solidifies into a gel at room and body temperature (Kleinman and Martin 2005). Subcutaneous injections of tumour suspended in matrigel induces rapid tumour development and growth of human tumours in athymic mice (Sato, Gleave et al. 1997, Kleinman and Martin 2005, Benton, Kleinman et al. 2011, Benton, Arnaoutova et al. 2014).

8.2.3 Preparation of matrigel and inoculation of cells:

Matrigel (storage temperature -20 C), is thawed overnight at 4 C to render it into the liquid state. Pre-cooled syringes and needles were used in handling matrigel to avoid it from solidifying into gel at room temperature. Matrigel was vortex mixed with cells (placed in Eppendorf containers on ice) and loaded into precooled syringes (total inoculation volume of 150 μ L). These were injected to right flank of athymic mice using a 20-guage needle while the mice were lightly anesthetized with halothane.

8.2.4 Treatment protocols:

We used 6 to 10 week nude athymic mice for the experiments. The mice were lightly anaesthetized with halothane. Test mice (n=5) received HT-1376 cells dispersed uniformly in matrigel and inoculated as described previously. Control mice (n=5) received vehicle solvent dispersed uniformly in matrigel (inoculation volume of 150 µL for both test and control mice). Exogenous doxazosin was given (3mg/kg) daily via intraperitoneal injection into tumour bearing mice. Mice were followed up weekly for up to 42 days and then killed using increasing concentrations of carbon dioxide in accordance with the schedule 1 guidelines of Home Office UK. The rate of change of established tumour growth was calculated using the formula previously described (Ahmed, Johnson et al. 2002):

Fractional tumour volume = (volume on day measure)/ (initial pre-treatment tumour volume)

8.3 Results

8.3.1 Effect of doxazosin on freshly implanted HT-1376 cells:

Daily intraperitoneal injections of doxazosin (3 mg/Kg) significantly reduced the rate of growth of freshly implanted HT-1376 cells when compared to control (n=5). After 42 days of treatment, doxazosin reduced mean fractional tumour volume significantly (Figure 67).

No obvious side effects relating to treatment were noted in the treatment or control groups. Histological analysis of the neoplasms using TEM showed the tumours maintained the characteristics of urinary transitional carcinomas. In the doxazosin treated group, TEM also revealed the presence of autophagy.

8.3.2 Effect of doxazosin on established HT-1376 tumour growth:

Daily intraperitoneal injections of doxazosin (3 mg/Kg) significantly reduced the rate of growth of established tumour compared to control (n=5). After 42 days of treatment, doxazosin reduced mean fractional tumour volume significantly (Figure 68).

No obvious side effects relating to treatment were noted in the treatment or control groups. Histological analysis of the neoplasms using TEM showed the tumours maintained the characteristics of urinary transitional carcinomas. In the doxazosin treated group, TEM also revealed the presence of autophagy.

Figure 67: Effect of doxazosin (3mg/kg) on the growth of freshly implanted HT1376 tumour *In Vivo* (versus control).

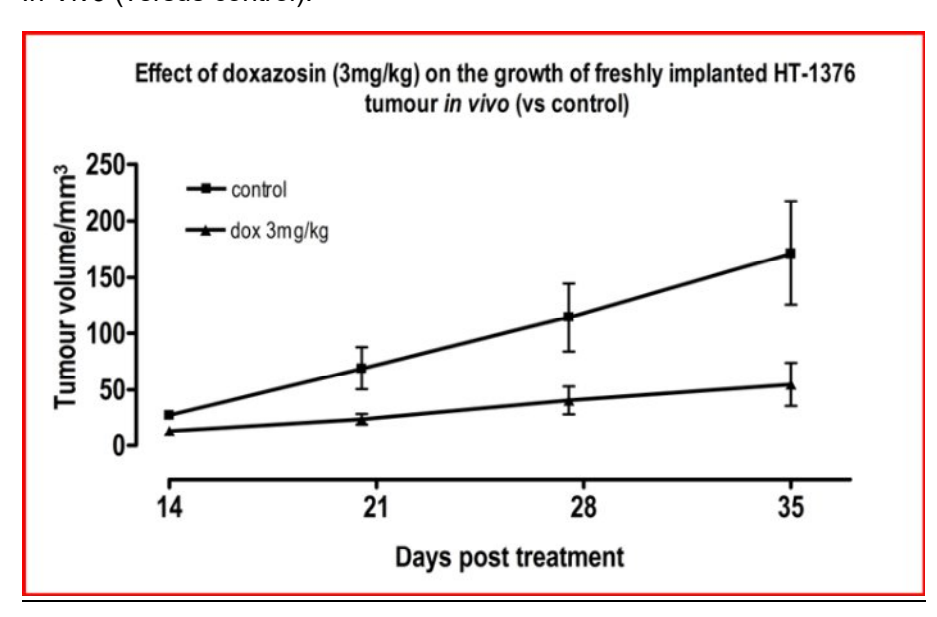


Figure 68: Effect of doxazosin (3mg/kg) on the fractional growth of established HT1376 tumour *In Vivo* (versus control).

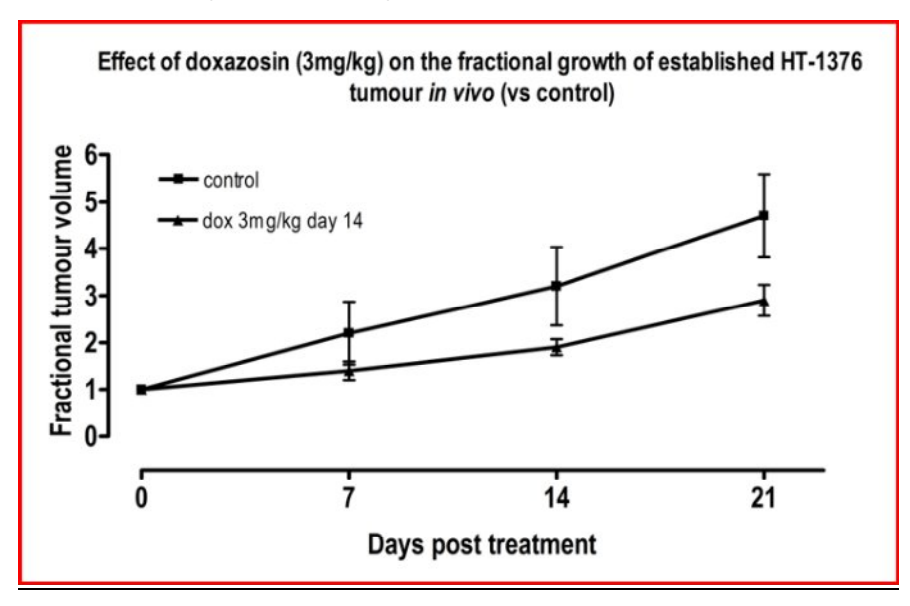


Figure 69: Effect of doxazosin (3mg/kg, intraperitoneal) on the growth of implanted HT1376 cells *In Vivo* after 14 days of initial growth. Lower mouse in the figure received doxazosin treatment versus vehicle only treatment in the upper mouse.



Figure 70: Resected specimens from the mice shown in figure 69 (above). The resection sample from the control is on the left and the resection sample of doxazosin treated mice is on the right.



8.4 Discussion

Athymic nude mice animal model is a widely used tool in cancer research especially for preclinical testing of drugs (Szadvari, Krizanova et al. 2016). These mice models have a deletion of *Foxn1* gene, which results in an absent thymus and consequent reduction in T cells and immunosuppression (Szadvari, Krizanova et al. 2016). The suitability of the athymic nude mice to xenograft models is due to their lack of an immune response to the xenografts. The shorter overall life span and the rapid disease progression are factors that contribute to the advantages of animal models in the experimental setting (Cekanova and Rathore 2014).

More recently, genetically engineered mice models have been used in the PCa research with over 40 different models described to date (van Weerden and Romijn 2000, Ittmann, Huang et al. 2013) and the choice of the model will be determined by the desired experimental conditions as well as the inherent advantages or disadvantages of a specific xenograft or genetically engineered model (Grabowska, DeGraff et al. 2014). Nonetheless, mice rarely develop spontaneous PCa (Suwa, Nyska et al. 2002) suggesting that there are fundamental differences between human and mouse prostate biology and tumorigenesis (Grabowska, DeGraff et al. 2014).

Our group has had previous experience using xenograft model in nude athymic mice with HT1376 cells (Shabbir, Ryten et al. 2008) and this dictated the choice of using an experimental model that had been previously tried and tested in our lab. Using HT1376 subcutaneous cell inoculations we were able to show for the first time that intraperitoneal injections of doxazosin (3mg/kg/day) significantly and effectively reduced the growth of both freshly implanted and established tumour outgrowths as

compared to vehicle controls (Pavithran, Shabbir et al. 2017). Using a combination of immunohistochemistry and TEM, we were able to show that the inoculated tumour cells retained their original phenotype and cellular characteristics, further validating the relevance of these results to the expected effects of doxazosin treatment for tumours in actual patients.

Experiments using animal models of PCa using quinazoline-based adrenergic receptor antagonists have been previously reported (Chiang, Son et al. 2005). Chiang et al, in their experiments on transgenic adenocarcinoma of the mouse prostate (TRAMP) models, found that late administration of doxazosin did not have any effect on established tumour whilst early administration of doxazosin supressed the growth of prostate tumour (Chiang, Son et al. 2005). Moreover, administration of doxazosin completely supressed metastasis irrespective of the stage of development of the tumour (Chiang, Son et al. 2005).

Our experiments showed that doxazosin reduced the growth of both freshly implanted –and –established tumours as compared to vehicle controls. The difference in the results (from previously reported *In Vivo* experiments with PCa) could be attributed to the differences in the cell line used, the mice models and the experimental conditions, particularly the dose of doxazosin used. Whilst 3mg/kg of doxazosin intraperitoneally was well tolerated by the nude athymic mice in our experiments, the experience with TRAMP models was considerably different with death resulting within 4-16 days of oral treatment with 2mg/kg of doxazosin – hence necessitating the use of a lower dosage of doxazosin in TRAMP mice models (Chiang, Son et al. 2005). The same group had been able to administer a high dose 100 mg/day of doxazosin (daily, orally) without adverse consequences in SCID nude athymic mice (Kyprianou and Benning 2000) further supporting the suggestion that

the reported deaths in TRAMP models were due to an intrinsic inability to tolerate higher doses of doxazosin by the TRAMP mice models.

Another aspect of this study was to assess the effect of doxazosin on the development of tumour metastasis. Unfortunately, no distant metastasis was seen in the doxazosin or vehicle treated group. Subcutaneous xenograft mice models do not fully replicate the disease process compared to that of orthotopic implanted tumours, and the inability to find distant metastasis could have been due to the subcutaneous tumour implantation or too short a time to allow for metastatic spread to become evident clinically.

By the time we had identified the presence of extensive autophagy in our *In Vitro* experiments, the *In Vivo* experiments had already been completed. As a result, we were unprepared at the time of experiment planning and assessment of histopathological analysis to assess specifically for the presence of autophagy in the xenograft implants. Nonetheless, we looked at the xenograft sections retrospectively and found evidence of autophagy as well as the presence of apoptosis in xenograft tumour specimens. However, these evaluations would need further confirmation using immunohistochemistry techniques that can specifically label and quantify the presence of anti-LC3II antibodies in the xenograft specimens as well as demonstration of characteristic morphological features of autophagy in sections that are suitably prepared for viewing on TEM.

We suggest that future experiments should take into consideration the evaluation of autophagy in xenograft specimens from the experiment planning stage itself and suitable sections for immunohistochemistry and TEM should be prepared as part of the histopathological analysis.

Chapter 9

Discussion

PCa is the most common cancer in men in developed countries; worldwide, it is the second most commonly diagnosed cancer in men (Bray, Ren et al. 2013, Torre, Bray et al. 2015, Shah, loffe et al. 2022). BCa accounted for 430,000 cases in 2012 and is the ninth most common cancer worldwide (Malats and Real 2015, Lobo, Afferi et al. 2022, Siegel, Miller et al. 2023).

Androgen ablation therapy is the mainstay for locally advanced or metastatic PCa, However, the inevitable development of androgen resistance is a major disadvantage of androgen ablation treatment and it offers only a short-term benefit to most patients (Wasim, Lee et al. 2022). Whilst second-generation AR antagonists such as enzalutamide, apalutamide and darolutamide has improved survival they do not result in cure, and these patients too progress to lethal neuroendocrine PCa (Chen, Zhou et al. 2022). More recently, Lutetium177 therapy has been used for treatment of such metastatic PCa (Fanti, Briganti et al. 2022).

At the start of this research, there was a growing body of evidence suggesting that alpha-1A adrenergic receptor antagonists inhibit the growth of various cancers, including PCa and BCa. This effect appeared to be independent of their ability to bind with the alpha-1A receptors and instead was linked to the quinazoline-based structure.

It was found that the cumulative incidence of developing BCa in those who were prescribed alpha-1 antagonists (doxazosin or terazosin) for BPE or hypertension was 0.24% as compared to 0.42% in the untreated group (Martin, Harris et al. 2008). The study concluded that men treated with alpha adrenoceptor antagonists have a 43%

lower attributable relative risk of developing BCa than untreated men (p=0.083) (Martin, Harris et al. 2008).

The same research group also conducted another study on the same cohort of 27,138 males to understand the relationship between PCa and the use of alpha-1 antagonists. This study revealed that in the treated group (doxazosin or terazosin for management of hypertension of BPE), the cumulative incidence of PCa was 1.65% as compared to 2.41% in the untreated group (Harris, Warner et al. 2007). This equates to 7.6 fewer cases of PCa per 1000 men when treated with alpha-1 antagonists, and these men had a 31.7% lower attributable relative risk of developing the disease (Harris, Warner et al. 2007).

The precise molecular and cell signalling mechanisms of doxazosin and other piperazinyl quinazoline alpha receptor antagonists remain unclear. Given that only quinazoline-based adrenergic receptor antagonists exhibited anticancer effects, the role of adrenergic receptors themselves has been questioned. (Kyprianou, Chon et al. 2000). Furthermore, in addition to its alpha-1 antagonist activity, quinazoline based alpha adrenergic receptor antagonists such as doxazosin can act as a HEGR ligand, (Bilbro, Mart et al. 2013) EGF receptor inhibitor (Hui, Fernando et al. 2008), VEGF-mediated angiogenic antagonist (Park, Kim et al. 2014), FGF receptor-2 antagonist (Ballou, Cross et al. 2000), and tyrosine kinase receptor agonist (Keledjian, Garrison et al. 2005, Petty, Myshkin et al. 2012). All these suggest that doxazosin can modulate several signalling pathways (Walden, Globina et al. 2004, Garrison and Kyprianou 2006, Park, Kim et al. 2014, Batty, Pugh et al. 2016). It has also been shown that doxazosin acts via the extrinsic apoptotic pathway on the death receptors (TGF-beta 1 receptor and TNF alpha). This leads to adaptor

protein complex formation, caspase-3 –and –caspase-8 activation, which in turn led to FADD-dependent apoptosis in the PCa cell lines PC-3 and BPH-1 (Garrison and Kyprianou 2006).

Alternatively, doxazosin can also mediate apoptosis via the intrinsic pathway via release of calcium from ER leading to mitochondrial release of cytochrome-*c* and caspase-9 activation (Batty, Pugh et al. 2016). Additionally, it can directly exert its action on DNA either by DNA fragmentation or by inhibiting topoisomerase 1 leading to DNA damage, intercalation of DNA and cell death (Batty, Pugh et al. 2016). In addition to these actions, doxazosin modulates PI3K/Akt signalling pathways by inhibiting downstream VEGFR-2/Akt/mTOR signalling as well as reducing HIF-1a expression and VEGF expression, and these have been postulated to explain its ability to inhibit angiogenesis (Park, Kim et al. 2014).

Previous experimental data had also already shown that that the anticancer actions of doxazosin on PCa and BCa were independent of its adrenergic receptor activity (Tahmatzopoulos, Rowland et al. 2004, Tahmatzopoulos, Lagrange et al. 2005). Furthermore, novel molecules were developed based on the quinazoline structure but devoid of adrenergic activity such as DZ-50 against PCa (Hensley, Desiniotis et al. 2014). However, despite this progress, the underlying mechanism through which quinazoline-based adrenergic receptor antagonists like doxazosin exert their anticancer effects remains unclear. Given the numerous signalling pathways modulated by doxazosin, we hypothesized that its anticancer activity is likely mediated through a receptor pathway. Initially, we speculated that doxazosin might exert its anticancer effects via a receptor that is structurally similar to the adrenergic receptor. The initial hypothesis was that doxazosin could be exerting its anticancer actions through a receptor that has a structural similarity to the adrenergic receptor

Using the UniprotKB/SwissProt databases, we performed BLAST searches for the adrenergic alpha receptor [P35348]. The resulting FASTA outputs were subsequently used to query the PSI-2 Search database (Lussi, Magrane et al. 2023). This showed that several members of the adrenergic receptor family and the serotonin or 5HT receptors had close structural similarities [Figure 8]. Interestingly, doxazosin interacts with serotonin receptors, which has been reported in studies on platelet activation (Jagroop and Mikhailidis 2001) and in cavernous smooth muscle contraction (Lau, Thompson et al. 2006). Pre-treatment with doxazosin prevented the early step in platelet activation thereby inhibiting the shape change in platelets (Jagroop and Mikhailidis 2001). Doxazosin also attenuated 5HT-mediated contractility of cavernous smooth muscles (Lau, Thompson et al. 2006). Furthermore, it has been hypothesized that 5HT receptors could possibly mediate the growth inhibitory effects of doxazosin (Siddiqui, Shabbir et al. 2005). Collectively, these suggested that doxazosin might influence the activity of 5HT receptors. Consequently, we decided to investigate the roles of doxazosin, other adrenergic receptors (besides the alpha-adrenergic receptor), and 5HT receptors, all of which share structural similarities with the alpha-adrenergic receptor.

First, we investigated the role of various adrenergic compounds in doxazosin-induced cell death. For our *In Vitro* experiments, we used three PCa cell lines (PC-3, DU145, and LNCaP) and one BCa cell line (HT1376). The adrenergic compounds tested included several agonists and antagonists: clonidine, idazoxan, and guanabenz (alpha-2 selective agonists), yohimbine (non-selective alpha antagonist), propranolol (non-selective beta antagonist), and imiloxan (alpha-2B antagonist). Given the structural similarity between alpha-1 and alpha-2 adrenergic receptors, we tested whether these compounds would alter the growth inhibition by doxazosin.

Our experiments with yohimbine, clonidine, guanabenz, imiloxan, and propranolol compounds demonstrated that pretreatment with these compounds did not attenuate the cell death induced by doxazosin. Whilst idazoxan inhibited the growth of PC3 cells and DU145 cells, it did not alter the growth of LNCaP or HT1376 cells. These findings suggest that growth inhibitory actions of idazoxan could be related to the androgen-resistant status of PC3 and DU145 cells. Not surprisingly, the growth inhibition of DU145 cells by idazoxan had already been reported previously though the mechanism of action remains to be fully elucidated (Eilon, Weisenthal et al. 2009). More importantly, idazoxan did not have any effect on doxazosin-induced growth inhibition in any of the cell lines tested. Based on these results, we concluded that adrenergic receptors do not mediate the anticancer actions of doxazosin.

Next, we assessed the role of 5HT receptors using serotonin hydrochloride and serotonin creatinine sulphate monohydrate, the latter being more water-soluble and resistant to photodecomposition. We found that 5HT induced proliferation in the cell lines tested. However, pre-treatment with 5HT did not mitigate doxazosin-induced cell death. These findings are consistent with previous studies showing that serotonin promotes the proliferation of PCa and BCa cells *In Vitro* (Siddiqui, Shabbir et al. 2005) and that this proliferative effect is inhibited by 5HT antagonists (Abdul, Anezinis et al. 1994). Our experiments with both these compounds (serotonin chloride and serotonin creatinine sulphate) were unable to demonstrate that 5HT receptors mediated doxazosin induced growth inhibition. We also repeated the experiment using BrdU assay with serotonin creatinine sulphate, obtained similar results to that of Cell-Titer 96® aqueous MTS assay. Taken together, we concluded that 5HT receptors did not mediate the cytotoxic effects of doxazosin in the PCa and BCa cell line we tested.

Though we concluded that doxazosin did not mediate its actions on cell viability via the receptors that have structural similarity to alpha-1 adrenergic receptor, at this stage of experiments, the receptor that mediated the cytotoxic actions of doxazosin remained elusive. However, our results were also in agreement with others that the cytotoxic actions of doxazosin in PCa and BCa were independent of the alpha-adrenergic receptor (Benning and Kyprianou 2002, Pavithran and Thompson 2012, Pavithran, Shabbir et al. 2017).

Following these findings, we initiated the development of doxazosin-resistant cells, as these cells could potentially exhibit up-regulation or down-regulation of receptors responsible for mediating the growth-inhibiting effects of doxazosin. Our hypothesis was that treating cell lines with a sub-lethal dose of doxazosin over time would prompt the emergence of doxazosin-resistant cancer cells. These resistant cells could then serve as a model to investigate the actions of doxazosin.

Using previously established experimental protocols (Chien, Astumian et al. 1999), we attempted to develop drug-resistant PCa cell lines (PC-3, DU-145 and LNCaP) in the first phase before extending the experiments to BCa cell lines. In brief, logarithmically growing PCa cells were exposed *In Vitro* to either serially increasing concentrations of doxazosin for short time intervals or a low dose doxazosin for longer periods. The attempts to develop PCa cell lines that are resistant to doxazosin were unsuccessful and therefore, we did not extend our experiments with BCa cell lines.

During the course of the above experiments to create resistant cell lines, we noted that all cell lines treated with doxazosin developed a granular appearance of the cytoplasm. These cytoplasmic granules, which could be seen on light microscopy,

were present in the doxazosin treated samples; control samples were devoid of such granular changes. PC-3 cells showed the most marked granular appearance whilst in HT-1376 cells these granulations were difficult to appreciate as these cells do not form a uniform monolayer and tend to grow into several layers. We also observed that the time taken for onset of granular appearance was directly proportional to the concentration of doxazosin to which the cells were exposed - the higher the concentration of doxazosin the faster these granulations appeared with the cytoplasm.

We, therefore, embarked on identifying and further characterizing the granulations. Initially, we stained using DAPS and aldehyde fuchsin as these granularities resembled lipofuscin granules. DAPS stains lipofuscin in magenta colour and aldehyde fuchsin in deep purple. (Perse, Injac et al. 2013). However, we were unable to demonstrate the presence of lipofuscin using these techniques.

Though we were unable to identify the nature of the granulations, we continued to study the relationship between the development of granulations and exposure to doxazosin. We focused on the relationship between concentration of doxazosin and the time taken for the granulations to appear. The morphological examination of the cell lines using light microscopy during these experiments suggested that:

- (a) appearance of granular cytoplasm was preceded by cell death
- (b) the actions of doxazosin were cumulative even when exposed to low doses of doxazosin but over a longer duration,
- (c) the effects were irreversible once the cells were exposed to concentrations over60 μM of doxazosin, and vice versa,
- (d) nutrient-depleted conditions, such as incubation in serum free media, potentiated doxazosin-induced cell death,

- (e) addition of lipoproteins to the culture medium negated the effects of nutrient depletion, and
- (e) the addition of cholesterol solution (1:1000) further abrogated the cell death induced by doxazosin.

We concluded, based on these observations, that developing doxazosin-resistant cell lines would not be feasible due to the cumulative effects of doxazosin and its reversibility at lower concentrations. This also led us to hypothesize that an active or passive transport mechanism might be involved in the entry of doxazosin into the cell, potentially bypassing receptor-mediated pathways and operating independently of receptor involvement. Considering the additive cytotoxic effects of doxazosin in serum-free and LPDS conditions, and the reversal of these effects with the addition of cholesterol, we postulated that doxazosin's action might be mediated by a receptor that undergoes endocytosis upon binding with doxazosin—potentially a lipid receptor.

To test this hypothesis, we used LDL receptor mutant fibroblast cell lines. Interestingly, doxazosin had no effect on cell viability at lower concentrations (12.5 μ M and 25 μ M) on these cells and over 50% of the cells were viable at 75 μ M of doxazosin. The LDL receptor mutant cell lines were difficult to grow in cell cultures and did not grow beyond 40% - 50% confluence. Despite our best efforts, establishing new batches of cells for experiments proved futile and therefore further experiments using this cell line had to be terminated. Hence, it is difficult to conclude if LDL receptors can be implicated in doxazosin-mediated toxicity.

To further explore how doxazosin is transported into cells, we examined the roles of common endocytic pathways and pinocytosis. We utilized chemical inhibitors

targeting clathrin and caveolin-mediated endocytosis, as well as inhibitors of pinocytosis.

It has been previously shown that cells can internalize small segments of its plasma membrane and this internalized segment could carry surface receptors and their bound ligands, nutrients, bacterial toxins, immunoglobulins, viruses and various extracellular soluble molecules into the cell by endocytosis (Lanzetti and Di Fiore 2008). Endocytosis had been shown to attenuate cell signalling and recent evidence in this field has given rise to the concept of signalling endosomes (von Zastrow and Sorkin 2007, Lanzetti and Di Fiore 2008).

Quinazoline compounds like doxazosin are small molecules, allowing them to enter the cell directly via endocytosis. Alternatively, doxazosin might first bind to a receptor, which is then internalized. Another possibility is that the lipophilic nature of doxazosin enables it to integrate into the lipid-rich cell membrane, which is subsequently internalized and transported into the cell. Previous studies using single-cell quantitative fluorescence imaging with BIODIPY-FL prazosin have shown that 40% of adrenergic binding sites are located intracellularly (Mackenzie, Daly et al. 2000). The mechanisms controlling the entry of macromolecules like doxazosin and prazosin, as well as the factors that regulate their subsequent trafficking within cells via endocytosis, remain poorly understood. Once these macromolecules enter the cells, they are sorted into different cellular destinations within early or sorting endosomes.

Molecular trafficking into the cell can occur by endocytosis and pinocytosis. The endocytic pathway can be further subdivided into clathrin-mediated, caveolin-

mediated and dynamin-mediated pathways though some overlaps exist between these individual pathways.

We investigated the role of endocytosis in doxazosin-induced cell death in *In Vitro* cell cultures of PCa and BCa cell lines by using chemical inhibitors of endocytosis that target the clathrin-mediated, caveolae-mediated, dynamin-mediated, and pinocytosis pathways. In brief, we observed that there was significant attenuation of doxazosin-induced cell death when clathrin-mediated or dynamin-mediated pathways were inhibited.

Since endocytosis is a temperature-dependent cellular process and at 10 C or below, the rate of endocytosis is negligible. Between 10 to 20 C endocytosis increases gradually and proportionately to the rise in temperature. Above 20 C, this rise is at a much higher rate when the temperatures are between 20 C to 41 C (Weigel and Oka 1981). Our results showed that the cell death induced by doxazosin was attenuated when cells were incubated on ice as compared to positive controls at 37 C. We did not observe a significant effect of temperature at lower concentrations of doxazosin (10⁻⁷ and 10⁻⁶). However, at concentrations of 10⁻⁵ and 10⁻⁴, we observed that there was a significant attenuation of doxazosin-induced cell death when cells were cooled on ice, suggesting that the effects of doxazosin of cell viability was temperature dependent. At these temperatures, both clathrin -and caveolae -mediated endocytic processes are inhibited and therefore does not provide information on the specific pathway that is inhibited. Moreover, the attenuation of cell death by cooling only provides indirect evidence of endocytic inhibition as the positive controls were not designed to show a direct inhibition of endocytosis but rather the consequence of such an effect on cell viability.

One limitation of using cell viability as an endpoint for the experiments was that cooling the cells had unintended effects on their ability to adhere to the MP, which was especially noticeable with LNCaP cells. Among the four cell lines tested, LNCaP cells were the least adherent under normal conditions. Cooling significantly impaired their adhesion. In contrast, androgen-independent cells (DU145 and PC-3) overexpress α6β4 integrin due to the loss of AR, which enhances cell adhesion (Baust, Klossner et al. 2010). This could likely explain the tolerance of androgenresistant cells (DU145 and PC3) to lower temperatures whilst androgen-dependent LNCaP cells underwent significant anoikis at lower temperatures even after a relatively short duration (4 h) of incubation with doxazosin. Though this added to an unwarranted artefactual error (due to loss of cells) to the interpretation of results, particularly with LNCaP cells, they may possibly have some clinical significance in dissemination and subsequent establishment of metastasis of such tumours especially when cryotherapy is used as a mode of treatment. On the other hand, exploitation of the accelerated cell death processes involved in temperature dependent cell death of androgen-dependent tumours may be useful in planning novel option of treatments for androgen-dependent PCa (Baust, Klossner et al. 2010).

Our next experiments focussed on dissecting the role of clathrin-mediated endocytic pathways in doxazosin-induced cell death of PCa and BCa cell lines. These inhibitors, besides interfering with specific steps of the endocytic pathway, are known to have several effects on other signalling processes within the cell thus confounding the validity of the results (Ivanov 2008). Chemical inhibitors of endocytosis serve as a preliminary step towards a broad understanding of the endocytic process (Ivanov 2008). Additionally, the different pathways of endocytosis are not clearly demarcated

and significant overlaps exist between the different endocytic pathways (Ivanov 2008). Moreover, endocytosis is linked to other unrelated cell processes such as apoptosis, autophagy and cell division, and these may have an influence on the results especially when cell viability is considered as an end point of the experiments (Polo, Pece et al. 2004, von Zastrow and Sorkin 2007, Fielding, Willox et al. 2012, Di Fiore and von Zastrow 2014). Conversely, whilst visualizing of molecular trafficking by confocal studies can more reliably quantify the endocytic transport of a molecule (in this case doxazosin) (Ivanov 2008, Di Fiore and von Zastrow 2014), the results will still need to be corroborated with cell viability studies to ascribe relevance to those findings to doxazosin-induced cell death. Therefore, designing studies to establish a direct relationship between endocytosis and cell viability is challenging due to several confounding factors. These include the overlap among various endocytic sub-pathways and the interaction between endocytic pathways and other cell viability-related pathways, such as autophagy, apoptosis, and endosomal signalling.

We selected sucrose, chlorpromazine, and dansylcadaverine as chemical inhibitors for clathrin-mediated endocytosis, following previously reported methods (Ostrom and Liu 2007, Ivanov 2008). We observed doxazosin-induced cell death in PC-3 was attenuated by pre-treatment with sucrose of 0.25 M and followed by exposure to doxazosin (10⁻⁵) significantly (p = 0.0256). At a higher concentration of sucrose of 0.4 M, this effect was significant for two different concentrations of doxazosin (p = 0.0122 for 10⁻⁵ and 0.0016 for 10⁻⁵ of doxazosin). Pre-treatment with sucrose 0.25 M and 0.4 M and followed by exposure to doxazosin (10⁻⁶) significantly (p = 0.0147 and 0.0475, respectively) attenuated the cell death induced by doxazosin in DU145 cells. In HT1376 cells, the only significant (p = 0.0004) attenuation was observed when

pre-treatment with sucrose 0.25 M was followed by exposure to doxazosin (10⁻⁶). Sucrose had no significant effect on viability of at all the other concentrations tested. Sucrose inhibits clathrin-mediated endocytosis by causing clathrin to become trapped in microcages, which is considered the primary mechanism of its action. Therefore, sucrose is experimentally used as an inhibitor of clathrin-mediated endocytosis, although it can also modulate macropinocytosis and reduce autophagic flux (Malek, Xu et al. 2007, Dutta and Donaldson 2012). Sucrose interferes with fluid phase of macropinocytosis (Carpentier, Sawano et al. 1989). Sucrose also induces vesicle accumulation and autophagy (Higuchi, Nishikawa et al. 2015). All these overlapping actions of sucrose on macropinocytosis and autophagy limits the ability to arrive at a conclusion on the basis of viability assays.

Another chemical inhibitor of clathrin-mediated endocytosis investigated was chlorpromazine. Chlorpromazine inhibits clathrin coated pit formation by a reversible translocation of clathrin and adaptor protein-2 from plasma membrane to intracellular vesicles (Wang, Rothberg et al. 1993, Ivanov 2008, Vercauteren, Vandenbroucke et al. 2010, Dutta and Donaldson 2012). One of the draw backs was that chlorpromazine can also reduce cell viability in concentrations required for inhibition of endocytosis (Vercauteren, Vandenbroucke et al. 2010). In our experimental data, not surprisingly, we noted a small but not significant reduction in cell populations exposed to doxazosin. However, chlorpromazine did not show any significant attenuation of doxazosin induced cell death in all the cell lines tested.

The next chemical inhibitor of clathrin-mediated endocytosis we investigated was dansylcadaverine. Dansylcadaverine and mono dansylcadaverine have been found to inhibit clathrin-mediated endocytosis as it stabilizes clathrin-coated vesicles and

reversibly inhibits the uptake of ligands and this process is selective for receptor-mediated ligands (Schlegel, Dickson et al. 1982). We conducted our experiments with dansylcadaverine as this is also lysosomotropic and autofluorescent and selectively concentrates within autophagosomes thus making it a very useful marker of autophagy (Ivanov 2008, Klionsky, Abdalla et al. 2012). Our results show that dansylcadaverine had a significant effect in attenuation of doxazosin induced cell death (p = <0.0001 in PC3, DU145 and HT1376 cells) and (p = 0.0002 in LNCaP cells), suggesting that these may have been mediated by inhibitory of effects of dansylcadaverine on clathrin-mediated endocytosis. As mentioned earlier, dansylcadaverine has significant overlapping actions on autophagic pathways and therefore the results could not be attributed to its clathrin-mediated endocytosis alone. Nonetheless, we exploited the autofluorescent properties of dansylcadaverine in our later experiments on autophagy to demonstrate the presence of autophagosomes in doxazosin treated cells.

Caveolin-mediated endocytosis is a clathrin-independent and dynamin-dependent pathway for endocytosis, and represents a parallel but distinct mechanism (Nabi and Le 2003). The caveolin –and –raft dependent pathways are characterized by their independence from the clathrin and a common sensitivity to cholesterol depletion and inhibition of dynamin function (Nabi and Le 2003). Caveolin-1 dependent endocytosis enhances chemosensitivity of Herceptin-2 positive breast cancers to trastuzumab and emtansine (Chung, Kuo et al. 2015) and a loss of caveolin-1 has been implicated in the pathogenesis of human cancers (Sotgia, Martinez-Outschoorn et al. 2012).

Caveolin-mediated –and –lipid raft mediated endocytosis happen at the caveolae (that are flask-shaped, 50-100 nm invaginations of plasma membrane), which are

enriched with specific lipids such as cholesterol and glycolipids (Ostrom and Liu 2007, Sotgia, Martinez-Outschoorn et al. 2012). These caveolae are similar to lipid rafts in that they are both enriched with sphingolipid and cholesterol, but caveolae also express a coat of caveolin proteins on the inner leaflet of the membrane bilayer; caveolin-1 is the predominant isoform of caveolin (Ostrom and Liu 2007).

In our experiments we used mevastatin, MBCD and cholesterol oxidase to assess the role of caveolin-mediated endocytosis pathway on doxazosin-induced cell death on PCa cell lines (PC-3, DU-145, LNCaP) and BCa cell line HT1376.

Mevastatin inhibits HMG-CoA reductase enzyme (Endo and Hasumi 1993), which controls the rate limiting step required for intracellular production of cholesterol (Feher, Webb et al. 1993). HMG-CoA inhibition results in inhibition of cholesterol synthesis, depletion of intermediates for small GTPase activation, disruption of vesicular trafficking and disruption of lipid rafts, and actin cytoskeleton disruption (Endo and Hasumi 1993, Hao, Mukherjee et al. 2004, Sidaway, Davidson et al. 2004, Liao and Laufs 2005, Cheng, Ohsaki et al. 2006, Ivanov 2008).

Incubation of cells with 10- 100 µM concentration of statins (simvastatin, lovastatin, mevastatin, pravastatin etc), results in nearly 100 % blockage of intracellular cholesterol synthesis (Sidaway, Davidson et al. 2004, Ivanov 2008). Statins also block the synthesis of franyl pyrophosphate and geranyl-geranyl pyrophosphate that are essential for post translation activation of intracellular proteins such as Ras, Rho and Rab families of small GTPases (de Toledo, Senic-Matuglia et al. 2003, Katoh and Katoh 2004, Liao and Laufs 2005). This results in accumulation of inactive GTPases and leads to profound and nonspecific disruption of the actin cytoskeleton (de Toledo, Senic-Matuglia et al. 2003, Liao and Laufs 2005, Ivanov 2008).

Mevastatin as a prototype statin given its well established role in preventing vesicle trafficking and disruption of caveolin mediated endocytic pathways (Hao, Mukherjee et al. 2004). Pre-incubating PC-3, DU145, LNCaP and HT-1376 with 20 μ M of mevastatin for 4 h followed by exposure to doxazosin 37 μ M had different effects on the above cell lines. Whilst in PC-3 and HT1376 cell lines the inhibition of cell death by doxazosin were unequivocally not significant (p = 0.1394 and p = 0.4635, respectively), this was not the case with DU145 cells where the p = 0.0507. Also, the attenuation of cell death by doxazosin by pre-incubation with mevastatin was unequivocally significant (p = 0.002) in LNCaP cells.

Since HMG-CoA inhibition also secondarily inhibits various downstream cellular processes (Endo and Hasumi 1993, Hao, Mukherjee et al. 2004, Sidaway, Davidson et al. 2004, Liao and Laufs 2005, Cheng, Ohsaki et al. 2006, Ivanov 2008), the results suggests that the cytotoxic effects of doxazosin may be contingent on the inter dependency of these processes for cell viability, and that these may be variable for each cell line. The attenuation of cytotoxic effects of doxazosin in LNCaP cells could be attributed to be the androgen-sensitive status of these cell lines as androgen-resistant cells have an increased aberrant HMG-CoA reductase activity (Kong, Cheng et al. 2018).

MBCD is a water soluble and hydrophobic compound that is capable of sequestering cholesterol molecules with a high affinity (Kilsdonk, Yancey et al. 1995). By this actions, MBCD depletes lipids and cholesterol available to the caveolae and lipid rafts, to inhibit this pathway of endocytosis (Ivanov 2008). In our experiments, we used MBCD at a concentration of 1 mM in serum free media to pre-treat PC3-, DU145, LNCaP and HT1376 to investigate if depletion of lipids and cholesterol from cells would result in an attenuation of cell death induced by doxazosin. We did not

observe any significant attenuation of the effects of doxazosin following pretreatment with MBCD.

Subsequently, we used cholesterol oxidase that converts cholesterol into 4-cholesten-3-one. This compound gets enriched in the caveolae, significantly altering its properties and disrupting caveolin-mediated internalization of endocytic vesicles (MacLachlan, Wotherspoon et al. 2000, Ivanov 2008). We did not observe a significant effect on doxazosin induced cell death any of the cell lines (PC-3, DU145, LNCaP and HT1376) were pre-incubated with cholesterol oxidase.

Taken together our results with mevastatin, MBCD and cholesterol oxidase suggests that caveolin mediated pathways were unlikely to have a significant role in intracellular trafficking of doxazosin.

Pinocytosis or macropinocytosis is an actin-dependent mechanism and functions in parallel to clathrin –and –caveolin mediated pathways (Thurn, Arora et al. 2011). We used amiloride, a specific inhibitor of pinocytosis, and acts by inhibiting the Na/K exchange (Ivanov 2008). We did not observe any significant attenuation of the effects of doxazosin following pre-treatment with 50 µM of amiloride in any of the cell lines tested, suggesting that the actions of doxazosin were independent of pinocytosis.

The caveat of interpreting this result is that pinocytosis is a dynamic process and other studies such as confocal microscopy would be required to confirm an inhibition of pinocytosis.

Next, we investigated whether the effects of doxazosin relied on dynamin, a 100-KDa GTPase crucial for vesicle formation in receptor-mediated endocytosis, synaptic vesicle recycling, caveolae internalization, and potentially vesicle trafficking to and from Golgi bodies (Hinshaw 2000). Dynasore is a relatively specific, cell permeable inhibitor of dynamin (Macia, Ehrlich et al. 2006).

In our experiments, we utilized dynasore at a concentration of 20 μ M in serum-free media to pre-treat PC3, DU145, LNCaP, and HT1376 cells, aiming to investigate whether inhibiting dynamin-dependent endocytosis would reduce the cell death induced by doxazosin. Dynasore exhibited a slight but statistically nonsignificant inhibitory effect on all four cell lines tested. However, our findings demonstrated that dynasore significantly mitigated the cell death induced by doxazosin. Specifically, pre-treatment with 20 μ M dynasore for 4 h, followed by treatment with 37 μ M doxazosin for 72 h, yielded significant results (p = 0.0243, p = 0.0019, p = 0.0766, and p = 0.0007 for PC-3, DU145, LNCaP, and HT1376 cells, respectively). This effect became more pronounced at a higher concentration of doxazosin (100 μ M), with p-values <0.0001 for PC-3, DU145, and HT1376 cells, and p = 0.0141 for LNCaP cells. These outcomes suggest that dynasore at 20 μ M led to greater attenuation of cell death at a higher concentration (100 μ M) of doxazosin compared to a lower concentration (37 μ M), indicating a quantitative inhibition of intracellular trafficking of doxazosin through a dynamin-dependent process.

Endocytosis is necessary for the execution of a wide range of cellular programs (Di Fiore 2009). Derailed endocytosis and its effects on the cellular processes is an emerging field of cancer research. Endocytosis serves as a tumour suppressor pathway by attenuating cell signalling (Polo, Pece et al. 2004, Di Fiore 2009). Endocytic signalling persists throughout the signalling route giving rise to the concept of signalling endosomes (von Zastrow and Sorkin 2007, Di Fiore and von Zastrow 2014). Defective trafficking of growth factor receptors, due to deranged endocytosis,

coupled with an unbalanced recycling of adhesion complexes are one of the hallmarks of malignant cells (Mosesson, Mills et al. 2008).

Prazosin had been shown to inhibit the sorting process by an off-target perturbation of GPCR of which alpha-1 adrenergic receptors were considered as a prime target (Zhang, Wang et al. 2012). Since the cell death induced by doxazosin and prazosin has been shown to be independent of its adrenergic receptor activity (Benning and Kyprianou 2002, Pavithran and Thompson 2012, Pavithran, Shabbir et al. 2017), the significance of the ability of prazosin to inhibit the sorting process of alpha-1 adrenergic receptors and its role in prazosin-induced cell death of cancer cells remains uncertain.

Our results shows that doxazosin induced cell death is a dynamin-dependent process and inhibition of this pathway using dynasore, the chemical inhibitor of dynamin, significantly attenuates the cytotoxic effects of doxazosin on PCa and BCa cell lines (Pavithran and Thompson 2012, Pavithran, Shabbir et al. 2017).

Our previous experiments demonstrated that cell death induced by doxazosin increased when cells were cultured in serum-free media. We also observed that serum starvation accelerated the onset of granulation. Additionally, we found that dansylcadaverine attenuated doxazosin-induced cell death. Besides inhibiting clathrin-mediated endocytosis, dansylcadaverine also inhibits the autophagic (Munafo and Colombo 2001). These led us to hypothesize that these granulations may represent autophagy within the cells exposed to doxazosin.

Autophagy is an evolutionarily conserved process of degradation of cytoplasm and organelles in the lysosomes for amino acid recycling and energy (Klionsky, Abeliovich et al. 2008). Autophagy serves as a survival strategy during starvation and plays a

pivotal role in energy homeostasis. It is also a critical component of the cellular recycling mechanism and quality control of macromolecules and intracellular organelles, with an important role in maintaining cellular fitness both in healthy and stressful conditions. Interestingly, it has both pro- and anti-tumorigenic roles and can crosstalk with apoptosis, and has a role in senescence; however, autophagy can lead to cell death if the process is uncontrolled. Autophagy thus plays a dual role in both cell survival and cell death (Klionsky, Abeliovich et al. 2008, Klionsky, Abdalla et al. 2012, Zhang 2015).

We initially used two commonly used inhibitors of autophagy, namely, dansylcadaverine and 3-MA to explore if the chemical inhibition of autophagy had any effect on cell death induced by doxazosin.

Dansylcadaverine is also autofluorescent and its accumulation in autophagic vacuoles can be demonstrated using fluorescent microscopy (Munafo and Colombo 2001). As the next step, we examined the accumulation of dansylcadaverine in cells exposed to doxazosin. We demonstrated that autofluorescent dansylcadaverine accumulated in the autophagosomes of these cells (Figure 44). Thus, the concentration of dansyl cadaverine serve as a marker for the presence of autophagosomes and the presence of autophagy (Davies, Cornwell et al. 1984, Pavithran and Thompson 2012, Pasquier 2016, Pavithran, Shabbir et al. 2017).

Our experiments with 3-MA-1 showed that it significantly inhibited the growth of PC-3 (p <0.0006) and LNCaP cells (p <0.0001) whilst it had no significant effect on growth of DU-145 (p <0.01) and HT-1376 cells (p = 0.0579). There was a significant reduction in the cytotoxic effect of doxazosin when the above cells lines were pre-incubated with 2 mM of 3-MA-1 for 4 h. 3-MA-1 is an inhibitor of autophagy and exerts its actions by

inhibition of PI3K inhibition (Wang, Yang et al. 2017), which in turn regulates cellular processes such as proliferation, RNA processing, protein translation and autophagy (Wang, Yang et al. 2017, Chen, Tseng et al. 2023).

TEM is the gold standard for demonstration of autophagy. The characteristic appearances of autophagy within cells when viewed using TEM are also well described (Tabata, Hayashi-Nishino et al. 2013). We examined the cells exposed to doxazosin under TEM and compared the appearances to that of unexposed controls. Additionally, we also observed the cells using SEM to evaluate if the cell surface demonstrated any changes that could account for its granular appearance.

We demonstrated the presence of mitophagy on TEM and the granulations observed on light microscopy were fragmented mitochondria within autophagosomes in doxazosin treated cells (Figures 45-52). Imaging with SEM revealed the various stages of doxazosin-treated cells undergoing anoikis but did not provide with any features that could account for the granulations (Figures 53-57).

We were the first to report widespread autophagy by doxazosin in PCa and BCa cell lines using TEM (Pavithran and Thompson 2012, Pavithran, Shabbir et al. 2017) and our experiments with TEM suggests that exposure to doxazosin 37 µM for 24 h to 72 h resulted in autophagy with a predominantly selective mitophagy in PC-3, fibroblasts and HT1376 cells. Furthermore, these autophagic changes were not accompanied by karyorrhexis and chromatin condensation in these cells and possibly the autophagic component was more significant than apoptosis, even though both apoptotic and autophagic gene families exhibited significant fold changes in our later experiments with next generation transcriptome sequencing on PC-3 cell line.

A reliable marker of autophagy is the presence of LC3-II (Tanida, Ueno et al. 2008). LC3 is a soluble microtubule-associated protein 1A/1B (with a molecular mass of approximately 17 KDa), ubiquitously distributed, and found in mammalian tissues and cultured cells. The cytosolic form of LC3 (LC3-I) is conjugated to phosphatidylethanolamine to form LC3-II, and these are recruited into the autophagosomal membranes (Wild, McEwan et al. 2014). In our next experiment, we investigated the presence of LC3-II using immunohistochemistry in cells exposed to doxazosin (Rosenfeldt, Nixon et al. 2012) and demonstrated the presence of LC3-II in cells treated with doxazosin. Immunohistochemically labelled sections revealed densely stained areas of LC3 B (brown staining) in the cytoplasm of sections that had been exposed to doxazosin whilst this feature was absent in the control specimens (Figure 58) (Pavithran, Shabbir et al. 2017).

Autophagy commences with *de novo* formation of double-membrane vesicles called phagophores. The phagophores undergo invagination to eventually fuse to form a double-membrane structure called autophagosomes that sequester the transport cargo. The exact origin of the phagophore membrane that leads to formation of the autophagosomes remains unresolved with ER-Golgi intermediate compartment and ER-mitochondria considered to be among the possible candidates (Rubinsztein, Shpilka et al. 2012, Chan and Tang 2013, Lamb, Yoshimori et al. 2013, Tooze 2013, Ge and Schekman 2014). The autophagosomes fuse with the lysosome to form the autophagolysosome which then degrades the cargo within it (Parzych and Klionsky 2014).

Currently, over 30 genes involved in autophagy have been identified in mammals of which 16 genes are involved in all types of autophagy (Klionsky, Abdalla et al. 2012, Pyo, Nah et al. 2012). The ubiquitin-like protein LC3 is a mammalian homolog of

ATG8 gene and is essential for the formation of autophagosomes. LC3 is lipidated with phosphatidylethanolamine to form LC3-II which remains on the membranes of the autophagosomes until its fusion with the lysosomes (Burman and Ktistakis 2010, Pyo, Nah et al. 2012). The conversion of LC3 to LC3-II is therefore considered a reliable molecular indicator of autophagy (Klionsky, Abeliovich et al. 2008, Klionsky, Abdalla et al. 2012, Pyo, Nah et al. 2012). Nonetheless, as mentioned earlier, TEM is still considered to be the gold standard for detection of autophagy.

Chemical inhibitors of autophagy serve as an initial tool to assess the presence or absence of autophagy; however, they are not specific in their actions (Yang, Hu et al. 2013, Vinod, Padmakrishnan et al. 2014, Pasquier 2016). This is compounded by the fact that autophagy is intrinsically linked to other cellular functions such as endocytosis (Lamb, Dooley et al. 2013).

Our experiments were designed to identify the causative factor for development of granulations within the cells when exposed to doxazosin, when attempting to create doxazosin-resistant cells. We had previously looked at the possibility of these granules being lipofuscin granules but specific staining for these were negative and focussed out attention to autophagy. As a first step, we used 2 main chemical inhibitors of autophagy, namely, 3-MA and dansylcadaverine to evaluate their effects on doxazosin induced cell death. Subsequently, we demonstrated the presence of autophagy in cells treated with doxazosin using TEM and fluorescent microscopy (accumulation of dansylcadaverine in autophagosomes) and by demonstrating the presence of LC3-II. As a result of these findings, we were the first to report extensive autophagy in PCa cell lines, BCa cell lines, and fibroblasts following exposure to doxazosin (Pavithran and Thompson 2012, Pavithran, Shabbir et al. 2017).

Additionally, the autophagic process was independent of *p53* gene as we were able to replicate these findings in PC-3 cells, which have a *p-53-null* status.

Taken together, these observations suggest that autophagy (especially mitophagy) plays an important role in the doxazosin-induced cell death in the cell lines tested. These findings, however, cannot directly attribute the cell death from doxazosin to autophagy (Klionsky, Abdalla et al. 2012).

After having shown that autophagy was involved in doxazosin-mediated cell death, we set out to conduct next generation entire transcriptome sequencing with a view to identify the fold changes that occur when cells are exposed to doxazosin as compared to the controls. We limited to studying PC-3 cells initially given that these were androgen-independent cells and exhibited the greatest autophagy morphology among all cells tested. We conducted the transcriptome readings at two time points (24h and 48h). We chose these time points, as the more significant gene changes were likely to happen during the earlier part of the exposure, and late exposure times were likely to only reveal terminal cell death. Another reason was the differences that occur to cell adhesion and confluence when cells are exposed to doxazosin. Cells exposed to doxazosin are less adherent, likely to undergo anoikis and less confluent due to increased cell death and reduced growth rate or both. We felt that the differences in confluence would result in additional artefactual errors where pathways involving cell adhesions, integrins and anoikis are involved, and therefore, chose earlier time points.

Our data showed that significant changes occur in gene expression levels of cells exposed to doxazosin as compared to controls. All genes examined in the apoptosis gene family exhibited fold changes, most of the autophagy genes, TNF family of

genes also exhibited fold changes greater than 2. However, it remains unknown if these changes would result in altered protein transcription and these experiments could not be completed. Furthermore, due to the high costs we performed the next generation sequencing in only a single cell line with a single quinazoline adrenergic receptor antagonist, namely, doxazosin. To validate the results of our experiments, it would require repeating the experiments to check if the present data can be replicated in the same cell line and with other cell lines as well as with other quinazoline derivatives.

Though autophagy and apoptosis appear to be divergent pathways in cell survival, several studies have shown that these are closely related and capable of switching from one pathway to the other (Bhutia, Dash et al. 2010, Bhutia, Das et al. 2011). Apoptosis signalling can regulate autophagy and conversely autophagy can regulate apoptosis (Yonekawa and Thorburn 2013). Not surprisingly, we found that the gene families involved in regulation of autophagy and apoptosis showed significant fold changes. Given the extensive crosstalk between autophagy and apoptosis (and the existence of both these processes simultaneously), it is often difficult to attribute quantitatively the cell death to each of these two processes. Nonetheless, our results therefore suggests that autophagy is a predominant process involved in doxazosin-induced cell death.

Among the genes with the highest positive fold change after 48 h of exposure to doxazosin, we found the *LOC100271832* had a +9.77-fold change. The *LOC100271832* is an uncharacterized gene that is expressed at low levels in several tissues in humans (Fagerberg, Hallstrom et al. 2014). Therefore, an increase in fold change by a factor of 9.77 in our data is intriguing. Further studies into

understanding the functions of this gene and the protein expressed by this gene could shed light into novel pathways that are involved in androgen resistant PCa.

Among the genes with the most significant negative fold change after 48 hours of doxazosin exposure, the CD3D gene exhibited a -10.54-fold reduction in the log2 ratio, indicating substantial suppression in the presence of doxazosin. The CD3D gene, known as the CD3-Delta unit of the T-cell receptor complex, was initially identified in T cell lymphocytes. It has since been found to be expressed in both benign and malignant prostate tissues (Essand, Vasmatzis et al. 1999). *CD3D* expression levels is known to be a prognostic marker for a wide range of cancers or their response to treatment including muscle-invasive BCa (Shi, Meng et al. 2019), gastric cancer (Yuan, Xu et al. 2022), colon cancer (Yang, Zang et al. 2020), and is a marker for response to radiotherapy in PCa (Fortis, Goulielmaki et al. 2022). However, there has been no previous studies to our knowledge that has previously examined the relationship between *CD3D* gene expression and PCa cells.

The *SLC25A3* gene demonstrated a -9.77 reduction. This gene belongs to a family of mitochondrial transport proteins and is involved in transport of copper ions which is need for cytochrome oxidase for cytochrome-*c* release – this recently described pathway sometimes referred to as cuproptosis (Wang, Zhang et al. 2022). There have been no previous studies that have examined the relationship between adrenergic receptors or its antagonists with cuproptosis. Whilst suppression of cuproptosis could be a possible pathway in doxazosin induced cell death, further studies will be needed to clarify this. Moreover, the reduction in expression could be reflection of disruption to the mitochondrial membrane and subsequent autophagy.

In all we observed that over 250 genes underwent fold changes greater than 2 in PC3 cells when exposed to doxazosin. Since our experiments were conducted in only a single cell line, it would be beneficial to replicate these studies in additional PCa and BCa cell lines to identify genes that exhibit significant fold changes associated with doxazosin-induced cell death. This information would aid in identifying the involved proteins and elucidating the various cell signaling pathways mediating doxazosin-induced cell death in PCa and BCa cells.

Finally, we conducted In Vivo experiments to identify if the In Vitro experimental data could be replicated in animal studies. Using HT1376 subcutaneous cell inoculations we were able to show for the first time that intraperitoneal injections of doxazosin (3mg/kg/day) significantly and effectively reduced the growth of both freshly implanted and established tumour outgrowths as compared to vehicle controls (Pavithran, Shabbir et al. 2017). Using a combination of immunohistochemistry and TEM, we were able to show that the inoculated tumour cells retained their original phenotype and cellular characteristics, further validating the relevance of these results to the expected effects of doxazosin treatment for tumours in actual patients. In summary, our experimental data suggests that doxazosin exerts its anti-tumour activity by initially entering the cell via a dynamin-dependent endocytic process (independent of the adrenergic receptor). The presence of significant mitophagy in TEM experiments suggests that doxazosin is potentially mitochondriotoxic whereby the damaged mitochondria undergo mitophagy. The highest fold change of a yet uncharacterized gene (LOC100271832) suggests that the actions of doxazosin may be mediated by proteins and signalling pathways that has not been elucidated to date, and future work into this could help to understand novel mechanisms involved in cancer cell death.

Chapter 10

Future work

We were able demonstrate that dynamin-mediated endocytic process played a critical role in the widespread autophagy (mitophagy) and cell death, following exposure to doxazosin. The effects of doxazosin were demonstrated *In Vitro* and also shown to be present lin Vivo. However, the exact molecular mechanisms involved in this process are still unknown.

While our research was conducted on 2D cell cultures, future studies could utilize 3D cell cultures to validate our results in a more complex environment, especially since anoikis has been identified as a significant upstream event leading to doxazosin-induced cell death.

Future confocal microscopy studies could enhance our understanding of the role of endocytosis in doxazosin-induced cell death. Although cell viability assays can determine cell viability as an endpoint, they are inadequate for studying the dynamic vesicle trafficking involved in endocytosis. Custom-made fluorescent trackers that tag doxazosin could be developed to study its trafficking within cells using confocal microscopy and single live cell imaging.

Additionally, next-generation sequencing revealed that doxazosin increased the expression of several gene families related to autophagy, apoptosis, anoikis, and lipid metabolism in the PC-3 cell line. Among the genes identified, LOC100271832, which remains uncharacterized, showed the second highest fold change in cells exposed to doxazosin. Since the role of this gene and its encoded protein in cancer

cell death is unknown, further characterization could uncover novel molecular mechanisms and potentially lead to new cancer therapies.

Chapter 11

Summary

Doxazosin, an alpha-1 adrenergic receptor antagonist, is commonly used to manage hypertension and benign prostatic enlargement (BPE). Besides its adrenergic receptor antagonism, doxazosin also demonstrates antineoplastic effects against various cancers, including prostate cancer (PCa) and bladder cancer (BCa). Although these effects are known to be linked to its quinazoline-based chemical structure, the precise mechanisms underlying its antineoplastic activity are not yet fully understood. This study aimed to investigate the cellular mechanisms by which doxazosin induces cell death in PCa and BCa.

Initially we hypothesised that the antineoplastic activity could be mediated by receptors that have structurally similarity to the adrenergic receptors. Therefore, using UniProtKB/SwissProt and PSI-2-Search we identified that 5HT share close structural similarity to alpha adrenergic receptors as well to other (1D and Beta) adrenergic receptors. However, our experimental data did not yield any positive results and refuted this hypothesis.

As a next step, we attempted to develop doxazosin-resistant cell lines with a view to investigate up regulation and/or down regulation of receptor types. We hypothesised that by developing doxazosin-resistant cell lines, the receptors mediating doxazosin-induced cell death would be down-regulated and that these cell lines would serve as useful tool in the study of doxazosin-induced cell death. However, we were unable to develop a doxazosin-resistant cell line.

Coincidentally, during the experiments to develop doxazosin-resistant cells, we observed a granular appearance in cells treated with doxazosin.

We then embarked on characterizing and identifying the granulations developing within doxazosin treated cells. These studies led us to hypothesise that a non-

receptor mediated pathways (such as endocytosis and pinocytosis) was involved in doxazosin induced cell death.

We also further explored, the incidental finding of granular appearances within cells exposed to doxazosin, using SEM and TEM and immunostaining techniques. Our experiments in non-receptor mediated trafficking were able to demonstrate that the inhibition of dynamin-mediated endocytic trafficking attenuates the cell death induced by doxazosin as well as by other quinazoline based adrenergic receptor antagonists. Our experiments with TEM demonstrated widespread autophagy (mitophagy) in prostate, bladder and fibroblast cells that were undergoing cell death following exposure to doxazosin.

We conducted further experiments using chemical inhibitors of autophagy to identify the precise steps in autophagy that mediated doxazosin induced cell death.

Subsequently, we also performed next-generation sequencing of the PC3 cell line to investigate the changes in gene expression following exposure to doxazosin. The experiments revealed that doxazosin increased the expression of several gene families related to autophagy, apoptosis, anoikis, and lipid metabolism in the PC-3 cell line. Among the genes identified, LOC100271832, which remains uncharacterized, showed the second highest fold change in cells exposed to doxazosin. The significance of this very high level of expression of this gene in cells undergoing cell death following exposure to doxazosin, remains to be understood.

Finally, we conducted *In Vivo* experiments to ascertain if the experiments findings translated to similar actions in nude athymic mice. Our experiments showed that doxazosin reduced the growth of both freshly implanted –and –established tumours as compared to vehicle controls.

Our results raise the possibility that doxazosin could be useful in the management of advanced urological malignancy, possibly as an adjunct to complement existing treatments.

REFERENCES:

Abdul, M., P. E. Anezinis, C. J. Logothetis and N. M. Hoosein (1994). "Growth inhibition of human prostatic carcinoma cell lines by serotonin antagonists." <u>Anticancer Res</u> **14**(3A): 1215-1220.

Agarwal, C., S. Dhanalakshmi, R. P. Singh and R. Agarwal (2004). "Inositol hexaphosphate inhibits growth and induces G1 arrest and apoptotic death of androgen-dependent human prostate carcinoma LNCaP cells." <u>Neoplasia</u> **6**(5): 646-659.

Aguilar, R. C. and B. Wendland (2005). "Endocytosis of membrane receptors: two pathways are better than one." <u>Proc Natl Acad Sci U S A</u> **102**(8): 2679-2680.

Ahmad, I., O. J. Sansom and H. Y. Leung (2012). "Exploring molecular genetics of bladder cancer: lessons learned from mouse models." <u>Dis Model Mech</u> **5**(3): 323-332.

Ahmed, S., C. S. Johnson, R. M. Rueger and D. L. Trump (2002). "Calcitriol (1,25-

dihydroxycholecalciferol) potentiates activity of mitoxantrone/dexamethasone in an androgen independent prostate cancer model." J Urol **168**(2): 756-761.

Akhoundova, D., F. Y. Feng, C. C. Pritchard and M. A. Rubin (2022). "Molecular Genetics of Prostate Cancer and Role of Genomic Testing." <u>Surg Pathol Clin</u> **15**(4): 617-628.

Akhtar, S., A. Al-Shammari and J. Al-Abkal (2018). "Chronic urinary tract infection and bladder carcinoma risk: a meta-analysis of case-control and cohort studies." World J Urol.

Alberti, C. (2007). "Apoptosis induction by quinazoline-derived alpha1-blockers in prostate cancer cells: biomolecular implications and clinical relevance." <u>Eur Rev Med Pharmacol Sci</u> **11**(1): 59-64. Altman, B. J. and J. C. Rathmell (2012). "Metabolic stress in autophagy and cell death pathways." Cold Spring Harb Perspect Biol **4**(9): a008763.

Andriole, G. L., D. G. Bostwick, O. W. Brawley, L. G. Gomella, M. Marberger, F. Montorsi, C. A. Pettaway, T. L. Tammela, C. Teloken, D. J. Tindall, M. C. Somerville, T. H. Wilson, I. L. Fowler, R. S. Rittmaster and R. S. Group (2010). "Effect of dutasteride on the risk of prostate cancer." N Engl J Med 362(13): 1192-1202.

Antonny, B. (2006). "Membrane deformation by protein coats." <u>Curr Opin Cell Biol</u> **18**(4): 386-394. Aranha, O., D. P. Wood, Jr. and F. H. Sarkar (2000). "Ciprofloxacin mediated cell growth inhibition, S/G2-M cell cycle arrest, and apoptosis in a human transitional cell carcinoma of the bladder cell line." <u>Clin Cancer Res</u> **6**(3): 891-900.

Arora, S., Y. Wang, Z. Jia, S. Vardar-Sengul, A. Munawar, K. S. Doctor, M. Birrer, M. McClelland, E. Adamson and D. Mercola (2008). "Egr1 regulates the coordinated expression of numerous EGF receptor target genes as identified by ChIP-on-chip." <u>Genome Biol</u> **9**(11): R166.

Ashrafizadeh, M., M. D. A. Paskeh, S. Mirzaei, M. H. Gholami, A. Zarrabi, F. Hashemi, K. Hushmandi, M. Hashemi, N. Nabavi, F. Crea, J. Ren, D. J. Klionsky, A. P. Kumar and Y. Wang (2022). "Targeting autophagy in prostate cancer: preclinical and clinical evidence for therapeutic response." <u>J Exp Clin Cancer Res</u> **41**(1): 105.

Babcook, M. A., R. M. Sramkoski, H. Fujioka, F. Daneshgari, A. Almasan, S. Shukla, R. R. Nanavaty and S. Gupta (2014). "Combination simvastatin and metformin induces G1-phase cell cycle arrest and Ripk1- and Ripk3-dependent necrosis in C4-2B osseous metastatic castration-resistant prostate cancer cells." <u>Cell Death Dis</u> **5**: e1536.

Balakumaran, B. S., J. T. Herbert and P. G. Febbo (2010). "MYC activity mitigates response to rapamycin in prostate cancer through 4EBP1-mediated inhibition of autophagy." <u>Autophagy</u> **6**(2): 281-282

Balakumaran, B. S., A. Porrello, D. S. Hsu, W. Glover, A. Foye, J. Y. Leung, B. A. Sullivan, W. C. Hahn, M. Loda and P. G. Febbo (2009). "MYC activity mitigates response to rapamycin in prostate cancer through eukaryotic initiation factor 4E-binding protein 1-mediated inhibition of autophagy." <u>Cancer Res 69</u>(19): 7803-7810.

Ballou, L. M., M. E. Cross, S. Huang, E. M. McReynolds, B. X. Zhang and R. Z. Lin (2000). "Differential regulation of the phosphatidylinositol 3-kinase/Akt and p70 S6 kinase pathways by the alpha(1A)-adrenergic receptor in rat-1 fibroblasts." J Biol Chem **275**(7): 4803-4809.

- Batty, M., R. Pugh, I. Rathinam, J. Simmonds, E. Walker, A. Forbes, S. Anoopkumar-Dukie, C. M. McDermott, B. Spencer, D. Christie and R. Chess-Williams (2016). "The Role of alpha1-Adrenoceptor Antagonists in the Treatment of Prostate and Other Cancers." Int J Mol Sci 17(8).
- Baust, J. G., D. P. Klossner, R. G. Vanbuskirk, A. A. Gage, V. Mouraviev, T. J. Polascik and J. M. Baust (2010). "Integrin involvement in freeze resistance of androgen-insensitive prostate cancer." <u>Prostate Cancer Prostatic Dis</u> **13**(2): 151-161.
- Beauchamp, E. M. and L. C. Platanias (2013). "The evolution of the TOR pathway and its role in cancer." Oncogene **32**(34): 3923-3932.
- Beck, R., M. Rawet, F. T. Wieland and D. Cassel (2009). "The COPI system: molecular mechanisms and function." <u>FEBS Lett</u> **583**(17): 2701-2709.
- Becker, A. L., N. I. Orlotti, M. Folini, F. Cavalieri, A. N. Zelikin, A. P. Johnston, N. Zaffaroni and F. Caruso (2011). "Redox-active polymer microcapsules for the delivery of a survivin-specific siRNA in prostate cancer cells." ACS Nano **5**(2): 1335-1344.
- Beckers, A., S. Organe, L. Timmermans, K. Scheys, A. Peeters, K. Brusselmans, G. Verhoeven and J. V. Swinnen (2007). "Chemical inhibition of acetyl-CoA carboxylase induces growth arrest and cytotoxicity selectively in cancer cells." <u>Cancer Res</u> **67**(17): 8180-8187.
- Belayneh, M. and C. Korownyk (2016). "Treatment of lower urinary tract symptoms in benign prostatic hypertrophy with alpha-blockers." <u>Can Fam Physician</u> **62**(9): e523.
- Beljanski, V., C. Knaak and C. D. Smith (2010). "A novel sphingosine kinase inhibitor induces autophagy in tumor cells." <u>J Pharmacol Exp Ther</u> **333**(2): 454-464.
- Ben Sahra, I., K. Laurent, S. Giuliano, F. Larbret, G. Ponzio, P. Gounon, Y. Le Marchand-Brustel, S. Giorgetti-Peraldi, M. Cormont, C. Bertolotto, M. Deckert, P. Auberger, J. F. Tanti and F. Bost (2010). "Targeting cancer cell metabolism: the combination of metformin and 2-deoxyglucose induces p53-dependent apoptosis in prostate cancer cells." <u>Cancer Res</u> **70**(6): 2465-2475.
- Ben Sahra, I., J. F. Tanti and F. Bost (2010). "The combination of metformin and 2-deoxyglucose inhibits autophagy and induces AMPK-dependent apoptosis in prostate cancer cells." <u>Autophagy</u> **6**(5): 670-671.
- Bennett, H. L., J. T. Fleming, J. O'Prey, K. M. Ryan and H. Y. Leung (2010). "Androgens modulate autophagy and cell death via regulation of the endoplasmic reticulum chaperone glucose-regulated protein 78/BiP in prostate cancer cells." <u>Cell Death Dis</u> 1: e72.
- Bennett, H. L., J. Stockley, J. T. Fleming, R. Mandal, J. O'Prey, K. M. Ryan, C. N. Robson and H. Y. Leung (2013). "Does androgen-ablation therapy (AAT) associated autophagy have a pro-survival effect in LNCaP human prostate cancer cells?" <u>BJU Int</u> **111**(4): 672-682.
- Benning, C. M. and N. Kyprianou (2002). "Quinazoline-derived alpha1-adrenoceptor antagonists induce prostate cancer cell apoptosis via an alpha1-adrenoceptor-independent action." <u>Cancer Res</u> **62**(2): 597-602.
- Benton, G., I. Arnaoutova, J. George, H. K. Kleinman and J. Koblinski (2014). "Matrigel: from discovery and ECM mimicry to assays and models for cancer research." <u>Adv Drug Deliv Rev</u> **79-80**: 3-18
- Benton, G., H. K. Kleinman, J. George and I. Arnaoutova (2011). "Multiple uses of basement membrane-like matrix (BME/Matrigel) in vitro and in vivo with cancer cells." <u>Int J Cancer</u> **128**(8): 1751-1757.
- Bhat, P., J. Kriel, B. Shubha Priya, Basappa, N. S. Shivananju and B. Loos (2018). "Modulating autophagy in cancer therapy: Advancements and challenges for cancer cell death sensitization." <u>Biochem Pharmacol</u> **147**: 170-182.
- Bhutia, S. K., S. K. Das, B. Azab, R. Dash, Z. Z. Su, S. G. Lee, P. Dent, D. T. Curiel, D. Sarkar and P. B. Fisher (2011). "Autophagy switches to apoptosis in prostate cancer cells infected with melanoma differentiation associated gene-7/interleukin-24 (mda-7/IL-24)." <u>Autophagy</u> **7**(9): 1076-1077. Bhutia, S. K., R. Dash, S. K. Das, B. Azab, Z. Z. Su, S. G. Lee, S. Grant, A. Yacoub, P. Dent, D. T. Curiel, D.
- Sarkar and P. B. Fisher (2010). "Mechanism of autophagy to apoptosis switch triggered in prostate

cancer cells by antitumor cytokine melanoma differentiation-associated gene 7/interleukin-24." Cancer Res **70**(9): 3667-3676.

Bilbro, J., M. Mart and N. Kyprianou (2013). "Therapeutic value of quinazoline-based compounds in prostate cancer." <u>Anticancer Res</u> **33**(11): 4695-4700.

Bommareddy, A., E. R. Hahm, D. Xiao, A. A. Powolny, A. L. Fisher, Y. Jiang and S. V. Singh (2009). "Atg5 regulates phenethyl isothiocyanate-induced autophagic and apoptotic cell death in human prostate cancer cells." <u>Cancer Res</u> **69**(8): 3704-3712.

Bonaccorsi, L., D. Nosi, M. Muratori, L. Formigli, G. Forti and E. Baldi (2007). "Altered endocytosis of epidermal growth factor receptor in androgen receptor positive prostate cancer cell lines." <u>J Mol</u> Endocrinol **38**(1-2): 51-66.

Bourbon, M., A. M. Fowler, X. M. Sun and A. K. Soutar (1999). "Inheritance of two different alleles of the low-density lipoprotein (LDL)-receptor gene carrying the recurrent Pro664Leu mutation in a patient with homozygous familial hypercholesterolaemia." <u>Clin Genet</u> **56**(3): 225-231.

Boutin, B., N. Tajeddine, P. Vandersmissen, N. Zanou, M. Van Schoor, L. Mondin, P. J. Courtoy, B. Tombal and P. Gailly (2013). "Androgen deprivation and androgen receptor competition by bicalutamide induce autophagy of hormone-resistant prostate cancer cells and confer resistance to apoptosis." <u>Prostate</u> **73**(10): 1090-1102.

Boya, P., F. Reggiori and P. Codogno (2013). "Emerging regulation and functions of autophagy." <u>Nat</u> Cell Biol **15**(7): 713-720.

Bray, F., J. S. Ren, E. Masuyer and J. Ferlay (2013). "Global estimates of cancer prevalence for 27 sites in the adult population in 2008." Int J Cancer 132(5): 1133-1145.

Brownson, R. C., J. C. Chang and J. R. Davis (1987). "Occupation, smoking, and alcohol in the epidemiology of bladder cancer." <u>Am J Public Health</u> **77**(10): 1298-1300.

Bruner, R. H., M. N. Novilla, C. A. Picut, J. B. Kirkpatrick, T. P. O'Neill, K. L. Scully, W. B. Lawrence, D. G. Goodman, B. H. Saladino, D. G. Peters and G. A. Parker (2009). "Spontaneous hibernomas in Sprague-Dawley rats." Toxicol Pathol **37**(4): 547-552.

Bulbul, M. A., J. L. Chin, R. P. Huben, L. S. Englander and J. E. Pontes (1985). "The effect of nitrofurantoin on bladder tumor cell lines: in vitro growth and implantation in the cauterized mouse bladder." <u>J Urol</u> **134**(6): 1231-1235.

Burger, M., J. W. Catto, G. Dalbagni, H. B. Grossman, H. Herr, P. Karakiewicz, W. Kassouf, L. A. Kiemeney, C. La Vecchia, S. Shariat and Y. Lotan (2013). "Epidemiology and risk factors of urothelial bladder cancer." <u>Eur Urol</u> **63**(2): 234-241.

Burman, C. and N. T. Ktistakis (2010). "Autophagosome formation in mammalian cells." <u>Semin</u> Immunopathol **32**(4): 397-413.

Cao, C., T. Subhawong, J. M. Albert, K. W. Kim, L. Geng, K. R. Sekhar, Y. J. Gi and B. Lu (2006). "Inhibition of mammalian target of rapamycin or apoptotic pathway induces autophagy and radiosensitizes PTEN null prostate cancer cells." <u>Cancer Res</u> **66**(20): 10040-10047.

Cao, X., R. Mahendran, G. R. Guy and Y. H. Tan (1993). "Detection and characterization of cellular EGR-1 binding to its recognition site." <u>J Biol Chem</u> **268**(23): 16949-16957.

Carpentier, J. L., F. Sawano, D. Geiger, P. Gorden, A. Perrelet and L. Orci (1989). "Potassium depletion and hypertonic medium reduce "non-coated" and clathrin-coated pit formation, as well as endocytosis through these two gates." <u>J Cell Physiol</u> **138**(3): 519-526.

Carter, H. B., A. Kettermann, C. Warlick, E. J. Metter, P. Landis, P. C. Walsh and J. I. Epstein (2007). "Expectant management of prostate cancer with curative intent: an update of the Johns Hopkins experience." <u>J Urol</u> **178**(6): 2359-2364; discussion 2364-2355.

Cekanova, M. and K. Rathore (2014). "Animal models and therapeutic molecular targets of cancer: utility and limitations." <u>Drug Des Devel Ther</u> **8**: 1911-1921.

Chae, Y. C., M. C. Caino, S. Lisanti, J. C. Ghosh, T. Dohi, N. N. Danial, J. Villanueva, S. Ferrero, V. Vaira, L. Santambrogio, S. Bosari, L. R. Languino, M. Herlyn and D. C. Altieri (2012). "Control of tumor bioenergetics and survival stress signaling by mitochondrial HSP90s." <u>Cancer Cell</u> **22**(3): 331-344.

- Chan, S. N. and B. L. Tang (2013). "Location and membrane sources for autophagosome formation from ER-mitochondria contact sites to Golgi-endosome-derived carriers." <u>Mol Membr Biol</u> **30**(8): 394-402.
- Chang, C. L., M. C. Ho, P. H. Lee, C. Y. Hsu, W. P. Huang and H. Lee (2009). "S1P(5) is required for sphingosine 1-phosphate-induced autophagy in human prostate cancer PC-3 cells." <u>Am J Physiol Cell Physiol</u> **297**(2): C451-458.
- Chang, C. L., J. J. Liao, W. P. Huang and H. Lee (2007). "Lysophosphatidic acid inhibits serum deprivation-induced autophagy in human prostate cancer PC-3 cells." <u>Autophagy</u> **3**(3): 268-270.
- Chang, L., J. Zhang, Y. H. Tseng, C. Q. Xie, J. Ilany, J. C. Bruning, Z. Sun, X. Zhu, T. Cui, K. A. Youker, Q. Yang, S. M. Day, C. R. Kahn and Y. E. Chen (2007). "Rad GTPase deficiency leads to cardiac hypertrophy." <u>Circulation</u> **116**(25): 2976-2983.
- Changou, C. A., Y. R. Chen, L. Xing, Y. Yen, F. Y. Chuang, R. H. Cheng, R. J. Bold, D. K. Ann and H. J. Kung (2014). "Arginine starvation-associated atypical cellular death involves mitochondrial dysfunction, nuclear DNA leakage, and chromatin autophagy." Proc Natl Acad Sci U S A 111(39): 14147-14152.
- Cheluvappa, R., D. P. Smith, S. Cerimagic and M. I. Patel (2014). "A comprehensive evaluation of bladder cancer epidemiology and outcomes in Australia." Int Urol Nephrol **46**(7): 1351-1360.
- Chen, K., X. Li, H. Zhu, Q. Gong and K. Luo (2017). "Endocytosis of Nanoscale Systems for Cancer Treatments." Curr Med Chem.
- Chen, N. and V. Karantza-Wadsworth (2009). "Role and regulation of autophagy in cancer." <u>Biochim Biophys Acta</u> **1793**(9): 1516-1523.
- Chen, P., J. Yu, B. Chalmers, J. Drisko, J. Yang, B. Li and Q. Chen (2012). "Pharmacological ascorbate induces cytotoxicity in prostate cancer cells through ATP depletion and induction of autophagy." Anticancer Drugs **23**(4): 437-444.
- Chen, P. J., H. H. Tseng, Y. H. Wang, S. Y. Fang, S. H. Chen, C. H. Chen, S. C. Tsai, Y. C. Chang, Y. F. Tsai and T. L. Hwang (2023). "Palbociclib blocks neutrophilic PI3K activity to alleviate psoriasiform dermatitis." <u>Br J Pharmacol</u>.
- Chen, Y., X. R. Liu, Y. Q. Yin, C. J. Lee, F. T. Wang, H. Q. Liu, X. T. Wu and J. Liu (2014). "Unravelling the multifaceted roles of Atg proteins to improve cancer therapy." <u>Cell Prolif</u> **47**(2): 105-112.
- Chen, Y., Q. Zhou, W. Hankey, X. Fang and F. Yuan (2022). "Second generation androgen receptor antagonists and challenges in prostate cancer treatment." <u>Cell Death Dis</u> **13**(7): 632.
- Chen, Z. J. and K. P. Minneman (2005). "Recent progress in alpha1-adrenergic receptor research." Acta Pharmacol Sin **26**(11): 1281-1287.
- Cheng, J., Y. Ohsaki, K. Tauchi-Sato, A. Fujita and T. Fujimoto (2006). "Cholesterol depletion induces autophagy." <u>Biochem Biophys Res Commun</u> **351**(1): 246-252.
- Chhipa, R. R., Y. Wu and C. Ip (2011). "AMPK-mediated autophagy is a survival mechanism in androgen-dependent prostate cancer cells subjected to androgen deprivation and hypoxia." <u>Cell Signal</u> **23**(9): 1466-1472.
- Chiang, C. F., E. L. Son and G. J. Wu (2005). "Oral treatment of the TRAMP mice with doxazosin suppresses prostate tumor growth and metastasis." <u>Prostate</u> **64**(4): 408-418.
- Chien, M., M. Astumian, D. Liebowitz, C. Rinker-Schaeffer and W. M. Stadler (1999). "In vitro evaluation of flavopiridol, a novel cell cycle inhibitor, in bladder cancer." <u>Cancer Chemother Pharmacol</u> **44**(1): 81-87.
- Chinni, S. R., Y. Li, S. Upadhyay, P. K. Koppolu and F. H. Sarkar (2001). "Indole-3-carbinol (I3C) induced cell growth inhibition, G1 cell cycle arrest and apoptosis in prostate cancer cells." <u>Oncogene</u> **20**(23): 2927-2936.
- Chiu, H. W., Y. A. Chen, S. Y. Ho and Y. J. Wang (2012). "Arsenic trioxide enhances the radiation sensitivity of androgen-dependent and -independent human prostate cancer cells." <u>PLoS One</u> **7**(2): e31579.
- Choi, K. S. (2012). "Autophagy and cancer." Exp Mol Med **44**(2): 109-120.

- Chon, J. K., A. Borkowski, A. W. Partin, J. T. Isaacs, S. C. Jacobs and N. Kyprianou (1999). "Alpha 1-adrenoceptor antagonists terazosin and doxazosin induce prostate apoptosis without affecting cell proliferation in patients with benign prostatic hyperplasia." J Urol 161(6): 2002-2008.
- Chu, H., M. Wang and Z. Zhang (2013). "Bladder cancer epidemiology and genetic susceptibility." <u>J</u> <u>Biomed Res</u> **27**(3): 170-178.
- Chuang, K. H., H. E. Wang, F. M. Chen, S. C. Tzou, C. M. Cheng, Y. C. Chang, W. L. Tseng, J. Shiea, S. R. Lin, J. Y. Wang, B. M. Chen, S. R. Roffler and T. L. Cheng (2010). "Endocytosis of PEGylated agents enhances cancer imaging and anticancer efficacy." <u>Mol Cancer Ther</u> **9**(6): 1903-1912.
- Chung, Y. C., J. F. Kuo, W. C. Wei, K. J. Chang and W. T. Chao (2015). "Caveolin-1 Dependent Endocytosis Enhances the Chemosensitivity of HER-2 Positive Breast Cancer Cells to Trastuzumab Emtansine (T-DM1)." PLoS One **10**(7): e0133072.
- Chuu, C. P., R. A. Hiipakka, J. M. Kokontis, J. Fukuchi, R. Y. Chen and S. Liao (2006). "Inhibition of tumor growth and progression of LNCaP prostate cancer cells in athymic mice by androgen and liver X receptor agonist." Cancer Res **66**(13): 6482-6486.
- Cole, S. W. and A. K. Sood (2012). "Molecular pathways: beta-adrenergic signaling in cancer." <u>Clin Cancer Res</u> **18**(5): 1201-1206.
- Cooperberg, M. R. and J. M. Chan (2017). "Epidemiology of prostate cancer." <u>World J Urol</u> **35**(6): 849. Cooperberg, M. R., J. Cowan, J. M. Broering and P. R. Carroll (2008). "High-risk prostate cancer in the United States, 1990-2007." World J Urol **26**(3): 211-218.
- da Silva, C. G., D. C. Minussi, C. Ferran and M. Bredel (2014). "A20 expressing tumors and anticancer drug resistance." <u>Adv Exp Med Biol</u> **809**: 65-81.
- Daniyal, M., Z. A. Siddiqui, M. Akram, H. M. Asif, S. Sultana and A. Khan (2014). "Epidemiology, etiology, diagnosis and treatment of prostate cancer." <u>Asian Pac J Cancer Prev</u> **15**(22): 9575-9578. Das, G., B. V. Shravage and E. H. Baehrecke (2012). "Regulation and function of autophagy during cell
- Dash, R., B. Azab, B. A. Quinn, X. Shen, X. Y. Wang, S. K. Das, M. Rahmani, J. Wei, M. Hedvat, P. Dent, I. P. Dmitriev, D. T. Curiel, S. Grant, B. Wu, J. L. Stebbins, M. Pellecchia, J. C. Reed, D. Sarkar and P. B. Fisher (2011). "Apogossypol derivative BI-97C1 (Sabutoclax) targeting McI-1 sensitizes prostate cancer cells to mda-7/IL-24-mediated toxicity." Proc Natl Acad Sci U S A 108(21): 8785-8790.
- Davies, P. J., M. M. Cornwell, J. D. Johnson, A. Reggianni, M. Myers and M. P. Murtaugh (1984). "Studies on the effects of dansylcadaverine and related compounds on receptor-mediated endocytosis in cultured cells." <u>Diabetes Care</u> **7 Suppl 1**: 35-41.

survival and cell death." Cold Spring Harb Perspect Biol 4(6).

- de Bekker-Grob, E. W., M. N. van der Aa, E. C. Zwarthoff, M. J. Eijkemans, B. W. van Rhijn, T. H. van der Kwast and E. W. Steyerberg (2009). "Non-muscle-invasive bladder cancer surveillance for which cystoscopy is partly replaced by microsatellite analysis of urine: a cost-effective alternative?" <u>BJU Int</u> **104**(1): 41-47.
- de Resende, M. F., S. Vieira, L. T. Chinen, F. Chiappelli, F. P. da Fonseca, G. C. Guimaraes, F. A. Soares, I. Neves, S. Pagotty, P. A. Pellionisz, A. Barkhordarian, X. Brant and R. M. Rocha (2013).
- "Prognostication of prostate cancer based on TOP2A protein and gene assessment: TOP2A in prostate cancer." J Transl Med 11: 36.
- de Toledo, M., F. Senic-Matuglia, J. Salamero, G. Uze, F. Comunale, P. Fort and A. Blangy (2003). "The GTP/GDP cycling of rho GTPase TCL is an essential regulator of the early endocytic pathway." <u>Mol Biol Cell</u> **14**(12): 4846-4856.
- Deep, G., R. P. Singh, C. Agarwal, D. J. Kroll and R. Agarwal (2006). "Silymarin and silibinin cause G1 and G2-M cell cycle arrest via distinct circuitries in human prostate cancer PC3 cells: a comparison of flavanone silibinin with flavanolignan mixture silymarin." Oncogene **25**(7): 1053-1069.
- Delmulle, L., T. Vanden Berghe, D. D. Keukeleire and P. Vandenabeele (2008). "Treatment of PC-3 and DU145 prostate cancer cells by prenylflavonoids from hop (Humulus lupulus L.) induces a caspase-independent form of cell death." <u>Phytother Res</u> **22**(2): 197-203.
- Dennis, L. K. and D. V. Dawson (2002). "Meta-analysis of measures of sexual activity and prostate cancer." <u>Epidemiology</u> **13**(1): 72-79.

- Di Fiore, P. P. (2009). "Endocytosis, signaling and cancer, much more than meets the eye. Preface." Mol Oncol **3**(4): 273-279.
- Di Fiore, P. P. and M. von Zastrow (2014). "Endocytosis, signaling, and beyond." <u>Cold Spring Harb</u> Perspect Biol **6**(8).
- Ding, J., D. Xu, C. Pan, M. Ye, J. Kang, Q. Bai and J. Qi (2014). "Current animal models of bladder cancer: Awareness of translatability (Review)." Exp Ther Med **8**(3): 691-699.
- Ding, W. X., H. M. Ni, W. Gao, Y. F. Hou, M. A. Melan, X. Chen, D. B. Stolz, Z. M. Shao and X. M. Yin (2007). "Differential effects of endoplasmic reticulum stress-induced autophagy on cell survival." <u>J Biol Chem</u> **282**(7): 4702-4710.
- DiPaola, R. S., D. Dvorzhinski, A. Thalasila, V. Garikapaty, D. Doram, M. May, K. Bray, R. Mathew, B. Beaudoin, C. Karp, M. Stein, D. J. Foran and E. White (2008). "Therapeutic starvation and autophagy in prostate cancer: a new paradigm for targeting metabolism in cancer therapy." <u>Prostate</u> **68**(16): 1743-1752.
- Docherty, J. R. (1998). "Subtypes of functional alpha1- and alpha2-adrenoceptors." <u>Eur J Pharmacol</u> **361**(1): 1-15.
- Dokladny, K., O. B. Myers and P. L. Moseley (2015). "Heat shock response and autophagy-cooperation and control." <u>Autophagy</u> **11**(2): 200-213.
- Draisma, G., R. Etzioni, A. Tsodikov, A. Mariotto, E. Wever, R. Gulati, E. Feuer and H. de Koning (2009). "Lead time and overdiagnosis in prostate-specific antigen screening: importance of methods and context." J Natl Cancer Inst **101**(6): 374-383.
- Duffield, A. S., T. K. Lee, H. Miyamoto, H. B. Carter and J. I. Epstein (2009). "Radical prostatectomy findings in patients in whom active surveillance of prostate cancer fails." <u>J Urol</u> **182**(5): 2274-2278. Dutta, D. and J. G. Donaldson (2012). "Search for inhibitors of endocytosis: Intended specificity and unintended consequences." <u>Cell Logist</u> **2**(4): 203-208.
- Eastham, J. A., S. J. Hall, I. Sehgal, J. Wang, T. L. Timme, G. Yang, L. Connell-Crowley, S. J. Elledge, W. W. Zhang, J. W. Harper and et al. (1995). "In vivo gene therapy with p53 or p21 adenovirus for prostate cancer." <u>Cancer Res</u> **55**(22): 5151-5155.
- Eilon, G. F., L. Weisenthal, M. Stupecky, G. Landucci and L. M. Slater (2009). "Antineoplastic activity of idazoxan hydrochloride." <u>Cancer Chemother Pharmacol</u> **64**(6): 1157-1163.
- El-Sebaie, M., M. S. Zaghloul, G. Howard and A. Mokhtar (2005). "Squamous cell carcinoma of the bilharzial and non-bilharzial urinary bladder: a review of etiological features, natural history, and management." Int J Clin Oncol **10**(1): 20-25.
- Endo, A. and K. Hasumi (1993). "HMG-CoA reductase inhibitors." <u>Nat Prod Rep</u> **10**(6): 541-550. Essand, M., G. Vasmatzis, U. Brinkmann, P. Duray, B. Lee and I. Pastan (1999). "High expression of a specific T-cell receptor gamma transcript in epithelial cells of the prostate." <u>Proc Natl Acad Sci U S A</u> **96**(16): 9287-9292.
- Fagerberg, L., B. M. Hallstrom, P. Oksvold, C. Kampf, D. Djureinovic, J. Odeberg, M. Habuka, S. Tahmasebpoor, A. Danielsson, K. Edlund, A. Asplund, E. Sjostedt, E. Lundberg, C. A. Szigyarto, M. Skogs, J. O. Takanen, H. Berling, H. Tegel, J. Mulder, P. Nilsson, J. M. Schwenk, C. Lindskog, F. Danielsson, A. Mardinoglu, A. Sivertsson, K. von Feilitzen, M. Forsberg, M. Zwahlen, I. Olsson, S. Navani, M. Huss, J. Nielsen, F. Ponten and M. Uhlen (2014). "Analysis of the human tissue-specific expression by genome-wide integration of transcriptomics and antibody-based proteomics." <u>Mol Cell Proteomics</u> **13**(2): 397-406.
- Fanti, S., A. Briganti, L. Emmett, K. Fizazi, S. Gillessen, K. Goffin, B. A. Hadaschik, K. Herrmann, J. Kunikowska, T. Maurer, S. MacLennan, N. Mottet, D. G. Murphy, D. E. Oprea-Lager, J. M. O'Sullivan, W. J. G. Oyen, O. Rouviere, O. Sartor, A. Stenzl, H. Van Poppel, J. Walz, W. Witjes and A. Bjartell (2022). "EAU-EANM Consensus Statements on the Role of Prostate-specific Membrane Antigen Positron Emission Tomography/Computed Tomography in Patients with Prostate Cancer and with Respect to [(177)Lu]Lu-PSMA Radioligand Therapy." <u>Eur Urol Oncol</u> **5**(5): 530-536.

- Farrall, A. L. and M. L. Whitelaw (2009). "The HIF1alpha-inducible pro-cell death gene BNIP3 is a novel target of SIM2s repression through cross-talk on the hypoxia response element." Oncogene **28**(41): 3671-3680.
- Farrow, J. M., J. C. Yang and C. P. Evans (2014). "Autophagy as a modulator and target in prostate cancer." Nat Rev Urol 11(9): 508-516.
- Fateye, B., W. Li, C. Wang and B. Chen (2012). "Combination of phosphatidylinositol 3-kinases pathway inhibitor and photodynamic therapy in endothelial and tumor cells." <u>Photochem Photobiol</u> **88**(5): 1265-1272.
- Feher, M. D., J. C. Webb, D. D. Patel, A. F. Lant, P. D. Mayne, B. L. Knight and A. K. Soutar (1993). "Cholesterol-lowering drug therapy in a patient with receptor-negative homozygous familial hypercholesterolaemia." <u>Atherosclerosis</u> **103**(2): 171-180.
- Feng, Y., D. He, Z. Yao and D. J. Klionsky (2014). "The machinery of macroautophagy." <u>Cell Res</u> **24**(1): 24-41.
- Fielding, A. B., A. K. Willox, E. Okeke and S. J. Royle (2012). "Clathrin-mediated endocytosis is inhibited during mitosis." <u>Proc Natl Acad Sci U S A</u> **109**(17): 6572-6577.
- Forbes, A., S. Anoopkumar-Dukie, R. Chess-Williams and C. McDermott (2016). "Relative cytotoxic potencies and cell death mechanisms of alpha1 -adrenoceptor antagonists in prostate cancer cell lines." Prostate **76**(8): 757-766.
- Fornace, A. J., Jr., J. Jackman, M. C. Hollander, B. Hoffman-Liebermann and D. A. Liebermann (1992). "Genotoxic-stress-response genes and growth-arrest genes. gadd, MyD, and other genes induced by treatments eliciting growth arrest." <u>Ann NY Acad Sci</u> **663**: 139-153.
- Fortis, S. P., M. Goulielmaki, N. Aubert, P. Batsaki, S. Ouzounis, D. Cavouras, G. Marodon, S. Stokidis, A. D. Gritzapis and C. N. Baxevanis (2022). "Radiotherapy-Related Gene Signature in Prostate Cancer." Cancers (Basel) **14**(20).
- Frandsen, J., A. Orton, D. Shrieve and J. Tward (2017). "Risk of Death from Prostate Cancer with and without Definitive Local Therapy when Gleason Pattern 5 is Present: A Surveillance, Epidemiology, and End Results Analysis." <u>Cureus</u> **9**(7): e1453.
- Frisbie, J. H., S. Kumar, E. J. Aguilera and S. Yalla (2006). "Prostate atrophy and spinal cord lesions." Spinal Cord **44**(1): 24-27.
- Fukuchi, J., J. M. Kokontis, R. A. Hiipakka, C. P. Chuu and S. Liao (2004). "Antiproliferative effect of liver X receptor agonists on LNCaP human prostate cancer cells." <u>Cancer Res</u> **64**(21): 7686-7689. Fulda, S. (2018). "Targeting autophagy for the treatment of cancer." <u>Biol Chem</u>.
- Fulton, B., A. J. Wagstaff and E. M. Sorkin (1995). "Doxazosin. An update of its clinical pharmacology and therapeutic applications in hypertension and benign prostatic hyperplasia." <u>Drugs</u> **49**(2): 295-320.
- Galvagni, F., M. Orlandini and S. Oliviero (2013). "Role of the AP-1 transcription factor FOSL1 in endothelial cells adhesion and migration." <u>Cell Adh Migr</u> **7**(5): 408-411.
- Garrison, J. B. and N. Kyprianou (2006). "Doxazosin induces apoptosis of benign and malignant prostate cells via a death receptor-mediated pathway." <u>Cancer Res</u> **66**(1): 464-472.
- Ge, L. and R. Schekman (2014). "The ER-Golgi intermediate compartment feeds the phagophore membrane." <u>Autophagy</u> **10**(1): 170-172.
- Ghoneim, M. A. and H. Abol-Enein (2008). "Management of muscle-invasive bladder cancer: an update." Nat Clin Pract Urol **5**(9): 501-508.
- Gillmore, R., V. Laurence, S. Raouf, J. Tobias, G. Blackman, T. Meyer, K. Goodchild, C. Collis and J. Bridgewater (2010). "Chemoradiotherapy with or without induction chemotherapy for locally advanced pancreatic cancer: a UK multi-institutional experience." <u>Clin Oncol (R Coll Radiol)</u> **22**(7): 564-569.
- Goepel, M., A. Wittmann, H. Rubben and M. C. Michel (1997). "Comparison of adrenoceptor subtype expression in porcine and human bladder and prostate." <u>Urol Res</u> **25**(3): 199-206.
- Golomb, E., A. Kruglikova, D. Dvir, N. Parnes and A. Abramovici (1998). "Induction of atypical prostatic hyperplasia in rats by sympathomimetic stimulation." <u>Prostate</u> **34**(3): 214-221.

Goossens, M. E., F. Isa, M. Brinkman, D. Mak, R. Reulen, A. Wesselius, S. Benhamou, C. Bosetti, B. Bueno-de-Mesquita, A. Carta, M. F. Allam, K. Golka, E. J. Grant, X. Jiang, K. C. Johnson, M. R. Karagas, E. Kellen, C. La Vecchia, C. M. Lu, J. Marshall, K. Moysich, H. Pohlabeln, S. Porru, G. Steineck, M. C. Stern, L. Tang, J. A. Taylor, P. van den Brandt, P. J. Villeneuve, K. Wakai, E. Weiderpass, E. White, A. Wolk, Z. F. Zhang, F. Buntinx and M. P. Zeegers (2016). "International pooled study on diet and bladder cancer: the bladder cancer, epidemiology and nutritional determinants (BLEND) study: design and baseline characteristics." Arch Public Health 74: 30.

Gordetsky, J. and J. Epstein (2016). "Grading of prostatic adenocarcinoma: current state and prognostic implications." <u>Diagn Pathol</u> **11**: 25.

Gotoh, A., H. Nagaya, T. Kanno and T. Nishizaki (2012). "Antitumor action of alpha(1)-adrenoceptor blockers on human bladder, prostate and renal cancer cells." Pharmacology 90(5-6): 242-246. Grabowska, M. M., D. J. DeGraff, X. Yu, R. J. Jin, Z. Chen, A. D. Borowsky and R. J. Matusik (2014). "Mouse models of prostate cancer: picking the best model for the question." Cancer Metastasis Rev 33(2-3): 377-397.

Griffin, C., J. McNulty and S. Pandey (2011). "Pancratistatin induces apoptosis and autophagy in metastatic prostate cancer cells." <u>Int J Oncol</u> **38**(6): 1549-1556.

Guan, M., K. Fousek and W. A. Chow (2012). "Nelfinavir inhibits regulated intramembrane proteolysis of sterol regulatory element binding protein-1 and activating transcription factor 6 in castration-resistant prostate cancer." FEBS J **279**(13): 2399-2411.

Halaseh, S. A., S. Halaseh, Y. Alali, M. E. Ashour and M. J. Alharayzah (2022). "A Review of the Etiology and Epidemiology of Bladder Cancer: All You Need To Know." <u>Cureus</u> **14**(7): e27330. Hall, R. A. and R. J. Lefkowitz (2002). "Regulation of G protein-coupled receptor signaling by scaffold proteins." <u>Circ Res</u> **91**(8): 672-680.

Hammarsten, J. and B. Hogstedt (1999). "Clinical, anthropometric, metabolic and insulin profile of men with fast annual growth rates of benign prostatic hyperplasia." <u>Blood Press</u> **8**(1): 29-36. Han, C., W. C. Bowen, G. K. Michalopoulos and T. Wu (2008). "Alpha-1 adrenergic receptor transactivates signal transducer and activator of transcription-3 (Stat3) through activation of Src and epidermal growth factor receptor (EGFR) in hepatocytes." <u>J Cell Physiol</u> **216**(2): 486-497. Hao, M., S. Mukherjee, Y. Sun and F. R. Maxfield (2004). "Effects of cholesterol depletion and increased lipid unsaturation on the properties of endocytic membranes." <u>J Biol Chem</u> **279**(14): 14171-14178.

Harris, A. M., B. W. Warner, J. M. Wilson, A. Becker, R. G. Rowland, W. Conner, M. Lane, K. Kimbler, E. B. Durbin, A. T. Baron and N. Kyprianou (2007). "Effect of alpha1-adrenoceptor antagonist exposure on prostate cancer incidence: an observational cohort study." <u>J Urol</u> **178**(5): 2176-2180. Hasegawa, R., G. Murasaki, M. K. St John, T. V. Zenser and S. M. Cohen (1990). "Evaluation of nitrofurantoin on the two stages of urinary bladder carcinogenesis in the rat." <u>Toxicology</u> **62**(3): 333-347.

Hayashi, T., K. Nishiyama and T. Shirahama (2006). "Inhibition of 5-lipoxygenase pathway suppresses the growth of bladder cancer cells." Int J Urol **13**(8): 1086-1091.

He, Z., L. S. Mangala, C. A. Theriot, L. H. Rohde, H. Wu and Y. Zhang (2012). "Cell killing and radiosensitizing effects of atorvastatin in PC3 prostate cancer cells." <u>J Radiat Res</u> **53**(2): 225-233. Hennenberg, M., C. G. Stief and C. Gratzke (2014). "Prostatic alpha1-adrenoceptors: new concepts of function, regulation, and intracellular signaling." <u>Neurourol Urodyn</u> **33**(7): 1074-1085. Hensley, P. J., A. Desiniotis, C. Wang, A. Stromberg, C. S. Chen and N. Kyprianou (2014). "Novel pharmacologic targeting of tight junctions and focal adhesions in prostate cancer cells." <u>PLoS One</u>

pharmacologic targeting of tight junctions and focal adhesions in prostate cancer cells." <u>PLoS One</u> **9**(1): e86238. Herman-Antosiewicz, A., D. F. Johnson and S. V. Singh (2006), "Sulforaphane causes autophagy to

Herman-Antosiewicz, A., D. E. Johnson and S. V. Singh (2006). "Sulforaphane causes autophagy to inhibit release of cytochrome C and apoptosis in human prostate cancer cells." <u>Cancer Res</u> **66**(11): 5828-5835.

Higuchi, T., J. Nishikawa and H. Inoue (2015). "Sucrose induces vesicle accumulation and autophagy." J Cell Biochem **116**(4): 609-617.

- Hinata, N. and M. Fujisawa (2022). "Racial Differences in Prostate Cancer Characteristics and Cancer-Specific Mortality: An Overview." <u>World J Mens Health</u> **40**(2): 217-227.
- Hinshaw, J. E. (2000). "Dynamin and its role in membrane fission." <u>Annu Rev Cell Dev Biol</u> **16**: 483-519.
- Hird, A. E., E. Dvorani, R. Saskin, U. Emmenegger, S. Herschorn, R. Kodama, G. S. Kulkarni and R. K. Nam (2022). "Prevalence and Natural History of Non-metastatic Castrate Resistant Prostate Cancer: A Population-Based Analysis." <u>Clin Genitourin Cancer</u>.
- Hsu, T. C., M. R. Young, J. Cmarik and N. H. Colburn (2000). "Activator protein 1 (AP-1)- and nuclear factor kappaB (NF-kappaB)-dependent transcriptional events in carcinogenesis." <u>Free Radic Biol Med</u> **28**(9): 1338-1348.
- Hsueh, E. C., S. M. Knebel, W. H. Lo, Y. C. Leung, P. N. Cheng and C. T. Hsueh (2012). "Deprivation of arginine by recombinant human arginase in prostate cancer cells." J Hematol Oncol 5: 17.
- Hu, H., Y. Chai, L. Wang, J. Zhang, H. J. Lee, S. H. Kim and J. Lu (2009). "Pentagalloylglucose induces autophagy and caspase-independent programmed deaths in human PC-3 and mouse TRAMP-C2 prostate cancer cells." <u>Mol Cancer Ther</u> **8**(10): 2833-2843.
- Hui, H., M. A. Fernando and A. P. Heaney (2008). "The alpha1-adrenergic receptor antagonist doxazosin inhibits EGFR and NF-kappaB signalling to induce breast cancer cell apoptosis." <u>Eur J Cancer 44(1): 160-166</u>.
- Ibanez, E., A. Agliano, C. Prior, P. Nguewa, M. Redrado, I. Gonzalez-Zubeldia, D. Plano, J. A. Palop, C. Sanmartin and A. Calvo (2012). "The quinoline imidoselenocarbamate EI201 blocks the AKT/mTOR pathway and targets cancer stem cells leading to a strong antitumor activity." <u>Curr Med Chem</u> **19**(18): 3031-3043.
- Ikemoto, S., K. Sugimura, K. Kuratukuri and T. Nakatani (2004). "Antitumor effects of lipoxygenase inhibitors on murine bladder cancer cell line (MBT-2)." <u>Anticancer Res</u> **24**(2B): 733-736.
- Ishida, R., M. Sato, T. Narita, K. R. Utsumi, T. Nishimoto, T. Morita, H. Nagata and T. Andoh (1994). "Inhibition of DNA topoisomerase II by ICRF-193 induces polyploidization by uncoupling chromosome dynamics from other cell cycle events." <u>J Cell Biol</u> **126**(6): 1341-1351.
- Ito, H., H. Aoki, F. Kuhnel, Y. Kondo, S. Kubicka, T. Wirth, E. Iwado, A. Iwamaru, K. Fujiwara, K. R. Hess, F. F. Lang, R. Sawaya and S. Kondo (2006). "Autophagic cell death of malignant glioma cells induced by a conditionally replicating adenovirus." J Natl Cancer Inst **98**(9): 625-636.
- Ittmann, M., J. Huang, E. Radaelli, P. Martin, S. Signoretti, R. Sullivan, B. W. Simons, J. M. Ward, B. D. Robinson, G. C. Chu, M. Loda, G. Thomas, A. Borowsky and R. D. Cardiff (2013). "Animal models of human prostate cancer: the consensus report of the New York meeting of the Mouse Models of Human Cancers Consortium Prostate Pathology Committee." <u>Cancer Res</u> **73**(9): 2718-2736.
- Ivanov, A. I. (2008). Exocytosis and endocytosis. Totowa, N.J., Humana Press.
- Jagroop, I. A. and D. P. Mikhailidis (2001). "Doxazosin, an alpha1-adrenoceptor antagonist, inhibits serotonin-induced shape change in human platelets." J Hum Hypertens **15**(3): 203-207.
- Jahn, J. L., E. L. Giovannucci and M. J. Stampfer (2015). "The high prevalence of undiagnosed prostate cancer at autopsy: implications for epidemiology and treatment of prostate cancer in the Prostate-specific Antigen-era." Int J Cancer 137(12): 2795-2802.
- Janssen, K., S. Horn, M. T. Niemann, P. T. Daniel, K. Schulze-Osthoff and U. Fischer (2009). "Inhibition of the ER Ca2+ pump forces multidrug-resistant cells deficient in Bak and Bax into necrosis." <u>J Cell Sci</u> **122**(Pt 24): 4481-4491.
- Jia, J., T. Ye, P. Cui, Q. Hua, H. Zeng and D. Zhao (2016). "AP-1 transcription factor mediates VEGF-induced endothelial cell migration and proliferation." <u>Microvasc Res</u> **105**: 103-108.
- Jiang, M., S. Fernandez, W. G. Jerome, Y. He, X. Yu, H. Cai, B. Boone, Y. Yi, M. A. Magnuson, P. Roy-Burman, R. J. Matusik, S. B. Shappell and S. W. Hayward (2010). "Disruption of PPARgamma signaling results in mouse prostatic intraepithelial neoplasia involving active autophagy." <u>Cell Death Differ</u> **17**(3): 469-481.
- Jiang, M., W. G. Jerome and S. W. Hayward (2010). "Autophagy in nuclear receptor PPARgamma-deficient mouse prostatic carcinogenesis." <u>Autophagy</u> **6**(1): 175-176.

- Jiang, Q., X. Rao, C. Y. Kim, H. Freiser, Q. Zhang, Z. Jiang and G. Li (2012). "Gamma-tocotrienol induces apoptosis and autophagy in prostate cancer cells by increasing intracellular dihydrosphingosine and dihydroceramide." Int J Cancer 130(3): 685-693.
- John, B. A. and N. Said (2017). "Insights from animal models of bladder cancer: recent advances, challenges, and opportunities." Oncotarget **8**(34): 57766-57781.
- Kaini, R. R., L. O. Sillerud, S. Zhaorigetu and C. A. Hu (2012). "Autophagy regulates lipolysis and cell survival through lipid droplet degradation in androgen-sensitive prostate cancer cells." <u>Prostate</u> **72**(13): 1412-1422.
- Kamat, A. M. and D. L. Lamm (2004). "Antitumor activity of common antibiotics against superficial bladder cancer." Urology **63**(3): 457-460.
- Kanda, H., K. Ishii, Y. Ogura, T. Imamura, M. Kanai, K. Arima and Y. Sugimura (2008). "Naftopidil, a selective alpha-1 adrenoceptor antagonist, inhibits growth of human prostate cancer cells by G1 cell cycle arrest." Int J Cancer **122**(2): 444-451.
- Kar, R., P. K. Singha, M. A. Venkatachalam and P. Saikumar (2009). "A novel role for MAP1 LC3 in nonautophagic cytoplasmic vacuolation death of cancer cells." <u>Oncogene</u> **28**(28): 2556-2568. Karna, P., S. Zughaier, V. Pannu, R. Simmons, S. Narayan and R. Aneja (2010). "Induction of reactive oxygen species-mediated autophagy by a novel microtubule-modulating agent." <u>J Biol Chem</u> **285**(24): 18737-18748.
- Katoh, Y. and M. Katoh (2004). "Identification and characterization of ARHGAP27 gene in silico." <u>Int J</u> Mol Med **14**(5): 943-947.
- Kaye, B., N. J. Cussans, J. K. Faulkner, D. A. Stopher and J. L. Reid (1986). "The metabolism and kinetics of doxazosin in man, mouse, rat and dog." <u>Br J Clin Pharmacol</u> **21 Suppl 1**: 19S-25S. Keedwell, R. G., Y. Zhao, L. A. Hammond, K. Wen, S. Qin, L. I. Atangan, D. L. Shurland, D. M. Wallace, R. Bird, A. Reitmair, R. A. Chandraratna and G. Brown (2004). "An antagonist of retinoic acid receptors more effectively inhibits growth of human prostate cancer cells than normal prostate epithelium." Br J Cancer **91**(3): 580-588.
- Keledjian, K., A. Borkowski, G. Kim, J. T. Isaacs, S. C. Jacobs and N. Kyprianou (2001). "Reduction of human prostate tumor vascularity by the alpha1-adrenoceptor antagonist terazosin." <u>Prostate</u> **48**(2): 71-78.
- Keledjian, K., J. B. Garrison and N. Kyprianou (2005). "Doxazosin inhibits human vascular endothelial cell adhesion, migration, and invasion." <u>J Cell Biochem</u> **94**(2): 374-388.
- Keledjian, K. and N. Kyprianou (2003). "Anoikis induction by quinazoline based alpha 1-adrenoceptor antagonists in prostate cancer cells: antagonistic effect of bcl-2." J Urol 169(3): 1150-1156.
- Kennedy, D., R. Jager, D. D. Mosser and A. Samali (2014). "Regulation of apoptosis by heat shock proteins." <u>IUBMB Life</u> **66**(5): 327-338.
- Khwaja, F., J. Allen, J. Lynch, P. Andrews and D. Djakiew (2004). "Ibuprofen inhibits survival of bladder cancer cells by induced expression of the p75NTR tumor suppressor protein." <u>Cancer Res</u> **64**(17): 6207-6213.
- Kilsdonk, E. P., P. G. Yancey, G. W. Stoudt, F. W. Bangerter, W. J. Johnson, M. C. Phillips and G. H. Rothblat (1995). "Cellular cholesterol efflux mediated by cyclodextrins." <u>J Biol Chem</u> **270**(29): 17250-17256.
- Kim, D. K., J. S. Yang, K. Maiti, J. I. Hwang, K. Kim, D. Seen, Y. Ahn, C. Lee, B. C. Kang, H. B. Kwon, J. Cheon and J. Y. Seong (2009). "A gonadotropin-releasing hormone-II antagonist induces autophagy of prostate cancer cells." <u>Cancer Res</u> **69**(3): 923-931.
- Kim, K. H. and M. S. Lee (2014). "Autophagy--a key player in cellular and body metabolism." <u>Nat Rev Endocrinol</u> **10**(6): 322-337.
- Kim, M. S., S. Y. Song, J. Y. Lee, N. J. Yoo and S. H. Lee (2011). "Expressional and mutational analyses of ATG5 gene in prostate cancers." <u>APMIS</u> **119**(11): 802-807.
- Kim, R. H., R. J. Bold and H. J. Kung (2009). "ADI, autophagy and apoptosis: metabolic stress as a therapeutic option for prostate cancer." <u>Autophagy</u> **5**(4): 567-568.

Kim, R. H., J. M. Coates, T. L. Bowles, G. P. McNerney, J. Sutcliffe, J. U. Jung, R. Gandour-Edwards, F. Y. Chuang, R. J. Bold and H. J. Kung (2009). "Arginine deiminase as a novel therapy for prostate cancer induces autophagy and caspase-independent apoptosis." Cancer Res 69(2): 700-708. Kim, S. H., E. J. Park, C. R. Lee, J. N. Chun, N. H. Cho, I. G. Kim, S. Lee, T. W. Kim, H. H. Park, I. So and J. H. Jeon (2012). "Geraniol induces cooperative interaction of apoptosis and autophagy to elicit cell death in PC-3 prostate cancer cells." Int J Oncol 40(5): 1683-1690. Kim, Y. A., S. H. Rhee, K. Y. Park and Y. H. Choi (2003). "Antiproliferative effect of resveratrol in human prostate carcinoma cells." J Med Food 6(4): 273-280. Kleinman, H. K. and G. R. Martin (2005). "Matrigel: basement membrane matrix with biological activity." Semin Cancer Biol 15(5): 378-386. Klionsky, D. J., F. C. Abdalla, H. Abeliovich, R. T. Abraham, A. Acevedo-Arozena, K. Adeli, L. Agholme, M. Agnello, P. Agostinis, J. A. Aguirre-Ghiso, H. J. Ahn, O. Ait-Mohamed, S. Ait-Si-Ali, T. Akematsu, S. Akira, H. M. Al-Younes, M. A. Al-Zeer, M. L. Albert, R. L. Albin, J. Alegre-Abarrategui, M. F. Aleo, M. Alirezaei, A. Almasan, M. Almonte-Becerril, A. Amano, R. Amaravadi, S. Amarnath, A. O. Amer, N. Andrieu-Abadie, V. Anantharam, D. K. Ann, S. Anoopkumar-Dukie, H. Aoki, N. Apostolova, G. Arancia, J. P. Aris, K. Asanuma, N. Y. Asare, H. Ashida, V. Askanas, D. S. Askew, P. Auberger, M. Baba, S. K. Backues, E. H. Baehrecke, B. A. Bahr, X. Y. Bai, Y. Bailly, R. Baiocchi, G. Baldini, W. Balduini, A. Ballabio, B. A. Bamber, E. T. Bampton, G. Banhegyi, C. R. Bartholomew, D. C. Bassham, R. C. Bast, Jr., H. Batoko, B. H. Bay, I. Beau, D. M. Bechet, T. J. Begley, C. Behl, C. Behrends, S. Bekri, B. Bellaire, L. J. Bendall, L. Benetti, L. Berliocchi, H. Bernardi, F. Bernassola, S. Besteiro, I. Bhatia-Kissova, X. Bi, M. Biard-Piechaczyk, J. S. Blum, L. H. Boise, P. Bonaldo, D. L. Boone, B. C. Bornhauser, K. R. Bortoluci, I. Bossis, F. Bost, J. P. Bourquin, P. Boya, M. Boyer-Guittaut, P. V. Bozhkov, N. R. Brady, C. Brancolini, A. Brech, J. E. Brenman, A. Brennand, E. H. Bresnick, P. Brest, D. Bridges, M. L. Bristol, P. S. Brookes, E. J. Brown, J. H. Brumell, N. Brunetti-Pierri, U. T. Brunk, D. E. Bulman, S. J. Bultman, G. Bultynck, L. F. Burbulla, W. Bursch, J. P. Butchar, W. Buzgariu, S. P. Bydlowski, K. Cadwell, M. Cahova, D. Cai, J. Cai, Q. Cai, B. Calabretta, J. Calvo-Garrido, N. Camougrand, M. Campanella, J. Campos-Salinas, E. Candi, L. Cao, A. B. Caplan, S. R. Carding, S. M. Cardoso, J. S. Carew, C. R. Carlin, V. Carmignac, L. A. Carneiro, S. Carra, R. A. Caruso, G. Casari, C. Casas, R. Castino, E. Cebollero, F. Cecconi, J. Celli, H. Chaachouay, H. J. Chae, C. Y. Chai, D. C. Chan, E. Y. Chan, R. C. Chang, C. M. Che, C. C. Chen, G. C. Chen, G. Q. Chen, M. Chen, Q. Chen, S. S. Chen, W. Chen, X. Chen, X. Chen, X. Chen, Y. G. Chen, Y. Chen, Y. J. Chen, Z. Chen, A. Cheng, C. H. Cheng, Y. Cheng, H. Cheong, J. H. Cheong, S. Cherry, R. Chess-Williams, Z. H. Cheung, E. Chevet, H. L. Chiang, R. Chiarelli, T. Chiba, L. S. Chin, S. H. Chiou, F. V. Chisari, C. H. Cho, D. H. Cho, A. M. Choi, D. Choi, K. S. Choi, M. E. Choi, S. Chouaib, D. Choubey, V. Choubey, C. T. Chu, T. H. Chuang, S. H. Chueh, T. Chun, Y. J. Chwae, M. L. Chye, R. Ciarcia, M. R. Ciriolo, M. J. Clague, R. S. Clark, P. G. Clarke, R. Clarke, P. Codogno, H. A. Coller, M. I. Colombo, S. Comincini, M. Condello, F. Condorelli, M. R. Cookson, G. H. Coombs, I. Coppens, R. Corbalan, P. Cossart, P. Costelli, S. Costes, A. Coto-Montes, E. Couve, F. P. Coxon, J. M. Cregg, J. L. Crespo, M. J. Cronje, A. M. Cuervo, J. J. Cullen, M. J. Czaja, M. D'Amelio, A. Darfeuille-Michaud, L. M. Davids, F. E. Davies, M. De Felici, J. F. de Groot, C. A. de Haan, L. De Martino, A. De Milito, V. De Tata, J. Debnath, A. Degterev, B. Dehay, L. M. Delbridge, F. Demarchi, Y. Z. Deng, J. Dengjel, P. Dent, D. Denton, V. Deretic, S. D. Desai, R. J. Devenish, M. Di Gioacchino, G. Di Paolo, C. Di Pietro, G. Diaz-Araya, I. Diaz-Laviada, M. T. Diaz-Meco, J. Diaz-Nido, I. Dikic, S. P. Dinesh-Kumar, W. X. Ding, C. W. Distelhorst, A. Diwan, M. Djavaheri-Mergny, S. Dokudovskaya, Z. Dong, F. C. Dorsey, V. Dosenko, J. J. Dowling, S. Doxsey, M. Dreux, M. E. Drew, Q. Duan, M. A. Duchosal, K. Duff, I. Dugail, M. Durbeej, M. Duszenko, C. L. Edelstein, A. L. Edinger, G. Egea, L. Eichinger, N. T. Eissa, S. Ekmekcioglu, W. S. El-Deiry, Z. Elazar, M. Elgendy, L. M. Ellerby, K. E. Eng, A. M. Engelbrecht, S. Engelender, J. Erenpreisa, R. Escalante, A. Esclatine, E. L. Eskelinen, L. Espert, V. Espina, H. Fan, J. Fan, Q. W. Fan, Z. Fan, S. Fang, Y. Fang, M. Fanto, A. Fanzani, T. Farkas, J. C. Farre, M. Faure, M. Fechheimer, C. G. Feng, J. Feng, Q. Feng, Y. Feng, L. Fesus, R. Feuer, M. E. Figueiredo-Pereira, G. M. Fimia, D. C. Fingar, S. Finkbeiner, T. Finkel, K. D. Finley, F. Fiorito, E. A. Fisher, P. B. Fisher, M. Flajolet, M. L. Florez-McClure, S. Florio, E. A. Fon, F. Fornai, F. Fortunato, R. Fotedar, D. H. Fowler, H. S. Fox, R. Franco, L. B. Frankel, M. Fransen, J. M. Fuentes, J.

Fueyo, J. Fujii, K. Fujisaki, E. Fujita, M. Fukuda, R. H. Furukawa, M. Gaestel, P. Gailly, M. Gajewska, B. Galliot, V. Galy, S. Ganesh, B. Ganetzky, I. G. Ganley, F. B. Gao, G. F. Gao, J. Gao, L. Garcia, G. Garcia-Manero, M. Garcia-Marcos, M. Garmyn, A. L. Gartel, E. Gatti, M. Gautel, T. R. Gawriluk, M. E. Gegg, J. Geng, M. Germain, J. E. Gestwicki, D. A. Gewirtz, S. Ghavami, P. Ghosh, A. M. Giammarioli, A. N. Giatromanolaki, S. B. Gibson, R. W. Gilkerson, M. L. Ginger, H. N. Ginsberg, J. Golab, M. S. Goligorsky, P. Golstein, C. Gomez-Manzano, E. Goncu, C. Gongora, C. D. Gonzalez, R. Gonzalez, C. Gonzalez-Estevez, R. A. Gonzalez-Polo, E. Gonzalez-Rey, N. V. Gorbunov, S. Gorski, S. Goruppi, R. A. Gottlieb, D. Gozuacik, G. E. Granato, G. D. Grant, K. N. Green, A. Gregorc, F. Gros, C. Grose, T. W. Grunt, P. Gual, J. L. Guan, K. L. Guan, S. M. Guichard, A. S. Gukovskaya, I. Gukovsky, J. Gunst, A. B. Gustafsson, A. J. Halayko, A. N. Hale, S. K. Halonen, M. Hamasaki, F. Han, T. Han, M. K. Hancock, M. Hansen, H. Harada, M. Harada, S. E. Hardt, J. W. Harper, A. L. Harris, J. Harris, S. D. Harris, M. Hashimoto, J. A. Haspel, S. Hayashi, L. A. Hazelhurst, C. He, Y. W. He, M. J. Hebert, K. A. Heidenreich, M. H. Helfrich, G. V. Helgason, E. P. Henske, B. Herman, P. K. Herman, C. Hetz, S. Hilfiker, J. A. Hill, L. J. Hocking, P. Hofman, T. G. Hofmann, J. Hohfeld, T. L. Holyoake, M. H. Hong, D. A. Hood, G. S. Hotamisligil, E. J. Houwerzijl, M. Hoyer-Hansen, B. Hu, C. A. Hu, H. M. Hu, Y. Hua, C. Huang, J. Huang, S. Huang, W. P. Huang, T. B. Huber, W. K. Huh, T. H. Hung, T. R. Hupp, G. M. Hur, J. B. Hurley, S. N. Hussain, P. J. Hussey, J. J. Hwang, S. Hwang, A. Ichihara, S. Ilkhanizadeh, K. Inoki, T. Into, V. Iovane, J. L. Iovanna, N. Y. Ip, Y. Isaka, H. Ishida, C. Isidoro, K. Isobe, A. Iwasaki, M. Izquierdo, Y. Izumi, P. M. Jaakkola, M. Jaattela, G. R. Jackson, W. T. Jackson, B. Janji, M. Jendrach, J. H. Jeon, E. B. Jeung, H. Jiang, H. Jiang, J. X. Jiang, M. Jiang, Q. Jiang, X. Jiang, X. Jiang, A. Jimenez, M. Jin, S. Jin, C. O. Joe, T. Johansen, D. E. Johnson, G. V. Johnson, N. L. Jones, B. Joseph, S. K. Joseph, A. M. Joubert, G. Juhasz, L. Juillerat-Jeanneret, C. H. Jung, Y. K. Jung, K. Kaarniranta, A. Kaasik, T. Kabuta, M. Kadowaki, K. Kagedal, Y. Kamada, V. O. Kaminskyy, H. H. Kampinga, H. Kanamori, C. Kang, K. B. Kang, K. I. Kang, R. Kang, Y. A. Kang, T. Kanki, T. D. Kanneganti, H. Kanno, A. G. Kanthasamy, A. Kanthasamy, V. Karantza, G. P. Kaushal, S. Kaushik, Y. Kawazoe, P. Y. Ke, J. H. Kehrl, A. Kelekar, C. Kerkhoff, D. H. Kessel, H. Khalil, J. A. Kiel, A. A. Kiger, A. Kihara, D. R. Kim, D. H. Kim, D. H. Kim, E. K. Kim, H. R. Kim, J. S. Kim, J. H. Kim, J. C. Kim, J. K. Kim, P. K. Kim, S. W. Kim, Y. S. Kim, Y. Kim, A. Kimchi, A. C. Kimmelman, J. S. King, T. J. Kinsella, V. Kirkin, L. A. Kirshenbaum, K. Kitamoto, K. Kitazato, L. Klein, W. T. Klimecki, J. Klucken, E. Knecht, B. C. Ko, J. C. Koch, H. Koga, J. Y. Koh, Y. H. Koh, M. Koike, M. Komatsu, E. Kominami, H. J. Kong, W. J. Kong, V. I. Korolchuk, Y. Kotake, M. I. Koukourakis, J. B. Kouri Flores, A. L. Kovacs, C. Kraft, D. Krainc, H. Kramer, C. Kretz-Remy, A. M. Krichevsky, G. Kroemer, R. Kruger, O. Krut, N. T. Ktistakis, C. Y. Kuan, R. Kucharczyk, A. Kumar, R. Kumar, S. Kumar, M. Kundu, H. J. Kung, T. Kurz, H. J. Kwon, A. R. La Spada, F. Lafont, T. Lamark, J. Landry, J. D. Lane, P. Lapaquette, J. F. Laporte, L. Laszlo, S. Lavandero, J. N. Lavoie, R. Layfield, P. A. Lazo, W. Le, L. Le Cam, D. J. Ledbetter, A. J. Lee, B. W. Lee, G. M. Lee, J. Lee, J. H. Lee, M. Lee, M. S. Lee, S. H. Lee, C. Leeuwenburgh, P. Legembre, R. Legouis, M. Lehmann, H. Y. Lei, Q. Y. Lei, D. A. Leib, J. Leiro, J. J. Lemasters, A. Lemoine, M. S. Lesniak, D. Lev, V. V. Levenson, B. Levine, E. Levy, F. Li, J. L. Li, L. Li, S. Li, W. Li, X. J. Li, Y. B. Li, Y. P. Li, C. Liang, Q. Liang, Y. F. Liao, P. P. Liberski, A. Lieberman, H. J. Lim, K. L. Lim, K. Lim, C. F. Lin, F. C. Lin, J. Lin, J. D. Lin, K. Lin, W. W. Lin, W. C. Lin, Y. L. Lin, R. Linden, P. Lingor, J. Lippincott-Schwartz, M. P. Lisanti, P. B. Liton, B. Liu, C. F. Liu, K. Liu, L. Liu, Q. A. Liu, W. Liu, Y. C. Liu, Y. Liu, R. A. Lockshin, C. N. Lok, S. Lonial, B. Loos, G. Lopez-Berestein, C. Lopez-Otin, L. Lossi, M. T. Lotze, P. Low, B. Lu, B. Lu, B. Lu, Z. Lu, F. Luciano, N. W. Lukacs, A. H. Lund, M. A. Lynch-Day, Y. Ma, F. Macian, J. P. MacKeigan, K. F. Macleod, F. Madeo, L. Maiuri, M. C. Maiuri, D. Malagoli, M. C. Malicdan, W. Malorni, N. Man, E. M. Mandelkow, S. Manon, I. Manov, K. Mao, X. Mao, Z. Mao, P. Marambaud, D. Marazziti, Y. L. Marcel, K. Marchbank, P. Marchetti, S. J. Marciniak, M. Marcondes, M. Mardi, G. Marfe, G. Marino, M. Markaki, M. R. Marten, S. J. Martin, C. Martinand-Mari, W. Martinet, M. Martinez-Vicente, M. Masini, P. Matarrese, S. Matsuo, R. Matteoni, A. Mayer, N. M. Mazure, D. J. McConkey, M. J. McConnell, C. McDermott, C. McDonald, G. M. McInerney, S. L. McKenna, B. McLaughlin, P. J. McLean, C. R. McMaster, G. A. McQuibban, A. J. Meijer, M. H. Meisler, A. Melendez, T. J. Melia, G. Melino, M. A. Mena, J. A. Menendez, R. F. Menna-Barreto, M. B. Menon, F. M. Menzies, C. A. Mercer, A. Merighi, D. E. Merry, S. Meschini, C. G. Meyer, T. F. Meyer, C. Y. Miao, J. Y. Miao, P. A.

Michels, C. Michiels, D. Mijaljica, A. Milojkovic, S. Minucci, C. Miracco, C. K. Miranti, I. Mitroulis, K. Miyazawa, N. Mizushima, B. Mograbi, S. Mohseni, X. Molero, B. Mollereau, F. Mollinedo, T. Momoi, I. Monastyrska, M. M. Monick, M. J. Monteiro, M. N. Moore, R. Mora, K. Moreau, P. I. Moreira, Y. Moriyasu, J. Moscat, S. Mostowy, J. C. Mottram, T. Motyl, C. E. Moussa, S. Muller, S. Muller, K. Munger, C. Munz, L. O. Murphy, M. E. Murphy, A. Musaro, I. Mysorekar, E. Nagata, K. Nagata, A. Nahimana, U. Nair, T. Nakagawa, K. Nakahira, H. Nakano, H. Nakatogawa, M. Nanjundan, N. I. Naqvi, D. P. Narendra, M. Narita, M. Navarro, S. T. Nawrocki, T. Y. Nazarko, A. Nemchenko, M. G. Netea, T. P. Neufeld, P. A. Ney, I. P. Nezis, H. P. Nguyen, D. Nie, I. Nishino, C. Nislow, R. A. Nixon, T. Noda, A. A. Noegel, A. Nogalska, S. Noguchi, L. Notterpek, I. Novak, T. Nozaki, N. Nukina, T. Nurnberger, B. Nyfeler, K. Obara, T. D. Oberley, S. Oddo, M. Ogawa, T. Ohashi, K. Okamoto, N. L. Oleinick, F. J. Oliver, L. J. Olsen, S. Olsson, O. Opota, T. F. Osborne, G. K. Ostrander, K. Otsu, J. H. Ou, M. Ouimet, M. Overholtzer, B. Ozpolat, P. Paganetti, U. Pagnini, N. Pallet, G. E. Palmer, C. Palumbo, T. Pan, T. Panaretakis, U. B. Pandey, Z. Papackova, I. Papassideri, I. Paris, J. Park, O. K. Park, J. B. Parys, K. R. Parzych, S. Patschan, C. Patterson, S. Pattingre, J. M. Pawelek, J. Peng, D. H. Perlmutter, I. Perrotta, G. Perry, S. Pervaiz, M. Peter, G. J. Peters, M. Petersen, G. Petrovski, J. M. Phang, M. Piacentini, P. Pierre, V. Pierrefite-Carle, G. Pierron, R. Pinkas-Kramarski, A. Piras, N. Piri, L. C. Platanias, S. Poggeler, M. Poirot, A. Poletti, C. Pous, M. Pozuelo-Rubio, M. Praetorius-Ibba, A. Prasad, M. Prescott, M. Priault, N. Produit-Zengaffinen, A. Progulske-Fox, T. Proikas-Cezanne, S. Przedborski, K. Przyklenk, R. Puertollano, J. Puyal, S. B. Qian, L. Qin, Z. H. Qin, S. E. Quaggin, N. Raben, H. Rabinowich, S. W. Rabkin, I. Rahman, A. Rami, G. Ramm, G. Randall, F. Randow, V. A. Rao, J. C. Rathmell, B. Ravikumar, S. K. Ray, B. H. Reed, J. C. Reed, F. Reggiori, A. Regnier-Vigouroux, A. S. Reichert, J. J. Reiners, Jr., R. J. Reiter, J. Ren, J. L. Revuelta, C. J. Rhodes, K. Ritis, E. Rizzo, J. Robbins, M. Roberge, H. Roca, M. C. Roccheri, S. Rocchi, H. P. Rodemann, S. Rodriguez de Cordoba, B. Rohrer, I. B. Roninson, K. Rosen, M. M. Rost-Roszkowska, M. Rouis, K. M. Rouschop, F. Rovetta, B. P. Rubin, D. C. Rubinsztein, K. Ruckdeschel, E. B. Rucker, 3rd, A. Rudich, E. Rudolf, N. Ruiz-Opazo, R. Russo, T. E. Rusten, K. M. Ryan, S. W. Ryter, D. M. Sabatini, J. Sadoshima, T. Saha, T. Saitoh, H. Sakagami, Y. Sakai, G. H. Salekdeh, P. Salomoni, P. M. Salvaterra, G. Salvesen, R. Salvioli, A. M. Sanchez, J. A. Sanchez-Alcazar, R. Sanchez-Prieto, M. Sandri, U. Sankar, P. Sansanwal, L. Santambrogio, S. Saran, S. Sarkar, M. Sarwal, C. Sasakawa, A. Sasnauskiene, M. Sass, K. Sato, M. Sato, A. H. Schapira, M. Scharl, H. M. Schatzl, W. Scheper, S. Schiaffino, C. Schneider, M. E. Schneider, R. Schneider-Stock, P. V. Schoenlein, D. F. Schorderet, C. Schuller, G. K. Schwartz, L. Scorrano, L. Sealy, P. O. Seglen, J. Segura-Aguilar, I. Seiliez, O. Seleverstov, C. Sell, J. B. Seo, D. Separovic, V. Setaluri, T. Setoguchi, C. Settembre, J. J. Shacka, M. Shanmugam, I. M. Shapiro, E. Shaulian, R. J. Shaw, J. H. Shelhamer, H. M. Shen, W. C. Shen, Z. H. Sheng, Y. Shi, K. Shibuya, Y. Shidoji, J. J. Shieh, C. M. Shih, Y. Shimada, S. Shimizu, T. Shintani, O. S. Shirihai, G. C. Shore, A. A. Sibirny, S. B. Sidhu, B. Sikorska, E. C. Silva-Zacarin, A. Simmons, A. K. Simon, H. U. Simon, C. Simone, A. Simonsen, D. A. Sinclair, R. Singh, D. Sinha, F. A. Sinicrope, A. Sirko, P. M. Siu, E. Sivridis, V. Skop, V. P. Skulachev, R. S. Slack, S. S. Smaili, D. R. Smith, M. S. Soengas, T. Soldati, X. Song, A. K. Sood, T. W. Soong, F. Sotgia, S. A. Spector, C. D. Spies, W. Springer, S. M. Srinivasula, L. Stefanis, J. S. Steffan, R. Stendel, H. Stenmark, A. Stephanou, S. T. Stern, C. Sternberg, B. Stork, P. Stralfors, C. S. Subauste, X. Sui, D. Sulzer, J. Sun, S. Y. Sun, Z. J. Sun, J. J. Sung, K. Suzuki, T. Suzuki, M. S. Swanson, C. Swanton, S. T. Sweeney, L. K. Sy, G. Szabadkai, I. Tabas, H. Taegtmeyer, M. Tafani, K. Takacs-Vellai, Y. Takano, K. Takegawa, G. Takemura, F. Takeshita, N. J. Talbot, K. S. Tan, K. Tanaka, K. Tanaka, D. Tang, D. Tang, I. Tanida, B. A. Tannous, N. Tavernarakis, G. S. Taylor, G. A. Taylor, J. P. Taylor, L. S. Terada, A. Terman, G. Tettamanti, K. Thevissen, C. B. Thompson, A. Thorburn, M. Thumm, F. Tian, Y. Tian, G. Tocchini-Valentini, A. M. Tolkovsky, Y. Tomino, L. Tonges, S. A. Tooze, C. Tournier, J. Tower, R. Towns, V. Trajkovic, L. H. Travassos, T. F. Tsai, M. P. Tschan, T. Tsubata, A. Tsung, B. Turk, L. S. Turner, S. C. Tyagi, Y. Uchiyama, T. Ueno, M. Umekawa, R. Umemiya-Shirafuji, V. K. Unni, M. I. Vaccaro, E. M. Valente, G. Van den Berghe, I. J. van der Klei, W. van Doorn, L. F. van Dyk, M. van Egmond, L. A. van Grunsven, P. Vandenabeele, W. P. Vandenberghe, I. Vanhorebeek, E. C. Vaquero, G. Velasco, T. Vellai, J. M. Vicencio, R. D. Vierstra, M. Vila, C. Vindis, G. Viola, M. T. Viscomi, O. V. Voitsekhovskaja, C. von Haefen, M. Votruba, K. Wada, R. Wade-Martins, C. L. Walker, C. M. Walsh, J. Walter, X. B. Wan, A. Wang, C. Wang, D. Wang, F. Wang, F. Wang, G. Wang, H. Wang, H. G. Wang, H. D. Wang, J. Wang, K. Wang, M. Wang, R. C. Wang, X. Wang, X. Wang, Y. J. Wang, Y. Wang, Z. Wang, Z. C. Wang, Z. Wang, D. G. Wansink, D. M. Ward, H. Watada, S. L. Waters, P. Webster, L. Wei, C. C. Weihl, W. A. Weiss, S. M. Welford, L. P. Wen, C. A. Whitehouse, J. L. Whitton, A. J. Whitworth, T. Wileman, J. W. Wiley, S. Wilkinson, D. Willbold, R. L. Williams, P. R. Williamson, B. G. Wouters, C. Wu, D. C. Wu, W. K. Wu, A. Wyttenbach, R. J. Xavier, Z. Xi, P. Xia, G. Xiao, Z. Xie, Z. Xie, D. Z. Xu, J. Xu, L. Xu, X. Xu, A. Yamamoto, A. Yamamoto, S. Yamashina, M. Yamashita, X. Yan, M. Yanagida, D. S. Yang, E. Yang, J. M. Yang, S. Y. Yang, W. Yang, W. Y. Yang, Z. Yang, M. C. Yao, T. P. Yao, B. Yeganeh, W. L. Yen, J. J. Yin, X. M. Yin, O. J. Yoo, G. Yoon, S. Y. Yoon, T. Yorimitsu, Y. Yoshikawa, T. Yoshimori, K. Yoshimoto, H. J. You, R. J. Youle, A. Younes, L. Yu, L. Yu, S. W. Yu, W. H. Yu, Z. M. Yuan, Z. Yue, C. H. Yun, M. Yuzaki, O. Zabirnyk, E. Silva-Zacarin, D. Zacks, E. Zacksenhaus, N. Zaffaroni, Z. Zakeri, H. J. Zeh, 3rd, S. O. Zeitlin, H. Zhang, H. L. Zhang, J. Zhang, J. P. Zhang, L. Zhang, L. Zhang, M. Y. Zhang, X. D. Zhang, M. Zhao, Y. F. Zhao, Y. Zhao, Z. J. Zhao, X. Zheng, B. Zhivotovsky, Q. Zhong, C. Z. Zhou, C. Zhu, W. G. Zhu, X. F. Zhu, X. Zhu, Y. Zhu, T. Zoladek, W. X. Zong, A. Zorzano, J. Zschocke and B. Zuckerbraun (2012). "Guidelines for the use and interpretation of assays for monitoring autophagy." Autophagy 8(4): 445-544. Klionsky, D. J., H. Abeliovich, P. Agostinis, D. K. Agrawal, G. Aliev, D. S. Askew, M. Baba, E. H. Baehrecke, B. A. Bahr, A. Ballabio, B. A. Bamber, D. C. Bassham, E. Bergamini, X. Bi, M. Biard-Piechaczyk, J. S. Blum, D. E. Bredesen, J. L. Brodsky, J. H. Brumell, U. T. Brunk, W. Bursch, N. Camougrand, E. Cebollero, F. Cecconi, Y. Chen, L. S. Chin, A. Choi, C. T. Chu, J. Chung, P. G. Clarke, R. S. Clark, S. G. Clarke, C. Clave, J. L. Cleveland, P. Codogno, M. I. Colombo, A. Coto-Montes, J. M. Cregg, A. M. Cuervo, J. Debnath, F. Demarchi, P. B. Dennis, P. A. Dennis, V. Deretic, R. J. Devenish, F. Di Sano, J. F. Dice, M. Difiglia, S. Dinesh-Kumar, C. W. Distelhorst, M. Djavaheri-Mergny, F. C. Dorsey, W. Droge, M. Dron, W. A. Dunn, Jr., M. Duszenko, N. T. Eissa, Z. Elazar, A. Esclatine, E. L. Eskelinen, L. Fesus, K. D. Finley, J. M. Fuentes, J. Fueyo, K. Fujisaki, B. Galliot, F. B. Gao, D. A. Gewirtz, S. B. Gibson, A. Gohla, A. L. Goldberg, R. Gonzalez, C. Gonzalez-Estevez, S. Gorski, R. A. Gottlieb, D. Haussinger, Y. W. He, K. Heidenreich, J. A. Hill, M. Hoyer-Hansen, X. Hu, W. P. Huang, A. Iwasaki, M. Jaattela, W. T. Jackson, X. Jiang, S. Jin, T. Johansen, J. U. Jung, M. Kadowaki, C. Kang, A. Kelekar, D. H. Kessel, J. A. Kiel, H. P. Kim, A. Kimchi, T. J. Kinsella, K. Kiselyov, K. Kitamoto, E. Knecht, M. Komatsu, E. Kominami, S. Kondo, A. L. Kovacs, G. Kroemer, C. Y. Kuan, R. Kumar, M. Kundu, J. Landry, M. Laporte, W. Le, H. Y. Lei, M. J. Lenardo, B. Levine, A. Lieberman, K. L. Lim, F. C. Lin, W. Liou, L. F. Liu, G. Lopez-Berestein, C. Lopez-Otin, B. Lu, K. F. Macleod, W. Malorni, W. Martinet, K. Matsuoka, J. Mautner, A. J. Meijer, A. Melendez, P. Michels, G. Miotto, W. P. Mistiaen, N. Mizushima, B. Mograbi, I. Monastyrska, M. N. Moore, P. I. Moreira, Y. Moriyasu, T. Motyl, C. Munz, L. O. Murphy, N. I. Nagvi, T. P. Neufeld, I. Nishino, R. A. Nixon, T. Noda, B. Nurnberg, M. Ogawa, N. L. Oleinick, L. J. Olsen, B. Ozpolat, S. Paglin, G. E. Palmer, I. Papassideri, M. Parkes, D. H. Perlmutter, G. Perry, M. Piacentini, R. Pinkas-Kramarski, M. Prescott, T. Proikas-Cezanne, N. Raben, A. Rami, F. Reggiori, B. Rohrer, D. C. Rubinsztein, K. M. Ryan, J. Sadoshima, H. Sakagami, Y. Sakai, M. Sandri, C. Sasakawa, M. Sass, C. Schneider, P. O. Seglen, O. Seleverstov, J. Settleman, J. J. Shacka, I. M. Shapiro, A. Sibirny, E. C. Silva-Zacarin, H. U. Simon, C. Simone, A. Simonsen, M. A. Smith, K. Spanel-Borowski, V. Srinivas, M. Steeves, H. Stenmark, P. E. Stromhaug, C. S. Subauste, S. Sugimoto, D. Sulzer, T. Suzuki, M. S. Swanson, I. Tabas, F. Takeshita, N. J. Talbot, Z. Talloczy, K. Tanaka, K. Tanaka, I. Tanida, G. S. Taylor, J. P. Taylor, A. Terman, G. Tettamanti, C. B. Thompson, M. Thumm, A. M. Tolkovsky, S. A. Tooze, R. Truant, L. V. Tumanovska, Y. Uchiyama, T. Ueno, N. L. Uzcategui, I. van der Klei, E. C. Vaquero, T. Vellai, M. W. Vogel, H. G. Wang, P. Webster, J. W. Wiley, Z. Xi, G. Xiao, J. Yahalom, J. M. Yang, G. Yap, X. M. Yin, T. Yoshimori, L. Yu, Z. Yue, M. Yuzaki, O. Zabirnyk, X. Zheng, X. Zhu and R. L. Deter (2008). "Guidelines for the use and interpretation of assays for monitoring autophagy in higher eukaryotes." Autophagy **4**(2): 151-175.

Knaevelsrud, H. and A. Simonsen (2012). "Lipids in autophagy: constituents, signaling molecules and cargo with relevance to disease." <u>Biochim Biophys Acta</u> **1821**(8): 1133-1145.

- Kobalka, A. J., R. W. Keck and J. Jankun (2015). "Synergistic anticancer activity of biologicals from green and black tea on DU 145 human prostate cancer cells." Cent Eur J Immunol 40(1): 1-4. Konety, B. R., J. P. Lavelle, G. Pirtskalaishvili, R. Dhir, S. A. Meyers, T. S. Nguyen, P. Hershberger, M. R. Shurin, C. S. Johnson, D. L. Trump, M. L. Zeidel and R. H. Getzenberg (2001). "Effects of vitamin D (calcitriol) on transitional cell carcinoma of the bladder in vitro and in vivo." J Urol 165(1): 253-258. Kong, Y., L. Cheng, F. Mao, Z. Zhang, Y. Zhang, E. Farah, J. Bosler, Y. Bai, N. Ahmad, S. Kuang, L. Li and X. Liu (2018). "Inhibition of cholesterol biosynthesis overcomes enzalutamide resistance in castration-resistant prostate cancer (CRPC)." J Biol Chem.
- Kubler, H. R., H. van Randenborgh, U. Treiber, S. Wutzler, C. Battistel, A. Lehmer, S. Wagenpfeil, R. Hartung and R. Paul (2005). "In vitro cytotoxic effects of imatinib in combination with anticancer drugs in human prostate cancer cell lines." <u>Prostate</u> **63**(4): 385-394.
- Kubota, T., J. Hisatake, Y. Hisatake, J. W. Said, S. S. Chen, S. Holden, H. Taguchi and H. P. Koeffler (2000). "PC-SPES: a unique inhibitor of proliferation of prostate cancer cells in vitro and in vivo." <u>Prostate</u> **42**(3): 163-171.
- Kung, H. J. (2011). "Targeting tyrosine kinases and autophagy in prostate cancer." <u>Horm Cancer</u> **2**(1): 38-46
- Kyprianou, N. (2003). "Doxazosin and terazosin suppress prostate growth by inducing apoptosis: clinical significance." J Urol **169**(4): 1520-1525.
- Kyprianou, N. and C. M. Benning (2000). "Suppression of human prostate cancer cell growth by alpha1-adrenoceptor antagonists doxazosin and terazosin via induction of apoptosis." <u>Cancer Res</u> **60**(16): 4550-4555.
- Kyprianou, N., J. Chon and C. M. Benning (2000). "Effects of alpha(1)-adrenoceptor (alpha(1)-AR) antagonists on cell proliferation and apoptosis in the prostate: therapeutic implications in prostatic disease." Prostate Suppl **9**: 42-46.
- Kyprianou, N. and S. C. Jacobs (2000). "Induction of apoptosis in the prostate by alpha1-adrenoceptor antagonists: a novel effect of "old" drugs." Curr Urol Rep 1(2): 89-96.
- Kyprianou, N., J. P. Litvak, A. Borkowski, R. Alexander and S. C. Jacobs (1998). "Induction of prostate apoptosis by doxazosin in benign prostatic hyperplasia." <u>J Urol</u> **159**(6): 1810-1815.
- Lamb, C. A., H. C. Dooley and S. A. Tooze (2013). "Endocytosis and autophagy: Shared machinery for degradation." <u>Bioessays</u> **35**(1): 34-45.
- Lamb, C. A., T. Yoshimori and S. A. Tooze (2013). "The autophagosome: origins unknown, biogenesis complex." Nat Rev Mol Cell Biol **14**(12): 759-774.
- Lanzetti, L. and P. P. Di Fiore (2008). "Endocytosis and cancer: an 'insider' network with dangerous liaisons." Traffic **9**(12): 2011-2021.
- Lau, D. H., C. S. Thompson, J. F. Bellringer, P. J. Thomas, F. H. Mumtaz, R. J. Morgan and D. P. Mikhailidis (2006). "Doxazosin and serotonin (5-HT) receptor (1A, 2A, and 4) antagonists inhibit 5-HT-mediated human cavernosal contraction." <u>J Androl</u> **27**(5): 679-685.
- Le Roy, C. and J. L. Wrana (2005). "Clathrin- and non-clathrin-mediated endocytic regulation of cell signalling." Nat Rev Mol Cell Biol **6**(2): 112-126.
- Lee, D. J., K. Mallin, A. J. Graves, S. S. Chang, D. F. Penson, M. J. Resnick and D. A. Barocas (2017). "Recent Changes in Prostate Cancer Screening Practices and Epidemiology." <u>J Urol</u> **198**(6): 1230-1240.
- Lee, S. L., E. C. Hsu, C. C. Chou, H. C. Chuang, L. Y. Bai, S. K. Kulp and C. S. Chen (2011). "Identification and characterization of a novel integrin-linked kinase inhibitor." <u>J Med Chem</u> **54**(18): 6364-6374.
- Lee, Y. J., A. J. Won, J. Lee, J. H. Jung, S. Yoon, B. M. Lee and H. S. Kim (2012). "Molecular mechanism of SAHA on regulation of autophagic cell death in tamoxifen-resistant MCF-7 breast cancer cells." <u>Int J Med Sci</u> **9**(10): 881-893.
- Leggio, L. and G. A. Kenna (2013). "Commentary: Doxazosin for alcoholism." <u>Alcohol Clin Exp Res</u> **37**(2): 191-193.
- Leone, R. D. and R. K. Amaravadi (2013). "Autophagy: a targetable linchpin of cancer cell metabolism." <u>Trends Endocrinol Metab</u> **24**(4): 209-217.

- Li, H., N. Xie, M. E. Gleave and X. Dong (2015). "Catalytic inhibitors of DNA topoisomerase II suppress the androgen receptor signaling and prostate cancer progression." <u>Oncotarget</u> **6**(24): 20474-20484. Li, J. L., S. L. Han and X. Fan (2011). "Modulating autophagy: a strategy for cancer therapy." <u>Chin J Cancer</u> **30**(10): 655-668.
- Li, M., X. Jiang, D. Liu, Y. Na, G. F. Gao and Z. Xi (2008). "Autophagy protects LNCaP cells under androgen deprivation conditions." Autophagy **4**(1): 54-60.
- Lian, J., D. Karnak and L. Xu (2010). "The Bcl-2-Beclin 1 interaction in (-)-gossypol-induced autophagy versus apoptosis in prostate cancer cells." <u>Autophagy</u> **6**(8): 1201-1203.
- Lian, J., Z. Ni, X. Dai, C. Su, A. R. Smith, L. Xu and F. He (2012). "Sorafenib sensitizes (-)-gossypol-induced growth suppression in androgen-independent prostate cancer cells via Mcl-1 inhibition and Bak activation." Mol Cancer Ther **11**(2): 416-426.
- Lian, J., X. Wu, F. He, D. Karnak, W. Tang, Y. Meng, D. Xiang, M. Ji, T. S. Lawrence and L. Xu (2011). "A natural BH3 mimetic induces autophagy in apoptosis-resistant prostate cancer via modulating Bcl-2-Beclin1 interaction at endoplasmic reticulum." Cell Death Differ **18**(1): 60-71.
- Liao, J. K. and U. Laufs (2005). "Pleiotropic effects of statins." <u>Annu Rev Pharmacol Toxicol</u> **45**: 89-118.
- Lin, J. F., Y. C. Lin, Y. H. Lin, T. F. Tsai, K. Y. Chou, H. E. Chen and T. I. Hwang (2011). "Zoledronic acid induces autophagic cell death in human prostate cancer cells." J Urol **185**(4): 1490-1496.
- Liu, C., A. Calogero, G. Ragona, E. Adamson and D. Mercola (1996). "EGR-1, the reluctant suppression factor: EGR-1 is known to function in the regulation of growth, differentiation, and also has significant tumor suppressor activity and a mechanism involving the induction of TGF-beta1 is postulated to account for this suppressor activity." Crit Rev Oncog **7**(1-2): 101-125.
- Liu, C., P. Xu, D. Chen, X. Fan, Y. Xu, M. Li, X. Yang and C. Wang (2013). "Roles of autophagy-related genes Beclin-1 and LC3 in the development and progression of prostate cancer and benign prostatic hyperplasia." <u>Biomed Rep</u> **1**(6): 855-860.
- Liu, Y. Q., Y. Ji, X. Z. Li, K. L. Tian, C. Y. Young, H. X. Lou and H. Q. Yuan (2013). "Retigeric acid B-induced mitophagy by oxidative stress attenuates cell death against prostate cancer cells in vitro." <u>Acta Pharmacol Sin</u> **34**(9): 1183-1191.
- Lobo, N., L. Afferi, M. Moschini, H. Mostafid, S. Porten, S. P. Psutka, S. Gupta, A. B. Smith, S. B. Williams and Y. Lotan (2022). "Epidemiology, Screening, and Prevention of Bladder Cancer." <u>Eur Urol Oncol</u> **5**(6): 628-639.
- Loizzo, D., S. D. Pandolfo, D. Rogers, C. Cerrato, N. A. di Meo, R. Autorino, V. Mirone, M. Ferro, C. Porta, A. Stella, C. Bizzoca, L. Vincenti, M. Spilotros, M. Rutigliano, M. Battaglia, P. Ditonno and G. Lucarelli (2022). "Novel Insights into Autophagy and Prostate Cancer: A Comprehensive Review." Int J Mol Sci **23**(7).
- Long, J., J. Zhao, Z. Yan, Z. Liu and N. Wang (2009). "Antitumor effects of a novel sulfur-containing hydroxamate histone deacetylase inhibitor H40." Int J Cancer **124**(5): 1235-1244.
- Lower, G. M., Jr., T. Nilsson, C. E. Nelson, H. Wolf, T. E. Gamsky and G. T. Bryan (2007). "Nacetyltransferase phenotype and risk in urinary bladder cancer: approaches in molecular epidemiology. Preliminary results in Sweden and Denmark. Environmental Health Perspectives;1979:71-79." Int J Epidemiol **36**(1): 11-18.
- Lu, X., T. C. Hsieh and J. M. Wu (2004). "Equiguard suppresses androgen-dependent LNCaP prostate cancer cell proliferation by targeting cell cycle control via down regulation of the retinoblastoma protein Rb and induction of apoptosis via the release of cytochrome c." Int J Oncol 25(6): 1801-1807. Lussi, Y. C., M. Magrane, M. J. Martin, S. Orchard and C. UniProt (2023). "Searching and Navigating UniProt Databases." Curr Protoc 3(3): e700.
- Macia, E., M. Ehrlich, R. Massol, E. Boucrot, C. Brunner and T. Kirchhausen (2006). "Dynasore, a cell-permeable inhibitor of dynamin." <u>Dev Cell</u> **10**(6): 839-850.
- Mackenzie, J. F., C. J. Daly, J. D. Pediani and J. C. McGrath (2000). "Quantitative imaging in live human cells reveals intracellular alpha(1)-adrenoceptor ligand-binding sites." <u>J Pharmacol Exp Ther</u> **294**(2): 434-443.

MacLachlan, J., A. T. Wotherspoon, R. O. Ansell and C. J. Brooks (2000). "Cholesterol oxidase: sources, physical properties and analytical applications." <u>J Steroid Biochem Mol Biol</u> **72**(5): 169-195. Maede, Y., H. Shimizu, T. Fukushima, T. Kogame, T. Nakamura, T. Miki, S. Takeda, Y. Pommier and J. Murai (2014). "Differential and common DNA repair pathways for topoisomerase I- and II-targeted drugs in a genetic DT40 repair cell screen panel." <u>Mol Cancer Ther</u> **13**(1): 214-220.

Mah, L. Y. and K. M. Ryan (2012). "Autophagy and cancer." <u>Cold Spring Harb Perspect Biol</u> **4**(1): a008821.

Maida, Y., S. Kyo, T. Lassmann, Y. Hayashizaki and K. Masutomi (2013). "Off-target effect of endogenous siRNA derived from RMRP in human cells." Int J Mol Sci **14**(5): 9305-9318.

Malats N. and F. X. Real (2015). "Epidemiology of bladder cancer." Hematol Opcol Clin North A

Malats, N. and F. X. Real (2015). "Epidemiology of bladder cancer." <u>Hematol Oncol Clin North Am</u> **29**(2): 177-189, vii.

Malek, A. M., C. Xu, E. S. Kim and S. L. Alper (2007). "Hypertonicity triggers RhoA-dependent assembly of myosin-containing striated polygonal actin networks in endothelial cells." <u>Am J Physiol Cell Physiol</u> **292**(5): C1645-1659.

Mantena, S. K., S. D. Sharma and S. K. Katiyar (2006). "Berberine, a natural product, induces G1-phase cell cycle arrest and caspase-3-dependent apoptosis in human prostate carcinoma cells." <u>Mol Cancer Ther</u> **5**(2): 296-308.

Marinese, D., R. Patel and P. D. Walden (2003). "Mechanistic investigation of the adrenergic induction of ventral prostate hyperplasia in mice." Prostate **54**(3): 230-237.

Martarelli, D., B. Martarelli, D. Pediconi, M. I. Nabissi, M. Perfumi and P. Pompei (2004). "Hypericum perforatum methanolic extract inhibits growth of human prostatic carcinoma cell line orthotopically implanted in nude mice." Cancer Lett **210**(1): 27-33.

Martin, F. M., A. M. Harris, R. G. Rowland, W. Conner, M. Lane, E. Durbin, A. T. Baron and N. Kyprianou (2008). "Decreased risk of bladder cancer in men treated with quinazoline-based alpha1-adrenoceptor antagonists." <u>Gene Ther Mol Biol</u> **12**(2): 253-258.

Mathew, R., V. Karantza-Wadsworth and E. White (2007). "Role of autophagy in cancer." <u>Nat Rev Cancer</u> **7**(12): 961-967.

McGrath, J. C. (2015). "Localization of alpha-adrenoceptors: JR Vane Medal Lecture." <u>Br J Pharmacol</u> **172**(5): 1179-1194.

McGrath, J. C., J. F. Mackenzie and C. J. Daly (1999). "Pharmacological implications of cellular localization of alpha1-adrenoceptors in native smooth muscle cells." <u>J Auton Pharmacol</u> **19**(6): 303-310.

McMahon, H. T. and I. G. Mills (2004). "COP and clathrin-coated vesicle budding: different pathways, common approaches." Curr Opin Cell Biol **16**(4): 379-391.

McVary, K. T., A. Razzaq, C. Lee, M. F. Venegas, A. Rademaker and K. E. McKenna (1994). "Growth of the rat prostate gland is facilitated by the autonomic nervous system." <u>Biol Reprod</u> **51**(1): 99-107. Megalizzi, V., V. Mathieu, T. Mijatovic, P. Gailly, O. Debeir, N. De Neve, M. Van Damme, G. Bontempi, B. Haibe-Kains, C. Decaestecker, Y. Kondo, R. Kiss and F. Lefranc (2007). "4-IBP, a sigma1 receptor agonist, decreases the migration of human cancer cells, including glioblastoma cells, in vitro and

sensitizes them in vitro and in vivo to cytotoxic insults of proapoptotic and proautophagic drugs." Neoplasia **9**(5): 358-369.

Michel, M. C., R. F. Schafers and M. Goepel (2000). "Alpha-blockers and lower urinary tract function: more than smooth muscle relaxation?" <u>BJU Int</u> **86 Suppl 2**: 23-28; discussion 28-30.

Mimeault, M., N. Pommery, N. Wattez, C. Bailly and J. P. Henichart (2003). "Anti-proliferative and apoptotic effects of anandamide in human prostatic cancer cell lines: implication of epidermal growth factor receptor down-regulation and ceramide production." <u>Prostate</u> **56**(1): 1-12.

Mohammed, S. I., D. Dhawan, S. Abraham, P. W. Snyder, D. J. Waters, B. A. Craig, M. Lu, L. Wu, R. Zheng, J. Stewart and D. W. Knapp (2006). "Cyclooxygenase inhibitors in urinary bladder cancer: in vitro and in vivo effects." <u>Mol Cancer Ther</u> **5**(2): 329-336.

Montero, J. C., R. Rodriguez-Barrueco, A. Ocana, E. Diaz-Rodriguez, A. Esparis-Ogando and A. Pandiella (2008). "Neuregulins and cancer." <u>Clin Cancer Res</u> **14**(11): 3237-3241.

Morales, A. and A. S. Pang (1986). "Prophylaxis and therapy of an experimental bladder cancer with biological response modifiers." J Urol **135**(1): 191-193.

Mosesson, Y., G. B. Mills and Y. Yarden (2008). "Derailed endocytosis: an emerging feature of cancer." Nat Rev Cancer 8(11): 835-850.

Mostafa, M. H., S. A. Sheweita and P. J. O'Connor (1999). "Relationship between schistosomiasis and bladder cancer." Clin Microbiol Rev **12**(1): 97-111.

Munafo, D. B. and M. I. Colombo (2001). "A novel assay to study autophagy: regulation of autophagosome vacuole size by amino acid deprivation." J Cell Sci **114**(Pt 20): 3619-3629.

Munzar, P. and S. R. Goldberg (1999). "Noradrenergic modulation of the discriminative-stimulus effects of methamphetamine in rats." Psychopharmacology (Berl) **143**(3): 293-301.

Murphy, M. E. (2013). "The HSP70 family and cancer." Carcinogenesis 34(6): 1181-1188.

Murta-Nascimento, C., B. J. Schmitz-Drager, M. P. Zeegers, G. Steineck, M. Kogevinas, F. X. Real and N. Malats (2007). "Epidemiology of urinary bladder cancer: from tumor development to patient's death." World J Urol **25**(3): 285-295.

Nabi, I. R. and P. U. Le (2003). "Caveolae/raft-dependent endocytosis." <u>J Cell Biol</u> **161**(4): 673-677. Neuberg, M., J. Adamkiewicz, J. B. Hunter and R. Muller (1989). "A Fos protein containing the Jun leucine zipper forms a homodimer which binds to the AP1 binding site." <u>Nature</u> **341**(6239): 243-245. Neulander, E. Z., R. C. Duncan, R. Tiguert, J. T. Posey and M. S. Soloway (2000). "Deferred treatment of localized prostate cancer in the elderly: the impact of the age and stage at the time of diagnosis on the treatment decision." <u>BJU Int</u> **85**(6): 699-704.

Newton, T. F., R. De La Garza, 2nd, G. Brown, T. R. Kosten, J. J. Mahoney, 3rd and C. N. Haile (2012). "Noradrenergic alpha(1) receptor antagonist treatment attenuates positive subjective effects of cocaine in humans: a randomized trial." <u>PLoS One</u> **7**(2): e30854.

Nikoletopoulou, V., M. Markaki, K. Palikaras and N. Tavernarakis (2013). "Crosstalk between apoptosis, necrosis and autophagy." <u>Biochim Biophys Acta</u> **1833**(12): 3448-3459.

Nishimune, A., H. Yoshiki, J. Uwada, A. S. Anisuzzaman, H. Umada and I. Muramatsu (2012). "Phenotype pharmacology of lower urinary tract alpha(1)-adrenoceptors." <u>Br J Pharmacol</u> **165**(5): 1226-1234.

Nishizaki, T., T. Kanno, A. Tsuchiya, Y. Kaku, T. Shimizu and A. Tanaka (2014). "1-[2-(2-Methoxyphenylamino)ethylamino]-3-(naphthalene-1-yloxy)propan-2-ol may be a promising anticancer drug." Molecules 19(12): 21462-21472.

Oh, Y. S., H. S. Lee, H. J. Cho, S. G. Lee, K. C. Jung and J. H. Park (2003). "Conjugated linoleic acid inhibits DNA synthesis and induces apoptosis in TSU-Pr1 human bladder cancer cells." <u>Anticancer Res</u> **23**(6C): 4765-4772.

Oosterhoff, J. K., L. C. Kuhne, J. A. Grootegoed and L. J. Blok (2005). "EGF signalling in prostate cancer cell lines is inhibited by a high expression level of the endocytosis protein REPS2." <u>Int J Cancer</u> **113**(4): 561-567.

Ostrom, R. S. and X. Liu (2007). "Detergent and detergent-free methods to define lipid rafts and caveolae." Methods Mol Biol **400**: 459-468.

Ottenweller, J., K. Putt, E. J. Blumenthal, S. Dhawale and S. W. Dhawale (2004). "Inhibition of prostate cancer-cell proliferation by Essiac." J Altern Complement Med **10**(4): 687-691.

Pannu, V., P. C. Rida, A. Ogden, R. Clewley, A. Cheng, P. Karna, M. Lopus, R. C. Mishra, J. Zhou and R. Aneja (2012). "Induction of robust de novo centrosome amplification, high-grade spindle multipolarity and metaphase catastrophe: a novel chemotherapeutic approach." <u>Cell Death Dis</u> **3**: e346.

Papadopoulos, G., D. Vlachodimitropoulos, A. Kyroudi, M. Kouloukoussa, D. Perrea and D. Mitropoulos (2013). "Terazosin treatment induces caspase-3 expression in the rat ventral prostate." <u>J Clin Med Res</u> **5**(2): 127-131.

Parikh, A., C. Childress, K. Deitrick, Q. Lin, D. Rukstalis and W. Yang (2010). "Statin-induced autophagy by inhibition of geranylgeranyl biosynthesis in prostate cancer PC3 cells." <u>Prostate</u> **70**(9): 971-981.

- Park, M. S., B. R. Kim, S. M. Dong, S. H. Lee, D. Y. Kim and S. B. Rho (2014). "The antihypertension drug doxazosin inhibits tumor growth and angiogenesis by decreasing VEGFR-2/Akt/mTOR signaling and VEGF and HIF-1alpha expression." <u>Oncotarget</u> **5**(13): 4935-4944.
- Park, M. S., B. R. Kim, S. Kang, D. Y. Kim and S. B. Rho (2014). "The antihypertension drug doxazosin suppresses JAK/STATs phosphorylation and enhances the effects of IFN-alpha/gamma-induced apoptosis." Genes Cancer **5**(11-12): 470-479.
- Parkin, D. M. (2008). "The global burden of urinary bladder cancer." <u>Scand J Urol Nephrol Suppl(218)</u>: 12-20.
- Parzych, K. R. and D. J. Klionsky (2014). "An overview of autophagy: morphology, mechanism, and regulation." Antioxid Redox Signal **20**(3): 460-473.
- Pasquier, B. (2016). "Autophagy inhibitors." Cell Mol Life Sci 73(5): 985-1001.
- Patane, S. (2015). "Insights into cardio-oncology: Polypharmacology of quinazoline-based alpha1-adrenoceptor antagonists." World J Cardiol **7**(5): 238-242.
- Pavithran, N., M. Shabbir, S. El Sheikh, F. Mumtaz, J. Cooper, R. Al Jehani and C. Thompson (2017). <u>Doxazosin-induced cell death of HT1376 bladder cancer cells is mediated by autophagy both in vitro and in vivo</u>. BAUS Oncology, 5–16 November 2016, Wales Millennium Centre, Cardiff, Wales, Journal of Clinical Urology, Sage Publications.
- Pavithran, N. and C. Thompson (2012). <u>Doxazoin causes cell death by autophagy (mitophagy) in hormone resistant prostate cancer cells</u>. Physiology 2012, Edinburgh, UK, Proceedings of the Physiological Society.
- Pelucchi, C., C. Bosetti, E. Negri, M. Malvezzi and C. La Vecchia (2006). "Mechanisms of disease: The epidemiology of bladder cancer." Nat Clin Pract Urol **3**(6): 327-340.
- Peng, X., W. Li, L. Yuan, R. G. Mehta, L. Kopelovich and D. L. McCormick (2013). "Inhibition of proliferation and induction of autophagy by atorvastatin in PC3 prostate cancer cells correlate with downregulation of Bcl2 and upregulation of miR-182 and p21." PLoS One 8(8): e70442.
- Perabo, F. G., A. Wirger, S. Kamp, H. Lindner, D. H. Schmidt, S. C. Muller and E. C. Kohn (2004).
- "Carboxyamido-triazole (CAI), a signal transduction inhibitor induces growth inhibition and apoptosis in bladder cancer cells by modulation of Bcl-2." <u>Anticancer Res</u> **24**(5A): 2869-2877.
- Perez, D. M., M. T. Piascik, N. Malik, R. Gaivin and R. M. Graham (1994). "Cloning, expression, and tissue distribution of the rat homolog of the bovine alpha 1C-adrenergic receptor provide evidence for its classification as the alpha 1A subtype." <u>Mol Pharmacol</u> **46**(5): 823-831.
- Perse, M., R. Injac and A. Erman (2013). "Oxidative status and lipofuscin accumulation in urothelial cells of bladder in aging mice." <u>PLoS One</u> **8**(3): e59638.
- Petty, A., E. Myshkin, H. Qin, H. Guo, H. Miao, G. P. Tochtrop, J. T. Hsieh, P. Page, L. Liu, D. J. Lindner, C. Acharya, A. D. MacKerell, Jr., E. Ficker, J. Song and B. Wang (2012). "A small molecule agonist of EphA2 receptor tyrosine kinase inhibits tumor cell migration in vitro and prostate cancer metastasis in vivo." PLos One 7(8): e42120.
- Piazzon, M. C., G. Lutfalla and M. Forlenza (2016). "IL10, A Tale of an Evolutionarily Conserved Cytokine across Vertebrates." <u>Crit Rev Immunol</u> **36**(2): 99-129.
- Polo, S., S. Pece and P. P. Di Fiore (2004). "Endocytosis and cancer." <u>Curr Opin Cell Biol</u> **16**(2): 156-161.
- Poulet, F. M., M. R. Berardi, W. Halliwell, B. Hartman, C. Auletta and H. Bolte (2004). "Development of hibernomas in rats dosed with phentolamine mesylate during the 24-month carcinogenicity study." <u>Toxicol Pathol</u> **32**(5): 558-566.
- Powell, M. J., M. C. Casimiro, C. Cordon-Cardo, X. He, W. S. Yeow, C. Wang, P. A. McCue, M. W. McBurney and R. G. Pestell (2011). "Disruption of a Sirt1-dependent autophagy checkpoint in the prostate results in prostatic intraepithelial neoplasia lesion formation." <u>Cancer Res</u> **71**(3): 964-975. Prins, G. S. and K. S. Korach (2008). "The role of estrogens and estrogen receptors in normal prostate growth and disease." <u>Steroids</u> **73**(3): 233-244.
- Pruthi, R. S., E. Derksen and K. Gaston (2003). "Cyclooxygenase-2 as a potential target in the prevention and treatment of genitourinary tumors: a review." J Urol **169**(6): 2352-2359.

- Pyo, J. O., J. Nah and Y. K. Jung (2012). "Molecules and their functions in autophagy." <u>Exp Mol Med</u> **44**(2): 73-80.
- Qi, P., M. Chen, L. X. Zhang, R. X. Song, Z. H. He and Z. P. Wang (2015). "A Meta-Analysis and Indirect Comparison of Endothelin A Receptor Antagonist for Castration-Resistant Prostate Cancer." <u>PLoS One</u> **10**(7): e0133803.
- Radons, J. (2016). "The human HSP70 family of chaperones: where do we stand?" <u>Cell Stress Chaperones</u> **21**(3): 379-404.
- Rajecki, M., T. af Hallstrom, T. Hakkarainen, P. Nokisalmi, S. Hautaniemi, A. I. Nieminen, M. Tenhunen, V. Rantanen, R. A. Desmond, D. T. Chen, K. Guse, U. H. Stenman, R. Gargini, M. Kapanen, J. Klefstrom, A. Kanerva, S. Pesonen, L. Ahtiainen and A. Hemminki (2009). "Mre11 inhibition by oncolytic adenovirus associates with autophagy and underlies synergy with ionizing radiation." Int J Cancer 125(10): 2441-2449.
- Ramkumar, A., B. Y. Jong and K. M. Ori-McKenney (2018). "ReMAPping the microtubule landscape: How phosphorylation dictates the activities of microtubule-associated proteins." <u>Dev Dyn</u> **247**(1): 138-155.
- Ren, L. F., Y. Y. Ma, Q. H. Yue, M. Q. Su and X. K. Hao (2012). "[Effects of TFDP3 on regulating the autophagy and apoptosis of LNCaP cells]." Xi Bao Yu Fen Zi Mian Yi Xue Za Zhi 28(4): 347-349.
- Reyjal, J., K. Cormier and S. Turcotte (2014). "Autophagy and cell death to target cancer cells: exploiting synthetic lethality as cancer therapies." Adv Exp Med Biol **772**: 167-188.
- Roca, H., Z. Varsos and K. J. Pienta (2008). "CCL2 protects prostate cancer PC3 cells from autophagic death via phosphatidylinositol 3-kinase/AKT-dependent survivin up-regulation." <u>J Biol Chem</u> **283**(36): 25057-25073.
- Rodgman, C., C. D. Verrico, M. Holst, D. Thompson-Lake, C. N. Haile, R. De La Garza, 2nd, M. A. Raskind and T. F. Newton (2016). "Doxazosin XL reduces symptoms of posttraumatic stress disorder in veterans with PTSD: a pilot clinical trial." <u>J Clin Psychiatry</u> **77**(5): e561-565.
- Rogler, L. E., B. Kosmyna, D. Moskowitz, R. Bebawee, J. Rahimzadeh, K. Kutchko, A. Laederach, L. D. Notarangelo, S. Giliani, E. Bouhassira, P. Frenette, J. Roy-Chowdhury and C. E. Rogler (2014). "Small RNAs derived from IncRNA RNase MRP have gene-silencing activity relevant to human cartilage-hair hypoplasia." <u>Hum Mol Genet</u> **23**(2): 368-382.
- Rosenfeldt, M. T., C. Nixon, E. Liu, L. Y. Mah and K. M. Ryan (2012). "Analysis of macroautophagy by immunohistochemistry." <u>Autophagy</u> **8**(6): 963-969.
- Ross, J. S., T. A. Jennings, T. Nazeer, C. E. Sheehan, H. A. Fisher, R. A. Kauffman, S. Anwar and B. V. Kallakury (2003). "Prognostic factors in prostate cancer." <u>Am J Clin Pathol</u> **120 Suppl**: S85-100. Roy-Burman, P., H. Wu, W. C. Powell, J. Hagenkord and M. B. Cohen (2004). "Genetically defined mouse models that mimic natural aspects of human prostate cancer development." <u>Endocr Relat</u> Cancer **11**(2): 225-254.
- Rubinsztein, D. C., T. Shpilka and Z. Elazar (2012). "Mechanisms of autophagosome biogenesis." <u>Curr Biol</u> **22**(1): R29-34.
- Sahoo, S. K., W. Ma and V. Labhasetwar (2004). "Efficacy of transferrin-conjugated paclitaxel-loaded nanoparticles in a murine model of prostate cancer." Int J Cancer **112**(2): 335-340.
- Sastry, K. S., Y. Karpova, S. Prokopovich, A. J. Smith, B. Essau, A. Gersappe, J. P. Carson, M. J. Weber, T. C. Register, Y. Q. Chen, R. B. Penn and G. Kulik (2007). "Epinephrine protects cancer cells from apoptosis via activation of cAMP-dependent protein kinase and BAD phosphorylation." <u>J Biol Chem</u> **282**(19): 14094-14100.
- Satcher, R. L., T. Pan, M. A. Bilen, X. Li, Y. C. Lee, A. Ortiz, A. P. Kowalczyk, L. Y. Yu-Lee and S. H. Lin (2015). "Cadherin-11 endocytosis through binding to clathrin promotes cadherin-11-mediated migration in prostate cancer cells." J Cell Sci 128(24): 4629-4641.
- Sato, N., M. E. Gleave, N. Bruchovsky, P. S. Rennie, E. Beraldi and L. D. Sullivan (1997). "A metastatic and androgen-sensitive human prostate cancer model using intraprostatic inoculation of LNCaP cells in SCID mice." <u>Cancer Res</u> **57**(8): 1584-1589.

Sawada, N., M. Murata, K. Kikuchi, M. Osanai, H. Tobioka, T. Kojima and H. Chiba (2003). "Tight junctions and human diseases." Med Electron Microsc **36**(3): 147-156.

Scherr, D. S. (2014). "Commentary on "common genetic polymorphisms modify the effect of smoking on absolute risk of bladder cancer." Garcia-Closas M, Rothman N, Figueroa JD, Prokunina-Olsson L, Han SS, Baris D, Jacobs EJ, Malats N, De Vivo I, Albanes D, Purdue MP, Sharma S, Fu YP, Kogevinas M, Wang Z, Tang W, Tardon A, Serra C, Carrato A, Garcia-Closas R, Lloreta J, Johnson A, Schwenn M, Karagas MR, Schned A, Andriole G Jr., Grubb R 3rd, Black A, Gapstur SM, Thun M, Diver WR, Weinstein SJ, Virtamo J, Hunter DJ, Caporaso N, Landi MT, Hutchinson A, Burdett L, Jacobs KB, Yeager M, Fraumeni JF Jr., Chanock SJ, Silverman DT, Chatterjee N, Division of Cancer Epidemiology and Genetics, National Cancer Institute, Bethesda, MD, USA.: Cancer Res 2013;73(7):2211-20 [Epub 2013 Mar 27]." <u>Urol Oncol</u> **32**(2): 213-214.

Schlegel, R., R. B. Dickson, M. C. Willingham and I. H. Pastan (1982). "Amantadine and dansylcadaverine inhibit vesicular stomatitis virus uptake and receptor-mediated endocytosis of alpha 2-macroglobulin." Proc Natl Acad Sci U S A **79**(7): 2291-2295.

Schmid, S. L. (1997). "Clathrin-coated vesicle formation and protein sorting: an integrated process." Annu Rev Biochem **66**: 511-548.

Schmid, S. L., A. Sorkin and M. Zerial (2014). "Endocytosis: Past, present, and future." <u>Cold Spring</u> Harb Perspect Biol **6**(12): a022509.

Schmukler, E., B. Shai, M. Ehrlich and R. Pinkas-Kramarski (2012). "Neuregulin promotes incomplete autophagy of prostate cancer cells that is independent of mTOR pathway inhibition." <u>PLoS One</u> **7**(5): e36828.

Schwinn, D. A. and C. G. Roehrborn (2008). "Alpha1-adrenoceptor subtypes and lower urinary tract symptoms." Int J Urol **15**(3): 193-199.

Seager, C., A. M. Puzio-Kuter, C. Cordon-Cardo, J. McKiernan and C. Abate-Shen (2010). "Mouse models of human bladder cancer as a tool for drug discovery." <u>Curr Protoc Pharmacol</u> **Chapter 14**: Unit14 14.

Sensibar, J. A., D. M. Sutkowski, A. Raffo, R. Buttyan, M. D. Griswold, S. R. Sylvester, J. M. Kozlowski and C. Lee (1995). "Prevention of cell death induced by tumor necrosis factor alpha in LNCaP cells by overexpression of sulfated glycoprotein-2 (clusterin)." <u>Cancer Res</u> **55**(11): 2431-2437.

Shabbir, M., M. Ryten, C. Thompson, D. Mikhailidis and G. Burnstock (2008). "Purinergic receptor-mediated effects of ATP in high-grade bladder cancer." <u>BJU Int</u> **101**(1): 106-112.

Shabbir, M., C. Thompson, M. Jarmulowiczc, D. Mikhailidis and G. Burnstock (2008). "Effect of extracellular ATP on the growth of hormone-refractory prostate cancer in vivo." <u>BJU Int</u> **102**(1): 108-112.

Shah, N., V. Ioffe and J. C. Chang (2022). "Increasing aggressive prostate cancer." <u>Can J Urol</u> **29**(6): 11384-11390.

Shappell, S. B., G. V. Thomas, R. L. Roberts, R. Herbert, M. M. Ittmann, M. A. Rubin, P. A. Humphrey, J. P. Sundberg, N. Rozengurt, R. Barrios, J. M. Ward and R. D. Cardiff (2004). "Prostate pathology of genetically engineered mice: definitions and classification. The consensus report from the Bar Harbor meeting of the Mouse Models of Human Cancer Consortium Prostate Pathology Committee." Cancer Res 64(6): 2270-2305.

Sharkey, F. E. and J. Fogh (1984). "Considerations in the use of nude mice for cancer research." Cancer Metastasis Rev **3**(4): 341-360.

Shen, J. C., R. D. Klein, Q. Wei, Y. Guan, J. H. Contois, T. T. Wang, S. Chang and S. D. Hursting (2000). "Low-dose genistein induces cyclin-dependent kinase inhibitors and G(1) cell-cycle arrest in human prostate cancer cells." Mol Carcinog **29**(2): 92-102.

Shi, J., X. Zhang, T. Shi and H. Li (2017). "Antitumor effects of curcumin in human bladder cancer in vitro." Oncol Lett **14**(1): 1157-1161.

Shi, M. J., X. Y. Meng, Q. J. Wu and X. H. Zhou (2019). "High CD3D/CD4 ratio predicts better survival in muscle-invasive bladder cancer." <u>Cancer Manag Res</u> **11**: 2987-2995.

- Shibayama, T., M. Tachibana, N. Deguchi, S. Jitsukawa and H. Tazaki (1991). "SCID mice: a suitable model for experimental studies of urologic malignancies." <u>J Urol</u> **146**(4): 1136-1137.
- Shin, S. W., S. Y. Kim and J. W. Park (2012). "Autophagy inhibition enhances ursolic acid-induced apoptosis in PC3 cells." <u>Biochim Biophys Acta</u> **1823**(2): 451-457.
- Shubassi, G., T. Robert, F. Vanoli, S. Minucci and M. Foiani (2012). "Acetylation: a novel link between double-strand break repair and autophagy." Cancer Res **72**(6): 1332-1335.
- Sidaway, J. E., R. G. Davidson, F. McTaggart, T. C. Orton, R. C. Scott, G. J. Smith and N. J. Brunskill (2004). "Inhibitors of 3-hydroxy-3-methylglutaryl-CoA reductase reduce receptor-mediated endocytosis in opossum kidney cells." J Am Soc Nephrol 15(9): 2258-2265.
- Siddiqui, E. J., M. Shabbir, D. P. Mikhailidis, C. S. Thompson and F. H. Mumtaz (2006). "The role of serotonin (5-hydroxytryptamine1A and 1B) receptors in prostate cancer cell proliferation." <u>J Urol</u> **176**(4 Pt 1): 1648-1653.
- Siddiqui, E. J., M. Shabbir, C. S. Thompson, F. H. Mumtaz and D. P. Mikhailidis (2005). "Growth inhibitory effect of doxazosin on prostate and bladder cancer cells. Is the serotonin receptor pathway involved?" <u>Anticancer Res</u> **25**(6B): 4281-4286.
- Siegel, R. L., K. D. Miller, N. S. Wagle and A. Jemal (2023). "Cancer statistics, 2023." <u>CA Cancer J Clin</u> **73**(1): 17-48.
- Simpson, M. A., J. A. Weigel and P. H. Weigel (2012). "Systemic blockade of the hyaluronan receptor for endocytosis prevents lymph node metastasis of prostate cancer." Int J Cancer 131(5): E836-840. Singh, R. P., P. Agrawal, D. Yim, C. Agarwal and R. Agarwal (2005). "Acacetin inhibits cell growth and cell cycle progression, and induces apoptosis in human prostate cancer cells: structure-activity relationship with linarin and linarin acetate." Carcinogenesis 26(4): 845-854.
- Smith, G. R. (1981). "DNA supercoiling: another level for regulating gene expression." <u>Cell</u> **24**(3): 599-600.
- Soler, M., F. Mancini, O. Meca-Cortes, L. Sanchez-Cid, N. Rubio, S. Lopez-Fernandez, J. J. Lozano, J. Blanco, P. L. Fernandez and T. M. Thomson (2009). "HER3 is required for the maintenance of neuregulin-dependent and -independent attributes of malignant progression in prostate cancer cells." Int J Cancer **125**(11): 2565-2575.
- Sorkin, A. (2001). "Internalization of the epidermal growth factor receptor: role in signalling." <u>Biochemical Society Transactions</u> **29**: 480-484.
- Sotgia, F., U. E. Martinez-Outschoorn, A. Howell, R. G. Pestell, S. Pavlides and M. P. Lisanti (2012). "Caveolin-1 and cancer metabolism in the tumor microenvironment: markers, models, and mechanisms." <u>Annu Rev Pathol</u> **7**: 423-467.
- Sousa, R. and E. M. Lafer (2015). "The role of molecular chaperones in clathrin mediated vesicular trafficking." Front Mol Biosci 2: 26.
- Stein, M., H. Lin, C. Jeyamohan, D. Dvorzhinski, M. Gounder, K. Bray, S. Eddy, S. Goodin, E. White and R. S. Dipaola (2010). "Targeting tumor metabolism with 2-deoxyglucose in patients with castrateresistant prostate cancer and advanced malignancies." <u>Prostate</u> **70**(13): 1388-1394.
- Steinmuller, L., G. Cibelli, J. R. Moll, C. Vinson and G. Thiel (2001). "Regulation and composition of activator protein 1 (AP-1) transcription factors controlling collagenase and c-Jun promoter activities." <u>Biochem J</u> **360**(Pt 3): 599-607.
- Suh, Y., F. Afaq, N. Khan, J. J. Johnson, F. H. Khusro and H. Mukhtar (2010). "Fisetin induces autophagic cell death through suppression of mTOR signaling pathway in prostate cancer cells." <u>Carcinogenesis</u> **31**(8): 1424-1433.
- Sun, X., J. Bao, K. C. Nelson, K. C. Li, G. Kulik and X. Zhou (2013). "Systems modeling of anti-apoptotic pathways in prostate cancer: psychological stress triggers a synergism pattern switch in drug combination therapy." <u>PLoS Comput Biol</u> **9**(12): e1003358.
- Suwa, T., A. Nyska, J. K. Haseman, J. F. Mahler and R. R. Maronpot (2002). "Spontaneous lesions in control B6C3F1 mice and recommended sectioning of male accessory sex organs." <u>Toxicol Pathol</u> **30**(2): 228-234.

- Suy, S., J. B. Mitchell, A. Samuni, S. Mueller and U. Kasid (2005). "Nitroxide tempo, a small molecule, induces apoptosis in prostate carcinoma cells and suppresses tumor growth in athymic mice." <u>Cancer</u> **103**(6): 1302-1313.
- Swellam, T., N. Miyanaga, M. Onozawa, K. Hattori, K. Kawai, T. Shimazui and H. Akaza (2003). "Antineoplastic activity of honey in an experimental bladder cancer implantation model: in vivo and in vitro studies." Int J Urol **10**(4): 213-219.
- Szadvari, I., O. Krizanova and P. Babula (2016). "Athymic nude mice as an experimental model for cancer treatment." Physiol Res **65**(Supplementum 4): S441-S453.
- Szymanska, E., A. Skowronek and M. Miaczynska (2016). "Impaired dynamin 2 function leads to increased AP-1 transcriptional activity through the JNK/c-Jun pathway." <u>Cell Signal</u> **28**(1): 160-171.
- Tabata, K., M. Hayashi-Nishino, T. Noda, A. Yamamoto and T. Yoshimori (2013). "Morphological analysis of autophagy." Methods Mol Biol **931**: 449-466.
- Tahmatzopoulos, A. and N. Kyprianou (2004). "Apoptotic impact of alpha1-blockers on prostate cancer growth: a myth or an inviting reality?" <u>Prostate</u> **59**(1): 91-100.
- Tahmatzopoulos, A., C. A. Lagrange, L. Zeng, B. L. Mitchell, W. T. Conner and N. Kyprianou (2005). "Effect of terazosin on tissue vascularity and apoptosis in transitional cell carcinoma of bladder." <u>Urology</u> **65**(5): 1019-1023.
- Tahmatzopoulos, A., R. G. Rowland and N. Kyprianou (2004). "The role of alpha-blockers in the management of prostate cancer." Expert Opin Pharmacother **5**(6): 1279-1285.
- Tai, S., Y. Sun, N. Liu, B. Ding, E. Hsia, S. Bhuta, R. K. Thor, R. Damoiseaux, C. Liang and J. Huang (2012). "Combination of Rad001 (everolimus) and propachlor synergistically induces apoptosis through enhanced autophagy in prostate cancer cells." Mol Cancer Ther **11**(6): 1320-1331.
- Tal-Or, P., A. Di-Segni, Z. Lupowitz and R. Pinkas-Kramarski (2003). "Neuregulin promotes autophagic cell death of prostate cancer cells." <u>Prostate</u> **55**(2): 147-157.
- Tamirisa, P., K. J. Blumer and A. J. Muslin (1999). "RGS4 inhibits G-protein signaling in cardiomyocytes." Circulation **99**(3): 441-447.
- Tang, J., Z. Li, L. Lu and C. H. Cho (2013). "beta-Adrenergic system, a backstage manipulator regulating tumour progression and drug target in cancer therapy." <u>Semin Cancer Biol</u> **23**(6 Pt B): 533-542.
- Tanida, I., T. Ueno and E. Kominami (2008). "LC3 and Autophagy." <u>Methods Mol Biol</u> **445**: 77-88. Teiten, M. H., F. Gaascht, M. Cronauer, E. Henry, M. Dicato and M. Diederich (2011). "Antiproliferative potential of curcumin in androgen-dependent prostate cancer cells occurs through modulation of the Wingless signaling pathway." <u>Int J Oncol</u> **38**(3): 603-611.
- Thebault, S., M. Roudbaraki, V. Sydorenko, Y. Shuba, L. Lemonnier, C. Slomianny, E. Dewailly, J. L. Bonnal, B. Mauroy, R. Skryma and N. Prevarskaya (2003). "Alpha1-adrenergic receptors activate Ca(2+)-permeable cationic channels in prostate cancer epithelial cells." <u>J Clin Invest</u> **111**(11): 1691-1701.
- Thurn, K. T., H. Arora, T. Paunesku, A. Wu, E. M. Brown, C. Doty, J. Kremer and G. Woloschak (2011). "Endocytosis of titanium dioxide nanoparticles in prostate cancer PC-3M cells." <u>Nanomedicine</u> **7**(2): 123-130.
- Toepfer, N., C. Childress, A. Parikh, D. Rukstalis and W. Yang (2011). "Atorvastatin induces autophagy in prostate cancer PC3 cells through activation of LC3 transcription." <u>Cancer Biol Ther</u> **12**(8): 691-699. Tong, Q., F. Zeng, L. Zheng, J. Zhao and G. Lu (2001). "Apoptosis inducing effects of arsenic trioxide on human bladder cancer cell line BIU-87." Chin Med J (Engl) **114**(4): 402-406.
- Tooze, S. A. (2013). "Current views on the source of the autophagosome membrane." <u>Essays</u> Biochem **55**: 29-38.
- Torre, L. A., F. Bray, R. L. Siegel, J. Ferlay, J. Lortet-Tieulent and A. Jemal (2015). "Global cancer statistics, 2012." CA Cancer J Clin 65(2): 87-108.
- Tortorella, S. and T. C. Karagiannis (2014). "Transferrin receptor-mediated endocytosis: a useful target for cancer therapy." J Membr Biol **247**(4): 291-307.

- Tsao, A. S., S. Liu, J. Fujimoto, Wistuba, II, J. J. Lee, E. M. Marom, C. Charnsangavej, F. V. Fossella, H. T. Tran, G. R. Blumenschein, V. Papadimitrakopoulou, M. S. Kies, W. K. Hong and D. J. Stewart (2011).
- "Phase II trials of imatinib mesylate and docetaxel in patients with metastatic non-small cell lung cancer and head and neck squamous cell carcinoma." <u>J Thorac Oncol</u> **6**(12): 2104-2111.
- Tseng-Crank, J., T. Kost, A. Goetz, S. Hazum, K. M. Roberson, J. Haizlip, N. Godinot, C. N. Robertson and D. Saussy (1995). "The alpha 1C-adrenoceptor in human prostate: cloning, functional expression, and localization to specific prostatic cell types." <u>Br J Pharmacol</u> **115**(8): 1475-1485.
- Tung, W. L., Y. Wang, P. W. Gout, D. M. Liu, M. Gleave and Y. Wang (2011). "Use of irinotecan for treatment of small cell carcinoma of the prostate." <u>Prostate</u> **71**(7): 675-681.
- Ullen, A., M. Farnebo, L. Thyrell, S. Mahmoudi, P. Kharaziha, L. Lennartsson, D. Grander, T. Panaretakis and S. Nilsson (2010). "Sorafenib induces apoptosis and autophagy in prostate cancer cells in vitro." Int J Oncol **37**(1): 15-20.
- Vaidyanathan, S., B. M. Soni, P. Mansour, P. L. Hughes, G. Singh and T. Oo (2009). "Effect of spinal cord injury upon prostate: adenocarcinoma of prostate in a spinal cord injury patient a case report." <u>Cases J **2**</u>: 9374.
- Van Antwerp, D. J., S. J. Martin, I. M. Verma and D. R. Green (1998). "Inhibition of TNF-induced apoptosis by NF-kappa B." <u>Trends Cell Biol</u> **8**(3): 107-111.
- van der Zee, P. A. and A. de Boer (2014). "Pheochromocytoma: a review on preoperative treatment with phenoxybenzamine or doxazosin." Neth J Med **72**(4): 190-201.
- van Eenennaam, H., N. Jarrous, W. J. van Venrooij and G. J. Pruijn (2000). "Architecture and function of the human endonucleases RNase P and RNase MRP." <u>IUBMB Life</u> **49**(4): 265-272.
- van Rhijn, B. W., H. G. van der Poel and T. H. van der Kwast (2005). "Urine markers for bladder cancer surveillance: a systematic review." <u>Eur Urol</u> **47**(6): 736-748.
- van Weerden, W. M. and J. C. Romijn (2000). "Use of nude mouse xenograft models in prostate cancer research." Prostate **43**(4): 263-271.
- Vega, V. L., W. Charles and A. De Maio (2010). "A new feature of the stress response: increase in endocytosis mediated by Hsp70." <u>Cell Stress Chaperones</u> **15**(5): 517-527.
- Vercauteren, D., R. E. Vandenbroucke, A. T. Jones, J. Rejman, J. Demeester, S. C. De Smedt, N. N. Sanders and K. Braeckmans (2010). "The use of inhibitors to study endocytic pathways of gene carriers: optimization and pitfalls." Mol Ther **18**(3): 561-569.
- Verplaetse, T. L., A. H. Weinberger, L. M. Oberleitner, K. M. Smith, B. P. Pittman, J. M. Shi, J. M. Tetrault, M. E. Lavery, M. R. Picciotto and S. A. McKee (2017). "Effect of doxazosin on stress reactivity and the ability to resist smoking." <u>J Psychopharmacol</u> **31**(7): 830-840.
- Vickers, A. J., A. Elfiky, V. L. Freeman and M. Roach, 3rd (2022). "Race, Biology, Disparities, and Prostate Cancer." <u>Eur Urol</u> **81**(5): 463-465.
- Vineis, P. (1992). "The use of biomarkers in epidemiology: the example of bladder cancer." <u>Toxicol</u> <u>Lett</u> **64-65 Spec No**: 463-467.
- Vineis, P., T. Martone and D. Randone (1995). "Molecular epidemiology of bladder cancer: Known chemical causes of bladder cancer: Occupation and smoking." <u>Urol Oncol</u> **1**(4): 137-143.
- Vinod, V., C. J. Padmakrishnan, B. Vijayan and S. Gopala (2014). "'How can I halt thee?' The puzzles involved in autophagic inhibition." <u>Pharmacol Res</u> **82**: 1-8.
- von Zastrow, M. and A. Sorkin (2007). "Signaling on the endocytic pathway." <u>Curr Opin Cell Biol</u> **19**(4): 436-445.
- Vyas, A. R., E. R. Hahm, J. A. Arlotti, S. Watkins, D. B. Stolz, D. Desai, S. Amin and S. V. Singh (2013). "Chemoprevention of prostate cancer by d,l-sulforaphane is augmented by pharmacological inhibition of autophagy." Cancer Res **73**(19): 5985-5995.
- Walden, P. D., Y. Globina and A. Nieder (2004). "Induction of anoikis by doxazosin in prostate cancer cells is associated with activation of caspase-3 and a reduction of focal adhesion kinase." <u>Urol Res</u> **32**(4): 261-265.
- Wang, L., L. Yang, E. Fikrig and P. Wang (2017). "An essential role of PI3K in the control of West Nile virus infection." Sci Rep **7**(1): 3724.

- Wang, L. H., K. G. Rothberg and R. G. Anderson (1993). "Mis-assembly of clathrin lattices on endosomes reveals a regulatory switch for coated pit formation." <u>J Cell Biol</u> **123**(5): 1107-1117. Wang, M., W. Tan, J. Zhou, J. Leow, M. Go, H. S. Lee and P. J. Casey (2008). "A small molecule inhibitor of isoprenylcysteine carboxymethyltransferase induces autophagic cell death in PC3 prostate cancer cells." <u>J Biol Chem</u> **283**(27): 18678-18684.
- Wang, Q., Z. Chen, X. Diao and S. Huang (2011). "Induction of autophagy-dependent apoptosis by the survivin suppressant YM155 in prostate cancer cells." <u>Cancer Lett</u> **302**(1): 29-36.
- Wang, T., Y. Li, H. L. Lu, Q. W. Meng, L. Cai and X. S. Chen (2015). "beta-Adrenergic Receptors: New Target in Breast Cancer." <u>Asian Pac J Cancer Prev</u> **16**(18): 8031-8039.
- Wang, W. B., L. X. Feng, Q. X. Yue, W. Y. Wu, S. H. Guan, B. H. Jiang, M. Yang, X. Liu and D. A. Guo (2012). "Paraptosis accompanied by autophagy and apoptosis was induced by celastrol, a natural compound with influence on proteasome, ER stress and Hsp90." <u>J Cell Physiol</u> **227**(5): 2196-2206. Wang, Y., L. Zhang and F. Zhou (2022). "Cuproptosis: a new form of programmed cell death." <u>Cell Mol Immunol</u> **19**(8): 867-868.
- Warlick, C. A., M. E. Allaf and H. B. Carter (2006). "Expectant treatment with curative intent in the prostate-specific antigen era: triggers for definitive therapy." <u>Urol Oncol</u> **24**(1): 51-57.
- Wasim, S., S. Y. Lee and J. Kim (2022). "Complexities of Prostate Cancer." Int J Mol Sci 23(22).
- Wasko, B. M., A. Dudakovic and R. J. Hohl (2011). "Bisphosphonates induce autophagy by depleting geranylgeranyl diphosphate." J Pharmacol Exp Ther 337(2): 540-546.
- Waters, M. G., T. Serafini and J. E. Rothman (1991). "'Coatomer': a cytosolic protein complex containing subunits of non-clathrin-coated Golgi transport vesicles." <u>Nature</u> **349**(6306): 248-251.
- Weigel, P. H. and J. A. Oka (1981). "Temperature dependence of endocytosis mediated by the asialoglycoprotein receptor in isolated rat hepatocytes. Evidence for two potentially rate-limiting steps." J Biol Chem **256**(6): 2615-2617.
- Wein, A. J., L. R. Kavoussi, A. W. Partin and C. A. Peters (2016). <u>Campbell-Walsh urology</u>. Philadelphia, PA, Elsevier.
- Wiczk, A., D. Hofman, G. Konopa and A. Herman-Antosiewicz (2012). "Sulforaphane, a cruciferous vegetable-derived isothiocyanate, inhibits protein synthesis in human prostate cancer cells." <u>Biochim Biophys Acta</u> **1823**(8): 1295-1305.
- Wild, P., D. G. McEwan and I. Dikic (2014). "The LC3 interactome at a glance." <u>J Cell Sci</u> **127**(Pt 1): 3-9. Wong, M. C. S., F. D. H. Fung, C. Leung, W. W. L. Cheung, W. B. Goggins and C. F. Ng (2018). "The global epidemiology of bladder cancer: a joinpoint regression analysis of its incidence and mortality trends and projection." <u>Sci Rep</u> **8**(1): 1129.
- Wu, W. K., S. B. Coffelt, C. H. Cho, X. J. Wang, C. W. Lee, F. K. Chan, J. Yu and J. J. Sung (2012). "The autophagic paradox in cancer therapy." Oncogene **31**(8): 939-953.
- Wu, X., M. M. Ros, J. Gu and L. Kiemeney (2008). "Epidemiology and genetic susceptibility to bladder cancer." <u>BJU Int</u> **102**(9 Pt B): 1207-1215.
- Wu, Z., P. C. Chang, J. C. Yang, C. Y. Chu, L. Y. Wang, N. T. Chen, A. H. Ma, S. J. Desai, S. H. Lo, C. P. Evans, K. S. Lam and H. J. Kung (2010). "Autophagy Blockade Sensitizes Prostate Cancer Cells towards Src Family Kinase Inhibitors." Genes Cancer 1(1): 40-49.
- Xiao, D., A. A. Powolny, J. Antosiewicz, E. R. Hahm, A. Bommareddy, Y. Zeng, D. Desai, S. Amin, A. Herman-Antosiewicz and S. V. Singh (2009). "Cellular responses to cancer chemopreventive agent D,L-sulforaphane in human prostate cancer cells are initiated by mitochondrial reactive oxygen species." Pharm Res 26(7): 1729-1738.
- Xiao, D., A. A. Powolny, M. B. Moura, E. E. Kelley, A. Bommareddy, S. H. Kim, E. R. Hahm, D. Normolle, B. Van Houten and S. V. Singh (2010). "Phenethyl isothiocyanate inhibits oxidative phosphorylation to trigger reactive oxygen species-mediated death of human prostate cancer cells." J Biol Chem 285(34): 26558-26569.
- Xie, B., H. Zuhair, R. Henrique, M. Millar, T. Robson, C. Thrasivoulou, K. Dickens, J. Pendjiky, A. Muneer, H. Patel and A. Ahmed (2023). "Opposite changes in the expression of clathrin and caveolin-

- 1 in normal and cancerous human prostate tissue: putative clathrin-mediated recycling of EGFR." Histochem Cell Biol.
- Xu, J., K. C. Yang, N. E. Go, S. Colborne, C. J. Ho, E. Hosseini-Beheshti, A. H. Lystad, A. Simonsen, E. T. Guns, G. B. Morin and S. M. Gorski (2022). "Chloroquine treatment induces secretion of autophagy-related proteins and inclusion of Atg8-family proteins in distinct extracellular vesicle populations." <u>Autophagy</u> **18**(11): 2547-2560.
- Xue, L. Y., S. M. Chiu, K. Azizuddin, S. Joseph and N. L. Oleinick (2007). "The death of human cancer cells following photodynamic therapy: apoptosis competence is necessary for Bcl-2 protection but not for induction of autophagy." <u>Photochem Photobiol</u> **83**(5): 1016-1023.
- Xue, L. Y., S. M. Chiu, K. Azizuddin, S. Joseph and N. L. Oleinick (2008). "Protection by Bcl-2 against apoptotic but not autophagic cell death after photodynamic therapy." <u>Autophagy</u> **4**(1): 125-127.
- Xue, Q., D. Yan, X. Chen, X. Li, R. Kang, D. J. Klionsky, G. Kroemer, X. Chen, D. Tang and J. Liu (2023).
- "Copper-dependent autophagic degradation of GPX4 drives ferroptosis." <u>Autophagy</u>: 1-15.
- Yamada, D., H. Nishimatsu, S. Kumano, Y. Hirano, M. Suzuki, T. Fujimura, H. Fukuhara, Y. Enomoto, H. Kume and Y. Homma (2013). "Reduction of prostate cancer incidence by naftopidil, an alpha1 adrenoceptor antagonist and transforming growth factor-beta signaling inhibitor." Int J Urol 20(12): 1220-1227.
- Yang, J., Y. Takahashi, E. Cheng, J. Liu, P. F. Terranova, B. Zhao, J. B. Thrasher, H. G. Wang and B. Li (2010). "GSK-3beta promotes cell survival by modulating Bif-1-dependent autophagy and cell death." <u>J Cell Sci</u> **123**(Pt 6): 861-870.
- Yang, P., P. Collin, T. Madden, D. Chan, B. Sweeney-Gotsch, D. McConkey and R. A. Newman (2003). "Inhibition of proliferation of PC3 cells by the branched-chain fatty acid, 12-methyltetradecanoic acid, is associated with inhibition of 5-lipoxygenase." <u>Prostate</u> **55**(4): 281-291.
- Yang, W., J. Monroe, Y. Zhang, D. George, E. Bremer and H. Li (2006). "Proteasome inhibition induces both pro- and anti-cell death pathways in prostate cancer cells." <u>Cancer Lett</u> **243**(2): 217-227.
- Yang, Y., Y. Zang, C. Zheng, Z. Li, X. Gu, M. Zhou, Z. Wang, J. Xiang, Z. Chen and Y. Zhou (2020). "CD3D is associated with immune checkpoints and predicts favorable clinical outcome in colon cancer." Immunotherapy **12**(1): 25-35.
- Yang, Y. F., C. C. Wu, W. P. Chen, Y. L. Chen and M. J. Su (2011). "Prazosin induces p53-mediated autophagic cell death in H9C2 cells." Naunyn Schmiedebergs Arch Pharmacol **384**(2): 209-216.
- Yang, Y. P., L. F. Hu, H. F. Zheng, C. J. Mao, W. D. Hu, K. P. Xiong, F. Wang and C. F. Liu (2013). "Application and interpretation of current autophagy inhibitors and activators." <u>Acta Pharmacol Sin</u> **34**(5): 625-635.
- Yang, Z. J., C. E. Chee, S. Huang and F. A. Sinicrope (2011). "The role of autophagy in cancer: therapeutic implications." Mol Cancer Ther **10**(9): 1533-1541.
- Ye, L. H., W. J. Li, X. Q. Jiang, Y. L. Chen, S. X. Tao, W. L. Qian and J. S. He (2012). "Study on the autophagy of prostate cancer PC-3 cells induced by oridonin." <u>Anat Rec (Hoboken)</u> **295**(3): 417-422. Yeom, S. Y., D. H. Nam and C. Park (2014). "RRAD promotes EGFR-mediated STAT3 activation and

induces temozolomide resistance of malignant glioblastoma." Mol Cancer Ther 13(12): 3049-3061.

- Yim, D., R. P. Singh, C. Agarwal, S. Lee, H. Chi and R. Agarwal (2005). "A novel anticancer agent, decursin, induces G1 arrest and apoptosis in human prostate carcinoma cells." <u>Cancer Res</u> **65**(3): 1035-1044.
- Yin, P., Y. Li and L. Zhang (2017). "Sec24C-Dependent Transport of Claudin-1 Regulates Hepatitis C Virus Entry." J Virol **91**(18).
- Yo, Y. T., G. S. Shieh, K. F. Hsu, C. L. Wu and A. L. Shiau (2009). "Licorice and licochalcone-A induce autophagy in LNCaP prostate cancer cells by suppression of Bcl-2 expression and the mTOR pathway." J Agric Food Chem **57**(18): 8266-8273.
- Yonekawa, T. and A. Thorburn (2013). "Autophagy and cell death." <u>Essays Biochem</u> **55**: 105-117. Yono, M., H. E. Foster, Jr., D. Shin, S. Mane and J. Latifpour (2005). "Molecular classification of doxazosin-induced alterations in the rat prostate using gene expression profiling." <u>Life Sci</u> **77**(4): 470-479.

Yu, W., J. Lin, C. Jin and B. Xia (2009). "Solution structure of human zeta-COP: direct evidences for structural similarity between COP I and clathrin-adaptor coats." J Mol Biol **386**(4): 903-912.

Yuan, L., J. Xu, Y. Shi, Z. Jin, Z. Bao, P. Yu, Y. Wang, Y. Xia, J. Qin, B. Zhang and Q. Yao (2022). "CD3D Is an Independent Prognostic Factor and Correlates With Immune Infiltration in Gastric Cancer." <u>Front Oncol 12</u>: 913670.

Zeegers, M. P., A. Jellema and H. Ostrer (2003). "Empiric risk of prostate carcinoma for relatives of patients with prostate carcinoma: a meta-analysis." <u>Cancer</u> **97**(8): 1894-1903.

Zhan, H., S. Zhang, L. Li, Z. Chen, Y. Cai, J. Huang, D. Wu, B. Huang, B. Wu and X. Liu (2022).

"Naftopidil enantiomers suppress androgen accumulation and induce cell apoptosis via the UDP-glucuronosyltransferase 2B15 in benign prostate hyperplasia." J Steroid Biochem Mol Biol 221: 106117.

Zhan, Q., K. A. Lord, I. Alamo, Jr., M. C. Hollander, F. Carrier, D. Ron, K. W. Kohn, B. Hoffman, D. A. Liebermann and A. J. Fornace, Jr. (1994). "The gadd and MyD genes define a novel set of mammalian genes encoding acidic proteins that synergistically suppress cell growth." Mol Cell Biol **14**(4): 2361-2371.

Zhang, J. (2015). "Teaching the basics of autophagy and mitophagy to redox biologists-Mechanisms and experimental approaches." Redox Biol 4c: 242-259.

Zhang, J., Z. Yang, L. Xie, L. Xu, D. Xu and X. Liu (2013). "Statins, autophagy and cancer metastasis." Int J Biochem Cell Biol **45**(3): 745-752.

Zhang, X., W. Wang, A. V. Bedigian, M. L. Coughlin, T. J. Mitchison and U. S. Eggert (2012).

"Dopamine receptor D3 regulates endocytic sorting by a Prazosin-sensitive interaction with the coatomer COPI." Proc Natl Acad Sci U S A **109**(31): 12485-12490.

Zhang, X. Q., X. F. Huang, X. B. Hu, Y. H. Zhan, Q. X. An, S. M. Yang, A. J. Xia, J. Yi, R. Chen, S. J. Mu and D. C. Wu (2010). "Apogossypolone, a novel inhibitor of antiapoptotic Bcl-2 family proteins, induces autophagy of PC-3 and LNCaP prostate cancer cells in vitro." <u>Asian J Androl</u> **12**(5): 697-708.

Zhou, L., B. Zhao, L. Zhang, S. Wang, D. Dong, H. Lv and P. Shang (2018). "Alterations in Cellular Iron Metabolism Provide More Therapeutic Opportunities for Cancer." Int J Mol Sci 19(5).

Zhu, K., K. Dunner, Jr. and D. J. McConkey (2010). "Proteasome inhibitors activate autophagy as a cytoprotective response in human prostate cancer cells." <u>Oncogene</u> **29**(3): 451-462.

Zlotta, A. R. and C. C. Schulman (2000). "Biological response modifiers for the treatment of superficial bladder tumors." <u>Eur Urol</u> **37 Suppl 3**: 10-15.

Zwarthoff, E. C. (2008). "Detection of tumours of the urinary tract in voided urine." <u>Scand J Urol Nephrol Suppl(</u>218): 147-153.